ANOXIA AND Na^+/H^+ EXCHANGE ACTIVITY IN RAT HIPPOCAMPAL NEURONS

by

CLAIRE ALEXIS SHELDON

B.Sc. (Physiology), University of Alberta, 1996
M.Sc. (Physiology), University of British Columbia, 1999

A THESIS SUBMITTED IN PARTIAL FULFILLMENT OF

THE REQUIREMENTS FOR THE DEGREE OF

COMBINED DOCTOR OF MEDICINE
AND DOCTOR OF PHILOSOPHY

in

THE FACULTY OF GRADUATE STUDIES

(Department of Anatomy, Cell Biology & Physiology)

We accept this thesis as conforming to the required standard

...

THE UNIVERSITY OF BRITISH COLUMBIA
October, 2004

ABSTRACT

In the present study, the effects of anoxia on intracellular pH (pH_i) and intracellular free sodium concentration ($[Na^+]_i$) were examined in isolated rat hippocampal neurons loaded with H^+- and/or Na^+-sensitive fluorophores, and the contribution of changes in Na^+/H^+ exchange activity to the changes in pH_i and $[Na^+]_i$ observed during and after anoxia were assessed. This assessment was aided by the development of a microspectrofluorimetric technique which permitted concurrent measurements of pH_i and $[Na^+]_i$ in the same neuron. I found that, in hippocampal neurons, Na^+/H^+ exchange activity was reduced shortly following the onset of anoxia, possibly as a result of declining internal ATP levels, and did not contribute to the increases in pH_i or $[Na^+]_i$ observed at this time. In contrast, Na^+/H^+ exchange activity was stimulated immediately after anoxia and contributed to acid extrusion and Na^+ influx during this particularly vulnerable period. As a result, the reported neuroprotective actions of Na^+/H^+ exchange inhibitors are likely mediated in the immediate post-anoxic period, consequent upon reductions in acid extrusion and/or internal Na^+ loading. A Zn^{2+}-sensitive H^+ efflux pathway, possibly a voltage-activated H^+ conductance activated by membrane depolarization, also contributed to acid extrusion during and immediately after anoxia and may act to limit the potentially detrimental activation of Na^+/H^+ exchange activity observed after anoxia. The final series of experiments identified additional mechanisms that contribute to the changes in $[Na^+]_i$ evoked by anoxia in cultured postnatal rat hippocampal neurons. Na^+ influx occurred through multiple pathways, the relative contributions of which differed not only during and after anoxia but also in neurons maintained in culture for different durations of time. Understanding the fundamental cellular mechanisms that contribute to anoxia-evoked changes in pH_i and $[Na^+]_i$ in mammalian central neurons may uncover novel therapeutic strategies for the treatment of stroke.

TABLE OF CONTENTS

CHAPTER TWO - General Methods

CHAPTER THREE - Intracellular pH Response to Anoxia in Acutely Isolated Adult Rat Hippocampal CA1 Pyramidal Neurons: Reduced Na^+/H^+ exchange activity during anoxia

CHAPTER FOUR - Intracellular pH Response to Anoxia in Acutely Isolated Adult Rat Hippocampal CA1 Pyramidal Neurons: Increased Na^+/H^+ exchange activity after anoxia

CHAPTER FIVE - Changes in $[Na^+]_i$ Induced By Anoxia in Isolated Rat Hippocampal Neurons: Role of Na^+/H^+ exchange activity

CHAPTER SIX - Concurrent Measurement of pH_i and $[Na^+]_i$ with Fluorescent Indicators: A further evaluation of the role of Na^+/H^+ exchange in anoxia-evoked changes in pH_i and $[Na^+]_i$

CHAPTER SEVEN - Additional Mechanisms Contributing to Anoxia-Evoked Increases in $[Na^+]_i$ in Cultured Postnatal Rat Hippocampal Neurons

LIST OF TABLES

LIST OF FIGURES

ACKNOWLEDGEMENTS

I would first like to thank John Church for his support and guidance and for the seemingly endless time and energy he has dedicated towards my training. My sincerest thanks. I would also like to express my gratitude to the members of my supervisory committee, Drs. Kenneth Baimbridge, Steven Kehl and Lynn Raymond, for sharing their time, scientific knowledge and words of encouragement with me. To the members of the entire Departments of Physiology and Anatomy and Cell Biology (students and faculty alike), and especially to Sally Osborne, Pauline Dan, Claudia Krebs, Herman Fernandes, Tony Kelly, May Cheng - thank you for your camaraderie and support. To Val Smith, Candace Hofmann, Mareika Grant, Gord Rintoul, Mike Rauh and Paul Yong, thank you for always being such wonderful friends! Finally, to the people that I hold dearest to my heart, Craig, Mary, Bill, Tess, Mia, Jay, Signy, Toby and Tori, I could not have done this without your never-ending love, humor and, at times, ridicule.

CHAPTER ONE

INTRODUCTION

1.0. General Introduction

1.1. Clinical background

Stroke is the third leading cause of death in the Western world. In Canada, 16 000 people die as a result of strokes every year and, in addition to those, 300 000 people are living with the disabling effects of stroke (Heart and Stroke Foundation of Canada website, www.heartandstroke.ca). While the number of stroke patients across Canada is expected to increase in the next two decades, therapies to date have had limited success. Thrombolytic and neuroprotective therapies represent two fundamental approaches to the treatment of strokes. Approximately 80% of strokes occur when the blood supply to the brain has been interrupted (ischemic strokes) and, in the majority of these cases, are consequent upon a physical blockage of the arteries supplying the central nervous system by thrombi or emboli. Since the energy required to maintain neuronal function and integrity is derived principally from oxidative phosphorylation, thrombolytic therapies are aimed at restoring the supply of oxygen and glucose necessary for normal cerebral function (Erecińska & Silver, 1989; Silver *et al.* 1997). The use of the intravenous thrombolytic agent, tissue plasminogen activator (tPA), administered within 3 h after stroke onset, is the only clinically approved treatment for acute ischemic strokes (see NINDS group study, 1995). However, it is estimated that only 1% of all ischemic stroke patients are treated with tPA (Schellinger *et al.* 2004), the major reason for this failure of treatment being the arrival and identification of eligible patients more than 3 h after stroke onset. There are also inherent risks associated with the resumption of blood flow which demand careful patient monitoring during and after thrombolytic therapy: reperfusion may be associated with an

increased risk of haemorrhage (see NINDS group study, 1995), abnormal neuronal activity (e.g. Xu & Pulsinelli, 1996; Reese *et al.* 2002), vascular endothelial damage and reactive oxygen species generation (e.g. Kent *et al.* 2001), all of which may promote the development of subsequent tissue damage. Finally, the efficacy of thrombolytic therapies is also limited by variations in clot composition and size (Broderick & Hacke, 2002a). The second approach to the treatment of acute ischemic strokes is neuroprotective agents. These therapies are designed to limit the cellular mechanisms leading to neuronal death and are, in large part, based on basic science research examining the neuronal response to periods of ischemia. More than 40 potential neuroprotective agents, directed towards a number of different fundamental mechanisms, have been examined in human trials; however, the vast majority of these have had limited clinical efficacy (see Table 1.1: Dietrich, 1998; Lee *et al.* 1999; Lo *et al.* 2003), an observation which is perhaps not surprising considering the large number of factors involved in initiating and maintaining the mechanisms thought to be responsible for ischemic neuronal death (Fig. 1.1). It is notable that, by influencing several of these mechanisms, mild hypothermia represents a successful neuroprotective strategy, although its utility is also limited by the lack of feasible techniques to induce hypothermia in a large number of patients (Broderick & Hacke, 2002b). Despite the potentially tragic consequences for patients with stroke and their families, as well as the growing socio-economic impact, effective treatments for ischemic strokes are clearly lacking.

1.2. Neuropathology

In this section, I will outline some of the features of cell damage observed in response to periods of cerebral ischemia. It is recognized that "the immediate effect of ischemia is similar to that of anoxia" (Somjen, 2004) and, as a result, the initial events that occur in response to ischemia (i.e. oxygen and glucose deprivation) can be effectively represented by oxygen deprivation alone

(anoxia). Indeed, as described below in Section 1.3, the pattern of ionic and electrical events initiated during anoxia and ischemia are similar, although the period of time over which they occur is shorter with more severe insults (e.g. Silver *et al.* 1997; Centonze *et al.* 2001). As ischemia is experienced most often clinically, in the section that follows I will use the term ischemia, although in later sections, in light of the similar pathophysiological mechanisms initiated during anoxia and ischemia, both terms will be employed.

A number of key factors determine the extent and pattern of damage observed in response to periods of cerebral ischemia. *First,* cellular populations within the brain have differing intrinsic sensitivities to periods of ischemia: neurons are most sensitive while glia and endothelial cells are more tolerant to periods of ischemia (Pulsinelli *et al.* 1982; Bramlett & Dietrich, 2004). *Second,* the magnitude of ischemic cell damage is proportional to the severity and duration of the ischemic insult. Periods of complete ischemia will produce more pronounced cell damage than equivalent periods of incomplete ischemia and, similarly, longer durations of ischemia will produce increasing amounts of damage (see Silver & Erecińska, 1990; Dietrich, 1998). *Third,* the type of ischemic insult experienced will determine the pattern of cell damage. In response to periods of global ischemia, which occur following the interruption of the supply of oxygen and glucose to the entire brain, as in cardiac arrest, selectively vulnerable cells (for example, CA1 pyramidal neurons of the hippocampus and GABAergic spiny neurons of the striatum) are specifically damaged. Focal ischemia, which occurs following the occlusion of blood vessel(s) supplying a particular region of the brain, produces a 'core' region of severe neuronal damage and a surrounding penumbra where blood flow is less markedly reduced and neurons remain potentially salvageable (reviewed by Back, 1998; Lipton, 1999). *Fourth,* although events occurring during ischemia initiate cellular dysfunction, further cell damage can

be influenced significantly by events that occur during early recirculation (e.g. Gao *et al.* 1998; Taylor *et al.* 1999).

Despite these various considerations, ischemic neuronal death can be classified in two general ways: acute *vs.* delayed and necrotic *vs.* apoptotic. Acute neuronal death occurs as neurons die rapidly following the onset of ischemia and, in these cases, ischemia tends to be severe and/or the neurons are selectively vulnerable to the ischemic episode. Morphologically, acute neuronal death is, in large part, necrotic, characterized by the appearance of darkened nuclei, swollen organelles and a loss of plasma membrane integrity. There are 3 categories of necrotic cell death: edematous cell change, ischemic cell change, and homogenizing cell change (Fig. 1.1; Lipton, 1999). While each category has its own distinquishing features, in most cases, the morphological changes reflect excessive Na^+ and Ca^{2+} entry: accompanying anion (e.g. Cl^- and HCO_3^-) and water entry promote cell swelling while increases in intracellular free Ca^{2+} concentrations ($[Ca^{2+}]_i$) activate proteolytic and lipolytic enzymes (Goldberg & Choi, 1993; Lee *et al.* 1999; Lipton, 1999; Small *et al.* 1999; Yuan *et al.* 2003). In contrast to acute neuronal death, delayed neuronal death occurs from hours to days, or more, after an ischemic insult. In contrast to the necrotic changes associated with acute neuronal death, delayed neuronal death is, in many cases, apoptotic in nature, characterized by chromatin condensation, cell shrinkage and the generation of apoptotic cell bodies (Lipton, 1999; Small *et al.* 1999). Changes in $[Ca^{2+}]_i$ and the internal concentration of K^+ ions ($[K^+]_i$) appear to be early events that trigger downstream apoptotic cascades; however, the precise contribution of these (and other) mechanisms to the initiation of apoptosis, and the identities of the downstream effector mechanisms, remain an area of active investigation (Lee *et al.* 1999; Snider *et al.* 1999; also see Banasiak *et al.* 2004 for an illustration of the relationship between $[Na^+]_i$ and hypoxia-induced apoptosis). Recent evidence suggests that both necrosis and apoptosis may be activated in parallel in the ischemic brain, possibly

through common intracellular cascades, and that the resulting observed morphologies lie along a continuum between necrosis and apoptosis (see Snider *et al.* 1999). A final distinct form of cell death, characterized by a condensed cytoplasm containing many large lysosomes, is autophagocytotic cell death; however, there is limited information regarding both its underlying mechanisms and its relative contribution to ischemic neuronal death (Lipton, 1999; Yuan *et al.* 2003; also see Florez-McClure *et al.* 2004).

Taken together, these observations suggest that, while many factors influence the extent and pattern of ischemic cell damage, common pathophysiological events may contribute to the initiation and regulation of both necrotic and apoptotic forms of neuronal death. In the following section, I will discuss the contribution of early changes in the concentrations of intracellular ions to the pathophysiology of ischemic cell damage.

1.3. Pathophysiology

Ischemia is an extremely complex metabolic insult during which diverse cellular events are initiated that, in turn, are critical determinants of subsequent functional and structural changes and eventual cell death. It is generally acknowledged that declining intracellular ATP levels and the accompanying changes in the concentrations of internal ions are critically important in initiating ischemic cell damage (Fig. 1.1; also see Somjen, 2002). The extra- and intracellular ionic changes that occur during and following anoxia or ischemia have been studied extensively (for reviews see Hansen, 1985; Erecińska & Silver, 1994; Martin *et al.* 1994; Lipton, 1999). As illustrated in Fig. 1.2, anoxia- or ischemia-induced changes in ion concentrations (both extra- and intracellular) can be described in 3 consecutive phases: during phase 1, there are slow changes in extra- and intracellular ion concentrations, which presumably reflect the declining capacity of neurons to maintain internal ATP levels (and the consequent inhibition of the activities of ATP-

dependent ion pumps, notably the Na^+,K^+-ATPase); the onset of phase 2 is associated with a precipitous and striking depolarization (referred to as 'ischemic' or 'anoxic' depolarization) and is accompanied by marked ionic dysregulation and an increased likelihood of irreversible neuronal injury; finally, slow changes in extra- and intracellular ion concentrations occur during phase 3. Thus, in response to ischemia, there are reductions in the external concentrations of sodium, calcium and chloride ions ($[Na^+]_o$, $[Ca^{2+}]_o$ and $[Cl^-]_o$, respectively) and increases in the external concentration of potassium ions ($[K^+]_o$). Corresponding increases in $[Ca^{2+}]_i$ and the internal concentrations of Na^+ and Cl^- ions ($[Na^+]_i$ and $[Cl^-]_i$, respectively), and decreases in $[K^+]_i$, are also observed. Changes in extra- and intracellular pH (pH_o and pH_i, respectively) also occur: falls in pH_o and pH_i are seen soon after the onset of anoxia or ischemia and may be interrupted by external alkaline transients upon anoxic depolarization before giving way to further acidic shifts. The period of time over which this sequence of events occurs depends on the nature and severity of the insult. For example, during focal ischemia, neurons located within the penumbra exhibit less marked falls in pH_i, increases in $[Ca^{2+}]_i$ and $[Na^+]_i$ and are less likely to undergo 'anoxic depolarization', compared to the neurons located within the adjacent core of the ischemic tissue (Back, 1998; Lipton, 1999). Finally, if the anoxic or ischemic insult is transient in nature, the restoration of internal ATP levels, transmembrane ion gradients and membrane potential may be possible; however, this recovery does not occur consistently and the restoration of oxygen and glucose does not necessarily result in the return of ion homeostasis and membrane repolarization (Ekholm *et al.* 1993; O'Reilly *et al.* 1995; Tanaka *et al.* 1997).

In light of these marked ionic shifts, in the following sections (Section 1.3.1 - 1.3.4), I will outline the potential contributions of changes in the extra- and intracellular concentrations of Ca^{2+}, H^+ and Na^+ ions to the pathophysiology of ischemic cell death.

1.3.1. $[Ca^{2+}]_i$ and excitotoxicity

The contribution of Ca^{2+} ions to anoxia- or ischemia-induced neuronal damage has received particular attention, notably within the framework of the excitoxic model of cell injury (Olney *et al.* 1971). Both anoxia and ischemia are associated with the release of excitatory neurotransmitters (most notably glutamate) into the synaptic cleft (e.g. Benveniste *et al.* 1984; Santos *et al.* 1996). The resulting prolonged activation of *N*-methyl-D-aspartate (NMDA) and other subtypes of ionotropic glutamate receptors (e.g. α-amino-3-hydroxy-5-methyl-4-isoxazole propionic acid; AMPA) elicits rises in $[Na^+]_i$ and $[Ca^{2+}]_i$ which, acting together, initiate neuronal damage by aggravating the decline in internal ATP levels, further promoting ion dysregulation and activating a variety of intracellular degradative enzymes (Choi, 1990; Herman *et al.* 1990; Mitani *et al.* 1994; Kristián & Siesjö, 1997).

The central role of glutamate and $Ca^{2+}{}_i$ to anoxia-induced neuronal damage is supported by a number of key findings: *i)* extracellular glutamate levels increase during ischemia *in vivo* (e.g. Benveniste *et al.* 1984; Choi, 1990) or metabolic inhibition *in vitro* (e.g. Goldberg & Choi, 1993; Kimura *et al.* 1998); *ii)* glutamate receptor antagonists, under certain circumstances, may reduce neuronal death *in vivo* (e.g. Simon *et al.* 1984; Church *et al.* 1988; but see Nurse & Corbett, 1996) and reduce Ca^{2+} influx and neuronal death in neuronal cultures exposed to oxygen-glucose deprivation (e.g. Goldberg *et al.* 1987; Kaku *et al.* 1993; but see Newell *et al.* 1995); and *iii)* the susceptibility to ischemia *in vivo* (e.g. Jensen, 2002) and excitotoxicity *in vitro* (e.g. Cheng *et al.* 1999) parallel developmental increases in ionotropic glutamate receptor expression (but see Marks *et al.* 2000). Finally, postischemic enhancements of NMDA- and non-NMDA receptor-mediated Ca^{2+} influx have been observed 1 - 12 h following transient ischemia

(e.g. Pellegrini-Giampietro *et al.* 1997; Mitani *et al.* 1998; Xu *et al.* 1999) and may contribute to further neuronal dysfunction and death at this time (Gao *et al.* 1998; Lipton, 1999).

In contrast, glutamate receptor antagonists fail to influence neuronal survival following periods of prolonged (>90 min) oxygen and glucose deprivation *in vitro* (Aarts *et al.* 2003; also see Obeidat *et al.* 2000), and their proposed neuroprotective effects in *in vivo* animal models (see above) have been attributed to drug-induced reductions in cerebral temperature (e.g. Nurse & Corbett, 1996). Most importantly, however, glutamate receptor antagonists have proven ineffective in improving clinical outcome following a stroke (Table 1.1; e.g. Lee *et al.* 1999; Lees *et al.* 2000). These negative findings have supported suggestions that glutamate-mediated excitotoxicity cannot completely account for the detrimental effects of anoxia or ischemia on neuronal viability. Indeed, some studies have illustrated differences in the time course of glutamate-induced neuronal dysfunction compared with that induced by anoxia or ischemia (see Friedman & Haddad, 1993; Chow & Haddad, 1998). In addition, while increases in $[Ca^{2+}]_i$, specifically Ca^{2+} entry through NMDA receptor-operated channels (Tymianski *et al.* 1993; Sattler *et al.* 1998), contribute to glutamate-induced neuronal death *in vitro*, anoxia- and ischemia-induced neuronal death is not necessarily dependent on an increase in $[Ca^{2+}]_i$ (e.g. Friedman & Haddad, 1993; Li *et al.* 1996) and the increases in $[Ca^{2+}]_i$ that occur in selectively vulnerable hippocampal CA1 pyramidal neurons *in vivo* during and upon recovery from transient periods of global ischemia are only partially influenced by pharmacological inhibitors of NMDA receptors (Silver & Erecińska, 1990 and 1992). This may, at least in part, reflect the facts that NMDA receptors are inhibited by reductions in pH_o (e.g. Vyklicky *et al.* 1990; Traynelis & Cull-Candy, 1991) and that marked falls in pH_o occur during anoxia and ischemia *in vivo* (see above and Section 1.3.2).

These apparently contradictory findings have highlighted the complex regulation of anoxic/ischemic neuronal damage and have prompted renewed interest into the identification of additional glutamate receptor-independent events that might contribute to the pathogenesis of anoxic/ischemic neuronal damage.

1.3.2. Role of changes in pH

1.3.2.1. Historical background

The importance of pH to the effects of ischemia on neuronal function and death has been recognized for over 25 years (reviewed by Siesjö *et al.* 1996). Early studies demonstrated key relationships between pre-ischemic plasma glucose levels, the magnitudes of the interstitial acidosis during ischemia and the extent of subsequent neuronal damage observed in response to global ischemia (Ljunggren *et al.* 1974; Diemer & Siemkowicz, 1981; Siemkowicz & Hansen, 1981). Initially demonstrated by Myers and Yamaguchi (1977), and confirmed by many others, pre-ischemic hyperglycemia enhances infarct size and limits functional recovery following ischemia compared to normoglycemic controls, a relationship which appears to hold true clinically as patients hyperglycemic prior to stroke show significantly worse outcomes (see Kent *et al.* 2001; Parsons *et al.* 2002). After infusing animals with varying amounts of glucose, Li *et al.* (1995) observed a close correlation between intra-ischemic pH_o and extent of cell necrosis measured 7 days following 10 min global ischemia and further illustrated that the effect of hyperglycemia to aggravate neuronal damage occurs over a narrow range of glucose concentrations and pH_o values (with the toxic effects of pH_o observed at pH_o values $< 5.8 - 6.4$; Li *et al.* 1995; also see Hurn *et al.* 1991). In additional studies, normoglycemic animals were subjected to transient ischemia under hypercapnic conditions to lower intra-ischemic pH_o to values similar to those observed in hyperglycemic animals ($pH_o \sim 5.8 - 6.3$; Katsura *et al.* 1994;

also see Hurn *et al.* 1991) and, in these animals, ischemia-induced neuronal damage was similarly aggravated despite the absence of hyperglycemia, providing further support for a critical role of pH_o in the development of ischemia-induced neuronal damage *in vivo*. However, further studies, employing global and focal models of ischemia, have produced conflicting results; studies have reported reductions, increases and no changes in infarct size under hyperglycemic conditions (e.g. LeBlanc *et al.* 1993; Li *et al.* 1996; Schurr *et al.* 1999). In an attempt to reconcile these differences, Sapolsky *et al.* (1996) argued that the influence of acidity is not likely to be simply toxic or beneficial to an ischemic neuron but rather "represents the summation and counterbalancing of the salutary and deleterious effects of acidosis". In the following sections, the apparently dichotomous role that changes in pH_o/pH_i may have in the pathogenesis of ischemic neuronal damage will be discussed further.

1.3.2.2. pH: neurotoxic or neuroprotective?

Changes in pH_o, of varying magnitudes and directions, are commonly observed within the central nervous system and may function as signalling events. Normal synaptic transmission and postsynaptic receptor activation both elicit changes in pH_o (see Krishtal *et al.* 1987; Jarolimek *et al.* 1989; Chesler & Kaila, 1992; Rose & Deitmer, 1995). In hippocampal slices, orthodromic electrical stimulation (2.5 to 20 Hz for 20 - 60 s) evokes external alkaline transients of up to 0.2 pH units, often followed by prolonged (e.g. min) extracellular acidifications of up to 0.1 pH units (Jarolimek *et al.* 1989). These changes in pH_o may have important regulatory functions; for example, synaptic vesicle fusion releases protons into the synaptic cleft which may, in turn, feedback and inhibit the voltage-activated Ca^{2+} channels initially responsible for their release (DeVries, 2001; also see Balestrino & Somjen, 1988; Church & McLennan, 1989; Tombaugh, 1994; Tombaugh & Somjen, 1996; Church *et al.* 1998).

During pathological events, such as cerebral ischemia, epileptic seizures and spreading depression, dramatic alterations in cerebral pH_o, ranging in magnitude from 0.1 to greater than 1 pH units, can occur (e.g. Mutch & Hansen, 1984; Hansen, 1985; Menna *et al.* 2000; Tong & Chesler, 2000) and, as under normoxic conditions, may have important downstream consequences. Indeed, seizure activity induces decreases in pH_o that may act to limit or even terminate the seizure activity itself (e.g. Aram & Lodge, 1987; Tong & Chesler, 2000). Mild falls in pH_o, such as those observed during the early stages of anoxia or ischemia, suppress neuronal excitability and reduce neuronal energy demand by decreasing NMDA receptor-mediated currents (see above) and voltage-activated Na^+ and Ca^{2+} currents and augmenting $GABA_A$ receptor-mediated Cl^- currents (Krnjević & Walz, 1990; Cummins *et al.* 1991; Tombaugh & Somjen, 1996; Krishek *et al.* 1996). These, and other, effects may underlie the neuroprotective actions of mild extracellular acidosis beyond that produced by glutamate receptor antagonists alone (Tombaugh & Sapolsky, 1990; Kaku *et al.* 1993). In contrast to the neuroprotective effects of mild reductions in pH_o, marked falls in pH_o may kill neurons (reviewed by Tombaugh & Sapolsky, 1993; Siesjö *et al.* 1996; see also Kraig *et al.* 1987; Nedergaard *et al.* 1991). Excessive and/or prolonged extracellular acidosis rapidly depletes tissue ATP levels and, following an anoxic insult, stimulates lipid peroxidation, protein denaturation and the accumulation of free radicals (Nedergaard & Goldman, 1993; Tombaugh & Sapolsky, 1993; Siesjö *et al.* 1996; Trafton *et al.* 1996; Raley-Susman & Barnes, 1998), effects which may contribute to the observed ability of marked external acidosis ($pH_o <\sim 6.5$) to induce necrotic and apoptotic neuronal death in hippocampal slices (Ding *et al.* 2000). Finally, acting at least in part by enhancing the activities of NMDA receptors and high-voltage activated Ca^{2+} channels, increases in pH_o promote neuronal excitability and the development of seizure activity, enhance the propagation of spreading depression and worsen functional recovery from global

ischemia (Aram & Lodge, 1987; Church & McLennan, 1989; Tombaugh & Somjen, 1996; Hurn *et al.* 1997; Tong & Chesler, 2000).

All together, pH_o is a key determinant of neuronal function and viability during and following an anoxic/ischemic insult, although the basis for its effects remains incompletely understood.

1.3.2.3. pH: extracellular or intracellular?

The great majority of studies which have examined the effects of changes in pH_o on neuronal function, whether under physiological or pathophysiological conditions, have not assessed the possible involvement of concomitant changes in pH_i. In contrast to many peripheral cell types (e.g. myocytes, neutrophils and cardiac Purkinje fibers), wherein pH_o has only a minor influence on pH_i (the slope of linear regression line relating pH_i to pH_o, $\Delta pH_i:\Delta pH_o$, $\cong$ 0.35 - 0.40; see Aickin, 1984; Wilding *et al.* 1992), in many types of mammalian central neurons, pH_o is a critical determinant of pH_i ($\Delta pH_i:\Delta pH_o \cong 0.75$; Ou-Yang *et al.* 1993; Sánchez-Armass *et al.* 1994; Church *et al.* 1998; also see Ritucci *et al.* 1998 for data comparing the pH_o-dependency of pH_i in chemosensitive *vs.* nonchemosensitive medullary neurons). Thus, the influence of pH_o on neuronal function under normoxic and anoxic conditions may, at least in part, be secondary to changes in pH_i.

Changes in neuronal pH_i can also occur in the absence of marked changes in pH_o. Membrane depolarization can elicit falls in pH_i in invertebrate (e.g. Ahmed & Conner, 1980) and mammalian central neurons (Trapp *et al.* 1996a; Zhan *et al.* 1998; Meyer *et al.* 2000; Willoughby & Schwiening, 2002; reviewed by Ballanyi & Kaila, 1998). Through mechanisms dependent on Ca^{2+} influx and HCO_3^- efflux, respectively, glutamatergic and GABAergic neurotransmission can

similarly elicit falls in pH_i (Kaila & Voipio, 1987; Irwin *et al.* 1994; Wang *et al.* 1994; Trapp *et al.* 1996a; Wu *et al.* 1999). By influencing a range of intracellular processes, from the activities of internal metabolic pathways and intracellular second messenger systems to the activities of voltage- and ligand-gated ion channels, intrinsic changes in pH_i can modulate not only neuronal activity under normoxic conditions but may also be important determinants of neuronal viability in response to anoxic or ischemic insults. For example, the activity of phosphofructokinase is markedly pH_i dependent with a change as small as 0.1 pH unit being able to completely activate or inactivate the glycolytic pathway (Busa & Nuccitelli, 1984). Similarly, adenylate cyclase and cyclic nucleotide phosphodiesterase, those enzymes responsible for cAMP synthesis and hydrolysis, respectively, are regulated by pH_i such that an increase in pH_i causes an elevation in intracellular cAMP levels (Busa & Nuccitelli, 1984). Additional intracellular second messenger cascades, including Ca^{2+}/calmodulin (e.g. Busa & Nuccitelli, 1984), nitric oxide synthase (e.g. Anderson & Meyer, 2000; Conte, 2003) and phospholipase A_2/arachidonic acid (e.g. Stella *et al.* 1995), are also sensitive to changes in pH_i. The activities of these, and other, intracellular pathways are affected by anoxia and ischemia and appear to be important determinants of subsequent neuronal function and viability by regulating, for example, neurotransmitter release, the generation of reactive oxygen species and membrane integrity (reviewed by Meldrum, 1996; Wieloch *et al.* 1996; Sapirstein & Bonventre, 2000; Prast & Philippu, 2001); thus, the possibility exists that changes in pH_i may influence the neuronal response to anoxia or ischemia by regulating the activities of diverse intracellular signalling cascades.

Analogous to the protective effects of mild falls in pH_o (see above), mild reductions in pH_i may exert a neuroprotective effect by inhibiting, for example, voltage-activated Ca^{2+} currents (e.g. Takahashi & Copenhagen, 1996; Tombaugh & Somjen, 1997), neurotransmitter release (e.g. Drapeau & Nachshen, 1988; Chen *et al.* 1998b), and gap junctional conductances (thereby

reducing neuronal synchrony and, possibly, anoxia-induced epileptiform activity; Spray & Bennett, 1985; Church & Baimbridge, 1991; Perez-Velazquez *et al.* 1994; Xiong *et al.* 2000). On the other hand, the neurotoxicity associated with exposure to highly acidic media ($pH_o < 6.5$) appears to be a function of the degree and duration of the intracellular acidification produced consequent upon the fall in pH_o (Hurn *et al.* 1991; Nedergaard *et al.* 1991). Marked decreases in pH_i are capable of inducing cellular dysfunction by initiating DNA damage and the production of free radicals (Siesjö *et al.* 1996; Vincent *et al.* 1999), as well as inhibiting Ca^{2+}- and voltage-activated K^+ channels (see review by Tombaugh & Somjen, 1998; also see Church, 1992; Church *et al.* 1998; Liu *et al.* 1999; Kelly & Church, 2004) and promoting cellular swelling (Jakubovicz & Klip, 1989). Recent studies have also illustrated that falls in pH_i are early events in mitochondria-dependent apoptosis; considering that optimal caspase activity is observed between pH 6.3 to 6.8, marked falls in pH_i are capable of regulating downstream caspase activity (Matsuyama *et al.* 2000; Takahashi *et al.* 2004).

Finally, although changes in pH_i are determined by changes in $[H^+]_i$ and $[HCO_3^-]_i$, HCO_3^- ions themselves can have important effects independent from changes in pH_i: HCO_3^- ions can control cAMP signalling (Chen *et al.* 2000) and the production of reactive oxygen species (e.g. Konorev *et al.* 2000; Han *et al.* 2003) and can directly impact neuronal excitability (Bruehl *et al.* 2000; Gu *et al.* 2000; Bruehl & Witte, 2003), especially in the post-anoxic period (e.g. Roberts *et al.* 2000).

1.3.2.4. pH_i: relevance to anoxia and the timing of its actions

The studies cited above indicate that changes in pH_i *per se* can modulate neuronal activity under normoxic conditions as well as neuronal viability in response to anoxic or ischemic insults. Similar findings have been made in peripheral cell types, most notably in cardiac myocytes and

hepatocytes. In these cell types, it appears that the recovery of pH_i to physiological values during reperfusion, rather than the fall in pH_i observed during anoxia or ischemia, initiates an intracellular cascade of events, including attendant changes in $[Na^+]_i$ and $[Ca^{2+}]_i$, that finally results in cellular damage (Lazdunski *et al.* 1985; Currin *et al.* 1991; Bond *et al.* 1993). The relevance of this series of events has not been established in mammalian central neurons. On the one hand, decreases in pH_i *during* anoxia have been suggested to modulate the susceptibility of neurons to injury (e.g. LeBlanc *et al.* 1993; Tyson *et al.* 1993; Roberts & Chih, 1997). On the other hand, neuronal damage in cultured neocortical neurons evoked by metabolic inhibition (a combination of 2-deoxy-D-glucose and cyanide) can be reduced by inhibiting the rate of restoration of pH_i to normal values in the period *following* the metabolic inhibition (Vornov *et al.* 1996). An understanding of the basis for these apparently disparate findings requires the characterization of the intrinsic changes in pH_i which occur in mammalian central neurons during *and* following periods of anoxia or ischemia.

1.3.3. Role of changes in $[Na^+]_i$

Early increases in Na^+_i occur in response to anoxia or ischemia and appear to contribute to the pathophysiology of subsequent neuronal death (see Urenjak & Obrenovitch, 1996; Lipton, 1999). Thus, the removal of extracellular Na^+ reduces anoxia- and ischemia-evoked changes in neuronal morphology (e.g. Friedman & Haddad, 1994b; Chidekel *et al.* 1997; Raley-Susman *et al.* 2001) and promotes subsequent functional recovery (e.g. Fried *et al.* 1995; Raley-Susman *et al.* 2001). The beneficial effects of reduced Na^+ entry may reflect a number of factors, including: *i)* a reduced demand for cellular ATP to maintain the Na^+ gradient (e.g. Erecińska *et al.* 1991; Fowler & Li, 1998; Chinopoulos *et al.* 2000); *ii)* decreased neuronal swelling (e.g. Friedman & Haddad, 1994b; Chidekel *et al.* 1997); *iii)* a reduction in the magnitude and duration of 'anoxic'

membrane depolarization (e.g. Haddad & Jiang, 1993; Tanaka *et al.* 1997; Calabresi *et al.* 1999b); *iv)* limiting reverse-mode glutamate reuptake and/or Na^+/Ca^{2+} exchange (e.g. Taylor *et al.* 1995; Kimura *et al.* 1998; Breder *et al.* 2000); and *v)* preventing Na^+_i-dependent increases in NMDA receptor-mediated currents (Yu & Salter, 1998).

In direct contrast to studies in non-neuronal cell types (e.g. cardiac myocytes; Carmeliet, 1999) and myelinated central nervous system axons (Stys, 1998), the mechanisms which mediate Na^+ influx in response to anoxia or ischemia in mammalian central neurons remain relatively poorly defined. Although Na^+ influx through glutamate receptor-operated channels has received some attention (Müller & Somjen, 2000, LoPachin *et al.* 2001), glutamate-mediated excitotoxicity may not be a completely valid model for the direct actions of anoxia or ischemia on neurons (see Section 1.3.1) and few studies (e.g. Chen *et al.* 1999) have systematically addressed the potential contributions of other mechanisms integral to the cell (e.g. voltage-activated Na^+ channels (e.g. Fung & Haddad, 1997; Banasiak *et al.* 2004), Na^+/H^+ exchange (e.g. Kintner *et al.* 2004), forward-mode Na^+/Ca^{2+} exchange (e.g. Chidekel *et al.* 1997) and $Na^+/K^+/2Cl^-$ cotransport (e.g. Beck *et al.* 2003)) to the increases in neuronal $[Na^+]_i$ observed during anoxia or ischemia (see Pisani *et al.* 1998a; Guatteo *et al.* 1998; Calabresi *et al.* 1998 for studies in slice preparations). In addition, despite indications that continued Na^+ entry upon reperfusion may be more damaging than Na^+ entry during anoxia or ischemia (see Lipton, 1999), the pathways that mediate Na^+ entry in the period immediately after anoxia/ischemia have not been characterized and it remains unknown whether these pathways might differ from those active during an insult, as reported for Ca^{2+} (see Silver & Erecińska, 1990 and 1992). Further studies are necessary, *first*, to characterize the changes in $[Na^+]_i$ observed in mammalian central neurons during and following periods of anoxia or ischemia and, *second*, to examine the mechanism(s) contributing to the changes in $[Na^+]_i$ observed at these times.

1.3.4. Pathophysiology: Summary

Internal shifts in $[Ca^{2+}]$, pH and $[Na^+]$ occur in neurons in response to anoxia or ischemia. While the potential contribution of changes in $Ca^{2+}{}_i$ has received particular attention, the early changes in pH_i and $Na^+{}_i$ that occur during and/or following periods of anoxia or ischemia also contribute to the pathophysiology of anoxic and ischemic neuronal death. Nevertheless, the mechanisms that contribute to the production of anoxia-induced changes in pH_i and $[Na^+]_i$ in mammalian central neurons remain relatively poorly defined. Given the close inter-relationships and, in fact, linked regulation of the internal concentrations of these ions via the activities of plasma membrane pH_i regulating mechanisms, in the following Section, I will discuss the pH_i regulating mechanisms present in rat hippocampal neurons and examine their potential abilities to influence not only pH_i but also $[Na^+]_i$.

1.4. Maintenance of intracellular pH

Assuming a resting membrane potential of -60 mV and pH_o 7.3, the passive distribution of protons across the neuronal plasma membrane would drive pH_i to ~ 6.3 (Roos & Boron, 1981; Chesler, 2003). Given that the cytosolic compartment is significantly more alkaline than this value, mechanisms must be in place to extrude intracellular protons or other acid equivalents. However, compared to non-neuronal and invertebrate neuronal cell types, relatively few studies have investigated pH_i regulating mechanisms in vertebrate and, in particular, mammalian central neurons, even under normoxic conditions (reviewed by Chesler, 2003). Given the importance of pH_i (as well as $[Na^+]_i$) in regulating neuronal excitability and viability, the characteristics of the mechanisms involved in the regulation of pH_i (as well as $[Na^+]_i$) are of critical importance.

To date, two major classes of pH_i regulating mechanisms have been found to be present in neurons of the mammalian central nervous system: *i)* HCO_3^--independent Na^+/H^+ exchangers;

and *ii)* HCO_3^--dependent exchangers and co-transporters (Fig. 1.3). However, given the variety of mechanisms which have been found to participate in pH_i regulation in invertebrate neurons and vertebrate non-neuronal cells, it is likely that additional pH_i regulating mechanisms will be identified in mammalian central neurons.

1.4.1. Na^+/H^+ exchange

1.4.1.1. General structure and expression patterns in non-neuronal tissues

In many cell types, pH_i is regulated primarily by a family of Na^+/H^+ exchangers, transmembrane proteins that mediate the electroneutral exchange of an intracellular proton for an extracellular sodium ion. The first mammalian Na^+/H^+ exchanger isoform was cloned and sequenced in 1989 (NHE isoform 1, NHE1; Sardet *et al.* 1989) and since that time, seven additional mammalian isoforms have been cloned (NHE2 - 8), each demonstrating varying tissue and/or intracellular distributions (for reviews see Wakabayashi *et al.* 1997; Putney *et al.* 2002; Orlowski & Grinstein, 2004; also see Numata *et al.* 1998; Brett *et al.* 2002b). NHE1 is expressed on the plasma membrane of virtually all cell types and fulfills the role of a "house-keeping" acid extrusion mechanism, whereas other isoforms exhibit a more restricted distribution. NHE2 and NHE3, for example, are predominantly expressed in intestinal and renal epithelial cells, whereas NHE6 and NHE7, which share only ~20% amino acid homology with other isoforms, are expressed in membranes of intracellular organelles (see Brett *et al.* 2002b). Despite their varied tissue distributions, Na^+/H^+ exchangers share a common structure. Hydropathy profiles predict that Na^+/H^+ exchangers exist as integral membrane proteins with 12 transmembrane domains (see Fliegel, 2001). Located on the cytoplasmic face of the exchange mechanism is a 'H^+ sensor' which allosterically controls the activity of the exchange mechanism in response to an intracellular acidosis (see Aronson, 1985). Additional sites located on the large intracellular *C*-

terminus mediate isoform-specific regulation of transport activity by a variety of intracellular regulatory proteins and second-messenger pathways (see Fliegel, 2001). Thus, the activities of distinct Na^+/H^+ exchanger isoforms can be modulated by multiple mechanisms, ranging from direct interactions with regulatory proteins (e.g. calmodulin, Na^+/H^+ exchanger regulatory factors, NHERFs; Hall *et al.* 1998) and lipids (e.g. phosphatidylinositol-4,5-bisphosphate, PIP_2; Aharonovitz *et al.* 2000) to direct phosphorylation by protein kinases (e.g. cAMP-dependent protein kinase (PKA), mitogen-activated protein kinase) as well as phosphorylation-independent mechanisms (e.g. in some cases, the regulation of NHE1 by protein kinase C (PKC); Fliegel, 2001). The effects of these, and other, mechanisms vary between NHE isoforms: for example, while NHE1 activity, in some cells, does not appear to be regulated by the activity of the cAMP/PKA pathway (Borgese *et al.* 1992), the same signalling cascade inhibits NHE3 (and, possibly, NHE5) indirectly by influencing its interaction with NHERF (Hall *et al.* 1998; Attaphitaya *et al.* 2001; also see Szászi *et al.* 2001) and stimulates βNHE (the NHE isoform found in trout red blood cells) by direct phosphorylation (Borgese *et al.* 1992; also see Pedersen *et al.* 2003 for a similar stimulatory effect on the NHE isoform expressed in winter flounder red blood cells). Moreover, the regulation of the activity of a given Na^+/H^+ exchanger isoform by mitogens and hormones may occur through diverse signal transduction pathways. In enteric endocrine and astrocytoma cells, for example, adrenaline (acting via β_2 adrenoceptors) and somatostatin stimulate and inhibit, respectively, Na^+/H^+ exchange activity; despite the fact that these receptors are coupled to adenylate cyclase, the regulation of Na^+/H^+ exchange, in these cases, is independent of cAMP accumulation (Barber *et al.* 1989; also see Isom *et al.* 1987).

In addition to their established role in pH_i regulation, Na^+/H^+ exchangers also act to regulate $[Na^+]_i$. For example, basal permeability of cardiac myocytes to Na^+ is, in part,

determined by Na^+/H^+ exchange activity (e.g. Frelin *et al.* 1984; Despa *et al.* 2002). Na^+/H^+-exchanger-induced increases in $[Na^+]_i$ have also been observed following imposed internal acid loads (e.g. Deitmer & Ellis, 1980, Vaughan-Jones, 1988) and in response to various hormones (e.g. Hou & Delamere, 2002; Cingolani *et al.* 2003) and these increases in $[Na^+]_i$ can have several important consequences, from activating intracellular signalling cascades to regulating the activity of the Na^+/Ca^{2+} exchanger (e.g. Hayasaki-Kajiwara *et al.* 1999; Trudeau *et al.* 1999; Mukhin *et al.* 2004). Na^+/H^+ exchangers also act as plasma membrane anchors for the actin-based cytoskeleton and, thereby, are involved in the control of cellular adhesion and migration (Putney *et al.* 2002). Considering these diverse properties, it is not surprising that Na^+/H^+ exchangers are involved in many physiological functions, including not only the regulation of pH_i and $[Na^+]_i$ but also the control of cellular volume and growth.

1.4.1.2. Expression patterns in nervous tissue

Few studies have examined the expression of NHE isoforms in nervous tissue. Ma and Haddad (1997) and Douglas *et al.* (2001) used *in situ* hybridization and western blot analysis, respectively, to localize the distribution of NHE isoforms within various regions of rat brain. NHE1 was present in all regions of rat brain examined and, in a similar manner, NHE4 was also widely expressed, albeit at lower levels. The expressions of NHE2 and NHE3 were predominantly restricted to the cerebellum, although NHE3 expression was observed in some chemosensitive neurons of the brainstem (also see Wiemann *et al.* 1999). NHE5 is almost exclusively expressed in the brain (Baird *et al.* 1999; Szabó *et al.* 2000) and appears to accumulate in the dendrites and axons of cultured hippocampal neurons transiently transfected with NHE5 (Szászi *et al.* 2002). Finally, the intracellular NHE isoforms, NHE6 and NHE7, have

also been found in brain tissue (Numata *et al.* 1998; Numata & Orlowski, 2001; also see Brett *et al.* 2002b).

In the midst of this growing family of Na^+/H^+ exchange proteins, the specific NHE isoform(s) present in rat hippocampal neurons remains unclear despite the fact that this cell type has been the subject of the most extensive studies of neuronal intracellular pH regulation within the mammalian central nervous system (see Chelser, 2003). In contrast to NHE1-8 and functional Na^+/H^+ exchange activity found in other mammalian central neurons and glial cells (and, indeed, in mouse hippocampal neurons; e.g. Vornov *et al.* 1996; Bevensee *et al.* 1997; Pedersen *et al.* 1998; Yao *et al.* 1999), all of which can, to a greater or lesser extent, be pharmacologically inhibited by amiloride, amiloride analogues and benzoylguanidinium compounds (Tse *et al.* 1993; Yun *et al.* 1995), Na^+/H^+ exchange activity in rat hippocampal neurons is essentially insensitive to these compounds, with concentrations as large as 1 mM having no effect on antiport activity (Raley-Susman *et al.* 1991; Schwiening & Boron, 1994; Baxter & Church, 1996)[3]. Harmaline appears to be the only pharmacological inhibitor of Na^+/H^+ exchange activity in rat hippocampal neurons, although its poor selectivity for Na^+/H^+ exchange and its autofluorescent properties have restricted its use (see Raley-Susman *et al.* 1991; Schwiening & Boron, 1994; Baxter & Church, 1996). Although NHE4 mRNA has been detected in rat hippocampus and NHE4 exchange activity is relatively resistant to known pharmacological inhibitors, antiport activity apparently only contributes to acid extrusion under hyperosmotic conditions (~490 mOsm) and, as such, its contribution to cytosolic pH_i regulation under more physiological conditions remains unclear (Bookstein *et al.* 1996; Chambrey *et al.* 1997a and b).

---

[3] It is notable that, in rat cortical neurons, Ou-Yang *et al.* (1993) observed variable degrees of sensitivity to amiloride inhibition.

NHE5 mRNA has also been found in rat hippocampal neurons but, while this relatively amiloride-resistant isoform shares some functional similarities with Na^+/H^+ exchange activity in rat hippocampal neurons (Attaphitaya *et al.* 1999 and 2001; Szabó *et al.* 2000), distinct differences exist between the regulation of NHE5 activity (expressed in cell lines) and Na^+/H^+ exchange activity in rat hippocampal neurons. For example, NHE5 activity is inhibited by activation of the cAMP/PKA pathway (e.g. Attaphitaya *et al.* 2001) whereas functional Na^+/H^+ exchange activity in rat hippocampal neurons increases upon activation of this signalling pathway (see below), an effect that is shared by the βNHE in trout red blood cells (Borgese *et al.* 1992) and a novel sperm-specific NHE (Wang *et al.* 2003a). It is apparent that further studies are required to elucidate the protein(s) contributing to functional Na^+/H^+ exchange activity in rat hippocampal neurons; however, successful identification of the specific NHE isoform present in rat hippocampal neurons has been limited by the relative lack of specificity of available antibodies (see Hill *et al.* 2002).

1.4.1.3. Na^+/H^+ exchange activity in rat hippocampal neurons

Under normoxic conditions at 37°C, the resting pH_i of rat hippocampal neurons is maintained, at least in part, by Na^+/H^+ exchange activity (reviewed by Chesler 2003; also see Raley-Susman *et al.* 1991; Baxter & Church, 1996; Bevensee *et al.* 1996; Smith *et al.* 1998; and see Putnam 2001; Ou-Yang *et al.* 1993; Sánchez-Armass *et al.* 1994; Yao *et al.* 1999 for illustrations of similar findings in rat brainstem and neocortical neurons, rat brain synaptosomes and mouse hippocampal neurons, respectively). Although, as noted above, the identity of the NHE isoform(s) present in rat hippocampal neurons remains unclear, Na^+/H^+ exchange activity in these cells shares a number of key characteristics with Na^+/H^+ exchange in other cell types. *First,* acid

extrusion via Na^+/H^+ exchange is dependent on the presence of external Na^+, with a K_m value for external Na^+ ions similar to that found for other Na^+/H^+ exchangers (see Raley-Susman *et al.* 1991). Studies have suggested that Na^+/H^+ exchange activity in rat hippocampal neurons, as in other cell types, is electroneutral (Raley-Susman *et al.* 1991), although the reversal of NHE1 activity has been associated with the development of a proton conductance (Demaurex *et al.* 1995; see Section 1.4.3). *Second,* extracellular Li^+, but not *N*-methyl-D-glucamine ($NMDG^+$), is an effective external Na^+ substitute (Kinsella & Aronson, 1981; Raley-Susman *et al.* 1991; Baxter & Church, 1996). *Third,* in common with Na^+/H^+ exchangers in other cell types, Na^+/H^+ exchange activity in rat hippocampal neurons exhibits an exquisite sensitivity to changes in pH_i, presumably reflecting the presence of an allosteric intracellular H^+ modifier site (the 'H^+ sensor'; see Section 1.4.1.1). *Fourth,* Na^+/H^+ exchange activity in rat hippocampal neurons is inhibited by reductions in pH_o and ambient temperature, consistent with observations in other cell types (Vaughan-Jones & Wu, 1990; Baxter & Church, 1996). *Finally,* as in non-neuronal cell types (reviewed by Fliegel, 2001; Hayashi *et al.* 2002), rat hippocampal neuronal Na^+/H^+ exchange activity can be regulated by a number of intracellular signalling cascades, including the cAMP/PKA (Smith *et al.* 1998) and Ca^{2+}/calmodulin pathways (Church *et al.* 2001). It is important to note that the regulation of Na^+/H^+ exchange activity may differ between neurons in different areas of the brain (e.g. cerebellum *vs.* hippocampus) and even between different types of neurons in a given brain region (e.g. medulla). For example, in rat cerebellar granule cells, PKC is primarily involved in the regulation of Na^+/H^+ exchange (*cf* rat hippocampal neurons; Gaillard & Dupont, 1990) and Na^+/H^+ exchange activity in neurons of the ventrolateral medulla is more sensitive to inhibition by falls in pH_o than exchange activity in neurons located in the neighbouring inferior olive (Ritucci *et al.* 1997 and 1998). These data re-emphasize two key considerations about Na^+/H^+ exchange activity in rat hippocampal neurons: *i)* that Na^+/H^+

exchange activity in rat hippocampal neurons can respond to changes in both the external (e.g. changes in pH_o and $[Na^+]_o$) and internal (e.g. changes in pH_i and the activities of intracellular second messenger systems) microenvironments; and *ii)* that the control of Na^+/H^+ exchange activity varies between isoforms and/or the cell type in which the specific isoform is expressed; thus, the control of Na^+/H^+ exchange activity in rat hippocampal neurons cannot be predicted on the basis of findings in other cell types.

1.4.1.4. Na^+/H^+ exchange: relevance to anoxia

The contribution of Na^+/H^+ exchange to the regulation of pH_i and $[Na^+]_i$ during and following periods of ischemia has been extensively studied in cardiac myocytes (see reviews by Karmazyn, 1999; Avkiran, 2001). Key experiments performed by Karmazyn (1988) provided initial evidence that Na^+/H^+ exchange activity in the ischemic/reperfused heart contributes to cellular injury. Whether Na^+/H^+ exchange activity in cardiac myocytes remains functional during ischemia remains somewhat controversial (Hurtado & Pierce, 2001), but it is generally accepted that, in response to a marked intracellular acidosis and the accumulation of regulatory factors, such as catecholamines and lysophosphatidlycholine, Na^+/H^+ exchange activity in cardiac myocytes is markedly activated at the time of reperfusion (Avkiran & Haworth, 1999; Karmazyn *et al.* 1999). Although this acts to restore pH_i, concomitant Na^+ influx leads to reversal of the Na^+/Ca^{2+} exchanger and an elevation of $[Ca^{2+}]_i$ (Fig. 1.4); however, it remains unknown whether the cardioprotective effects of Na^+/H^+ exchange inhibitors are a result of limiting the recovery of pH_i and/or Na^+ entry (mediated by Na^+/H^+ exchange) or subsequent Ca^{2+} entry (mediated by reverse Na^+/Ca^{2+} exchange; Avkiran, 2001). Nevertheless, the relative resistance of NHE1 null mutant mice to cardiac ischemia-reperfusion injury underscores the importance of Na^+/H^+ exchange activity to the pathophysiology of cell death following cardiac ischemia (Wang *et al.* 2003b).

That Na^+/H^+ exchange may play an analogous role in cerebral ischemia was initially suggested in studies by Vornov *et al.* (1996) in cultured rat neocortical neurons, where Na^+/H^+ exchange inhibitors were found to inhibit pH_i recovery following periods of metabolic inhibition and improve neuronal survival. More recently, in cell types in which Na^+/H^+ exchange activity is sensitive to pharmacological inhibitors, Na^+/H^+ exchange inhibitors have been shown to reduce the extent of neuronal damage following periods of cerebral ischemia *in vivo* (Kuribayashi *et al.* 1999; Phillis *et al.* 1999) and following periods of oxygen-glucose deprivation or glutamate application *in vitro* (Horikawa *et al.* 2001a; Matsumoto *et al.* 2003). Thus, it is becoming increasingly apparent that changes in neuronal Na^+/H^+ exchange activity may, at least in part, determine the extent of neuronal cell damage observed following periods of anoxia or ischemia. Studies performed *in vivo* or in slice preparations *in vitro* have suggested that changes in Na^+/H^+ exchange activity contribute to anoxia/ischemia-evoked changes in pH_o and pH_i (Ohno *et al.* 1989; Obrenovitch *et al.* 1990; Pirttilä & Kauppinen, 1992). Few studies, however, have examined the effects of anoxia or ischemia on Na^+/H^+ exchange activity, either during or following the insult, under conditions in which the observed changes in Na^+/H^+ exchange activity can be attributed to an intrinsic neuronal response to the period of anoxia or ischemia. It also remains unclear whether changes in Na^+/H^+ exchange activity contribute to the potentially detrimental alterations in pH_i and $[Na^+]_i$ observed during and/or following anoxia/ischemia. In support, studies employing cultured postnatal rat hippocampal, cultured fetal mouse neocortical and acutely isolated mouse hippocampal neurons have illustrated that changes in Na^+/H^+ exchange activity occur in response to anoxia and contribute to the anoxia-evoked changes in pH_i (Diarra *et al.* 1999, Jørgensen *et al.* 1999; Yao *et al.* 2001).

1.4.2. HCO_3^--dependent pH_i regulating mechanisms

The HCO_3^--transporter family includes 10 related proteins with wide tissue distributions (Romero *et al.* 2004). According to their respective functions, these transporters can be classified into three groups: a family of electroneutral acid-loading anion exchangers (which, in forward-mode, exchange external Cl^- for internal HCO_3^-); electroneutral acid-extruding Na^+-coupled Cl^-/HCO_3^- transporters (which, in forward-mode, exchange internal Cl^- for external HCO_3^-); and electrogenic Na^+/HCO_3^- cotransporters which, depending on their transport stoichiometry and the prevailing membrane potential, can act as acid-loading or acid-extruding mechanisms. These diverse transport mechanisms share between 20 and 70% amino acid identity, exist as integral membrane proteins with 10 – 14 transmembrane domains, and share sensitivities to inhibition by disulfonic stilbene derivatives (Romero *et al.* 2004).

1.4.2.1. Neuronal HCO_3^--dependent pH_i regulation

That pH_i regulation in a given cell type may be dependent on the activities of more than one plasmalemmal transport mechanism was initially described in skeletal muscle (Aickin & Thomas, 1977) and, in the following years, in invertebrate (Moody, 1981; Schlue & Thomas, 1985) and vertebrate (Chelser, 1986) central neurons. It is now generally accepted that HCO_3^--dependent pH_i regulating mechanisms act in concert with Na^+/H^+ exchange in the maintenance of pH_i in many types of mammalian central neurons (reviewed by Chesler, 2003; also see Raley-Susman *et al.* 1991; Ou-Yang *et al.* 1993; Raley-Susman *et al.* 1993; Schwiening & Boron, 1994; Baxter & Church, 1996; Smith *et al.* 1998; Brett *et al.* 2002a). In rat hippocampal neurons, two HCO_3^--dependent pH_i regulating mechanisms have been identified to date: *i)* a Na^+-independent Cl^-/HCO_3^- antiporter which, acting in forward-mode, transports HCO_3^- out of the cell, thereby acting as an acid loader (alkali extruder); and *ii)* a Na^+-dependent Cl^-/HCO_3^-

antiporter, which transports HCO_3^- into the cell in exchange for internal Cl^-, thereby functioning as an acid extruder. The former mechanism can reverse under conditions of extreme intracellular acidosis to participate in acid extrusion (Baxter & Church, 1996). Both Cl^-/HCO_3^- exchange proteins (Na^+-independent and Na^+-dependent) have been found in brain homogenates (Kobayashi *et al.* 1994; Wang *et al.* 2000; Grichtchenko *et al.* 2001) and distinct neuronal populations of the brain (e.g. hippocampus, cerebellum and cortex; Douglas *et al.* 2003; Giffard *et al.* 2003). In addition, both are sensitive to inhibition by 4,4'-diisothiocyanatostilbene-2,2'-disulfonate (DIDS; Schwiening & Boron, 1994; Baxter & Church, 1996). There is less functional evidence for the contribution of Na^+/HCO_3^- cotransport to pH_i regulation in mammalian central neurons (see Pocock & Richards, 1992; Schwiening & Boron, 1994; Baxter & Church, 1996; Bevensee *et al.* 2000; Schmitt *et al.* 2000); however, recent studies have demonstrated electrogenic Na^+/HCO_3^- cotransporter expression in rat brain (possibly located on neuronal processes; see Giffard *et al.* 2000; Schmitt *et al.* 2000) and, in mouse hippocampal neurons, Na^+/HCO_3^- cotransport may be activated in response to anoxia (Yao *et al.* 2003).

Studies examining the regulation of the activities of Cl^-/HCO_3^- exchangers in hippocampal neurons are limited (see Brett *et al.* 2002a). However, in a manner similar to Na^+/H^+ exchange, Cl^-/HCO_3^- exchangers in non-neuronal cell types respond to a variety of extracellular and intracellular factors, such as changes in pH_o and the activities of various intracellular second messenger systems (e.g. Boron *et al.* 1979; Vigne *et al.* 1988; Ludt *et al.* 1991). Importantly, the regulation of the activity of a given Cl^-/HCO_3^- exchanger differs from cell type to cell type and, furthermore, Na^+/H^+ exchange and Cl^-/HCO_3^-exchange activities in a given cell type are often independently regulated. In osteoblasts, for example, a rise in $[Ca^{2+}]_i$ stimulates Na^+-independent Cl^-/HCO_3^- exchange but has no effect on Na^+/H^+ exchange activity whereas a rise in intracellular cAMP inhibits both exchangers (Green & Kleeman, 1992). In

acutely isolated adult rat hippocampal CA1 pyramidal neurons, Na^+/H^+ exchange activity is increased while Na^+-dependent Cl^-/HCO_3^- exchange activity is decreased upon activation of the cAMP/PKA pathway (Smith *et al.* 1998; Brett *et al.* 2002a). To complicate matters further, the control of Cl^-/HCO_3^- exchange activities (Na^+-dependent and Na^+-independent) by the cAMP/PKA pathway in rat hippocampal neurons is dependent on resting pH_i values; for example, in neurons with low resting pH_i values ($pH_i < \sim 7.20$), PKA activation increases Na^+-independent Cl^-/HCO_3^- exchange activity and decreases Na^+-dependent Cl^-/HCO_3^- exchange activity, whereas opposite effects are seen in neurons with high resting pH_i values ($pH_i > \sim 7.20$; Brett *et al.* 2002a).

1.4.2.2. <u>HCO_3^--dependent pH_i regulation: relevance to anoxia</u>

Acting alongside Na^+/H^+ exchange, HCO_3^--dependent transport mechanisms may contribute to the neuronal pH_i and $[Na^+]_i$ (and $[Cl^-]_i$) responses to anoxia or ischemia and may, in turn, be important determinants of the extent of cell damage observed. In cardiac myocytes, electrogenic Na^+/HCO_3^- cotransport may augment the increases pH_i and $[Na^+]_i$ observed in response to anoxia or ischemia (see Lemars, 2001). With the use of a neutralizing antibody, Khandoudi *et al.* (2001) demonstrated that, in isolated rat hearts, inhibition of electrogenic Na^+/HCO_3^- cotransport reduced cellular damage and improved functional recovery following an ischemic insult. On the basis of NMR-based pH_i measurements in hippocampal slices, Pirttilä and Kauppinen (1994) similarly suggested that anoxia caused changes in the activities of HCO_3^--dependent pH_i regulating mechanisms, although this study was unable to differentiate between the possible contributions of neuronal *vs.* glial elements to the results obtained. In isolated rat hippocampal neurons, Na^+-dependent Cl^-/HCO_3^- exchange activity leads to increases in $[Na^+]_i$ and pH_i under normoxic condititions (Rose & Ransom, 1997; Brett *et al.* 2002a) and, if electrogenic Na^+/HCO_3^-

cotransporters are expressed by neurons, membrane depolarizations observed during (and possibly following) anoxia may enhance inward Na^+/HCO_3^- cotransport activity that, in turn, may serve to increase $[Na^+]_i$, pH_i and hyperpolarize the membrane potential. In contrast, however, Na^+/HCO_3^- cotransport (with a 1:3 stoichiometry) in mouse hippocampal neurons is reportedly activated during anoxia and appears to contribute to anoxia-induced falls in pH_i and membrane depolarizations (Yao *et al.* 2003). It is similarly unclear whether Cl^-/HCO_3^- exchangers contribute to the production of the anoxia-, ischemia- and excitotoxin-induced increases in $[Cl^-]_i$ that have been measured in rat hippocampal and neocortical slices (Rothman, 1985; Jiang *et al.* 1992; Inglefield & Swartz-Bloom, 1998a and b). This uncertainty reflects that fact that Cl^-/HCO_3^- exchangers act in concert with a diverse family of channels (e.g. volume-sensitive anion channels), plasmalemmal pumps (e.g. Cl^--ATPases) and other transporters (e.g. $Na^+/K^+/2Cl^-$ cotransport) to maintain neuronal Cl^- homeostasis (see Vaughan-Jones, 1979; Aickin & Brading, 1984; Kaila, 1994; Irie *et al.* 1998).

In support of the contribution of Cl^-/HCO_3^- exchange to the neuronal response to anoxia or ischemia, DIDS reduces the extent of neuronal damage in cultured cortical neurons following periods of oxygen-glucose deprivation (Tauskela *et al.* 2003), protects against excitotoxic damage in chick retinal cells (Zeevalk *et al.* 1989), reduces apoptotic cell death in cultured cerebellar granule cells (Franco-Cea *et al.* 2004), prevents ouabain-induced release of glutamate (Estevez *et al.* 2000) and delays the onset of hypoxic depolarization (Müller, 2000). However, few studies have carefully examined the mechanisms underlying these effects (see Tauskela *et al.* 2003) and, as such, DIDS may be acting to inhibit not only Na^+-dependent and Na^+-independent Cl^-/HCO_3^- exchangers but also a range of HCO_3^--independent processes that may be of importance in modulating anoxic or ischemic cell death (e.g. chloride channels, K^+/Cl^- transport,

glutamate uptake and mitochondrial release of free radicals; see Han *et al.* 2003; Malek *et al.* 2003; Tauskela *et al.* 2003).

Although Na^+-dependent and Na^+-independent Cl^-/HCO_3^- exchange activities are capable of influencing pH_i, $[Na^+]_i$ and $[Cl^-]_i$ in neurons under normoxic conditions, further experiments are required to examine the potential contributions of these transport mechanisms to the changes in pH_i and $[Na^+]_i$ observed in hippocampal neurons in response to anoxia.

1.4.3. Additional pH_i regulating mechanisms

Although Na^+/H^+ exchange and Cl^-/HCO_3^- exchangers (Na^+-dependent and Na^+-independent) have been formally identified as important pH_i regulating mechanisms in rat hippocampal neurons, other mechanisms may also contribute (see Fig. 1.3). In the following paragraphs, I will briefly outline some of these potential mechanisms and discuss their possible relevance to the neuronal response to anoxia.

First, there is a close relationship between pH_i and $[Ca^{2+}]_i$, an appreciation of which has led to the development of techniques for the concurrent measurement of pH_i and $[Ca^{2+}]_i$ using microspectrofluorimetry or ion-selective microelectrodes (ISMs; e.g. Martínez-Zaguilán *et al.* 1991 and 1996; Wiegmann *et al.* 1993; Austin *et al.* 1996). In addition to H^+ and Ca^{2+} ions competing for common intracellular binding sites, Ca^{2+}, both directly and via intracellular second messenger cascades, can regulate the activities of pH_i regulating mechanisms and, thus, pH_i (Vaughan-Jones & Wu, 1990; Sánchez-Armass *et al.* 1994; see also Gordienko *et al.* 1996). It is also perhaps not surprising that one or more mechanisms exist to regulate in concert the internal concentrations of both ions. One such mechanism, initially described in snail neurons, is the Ca^{2+},H^+-ATPase which extrudes intracellular Ca^{2+} ions in exchange for extracellular protons

(Schwiening *et al.* 1993). This mechanism also exists in rat hippocampal CA1 (Trapp *et al.* 1996b) and rat cerebellar granule (Wu *et al.* 1999) neurons and, in the latter, contributes to glutamate receptor-mediated intracellular acidosis (also see Irwin *et al.* 1994; Wang *et al.* 1994). Ischemia or anoxia may affect the activity of this ATPase, given the facts that these insults lead to rises in $[Ca^{2+}]_i$ and an external acidosis, both of which would act to enhance to its activity (see Schwiening *et al.* 1993; Ou-Yang *et al.* 1994a). In contrast, other studies have found that Ca^{2+},H^+-ATPase activity is inhibited during metabolic insults (e.g. Kass & Lipton 1989; Pereira *et al.* 1996; Castilho *et al.* 1998; Wu *et al.* 1999; Zaidi & Michaelis 1999; Chinopoulos *et al.* 2000).

Second, in a variety of cell types, including snail neurons, a voltage-activated H^+ conductance (g_{H^+}) contributes to the recovery of pH_i following intracellular acid loads imposed during membrane depolarization (Meech & Thomas, 1987; Byerly & Suen, 1989; Kapus *et al.* 1993; Gordienko *et al.* 1996). g_{H^+}s demonstrate an extremely high selectivity for protons and, upon activation, are capable of producing dramatic shifts in pH_i without demonstrating rapid current inactivation or desensitization (Meech & Thomas, 1987; Kapus *et al.* 1993; Lukacs *et al.* 1993; DeCoursey & Cherny, 1994a). Although the existence of a g_{H^+} in mammalian central neurons has not been investigated, it is possible that it could contribute to acid efflux during anoxic or ischemic insults which are associated with prolonged membrane depolarizations. In addition, as noted above, evidence indicates that g_{H^+}s can couple to Na^+/H^+ exchange (Demaurex *et al.* 1995).

Third, H^+,K^+- ATPases and H^+-ATPases represent members of a diverse family of P- and V-type ATP-driven cation transporters: the former are primarily found in the stomach, colon and kidney (van Driel & Callaghan, 1995) while the latter have been primarily characterized in

cardiac myocytes, renal epithelia and osteoclasts (Kurtz, 1987; Nelson & Klionsky, 1996). Both types of ATPases contribute to pH_i regulation and, in the case of H^+-ATPases, may act to limit Na^+/H^+ exchange-induced Ca^{2+} overload observed during metabolic inhibition in cardiomyocytes (Karwatowska-Prokopcauk *et al.* 1998). Although Bevensee *et al.* (1996) speculated that H^+-ATPases may contribute to Na^+_o-independent acid extrusion from rat hippocampal neurons, this possibility has not been formally examined (see Yoshinaka *et al.* 2004 for an illustration of V-type ATPases localized to rat brain synaptic vesicles).

Finally, although neurons are primarily metabolically aerobic, during periods of intense neuronal activity or periods of ATP depletion, anaerobic metabolism becomes the key, albeit less efficient, energy-producing pathway and, as a result, lactic acid accumulates intracellularly (Ljunggren *et al.* 1974; Hope *et al.* 1988; Jarolimek *et al.* 1989). Given a pK_a of ~ 3.9, at physiological pH_i values lactic acid will exist primarily in its anionic form, limiting its ability to cross the lipid membrane (but see Dringen *et al.* 1995). Characterized in peripheral cell types and limited populations of mammalian central neurons, a lactate/H^+ cotransport mechanism removes intracellular lactate and, in this way, may contribute to pH_i regulation (Assaf *et al.* 1990; Nedergaard & Goldman, 1993; Juel, 1997). Although studies in non-neuronal cell types support a role for this mechanism in contributing to the recovery of pH_i following transient periods of anoxia (Vandenberg *et al.* 1993), studies in mammalian central neurons to date have failed to document a similar role (see Fujiwara *et al.* 1992; Diarra *et al.* 1999).

1.5. Synthesis and objectives

The contribution of changes in pH_i and $[Na^+]_i$ to the pathophysiology of ischemic cell damage has been best investigated in non-neuronal cell types, notably cardiac myocytes and hepatocytes.

In these cell types, Na^+/H^+ exchange activity is activated at the time of reperfusion and, although this acts to restore pH_i, concomitant Na^+ influx leads to reversal of the Na^+/Ca^{2+} exchanger and an elevation of $[Ca^{2+}]_i$. Nevertheless, it remains unknown whether the cardioprotective actions of Na^+/H^+ exchange inhibitors result from limiting the rate of recovery of pH_i, reducing internal Na^+ loading and/or decreasing the subsequent entry of Ca^{2+}.

Despite the fact that changes in pH_i and $[Na^+]_i$ play important roles in the pathophysiology of anoxic and ischemic neuronal death, much less is known about the changes in pH_i and $[Na^+]_i$ that occur in mammalian central neurons during or following periods of anoxia or ischemia, and few studies have examined the role of transport mechanism(s) in the production of the changes in pH_i and $[Na^+]_i$ observed. Thus, the overall aims of the present study were to characterize the changes in pH_i and $[Na^+]_i$ which occur in response to transient periods of anoxia in isolated rat hippocampal neurons and to assess the role of a variety of mechanisms, especially Na^+/H^+ exchange, in the production of the ionic changes observed. Experiments were performed using isolated rat hippocampal neurons in order to isolate the intrinsic changes in pH_i and $[Na^+]_i$ that occur in response to anoxia (the choice of experimental preparations employed in these studies is discussed further in Section 2.0.1).

The principal objectives of the present study are:

1) To characterize the changes in pH_i and $[Na^+]_i$ which occur in isolated rat hippocampal neurons during *and* following transient anoxic insults and to assess the role of changes in Na^+/H^+ exchange activity to the changes in pH_i and $[Na^+]_i$ observed at these times (Chapters 3, 4 and 5).

2) To examine further the contribution of Na^+/H^+ exchange to anoxia-evoked changes in pH_i and $[Na^+]_i$ in isolated hippocampal neurons by developing a microspectrofluorimetric technique for the concurrent measurement of both ions (Chapter 6).

3) To explore systematically the potential contributions of other mechanisms integral to the cell to the changes in $[Na^+]_i$ observed during *and* following anoxia observed in isolated rat hippocampal neurons (Chapter 7).

These studies were driven by the contention that an understanding of the fundamental cellular mechanisms that contribute to anoxia-evoked changes in pH_i and $[Na^+]_i$ in mammalian central neurons may provide novel insights into the pathogenesis of anoxic/ischemic cell death.

Table 1.1: Clinical trials of selected agents in acute stroke

Proposed principle mechanism of action	*Drug name*	*Trial Status*
Glutamate receptor antagonist	YM872	Phase II: ongoing
	ZK-200775	Phase II: abandoned
	CGS 19755	Phase III: no efficacy
	Aptiganel	Phase III: no efficacy
	Dextrorphan	Phase II: abandoned
	Dextromethorphan	Abandoned
	Magnesium	Phase III: no efficacy
	Remacemide	Phase III: borderline efficacy
	ACEA 1021	Phase I: abandoned
	GV 150526	Phase III: ongoing
	Eliprodil	Phase III: abandoned
Voltage-activated Ca^{2+} channel antagonist	Nimodipine	Phase III: no efficacy
	Flunarizine	Phase III: no efficacy
Voltage-dependent K^+ channel agonist	BMS-204352	Phase III: no efficacy
Na^+ channel antagonist	Fosphenytoin	Phase III: no efficacy
$GABA_A$ receptor agonist	Clomethiazole	Phase III: no efficacy

Table adapted from Lee *et al.* 1999.

Fig. 1.1. Pathways of ischemic cell death. This figure, taken from Lipton (1999), illustrates some of the major events that are hypothesized to contribute to ischemic cell death and also illustrates the extremely complex interactions between these events. *Column* **5** lists five principal morphological forms taken by dying or dead cells after an ischemic insult. Determining how these end stages are reached is the ultimate goal of research on ischemic cell death. *Column* **4** lists six critical functional or structural changes, all of which appear to occur as a result of ischemia. *Column* **3** lists actions that are likely to cause the long-term functional changes described in *column* **4**. These are termed "perpetrators" because they are considered to be key damaging events in ischemic cell death. No direct effects of the perpetrators listed on the critical functional changes, shown in *column* **4**, are implied, because none has been completely established. *Columns* **2** and **1** show changes in some of the many variables initiated by anoxia or ischemia, the most important end result of which is considered to be the activation of perpetrators, but which may also have more direct effects on cell viability. Events located within the same toned horizontal bands are linked by direct causal interactions. Causal interactions are also indicated by including changes in *column* **1** within a box whose outline color is same as that of the variable they are changing (shown in *column* **2**). Abbreviations: Depol, depolarization; pH_i, intracellular pH; Na_i, intracellular Na^+; Ca_i, intracellular Ca^{2+}; P, permeability; FFA, free fatty acids; PAF, platelet-activating factor; e^- Transport, electron transport; Δ carriers, changes in the activities of transport mechanisms.

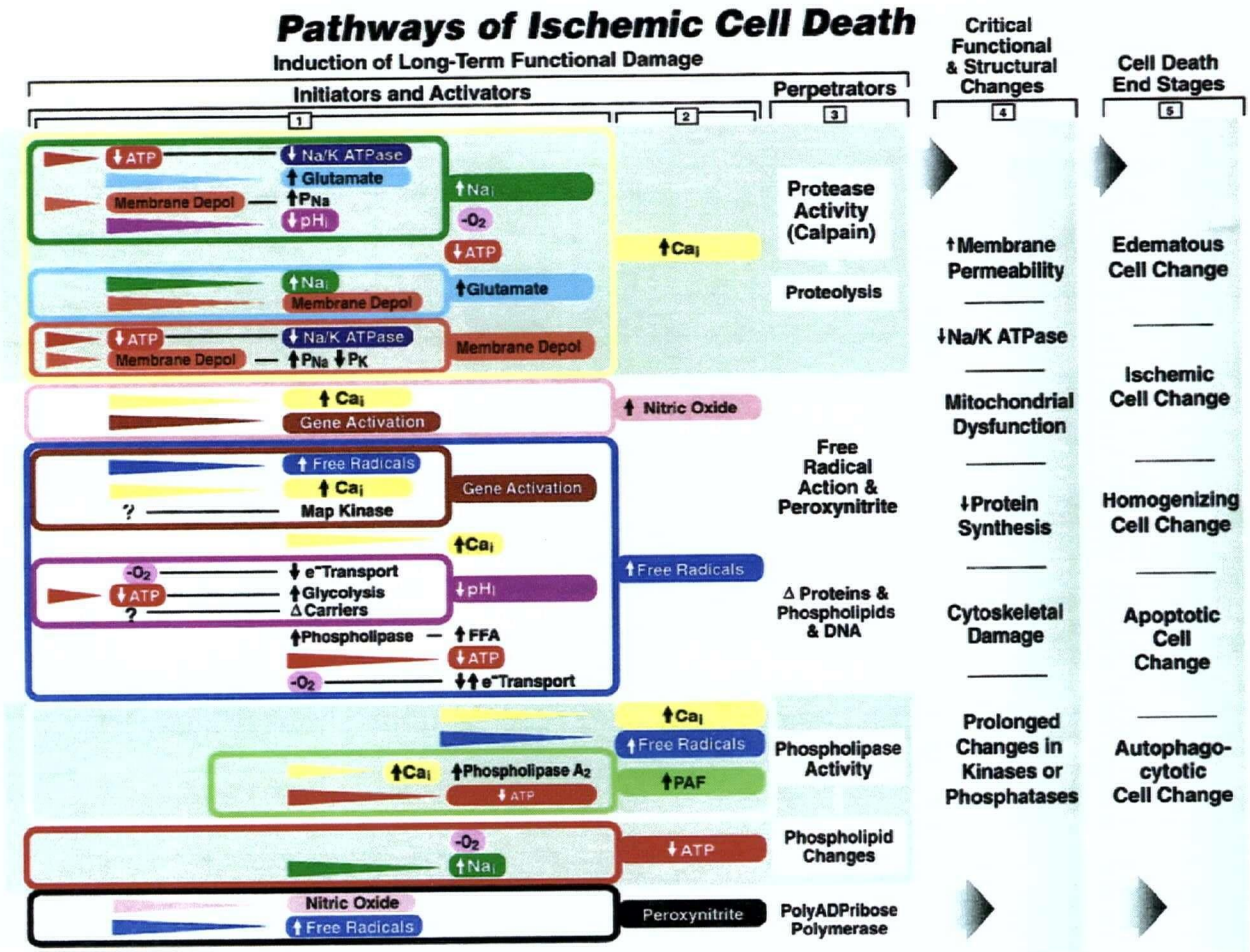
Pathways of Ischemic Cell Death
Induction of Long-Term Functional Damage
Initiators and Activators
Perpetrators
Critical Functional & Structural Changes
Cell Death End Stages
1
2
3
4
5
ATP
Na/K ATPase
Glutamate
Membrane Depol
PNa
pHi
Nai
-O2
ATP
Cai
Protease Activity (Calpain)
Nai
Membrane Depol
Glutamate
Proteolysis
ATP
Na/K ATPase
Membrane Depol
PNa PK
Membrane Depol
Cai
Gene Activation
Nitric Oxide
Free Radicals
Cai
Gene Activation
?
Map Kinase
Free Radical Action & Peroxynitrite
Cai
-O2
e⁻Transport
ATP
Glycolysis
?
Carriers
pHi
Free Radicals
Phospholipase
FFA
ATP
-O2
e⁻Transport
Δ Proteins & Phospholipids & DNA
Cai
Free Radicals
Cai
Phospholipase A2
ATP
PAF
Phospholipase Activity
-O2
Nai
ATP
Phospholipid Changes
Nitric Oxide
Free Radicals
Peroxynitrite
PolyADPribose Polymerase
Membrane Permeability
Na/K ATPase
Mitochondrial Dysfunction
Protein Synthesis
Cytoskeletal Damage
Prolonged Changes in Kinases or Phosphatases
Edematous Cell Change
Ischemic Cell Change
Homogenizing Cell Change
Apoptotic Cell Change
Autophago-cytotic Cell Change

Fig. 1.2. A schematic illustration of the pattern of ionic and electrical changes induced by anoxia or ischemia in mammalian central neurons (adapted from Martin *et al.* 1994). *Phase 1*: changes in membrane potential (V_m) usually begin shortly following the onset of anoxia or ischemia and neurons may respond with a slight membrane depolarization (upper record) or hyperpolarization (lower record), depending largely on the type of neuron from which recordings are made. Decreases in both pH_o and pH_i precede changes in V_m and the external and internal concentrations of other ions. As internal ATP levels decline, Na^+,K^+-ATPase activity becomes compromised: $[Na^+]_i$ and $[K^+]_o$ increase and further promote the gradual membrane depolarization seen after the initial transient depolarization or hyperpolarization. It is notable that the onset and magnitude of the electrical and ionic changes observed in Phase 1 vary between brain regions and even between different neurons within a given brain region (e.g. Leblond & Krnjević, 1989; Cowan & Martin, 1992). *Phase 2:* rapid depolarization (i.e. 'anoxic depolarization') with accompanying large changes in external and internal ion concentrations. *Phase 3:* without reperfusion, membrane repolarization will not occur and the internal and external concentrations of ions will not be restored. The period of time over which this sequence of events occurs depends on the nature and severity of the insult.

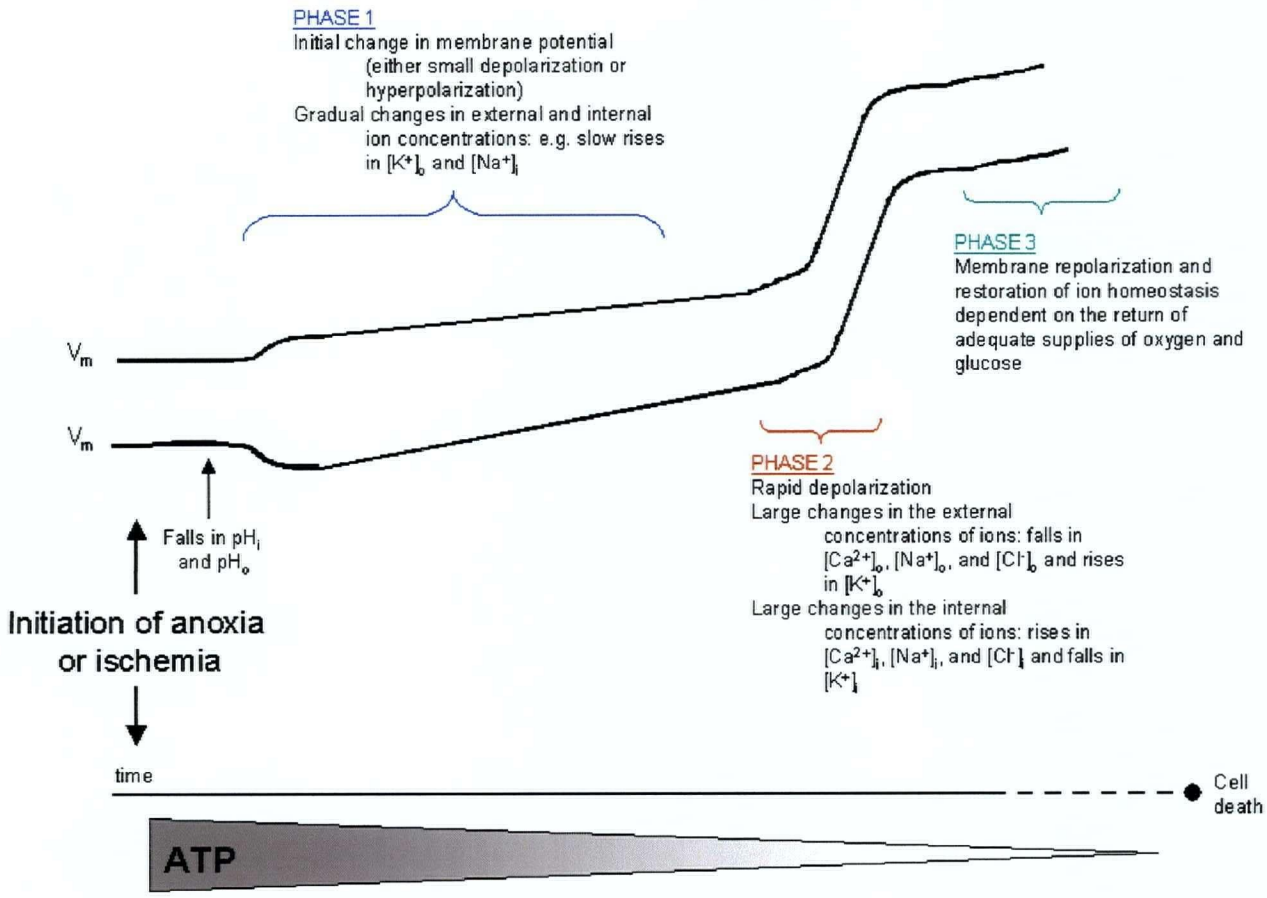
PHASE 1
Initial change in membrane potential (either small depolarization or hyperpolarization)
Gradual changes in external and internal ion concentrations: e.g. slow rises in $[K^+]_o$ and $[Na^+]_i$
PHASE 3
Membrane repolarization and restoration of ion homeostasis dependent on the return of adequate supplies of oxygen and glucose
V_m
V_m
PHASE 2
Rapid depolarization
Large changes in the external concentrations of ions: falls in $[Ca^{2+}]_o$, $[Na^+]_o$, and $[Cl^-]_o$ and rises in $[K^+]_o$
Large changes in the internal concentrations of ions: rises in $[Ca^{2+}]_i$, $[Na^+]_i$, and $[Cl^-]_i$ and falls in $[K^+]_i$
Falls in pH_i and pH_o
Initiation of anoxia or ischemia
time
Cell death
ATP

Fig. 1.3. An illustration of the pH_i regulating mechanisms present in rat hippocampal neurons (adapted from Schwiening, 2002). Two electroneutral mechanisms contribute to acid extrusion. First, a Na^+/H^+ exchanger which, in rat CA1 neurons, is insensitive to pharmacological inhibition with amiloride, amiloride analogues or benzoylguanidinium compounds (e.g. HOE 694). Second, a Na^+-dependent Cl^-/HCO_3^- exchanger which is sensitive to stilbenes such as DIDS. As in snail neurons, a putative g_{H^+} may also contribute to acid extrusion under depolarizing conditions. Two acid-loading mechanisms have also been identified. First, a DIDS-sensitive Na^+-independent Cl^-/HCO_3^- exchanger which is the primary means by which CA1 neurons recover from internal alkaline loads. Second, a plasmalemmal Ca^{2+},H^+-ATPase functions to extrude internal Ca^{2+} ions and, in doing so, generates a fall in pH_i. Although distinct isoforms of mammalian Na^+/H^+ and Na^+-independent Cl^-/HCO_3^- exchangers have been identified and the first mammalian members of the electroneutral Na^+-driven Cl^-/HCO_3^- exchanger family have been cloned, the precise molecular identities of the exchangers present in rat hippocampal CA1 neurons remains unknown.

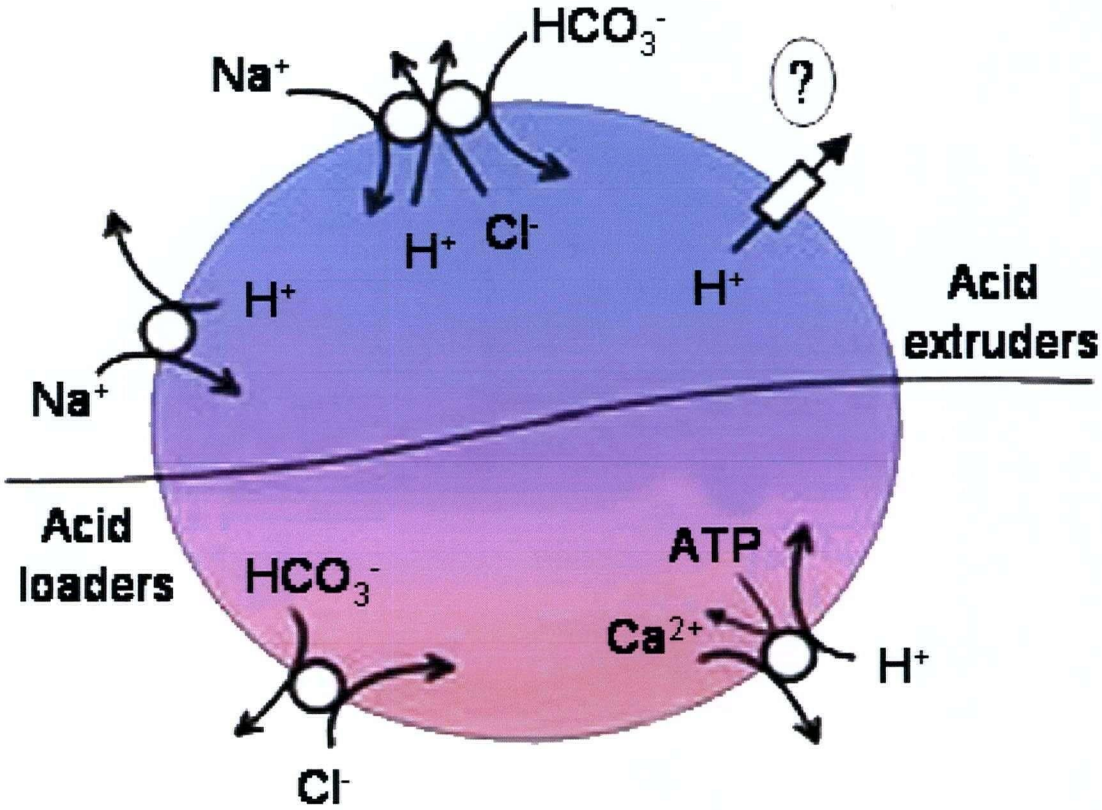
HCO3-
Na+
?
H+
Cl-
H+
H+
Acid
extruders
Na+
Acid
loaders
HCO3-
ATP
Ca2+
H+
Cl-

Fig. 1.4. The contribution of Na^+/H^+ exchange to myocardial injury induced by ischemia (adapted from Sheldon & Church, 2002b). *(1)* Before ischemia, Na^+/H^+ exchange and Na^+/Ca^{2+} exchange are operating to extrude H^+ and Ca^{2+} ions, respectively. Na^+,K^+-ATPase activity is functional and acts to maintain an inwardly directed Na^+ gradient. NHE, Na^+/H^+ exchange, NCX, Na^+/Ca^{2+} exchange operating in forward-mode. *(2)* In response to periods of ischemia/reperfusion, there is an inhibition of Na^+,K^+-ATPase activity and an activation of Na^+/H^+ exchange activity; this combination allows intracellular Na^+ ions to accumulate. As noted in the text, several, although not all, studies have suggested that Na^+/H^+ exchange activity in cardiac myocytes is inactive or minimally active during ischemia. It is acknowledged, however, that Na^+/H^+ exchange is activated immediately upon reperfusion. *(3)* The resulting increase in intracellular Na^+ ions helps to drive Na^+/Ca^{2+} exchange activity into reverse, importing Ca^{2+} ions. rNCX, Na^+/Ca^{2+} exchanger operating in reverse-mode. *(4)* Through a variety of intracellular cascades, the increase in intracellular Ca^{2+} initiates cellular damage and death. These cascades include Ca^{2+}-dependent proteases, phospholipases and the generation of free radicals. The thin arrow extending from Na^+/H^+ exchange to cell death indicates that, although the mechanisms are poorly understood, increased Na^+/H^+ exchange activity can contribute to cellular damage independent of changes in intracellular Ca^{2+}. This may include the damaging effects of increases in intracellular Na^+ and intracellular pH.

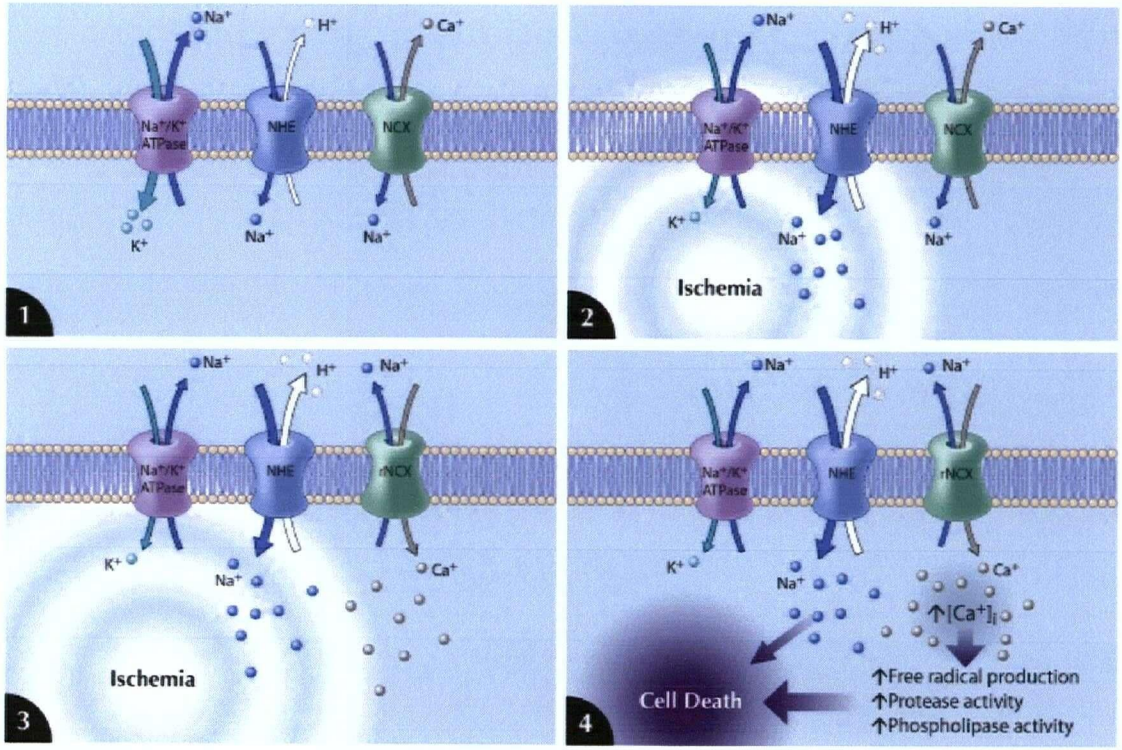
Na+
H+
Ca+
Na+/K+ ATPase
NHE
NCX
K+
Na+
Na+
1
Ischemia
2
rNCX
Ischemia
3
↑[Ca+]i
Cell Death
↑Free radical production
↑Protease activity
↑Phospholipase activity
4

CHAPTER TWO

GENERAL METHODS

2.0. CELL PREPARATION

2.0.1. Choice of experimental preparations

It has long been known that changes in neuronal pH_i occur during and following anoxia or ischemia *in vivo* and in slice preparations *in vitro* (for reviews see Erecińska & Silver, 1994; Siesjö *et al.* 1996; Lipton, 1999); however, it is difficult under these experimental conditions to separate the contribution of various cell types, including glia, to the changes observed from volume-averaged measurements and additional confounds, such as concurrent changes in pH_o, $[K^+]_o$ and neurotransmitter release (each of which can affect steady-state pH_i (and $[Na^+]_i$) and the activities of pH_i regulating mechanisms), complicate the characterization of underlying mechanisms (see Erecińska & Silver, 1994; Pirttilä & Kauppinen, 1994). In this regard, isolated neurons offer a distinct advantage and not only are hippocampal neurons, in particular, vulnerable to the effects of anoxia or ischemia but also they have been the subject of the most extensive studies of pH_i regulation in any type of mammalian central neuron (see Chesler, 2003). Thus, experiments were performed using isolated rat hippocampal neuronal preparations. Because the sensitivity to anoxic/ischemic cell damage (e.g. Rothman, 1983; Di Lorteo & Balestrino, 1997) and the mechanisms that regulate pH_i (e.g. Bevensee *et al.* 1996) are developmentally regulated, where possible, experiments were performed employing acutely isolated adult rat hippocampal CA1 pyramidal neurons in preference to cultured rat hippocampal neurons. Differences exist between the ischemic situation *in vivo* compared to isolated neuronal preparations (e.g. changes in extracellular fluid volume and composition; Lipton, 1999); however, similar to measurements made *in vivo* and in slice preparations *in vitro* (see Section 1.3), isolated neurons exhibit elevations in $[Ca^{2+}]_i$ and $[Na^+]_i$ and membrane depolarizations in

response to periods of anoxia or oxygen and glucose deprivation, and these insults lead to subsequent cell death (e.g. Goldberg & Choi, 1993; Friedman & Hadddad, 1994a; Chen *et al.* 1999; Diarra *et al.* 1999; Mazza *et al.* 2000; Fernandes, 2001; Aarts *et al.* 2003).

2.0.2. Acutely isolated adult rat hippocampal CA1 pyramidal neurons

Where possible, experiments were performed using acutely isolated adult rat hippocampal CA1 pyramidal neurons. Methods used to isolate these neurons were modified from techniques developed by Kay and Wong (1986) and Mody *et al.* (1989). Male Wistar rats (200 - 260 g) were obtained from The Animal Care Center (University of British Columbia) and housed under conditions of controlled temperature (20 - 22°C) and lighting (lights on 0600 - 1800). Food (Lab Diet, PMI Feeds Inc., St. Louis, MO) and water were available *ad libitum.* All procedures conformed to guidelines established by the Canadian Council on Animal Care and were approved by The University of British Columbia Animal Care Committee.

Animals were anesthetized with 3% halothane in air and decapitated. Brains were removed rapidly and placed in ice-cold (4 - 8°C) HCO_3^--containing medium previously equilibrated with 5%CO_2/95%O_2 (Solution 1; Table 2.1). One of the hippocampi was separated from the surrounding tissue, transverse hippocampal slices (450 μm) were obtained with a McIlwain tissue chopper and collected in ice-cold HCO_3^-/CO_2-buffered medium. The slices were transferred to an incubation chamber containing HCO_3^-/CO_2-buffered medium (at 32°C) and were allowed to recover for at least 1 h. Three hippocampal slices were then enzymatically digested at 32°C in 2 ml of HCO_3^-/CO_2-buffered medium containing 1.5 mg ml^{-1} pronase (protease type XIV bacterial from *Streptomyces griseus*; Sigma-Aldrich Canada Ltd., Oakville, ON). After 30 min, the CA1 regions were removed under a dissecting microscope and triturated with fire-polished Pasteur

pipettes of diminishing tip diameters (0.7, 0.5, 0.3 and 0.2 mm) in 0.5 ml of standard loading medium, pH 7.35 at room temperature (Solution 3; Table 2.1). The triturated suspension was deposited onto a cleaned glass coverslip mounted in a temperature-controlled perfusion chamber so as to form the floor of the chamber. Neurons were allowed to adhere to the substrate (i.e. coverslip) for 15 min at room temperature prior to loading with a fluorophore.

Freshly isolated hippocampal CA1 pyramidal neurons were chosen for study based on morphological criteria established by Schwiening and Boron (1994), i.e. a smooth, non-granular appearance; a single major process (presumably an apical dendrite) projecting from one pole of the soma which was at least three times (typically >5 times) the length of the diameter of the cell body; and the presence of two or more smaller processes (basal dendrites) at the opposite pole.

2.0.3. Postnatal rat hippocampal neuronal cultures

Due to the prolonged time required to load the acetoxymethyl ester (AM) form of the Na^+-sensitive dye sodium-binding benzofuran isophthalate (SBFI; see Section 2.3.1), cultured postnatal rat hippocampal neurons were employed in the majority of experiments examining the changes in $[Na^+]_i$ which occur in response to transient periods of anoxia. Primary cultures of hippocampal neurons were prepared from 2 - 4 day old postnatal Wistar rats. Rat pups were anesthetized and decapitated. Brains were removed rapidly and collected in ice-cold Leibovitz L-15 medium (Invitrogen Canada Inc., Burlington, ON) supplemented with 34 mM glucose (L-15/G). Hippocampi were removed, collected in ice-cold L-15/G and then incubated for 15 min at 37°C in L-15/G medium containing 1 mg ml^{-1} papain (from Papaya Latex; Sigma Chemical Co.) and 25 μg ml^{-1} DNAse (type II from Bovine pancreas; Sigma Chemical Co.). Afterwards, the L-15/G medium was discarded and replaced with Dulbecco's Modified Eagle Medium F-12

(Invitrogen Canada Inc.) supplemented with 29 mM $NaHCO_3$ and 10% fetal bovine serum (pH 7.4 at 37°C after equilibration with 5% CO_2; Sigma Chemical Co.). Hippocampi were then mechanically dissociated using fire-polished Pasteur pipettes of decreasing tip diameters. A hemocytometer chamber was used to count the number of cells within a sample of the cell suspension and a dilution factor was calculated in order to plate neurons at a density of 3 - 8 x 10^5 neurons cm^{-2} onto 18 mm glass coverslips. Coverslips were coated with poly-D-lysine (100 μg ml^{-1}; Sigma Chemical Co.) and laminin (16.7 μg ml^{-1}; Sigma Chemical Co.). Neurons were allowed to adhere to substrate for 2 h before coverslips were transferred into 12 well plates. After 24 h, the growth medium was fully changed to Neurobasal Medium A (Invitrogen Canada Inc.) supplemented with B-27 Supplement (Invitrogen Canada Inc.), 0.5 mM glutamine (Invitrogen Canada Inc.), 100 U ml^{-1} penicillin (Sigma Chemical Co.) and 100 μg ml^{-1} streptomycin (Sigma Chemical Co.). The cultures were fed every 4 - 5 days by half-changing the existing medium with fresh Neurobasal Medium A. Glial proliferation was inhibited 48 h after initial plating by adding 10 μM cytosine-β-D-arabinofuranoside hydrochloride (Sigma Chemical Co.). Each coverslip consisted primarily of hippocampal neurons with a maximum of 15% cells being glial. Neuronal cultures were used 6 - 14 days after plating.

2.1. SOLUTIONS AND TEST COMPOUNDS

The compositions of the HCO_3^-/CO_2-buffered media and nominally-HCO_3^-/CO_2-free, Hepes-buffered media commonly used in experiments are detailed in Table 2.1. Normoxic HCO_3^-/CO_2-buffered solutions were equilibrated with 5% CO_2/95% air, giving a final pH value of 7.35 (at 37°C); during perfusion with these media, the atmosphere in the recording chamber contained 5% CO_2/95% air. Hepes-buffered saline was titrated to pH 7.48 (at room temperature; 22°C) in

order to achieve a final pH of 7.35 - 7.36 at 37°C. Experiments were performed at 37°C, unless otherwise noted.

When external Na^+ was reduced to 2 - 4 mM, *N*-methyl-D-glucamine ($NMDG^+$) or Li^+ were employed as substitutes in Hepes-buffered media and solutions were titrated to pH 7.35 with 10 M HCl or 2 M LiOH, respectively (Solutions 4 and 5; Table 2.1). Given the use of sodium dithionite to induce anoxia (see below) and the need to maintain $[Na^+]_o$ constant during an experiment, external Na^+-free media could not be employed. Nevertheless, 2 - 4 mM Na^+_o is considerably less than the apparent K_m of Na^+/H^+ exchange in rat hippocampal neurons for external Na^+ (K_m = 23 - 26 mM; Raley-Susman *et al.* 1991) and rates of acid extrusion from rat hippocampal neurons in the complete absence of external Na^+ are not influenced by the addition of 2 - 4 mM Na^+ (C. Brett, C. Sheldon and J. Church, unpublished observations). In experiments in which Na^+-free, Hepes-buffered media were employed, NaCl and NaH_2PO_4 were omitted and $NMDG^+$ and/or KCl were employed as substitutes; solutions were titrated to pH 7.35 with 10 M HCl or KOH, respectively. For Ca^{2+}-free media, $CaCl_2$ was omitted, $[Mg^{2+}]$ was increased to 3.5 mM and 200 μM ethylene glycol-bis(β-aminoethyl ether) *N*, *N*, *N'*, *N'*-tetraacetic acid (EGTA) was added. Solutions containing 20 - 40 mM NH_4Cl were prepared by equimolar substitution for NaCl. In HCO_3^--free solutions containing Ni^{2+}, Zn^{2+} or Gd^{3+}, $MgSO_4$ was replaced with $MgCl_2$ and NaH_2PO_4 was omitted (see Caldwell *et al.* 1998). Corning 240 and 440 pH meters (Corning Inc., Corning, NY), calibrated daily, were utilized to measure the pH of all solutions.

A list of pharmacological agents used in the studies is presented in Table 2.2. Unless otherwise noted, test compounds were obtained from Sigma-Aldrich Canada Inc. 2',5'-dideoxyadenosine (DDA) was obtained from Biomol Research Laboratories Inc. (Plymouth Meeting, PA). The *R*p- isomer of adenosine-3',5'-cyclic monophosphorothioate (*R*p-cAMPS,

Na^+ salt) was obtained from Biolog Life Science Institute (La Jolla, CA). Arachidonyltrifluoromethyl ketone ($AACOCF_3$) was obtained from Calbiochem (San Diego, CA). (5*S*,10*R*)-(+)-5-methyl-10,11-dihydro-5*H*-dibenzo[a,d]cyclohepten-5,10-imine maleate (MK-801), 6-cyano-7-nitroquinoxaline-2,3-dione (CNQX, disodium salt), 2-[2-[4-(4-nitrobenzyloxy)phenyl]ethyl]isothiourea mesylate (KB-R7943) and 7-chloro-5-(2-chlorophenyl)-1,5-dihydro-4,1-benzothiazepin-2(3*H*)-one (CGP-37157) were obtained from Tocris Cookson Inc. (Ellisville, MO). Bafilomycin A_1, omeprazole and 2-methyl-8-(phenylmethoxy)imidazo[1,2-a]pyridine-3-acetonitrile (SCH-28080) were generous gifts from Dr. V. Palatý, AstraZeneca and Schering Canada Inc., respectively.

2.2. INDUCTION OF ANOXIA

In the great majority of experiments, anoxia was induced by the addition of 1 - 2 mM sodium dithionite ($Na_2S_2O_4$), an O_2 scavenger, to the superfusing medium (see Friedman & Haddad 1993; Nowicky & Duchen, 1998; Diarra *et al.* 1999; Yao *et al.* 2001 and 2003; Paquet-Durand & Bicker, 2004). Dithionite-containing media (50 ml) were prepared fresh prior to every experiment in which neurons were exposed to anoxia and solutions were equilibrated with 100% argon (Ar; in Hepes-buffered media) or 95% Ar/5% CO_2 (HCO_3^-/CO_2-buffered media) for 10 - 15 min immediately prior to use. During anoxia, the atmosphere in the recording chamber was switched from room air to 100% Ar (Hepes-buffered media) or from 95% air/5% CO_2 to 95% Ar/5% CO_2 (HCO_3^-/CO_2-buffered media). The P_{O_2} in media containing 1- 2 mM sodium dithionite was measured with a Radiometer ABL 500 blood gas analyzer calibrated for low P_{O_2} values; in samples obtained anaerobically from the recording chamber, P_{O_2} was <1 mm Hg (n = 6). Similar P_{O_2} values were measured during experiments in which an oxygen electrode (ISO_2;

World Precision Instruments Inc., Sarasota, FL) was placed in the recording chamber. Dithionite anions ($S_2O_4^{2-}$), or the associated SO_2^- monomers, act to reduce soluble O_2 and in doing so produce SO_4^{2-}, SO_3^{2-} and H_2O (see Lambeth & Palmer, 1973; Camacho *et al.* 1995). By-products of these reactions (see Camacho *et al.* 1995) may account for the ability of sodium dithionite to influence pulmonary vasoconstriction (Archer *et al.* 1995) and catecholamine release (Carpenter *et al.* 2000) in a manner independent of its ability to reduce P_{O_2}. Therefore, control experiments were performed to verify that the observed changes in pH_i and $[Na^+]_i$ evoked by exposure to solutions containing sodium dithionite were related to its O_2 scavenging property (see Chapters 3 and 5).

2.3. MICROSPECTROFLUORIMETRY

All ion-sensitive fluorescent probes were obtained from Molecular Probes Inc. (Eugene, OR). In the majority of experiments, pH_i measurements were obtained with the dual-excitation ratiometric fluorophore, 2′,7′-bis-(2-carboxyethyl)-5(6)-carboxyfluorescein (BCECF), or either of the dual emission seminaphthorhodafluor ratiometric indicators, carboxy SNARF-1 or SNARF-5F carboxylic acid. In some experiments, 8-hydroxypyrene-1,3,6-trisulfonic acid (HPTS) was used to measure pH_i. Changes in $[Na^+]_i$ and $[Ca^{2+}]_i$ were measured using the dual-excitation fluorophores SBFI and fura-2, respectively. Details of the techniques used for dye loading, dye calibration and the conversion of ratio values to ion concentrations (i.e. pH_i, $[Na^+]_i$ and $[Ca^{2+}]_i$) for BCECF, HPTS, SBFI and fura-2 are presented in the following Sections 2.3.1 - 2.3.3. Details regarding the use of carboxy SNARF-1 and SNARF-5F for measurements of pH_i are provided in Chapter 6.

2.3.1. Dye loading

Fluorophores, except HPTS (see below), were loaded into neurons in their AM esters form. AM esters are hydrophobic and uncharged, allowing passage across plasma membranes; upon entry into cells, AM esters are hydrolysed by intracellular esterases to produce the hydrophilic, polyanionic free acid forms of the fluorophores which become trapped intracellularly. BCECF-AM and SBFI-AM were prepared as 1 and 5 mM stock solutions, respectively, in DMSO and were stored at -60°C. Fura-2-AM was dissolved in chloroform and divided into 30 μl aliquots (1 μg μl^{-1}) after which the chloroform was removed by vacuum evaporation. Fura-2-AM-containing vials were stored at -60°C and, on the day of use, fura-2-AM was prepared as a 1 mM stock in anhydrous DMSO.

Acutely isolated neurons were loaded with BCECF or fura-2 by incubation with 2 μM BCECF-AM for 15 min at room temperature or 7 μM fura-2-AM for 30 min at 36°C. To load acutely isolated neurons with HPTS, a membrane-impermeant dye, neurons were exposed to 40 mM HPTS during the enzymatic treatment of hippocampal slices with protease and the mechanical trituration of microdissected hippocampal CA1 regions. To load acutely isolated neurons with SBFI, cells were triturated in the presence of 25 μM SBFI-AM and 5 mg ml^{-1} bovine serum albumin; following trituration, neurons were incubated with 25 μM SBFI-AM in the presence of 0.05% Pluronic acid F-127 for 30 - 45 min (see Chapter 5 for details of the SBFI-loading procedure used for postnatal hippocampal neuronal cultures). Following loading, neurons were superfused (2 ml min^{-1}) with the initial experimental solution at 37°C for 15 min prior to the acquisition of data.

2.3.2. Imaging equipment

Microspectrofluorimetric measurements were made employing a fluorescence ratio-imaging system (Atto Instruments Inc., Rockville, MD; Carl Zeiss Canada Ltd., Don Mills, ON) equipped with two intensified charge-coupled device cameras (Atto Instruments Inc.). The dual-excitation ratio method was used to determine pH_i, $[Na^+]_i$ and $[Ca^{2+}]_i$ with BCECF (or HPTS), SBFI and fura-2, respectively; Fig. 2.1 provides a schematic illustration of the equipment used and details of the excitation and emission filters employed with each fluorophore. Following excitation at the appropriate wavelengths, BCECF, HPTS, SBFI or fura-2 fluorescence emissions were measured by one of two intensified charge-coupled device cameras (Camera 1 in Fig. 2.1). The camera gains at each excitation wavelength for a given dye were set to maximize image intensity, minimize the possibility of camera saturation, and were held constant throughout an experiment. Images were digitized at 8 bit resolution. Data were obtained from multiple neuronal cell bodies simultaneously, with each cell body delineated as a region of interest (ROI). As an indication of background fluorescence, data were also obtained from a cell-free zone throughout the course of an experiment. In order to minimize photobleaching of the dye and UV light-induced damage to the neurons, a computer-controlled high-speed shutter restricted the exposure of neurons to light to periods of data acquisition. Where possible, a variable intensity lamp control (Attoarc, Carl Zeiss Canada Ltd.) was employed to reduce the intensity of the mercury arc lamp and neutral density filters were placed in the light path to reduce the intensity of the incident light at each excitation wavelength. Ratio pairs were acquired at 1 - 15 s intervals throughout the course of an experiment.

2.3.3. Calculation of pH_i, $[Na^+]_i$ and $[Ca^{2+}]_i$

2.3.3.1. BCECF

Fluorescence emissions at >520 nm were obtained from ROIs placed on individual neuronal somata and raw intensity data at each excitation wavelength (488 and 452 nm) were corrected for background fluorescence prior to calculation of the background-corrected BCECF emission intensity ratio (BI_{488}/BI_{452}). Analysis was restricted to those neurons able to retain BCECF throughout the course of an experiment (see Bevensee *et al.* 1995). The one-point high-$[K^+]$/nigericin technique was employed to convert BI_{488}/BI_{452} ratio values into pH_i values. At the end of an experiment, neurons loaded with BCECF were exposed to a pH 7.00, high-$[K^+]$ solution containing 10 μM nigericin (Solution 7; Table 2.3; see Baxter & Church, 1996). Nigericin, a carboxylic ionophore, equilibrates cytoplasmic and extracellular $[K^+]$ and, in doing so, equilibrates pH_o to pH_i (see Thomas *et al.* 1979). This method provided, for every cell from which experimentally-derived ratio values were analyzed, a BI_{488}/BI_{452} ratio value corresponding to pH 7.00. It has been suggested that the high-$[K^+]$/nigericin technique may introduce errors when employed to measure absolute pH_i values (Boyarsky *et al.* 1996a and 1996b). It is important to note, however, that the interpretation of BCECF-derived measurements of changes in pH_i and rates of pH_i recovery from imposed internal acid loads (see Section 2.4) are minimally affected by the application of the correction factors determined in the studies of Boyarsky and colleagues (1996a and 1996b). In addition, activity-induced changes in pH_i observed in invertebrate glia were not different when comparing measurements made simultaneously using ISMs and BCECF (the latter being calibrated by the high-$[K^+]$/nigericin technique; Nett & Deitmer, 1996). BI_{488}/BI_{452} ratio values obtained during the calibration period (at pH 7.00) were used as normalization factors for

experimentally-derived BI_{488}/BI_{452} ratio values and the resulting normalized ratio values were converted to pH_i using the equation

$$pH = pK_a + \log [(R_n - R_{n(min)}) / (R_{n(max)} - R_n)] \qquad \textit{(Equation 2.1)}$$

where R_n is the experimentally-derived BI_{488}/BI_{452} ratio value normalized to pH 7.00, $R_{n(min)}$ and $R_{n(max)}$ are the minimum and maximum obtainable values for the normalized ratio (i.e. at low and high pH values, respectively) and pK_a represents the -log of the dissociation constant for BCECF. $R_{n(min)}$, $R_{n(max)}$ and pK_a were derived from non-linear least-squares regression fits to normalized background-subtracted ratio values *vs.* pH data obtained in full calibration experiments (Fig. 2.2*A*). Full *in situ* calibrations of BCECF were performed by exposing neurons to 10 μM nigericin-containing, high-$[K^+]$ media (Solution 7, Table 2.3) titrated to a range of pH values (pH ~5.5 to ~8.5 in 0.5 pH unit increments). BI_{488}/BI_{452} ratio values obtained during the course of a full calibration were normalized to the BI_{488}/BI_{452} ratio value obtained at pH 7.00 and the resulting normalized BI_{488}/BI_{452} ratio values (R_n) were plotted as a function of pH (Fig. 2.2*B*). For the fourteen full calibration experiments utilized in analyzing all BCECF-derived experimental data, the mean values for $R_{n(max)}$, $R_{n(min)}$ and pK_a were (mean ± S.E.M.) 1.98 ± 0.04, 0.52 ± 0.01 and 7.31 ± 0.02, respectively. These values were not dependent on the temperature at which the full calibration was conducted nor the age of the hippocampal neurons used (data not shown). Full calibrations were performed whenever the mercury arc lamp was replaced or the optical set-up of the imaging system was altered.

Nigericin can adhere to perfusion tubing and/or perfusion chambers and, by acting as an acid-loading K^+/H^+ exchanger, can alter pH_i (Richmond & Vaughan-Jones, 1997; Bevensee *et al.*

1999a). Thus, after every one-point calibration or full *in situ* calibration in which nigericin was employed, perfusion lines were replaced and the imaging chamber was decontaminated by soaking first in ethanol, then in 20% Decon 75 (BDH Inc., Toronto, ON) and rinsed vigorously with water (see Richmond & Vaughan-Jones, 1997; Bevensee *et al.* 1999a). Selected experiments, in which BCECF was used as the pH_i indicator, were also repeated using an experimental chamber that had never been exposed to nigericin; although the data from these experiments were not calibrated (and, therefore, are not presented in Chapters 3 or 4), the BCECF-derived BI_{488}/BI_{452} ratio values obtained were not different from those recorded during the course of equivalent experiments conducted in nigericin-decontaminated chambers, suggesting that nigericin contamination does not contribute to the results obtained in the present studies.

2.3.3.2. HPTS

Fluorescence emissions were measured at >520 nm and raw intensity data at each excitation wavelength (452 and 380 nm) were corrected for background fluorescence prior to calculation of the background-corrected HPTS emission intensity ratio (BI_{452}/BI_{380}). The one-point high-$[K^+]$/nigericin technique was employed to convert BI_{452}/BI_{380} ratio values into pH_i values using the equation

$$pH = [pK_a + \log(1/\beta)] + \log[(R_n - R_{n(min)})/(R_{n(max)} - R_n)] \qquad \textit{(Equation 2.2)}$$

where R_n is the BI_{452}/BI_{380} ratio normalized to unity at pH 7.00 and $1/\beta = f_{n2a}/f_{n2b}$, where f_{n2a} and f_{n2b} are the normalized background-subtracted fluorescence intensities at the acidic and basic

extremes while exciting the dye at 380 nm ($\lambda_{ex(2)}$ in Fig. 2.1). The parameters of Equation 2.2 were derived from full calibration experiments, as described for BCECF.

2.3.3.3. SBFI

SBFI-derived fluorescence emissions were obtained from ROIs placed on individual neuronal somata and raw intensity data at each excitation wavelength (334 and 380 nm) were corrected for background fluorescence prior to calculation of the background-corrected SBFI emission intensity ratio (BI_{334}/BI_{380}; see Fig. 2.1). A one-point calibration technique was developed to convert BI_{334}/BI_{380} ratio values into $[Na^+]_i$ values (see Diarra *et al.* 2001 for full details). In brief, at the end of an experiment in which changes in $[Na^+]_i$ were measured, SBFI-loaded neurons were exposed to a pH 7.35 medium containing 10 mM Na^+ and 4 μM gramicidin D, a channel-forming ionophore which acts to rapidly equilibrate external and internal monovalent cations (Solution 11, Table 2.3). BI_{334}/BI_{380} ratio values obtained during the calibration period ($[Na^+]_i$ = 10 mM) were used as normalization factors for experimentally-derived BI_{334}/BI_{380} ratio values and the resulting normalized ratio values were converted to $[Na^+]_i$ using the equation

$$[Na^+] = \beta K_d[(R_n - R_{n(min)})/(R_{n(max)} - R_n)] \qquad \textit{(Equation 2.3)}$$

where R_n is the experimentally-derived BI_{334}/BI_{380} ratio value normalized to $[Na^+]$ = 10 mM, $R_{n(min)}$ and $R_{n(max)}$ are the minimum and maximum obtainable values for the normalized ratio (i.e. at low and high $[Na^+]_i$ values, respectively) and βK_d is the product of K_d, the dissociation constant of SBFI for Na^+, and β (see below). Parameters required for the conversion of experimentally-derived BI_{334}/BI_{380} ratio values to $[Na^+]_i$ (i.e. β, K_d, $R_{n(min)}$, and $R_{n(max)}$) were

determined from full *in situ* calibrations in which neurons were exposed to pH 7.35 media containing eight different $[Na^+]$ values (range, 0 - 130 mM; Solutions 8 - 15, Table 2.3) in the presence of 4 μM gramicidin D (Fig. 2.3*A*). BI_{334}/BI_{380} ratio values measured at each $[Na^+]$ were normalized to BI_{334}/BI_{380} ratio values obtained at $[Na^+]$ = 10 mM; the resulting normalized BI_{334}/BI_{380} ratio values were plotted as a function of $[Na^+]$ and fit to the equation

$$R_n = R_{n(min)} + [A([Na^+])/(B + [Na^+])] \qquad \textit{(Equation 2.4)}$$

where A is a constant from which $R_{n(max)}$ can be calculated ($R_{n(max)} = A + R_{n(min)}$) and B represents the product of βK_d (Fig. 2.3*B*). Measured following excitation at 380 nm ($\lambda_{ex(2)}$ in Fig. 2.1), β represents the ratio of the normalized fluorescence intensity of SBFI in its 'free' and 'bound' forms (i.e. normalized background-subtracted emission intensities in absence of Na^+ and in the presence of saturating concentrations of Na^+; $BI_{n(380f)}$ and $BI_{n(380b)}$, respectively). To determine β (and, thus, K_d), BI_{380} values from full calibrations were normalized to BI_{380} values measured at $[Na^+]$ = 10 mM and the resulting $BI_{n(380)}$ values were plotted as a function of $[Na^+]$. $BI_{n(380f)}$ and $BI_{n(380b)}$ represent $BI_{n(380)}$ values at the maximum and minimum extremes of the graphed function, respectively (Fig. 2.3*C*). Illustrated in Fig. 2.3*C*, and data points were fit to the equation

$$BI_{n(380)} = C + [E\,(D)/(D + [Na^+])] \qquad \textit{(Equation 2.5)}$$

where C,D, and E are constants from which β can be derived; $BI_{n(380)} = C + E$ at $[Na^+]$ = 0 mM, $BI_{n(380)} = C$ at saturating concentrations of $[Na^+]$ and D is $[Na^+]_i$ at $(C + E)/2$ (this parameter is not required to calculate β).

For the eighteen full calibration experiments utilized in analyzing all SBFI-derived data, mean values of $R_{n(min)}$, $R_{n(max)}$, and βK_d were 0.79 ± 0.06, 2.37 ± 0.16 and 55.81 ± 4.32 mM, respectively. Representative mean values for β and K_d were 2.64 ± 0.45 and 21.32 ± 2.32 mM, respectively (n = 6). These values were not dependent on the temperature at which calibrations were conducted nor the age of the hippocampal neurons used (data not shown). Full calibrations were performed whenever the mercury arc lamp was replaced or the optical set-up of the imaging system was altered.

To prevent contamination of the perfusion chamber with gramicidin D, perfusion lines were replaced and the perfusion chamber was decontaminated after each experiment (see Section 2.3.3.1).

2.3.3.4. Fura-2

Calibration of the fura-2 signal was not attempted and the effects of experimental maneuvers on $[Ca^{2+}]_i$ are presented as changes in fura-2-derived BI_{334}/BI_{380} ratio values. Nevertheless, under conditions identical to those employed in the present experiments, this laboratory has found that a BI_{334}/BI_{380} ratio value of ~ 0.5 (as was observed in quiescent neurons in the present study) represents an $[Ca^{2+}]_i$ ~ 80 nM (see Church *et al.* 1998).

2.4. EXPERIMENTAL PROCEDURES AND DATA ANALYSIS

The effects of anoxia and other experimental maneuvers were examined on steady-state pH_i and rates of pH_i recovery from internal acid loads imposed by the NH_4^+-prepulse technique (as established by Boron & DeWeer, 1976). In experiments in which rates of pH_i recovery were examined, 2 - 3 consecutive intracellular acid loads were imposed, the first one (or two) being

employed to calculate control rates of pH_i recovery for a given neuron and the second (or third) being performed under a test condition. Rates of pH_i recovery from imposed acid loads were determined by fitting the recovery portions of the pH record to a single exponential function of the form

$$pH_i = a + b(1 - e^{-ct}) \qquad \textit{(Equation 2.6)}$$

where *a* represents the pH_i at the point of maximum acidification, *b* is the pH_i range of recovery and *c* is the time constant. The first derivative of this function was then used to determine rates of pH_i change as a function of time (see Wu & Vaughan-Jones, 1994; Baxter & Church, 1996; Smith *et al.* 1998)

$$dpH_i/dt = bc(e^{-ct}) \qquad \textit{(Equation 2.7)}$$

Instantaneous rates of pH_i recovery (dpH_i/dt) under control and test conditions were calculated at 0.05 unit intervals of pH_i from the point of maximum acidification: formal statistical comparisons were performed at the same absolute pH_i values. There were no significant differences between the rates in pH_i recovery observed when two (or more) consecutive internal acid loads were imposed under control conditions (Fig. 2.4).

Data are reported as mean ± S.E.M. In experiments employing acutely isolated neurons, the accompanying *n* value refers to the number of neurons from which data were obtained. In experiments in which neuronal cultures were used, the accompanying *n* value refers to the

number of neuron populations (i.e. coverslips) from which data were obtained (measurements made from 2 - 5 different batches of neuronal cultures).

Table 2.1: Composition of commonly used experimental solutions

	Standard HCO_3^-/CO_2-buffered (1)	Standard Hepes-buffered (2)	Standard loading (3)	Low Na^+ ($NMDG^+$) (4)	Low Na^+ (Li^+) (5)
NaCl	127.0	136.5	133.5	2.0 - 4.0	2.0 - 4.0
$NaHCO_3$	19.5	-	3.0	-	-
KCl	3.0	3.0	3.0	3.0	3.0
$CaCl_2$	2.0*	2.0	2.0	2.0	2.0
NaH_2PO_4	1.5	1.5	1.5	-	-
$MgSO_4$	1.5	1.5	1.5	1.5	1.5
D-glucose	17.5	17.5	17.5	17.5	17.5
$NMDG^+$	-	-	-	134 - 136	-
LiCl	-	-	-	-	134 - 136
Hepes	-	10.0	10.0	10.0	10.0
Titrated with:	-	10 M NaOH	10 M NaOH	10 M HCl	2 M LiOH

All concentrations are presented in mM. The standard HCO_3^--containing solution (Solution 1) was equilibrated with 5% CO_2 in balance air (normoxia) or balance argon (anoxia). Solutions for use with postnatal hippocampal neuronal cultures contained 10, not 17.5 mM, D-glucose. *HCO_3^-/CO_2-buffered medium used during the preparation of hippocampal slices and acutely isolated rat hippocampal CA1 pyramidal neurons contained 1 mM $CaCl_2$. Abbreviations: $NMDG^+$, *N*-methyl-D-glucamine$^+$

Table 2.2: List of pharmacological agents

Compound - proposed mechanism of action	Solvent	[Stock] mM	Storage	[Test] μM
$AACOCF_3$ - inhibitor of cytosolic PLA_2	DMSO	10	-60°C	15 - 30
Bafilomycin A_1 - inhibitor of H^+-ATPase	DMSO	2	-20°C	1 - 2
Bepridil - inhibitor of Na^+/Ca^{2+} exchange	Hepes-buffered media	-	-	50
Bumetanide - inhibitor of $Na^+/K^+/2Cl^-$ cotransport	DMSO	50	-	50 - 100
CGP-37157 - inhibitor of plasmalemmal and mitochondrial Na^+/Ca^{2+} exchange	DMSO	25	-3°C	25
CNQX - inhibitor of non-NMDA ionotropic glumate receptor-operated channels	Ultra-pure H_2O	20	-20°C	20
DDA - inhibitor of adenylate cyclase	DMSO	100	-60 °C	100
DIDS - inhibitor of HCO_3^--dependent pH_i regulating mechanisms	DMSO	100	-	200
Digitonin - selective permeabilization of the plasma membrane	Ultra-pure H_2O	20	-	20
Gramicidin D - pore-forming ionophore; equilibrates $[Na^+]_o$ and $[Na^+]_i$	50:50 ethanol/methanol (v/v)	50	-60 °C	4
KB-R7943 - inhibitor of reverse-mode Na^+/Ca^{2+} exchange	Ultra-pure H_2O	5	-60°C	1- 10
Lidocaine - inhibitor of voltage-gated Na^+ channels	Ultra-pure H_2O	500	-3°C	250 – 500
L-NAME - inhibitor of nitric oxide synthase	Hepes-buffered media	-	-	500
MK-801 - inhibitor of NMDA ionotropic glumate receptor-operated channels	Ultra-pure H_2O	20	-20°C	2
Nifedipine - inhibitor of L-type voltage-gated Ca^{2+} channels	DMSO	10	-	10
Nigericin - carboxylic carrier ionophore; equilibrates $[K^+]_i$ and $[K^+]_o$	Ethanol	10	-60°C	10
Noradrenaline - full β-adrenoceptor agonist	Ultra-pure H_2O	10	-60°C	10
Omeprazole - inhibitor of H^+,K^+ ATPase	DMSO	25	-60°C	50
Ouabain - inhibitor of Na^+,K^+ ATPase	Hepes-buffered media	-	-	500
Propranolol - full β-adrenoceptor antagonist	Ultra-pure H_2O	50	-60°C	20
*R*p-cAMPS - inhibitor of PKA	Ultra-pure H_2O	50	-20°C	50

SCH-28080 - inhibitor of H^+,K^+ ATPase	DMSO	250	-60°C	500
Tetrodotoxin - inhibitor of voltage-gated Na^+ channels	Ultra-pure H_2O	0.1	-3°C	1
Trolox - antioxidant	Ultra-pure H_2O	500	-	1000
Verapamil - non-selective inhibitor of voltage-gated Ca^{2+} channels	Hepes-buffered media	-	-	300

In the absence of an indicated stock concentration, test solutions were prepared directly in Hepes-buffered saline. In situations in which stock solutions were prepared fresh daily, no storage temperature is indicated. Ultra-pure H_2O was obtained with a Milli-Q UF Plus Reagent Grade Water Purification System (Millipore, Mississauga, ON). Abbreviations: $AACOCF_3$, arachidonyltrifluoromethyl ketone; CGP-37157, 7-chloro-5-(2-chlorophenyl)-1,5-dihydro-4,1-benzothiazepin-2(3*H*)-one; CNQX, 6-cyano-7-nitroquinoxaline-2,3-dione (disodium salt); DDA, 2',5'-dideoxyadenosine; DIDS, 4,4'-diisothiocyanatostilbene-2,2'-disulfonic acid; DMSO, dimethylsulphoxide; KB-R7943, 2-[2-[4-(4-nitrobenzyloxy)phenyl]ethyl]isothiourea mesylate; L-NAME, N^G-nitro-L-arginine methyl ester; MK-801, (5*S*,10*R*)-(+)-5-methyl-10,11-dihydro-5*H*-dibenzo[a,d]cyclohepten-5,10-imine maleate; *R*p-cAMPS, *R*p- isomer of adenosine-3',5'-cyclic monophosphorothioate; SCH-28080, 2-methyl-8-(phenylmethoxy)imidazo[1,2-a]pyridine-3-acetonitrile; Trolox, 6-hydroxy-2,5,7,8-tetramethylchroman-2-carboxylate.

Table 2.3: Composition of solutions used for *in situ* calibrations of pH and Na^+-sensitive fluorophores

	High $[K^+]$ (7)	0 Na^+ (8)	3 Na^+ (9)	6 Na^+ (10)	10 Na^+ (11)	20 Na^+ (12)	40 Na^+ (13)	80 Na^+ (14)	130 Na^+ (15)
NaCl	-	-	-	-	-	-	-	10.0	30.0
KCl	-	30.0	30.0	30.0	30.0	30.0	30.0	20.0	-
$CaCl_2$	1.0	0.5	0.5	0.5	0.5	0.5	0.5	0.5	0.5
NaH_2PO_4	1.5	-	-	-	-	-	-	-	-
$MgSO_4$	1.5	0.6	0.6	0.6	0.6	0.6	0.6	0.6	0.6
Na Glu	10.0	-	3.0	6.0	10.0	20.0	40.0	70.0	100.0
K Glu	130.5	100.0	97.0	94.0	90.0	80.0	60.0	30.0	-
D-glucose	17.5	10.0	10.0	10.0	10.0	10.0	10.0	10.0	10.0
Hepes	10.0	10.0	10.0	10.0	10.0	10.0	10.0	10.0	10.0

All concentrations are presented in mM. High-$[K^+]$ solutions (Solution 7) were titrated to a range of pH values (pH ~ 5.5 to ~8.5 in 0.5 pH unit increments) with 10 M KOH and contained 10 μM nigericin. High-$[K^+]$ solutions for use with postnatal hippocampal neuronal cultures contained 10 mM D-glucose. Solutions with different Na^+ concentrations (Solutions 8 – 15) were titrated to pH 7.35 (temperature-corrected) with 10 M KOH and contained 4 μM gramicidin D. Abbreviations: Na Glu, sodium gluconate; K Glu, potassium gluconate.

Fig. 2.1. A schematic representation of the optical equipment used in neurons single-loaded with a dual-excitation fluorophore (i.e. BCECF, HPTS, SBFI or fura-2). Neurons were excited with light provided by a 100 W Hg lamp (solid and dotted lines) and band-pass filtered through alternating interference excitation wavelength filters ($\lambda_{ex(1)}$ and $\lambda_{ex(2)}$). Filtered excitation light then reflected off a dichroic mirror (Dichroic 1), passed through the objective (Zeiss LD Achroplan, n.a. 0.60, 40x) and illuminated the fluorophore loaded into neurons. At each excitation wavelength, fluorescence emissions (thick dotted line) passed through Dichroic 1 and a subsequent emission filter (λ_{em}) before being detected by Camera 1. The table presented below the diagram details the filters employed to measure fluorescence from neurons loaded with BCECF, HPTS, SBFI or fura-2 (i.e. $\lambda_{ex(1)}$, $\lambda_{ex(2)}$, Dichroic 1 and λ_{em}). Ratio values (measured as the ratio of the background-subtracted emission intensity detected following excitation at the first excitation wavelength ($BI_{ex(1)}$) to the background-subtracted emission intensity detected following excitation at the second excitation wavelength ($BI_{ex(2)}$)) were measured for each of the indicated fluorophores. * different filters were employed when SBFI was employed simultaneously with carboxy SNARF-1 or SNARF-5F (see Chapter 6). LP indicates that the filter is a long-pass filter. Compare with Fig. 6.1, a schematic diagram of the same optical equipment with slight modifications to allow the concurrent measurement of pH_i and $[Na^+]_i$ in the same cell.

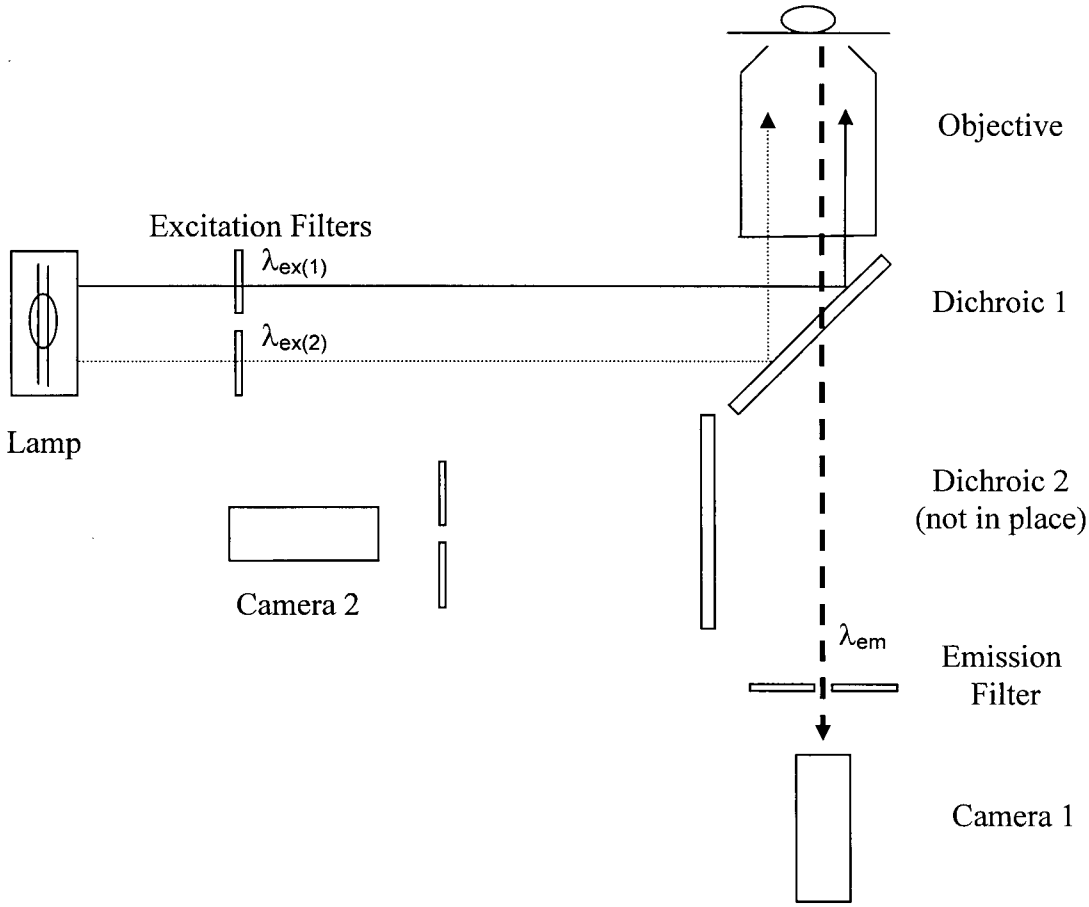

	Excitation Filters		Dichroic 1	Emission filter	Measured ratio
	$\lambda_{ex(1)}$	$\lambda_{ex(2)}$		λ_{em}	$BI_{ex(1)}/BI_{ex(2)}$
BCECF	488 ± 5	452 ± 5	510	520LP	BI_{488}/BI_{452}
HPTS	452 ± 5	380 ± 5	510	520LP	BI_{452}/BI_{380}
SBFI*	334 ± 5	380 ± 5	395	420LP	BI_{334}/BI_{380}
fura-2	334 ± 5	380 ± 5	395	420LP	BI_{334}/BI_{380}

Fig. 2.2. Sample *in situ* calibration plot for BCECF. *A*, cells were exposed to nominally HCO_3^- /CO_2-free, Hepes-buffered, high-[K^+] solutions containing 10 μM nigericin at 37°C and the pH_o (and therefore pH_i) values indicated above the record, which is the mean of data obtained from 17 cultured postnatal rat hippocampal neurons recorded on a single coverslip. *B*, plot of pH_i against the resulting background-subtracted normalized ratio value (R_n). R_n was calculated as the quotient of the average background-corrected ratios for all neurons on a given coverslip at each pH value and the average background subtracted ratio value determined in the same neurons at pH 7.0. The curve is a result of a non-linear least squares regression fit to Equation 2.1. For this particular calibration, the values of $R_{n(min)}$, $R_{n(max)}$, and pK_a were 0.44, 2.01, and 7.25, respectively. Error bars are S.E.M. ($n = 3$); where absent, error bars lie within the symbol area.

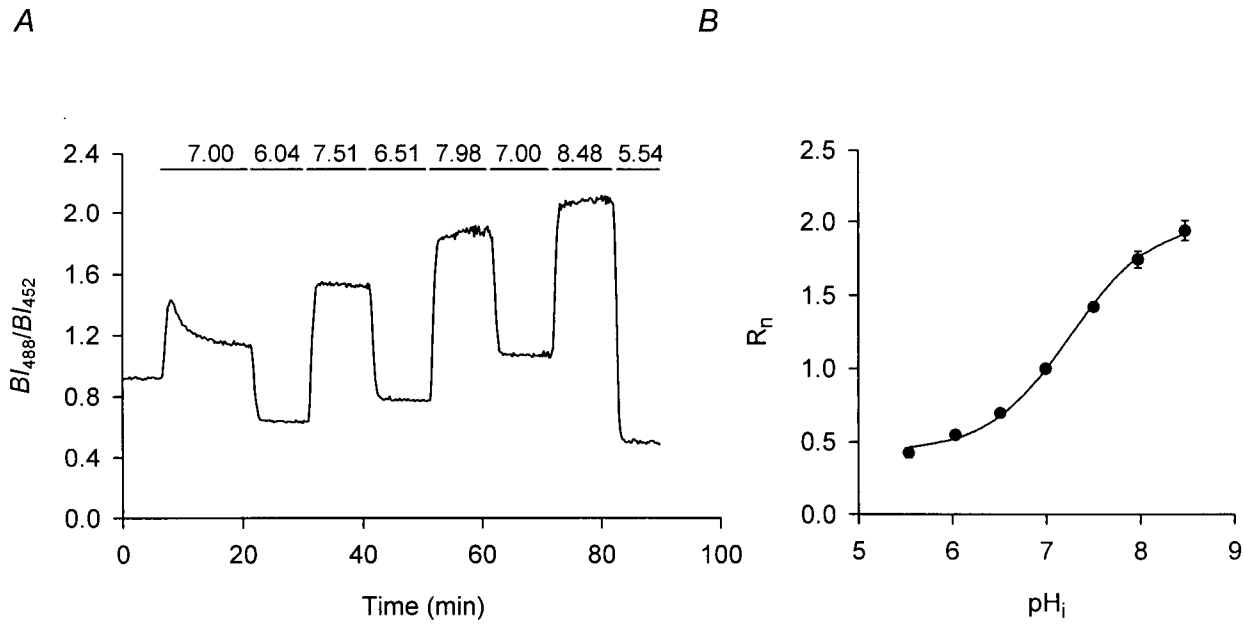
A
B
7.00
6.04
7.51
6.51
7.98
7.00
8.48
5.54
2.4
2.0
1.6
1.2
0.8
0.4
0.0
BI_{488}/BI_{452}
0
20
40
60
80
100
Time (min)
2.5
2.0
1.5
1.0
0.5
0.0
R_n
5
6
7
8
9
pH_i

Fig. 2.3. *In situ* calibration of SBFI at 37°C, pH_o 7.35. *A*, a full calibration experiment in which 7 SBFI-loaded cultured hippocampal neurons were exposed to 4 μM gramicidin D-containing solutions at the $[Na^+]$ values (in mM) indicated above the records. Shown are the mean changes in normalized BI_{334}/BI_{380} ratio values (R_n), which increased as $[Na^+]$ increased. *B*, plots of $[Na^+]$ *vs.* R_n obtained from experiments of the type shown in *A* (n = 4). The solid line represents the result of a three-parameter hyperbolic fit of the data points to Equation 2.4 and was used to determine the values of the SBFI calibration parameters (i.e. βK_d, $R_{n(min)}$ and $R_{n(max)}$). For this calibration, the values of $R_{n(min)}$, $R_{n(max)}$ and βK_d were 0.77, 2.52 and 66.02, respectively. *C*, plots of $[Na^+]$ *vs.* $BI_{n(380)}$ obtained from experiments of the type shown in *A* and from the same experiments used to determine the plot shown in *B*. The curve is the result of a three-parameter hyperbolic decay fit to Equation 2.5 and was used to determine the values of $BI_{n(380f)}$ and $BI_{n(380b)}$, $BI_{n(380)}$ values in the absence of Na^+_o and in the presence of saturating concentrations of $[Na^+]_o$, respectively. For this calibration, $BI_{n(380f)}$ and $BI_{n(380b)}$ were 1.26 and 0.37, respectively. Thus, the calculated β and K_d values were 3.41 and 19.36 mM, respectively. In *B* and *C*, error bars are S.E.M; where absent, error bars lie within the symbol area.

A

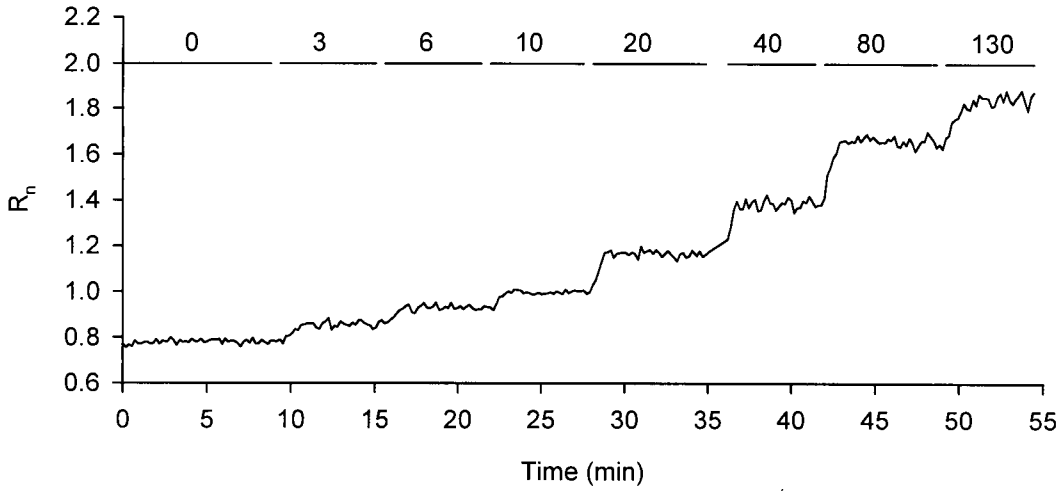
0
3
6
10
20
40
80
130
R_n
2.2
2.0
1.8
1.6
1.4
1.2
1.0
0.8
0.6
0
5
10
15
20
25
30
35
40
45
50
55
Time (min)

B

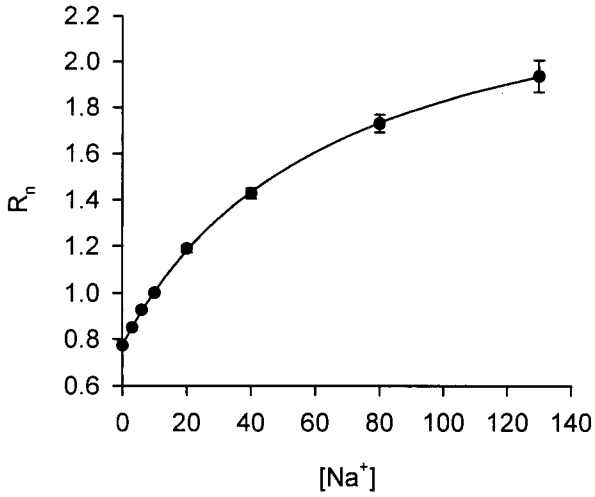
R_n
2.2
2.0
1.8
1.6
1.4
1.2
1.0
0.8
0.6
0
20
40
60
80
100
120
140
[Na+]

C

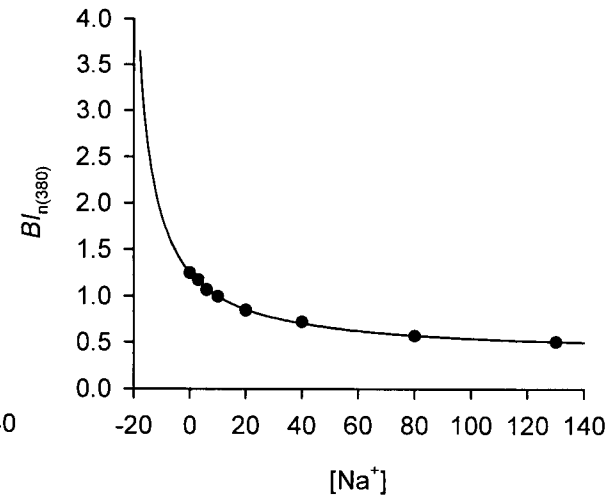
$BI_{n(380)}$
4.0
3.5
3.0
2.5
2.0
1.5
1.0
0.5
0.0
-20
0
20
40
60
80
100
120
140
[Na+]

Fig. 2.4. Consistency of rates of pH_i recovery from internal acid loads imposed under control conditions. *A*, a representative record of the changes in pH_i observed in an acutely isolated adult rat hippocampal CA1 pyramidal neuron in response to two consecutive internal acid loads, imposed under control conditions using the NH_4^+ pre-pulse technique. This trace was obtained under nominally-HCO_3^-free, Hepes-buffered conditions, pH_o 7.35, 37°C. *B*, the pH_i dependencies of rates of pH_i recovery following an initial (open circles) and a second (filled circles) internal acid load imposed under Hepes-buffered control conditions. Rates of pH_i recovery were evaluated at 0.05 pH unit intervals of pH_i and error bars represent S.E.M (n = 18). Continuous lines represent the weighted non-linear regression fits to the data points indicated for the first and second acid loads (see Motulsky & Ransnas, 1987).

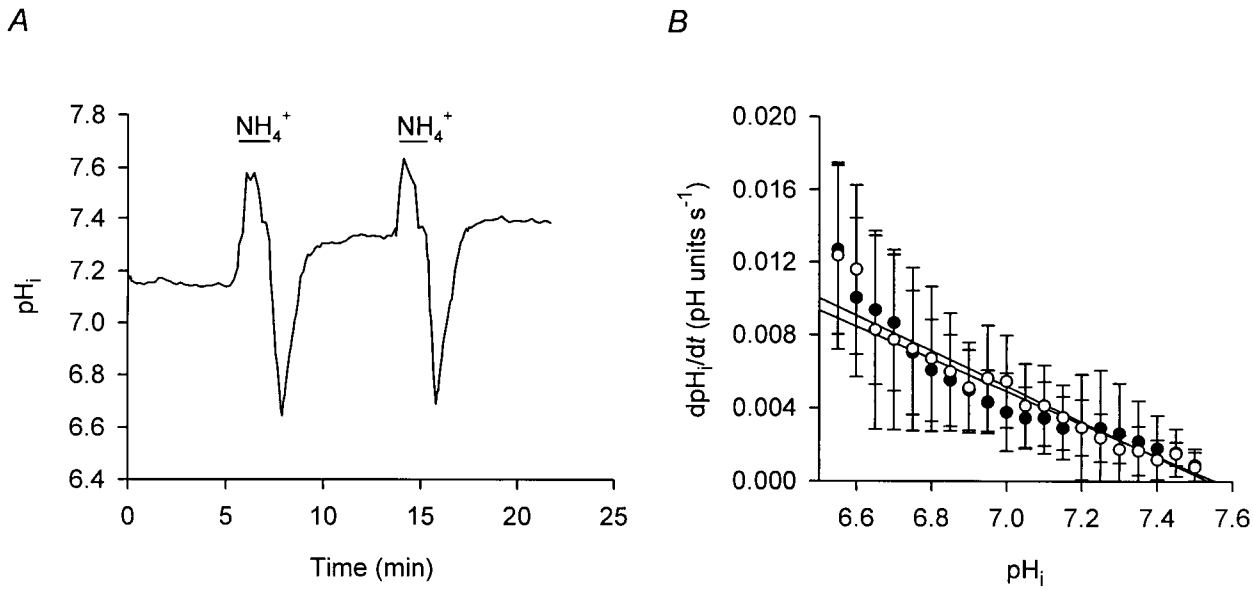
A
B
NH4+
NH4+
pHi
7.8
7.6
7.4
7.2
7.0
6.8
6.6
6.4
0
5
10
15
20
25
Time (min)
dpHi/dt (pH units s-1)
0.020
0.016
0.012
0.008
0.004
0.000
6.6
6.8
7.0
7.2
7.4
7.6
pHi

CHAPTER THREE

INTRACELLULAR pH RESPONSE TO ANOXIA IN ACUTELY ISOLATED ADULT RAT HIPPOCAMPAL CA1 PYRAMIDAL NEURONS: REDUCED Na^+/H^+ EXCHANGE ACTIVITY DURING ANOXIA[4]

3.0. INTRODUCTION

As noted in Chapter 1, while the contribution of Ca^{2+} ions to neuronal injury has received particular attention, there is renewed interest in the role of changes in pH_i in neurodegenerative phenomena. As outlined in Section 2.0.1, while it has long been known that changes in neuronal pH_i occur during and following anoxia or ischemia *in vivo* and in slice preparations *in vitro* (for reviews see Erecińska & Silver, 1994; Siesjö *et al.* 1996; Lipton, 1999), it is difficult under these experimental conditions to assess either the intrinsic changes in pH_i which occur in neurons in response to anoxia or ischemia or the contribution of intrinsic alterations in the activities of neuronal pH_i regulating mechanisms to the pH_i changes observed.

Recent studies, largely employing cultured fetal or postnatal neurons, point to the involvement of changes in Na^+/H^+ exchange activity in the neuronal pH_i response to anoxia (Diarra *et al.* 1999; Jørgensen *et al.* 1999; Messier *et al.* 2004; also see Yao *et al.* 2001 for studies in acutely isolated mouse hippocampal neurons). Moreover, examined *in vivo* and *in vitro*, selective pharmacological inhibitors of Na^+/H^+ exchange exert protective effects on neurons in which the transport mechanism is sensitive to such compounds (e.g. Vornov *et al.* 1996; Horikawa *et al.* 2001a and b). However, it remains unclear whether potentially detrimental changes in neuronal

[4] A version of this chapter has been published. Sheldon, C. and Church, J. (2004) Reduced contribution from Na^+/H^+ exchange to acid extrusion during anoxia in adult rat hippocampal CA1 neurons. J. Neurochem. 88: 594-603.

Na^+/H^+ exchange activity occur during and/or following anoxia (see Mutch & Hansen, 1984; Obrenovitch *et al.* 1990; Taylor *et al.* 1996). In addition, the sensitivity of mammalian central neurons to the damaging effects of anoxia (Kass & Lipton, 1989; Friedman & Haddad, 1993; Roberts & Chih, 1997; Isagai *et al.* 1999) and the mechanisms that serve to regulate neuronal pH_i (Raley-Susman *et al.* 1993; Bevensee *et al.* 1996; Roberts & Chih, 1997; Douglas *et al.* 2001) are developmentally regulated, and it remains unclear whether findings made in phenotypically relatively immature cells in culture can be applied to more mature neurons, especially rat hippocampal CA1 pyramidal neurons that are particularly vulnerable to the damaging effects of anoxia.

Thus, the aims of this first study were: *i)* to characterize the steady-state pH_i changes that occur during *and* following transient periods of anoxia in hippocampal CA1 pyramidal neurons acutely isolated from adult rats; and *ii)* to examine whether Na^+/H^+ exchange activity in adult rat hippocampal CA1 neurons remains functional during anoxia. Experiments examining changes in Na^+/H^+ exchange activity in the period immediately following anoxia are presented in Chapter 4.

3.1. MATERIALS AND METHODS

3.1.1. Experimental preparation

Acutely isolated adult rat hippocampal CA1 pyramidal neurons, loaded with either BCECF or fura-2, were used in the majority of experiments presented in this Chapter. Solutions containing 17.5 mM 2-deoxyglucose (2-DG) were prepared by equimolar substitution for D-glucose.

3.1.2. Recording techniques

Details of the techniques used for dye loading, dye calibration and the conversion of BCECF-derived BI_{488}/BI_{452} ratio values to pH_i values are presented in Chapter 2. It has been reported that BCECF inhibits the plasmalemmal Ca^{2+},H^+-ATPase in erythrocytes ($IC_{50} \approx 100$ μM; Gatto & Milanick, 1993). Because the Ca^{2+},H^+-ATPase in rat hippocampal neurons is an acid-loading Ca^{2+}/H^+ exchanger (Trapp *et al.* 1996b; see Fig. 1.3), anoxia-evoked changes in pH_i measured with BCECF may be influenced by a reduction in background acid loading consequent upon inhibition of the ATPase. Therefore, HPTS, a fluorescent ratiometric H^+-sensitive indicator that is reported not to inhibit activity-dependent pH_i changes in snail neurons (Willoughby *et al.* 1998), was employed in a limited number of experiments to measure anoxia-evoked changes in pH_i; details of the techniques used for dye loading, dye calibration and the conversion of HPTS-derived BI_{452}/BI_{380} ratio values to pH_i values are detailed in Chapter 2.

3.1.3. Experimental maneuvers

The effects of anoxia were examined on steady-state pH_i and rates of pH_i recovery from internal acid loads imposed by the NH_4^+-prepulse technique. To compare the steady-state pH_i changes evoked by anoxia under the various experimental conditions, three parameters were measured. The magnitude of the fall in pH_i observed during anoxia was measured as the difference between the pre-anoxic resting pH_i value and the minimum pH_i value observed during anoxia. The magnitudes of the increases in pH_i observed during and following anoxia were measured as the difference between the pH_i value observed immediately prior to the return to normoxia and the minimum pH_i value observed during anoxia, and the difference between the highest pH_i value observed after anoxia and the pre-anoxic steady-state pH_i value, respectively. In experiments in

which rates of pH_i recovery during anoxia were examined, acid loads were imposed such that the peak of the internal acidification occurred at approximately the same time at which steady-state pH_i during anoxia reached its minimum value (~2.5 min following the start of anoxia). Instantaneous rates of pH_i recovery were then determined at ~30 s after the peak acidification (i.e. at ~3 min after the start of anoxia).

3.1.4. ATP determination

Cellular ATP content was measured using the Molecular Probes ATP determination kit. The luciferin-luciferase assay is based on luciferase's requirement for ATP in the production of light. Experimental samples contained 5 - 6 CA1 principal cell layers microdissected from hippocampal slices, and were either exposed to anoxia or incubated under normoxic conditions with 5 $\mu g\ ml^{-1}$ antimycin A and 17.5 mM 2-DG (to block oxidative phosphorylation and glycolysis, respectively; see Aharonovitz *et al.* 2000; Szabó *et al.* 2000) for the durations indicated in the Results. At the same time as experimental samples were exposed to anoxia or metabolic inhibition, paired samples were maintained in Hepes-buffered saline for an equivalent period of time. In all subsequent steps, samples were kept on ice. Following control or test treatments, samples were lysed by the addition of 0.1 M NaOH/1 mM EDTA and, after centrifugation, the supernatant was neutralized with 0.5 M perchloric acid (see Sheline *et al.* 2000) and the pellet was used to determine protein content (see below). Ten microlitre aliquots of the supernatant were removed and mixed with 200 μl Reaction Solution which contained (in mM): 25 Tricine buffer (pH 7.8), 5 $MgSO_4$, 0.1 EDTA, 0.1 sodium azide, 1 dithiothreitol, 0.5 d-luciferin and 1.25 $\mu g\ ml^{-1}$ firefly luciferase. Sample bioluminescence was detected with a Berthold LB9507 Lumat luminometer (Fisher Scientific Ltd., Ottawa, ON). In all cases,

measurements were made in triplicate and data are presented as percentage declines from paired control measurements.

Low-concentration ATP standard solutions were prepared by diluting a 5 mM ATP-containing solution in ultra-pure distilled and autoclaved H_2O and were used to generate a standard curve relating measured luminescence to moles of ATP. Similarly, using the Bio-Rad DC Protein Assay kit (Bio-Rad Laboratories Inc., Mississauga, ON), standard curves relating absorbance measured at 595 nm (A_{595}) and concentration of protein were generated and the protein content of the pellet was determined. Thus, the total content of ATP (moles) and protein (mg) of the lysates prepared from CA1 regions could be determined and, assuming a cytosolic volume of 2.4 $\mu l\ mg^{-1}$ protein (Chinopoulos *et al.* 2000), concentrations of ATP could be estimated.

3.1.5. Statistical analysis

Data are reported as mean ± S.E.M. and the accompanying *n* value refers to the number of acutely isolated CA1 neurons from which data were obtained. In experiments in which internal ATP content was measured, *n* refers to the number of samples examined under a given experimental condition. Statistical analysis was performed with Student's two-tailed *t* test, paired or unpaired as appropriate, with significance assumed at the 5% level.

3.2. RESULTS

3.2.1. Steady-state pH_i under normoxic conditions

Under HCO_3^-/CO_2-buffered conditions at pH_o 7.35 and 37°C, resting pH_i was distributed in a Gaussian manner around a mean of 7.34 ± 0.05 (range pH 7.07 – 7.78; $n = 18$). In nominally

HCO_3^-/CO_2-free, Hepes-buffered medium at pH 7.35 and 37°C, steady-state pH_i was 7.19 ± 0.01 (range pH 6.34 - 7.74; n = 330) and the distribution of resting pH_i values was fit with the sum of two Gaussian distributions with means at pH_i 6.90 ± 0.02 and pH_i 7.35 ± 0.01. The mean resting pH_i values and their distributions under both HCO_3^-/CO_2- and Hepes-buffered conditions were similar to those reported previously by our laboratory (Smith *et al.* 1998; Brett *et al.* 2002a) and others (Bevensee *et al.* 1996) for acutely isolated mature rat hippocampal CA1 pyramidal neurons at 37°C.

3.2.2. Steady-state pH_i response to anoxia

The steady-state pH_i changes evoked by 5 min periods of anoxia, induced by sodium dithionite, were first examined under HCO_3^-/CO_2-buffered conditions at pH_o 7.35. The results are presented in Table 3.1 and a representative response is illustrated in Fig. 3.1*A*. Anoxia elicited a triphasic pattern of steady-state pH_i changes which consisted of an initial acidic shift following the induction of anoxia, a subsequent rise in pH_i in the continued absence of O_2 and, finally, a further internal alkalinization upon the return to normoxia which recovered slowly towards resting pH_i values. A clear change in the rate of increase of pH_i was observed during the transition from anoxia to normoxia in 10/14 neurons subjected to 5 min anoxia under HCO_3^-/CO_2-buffered conditions (corresponding changes were observed in 29/38 "high" pH_i neurons under nominally HCO_3^-/CO_2-free conditions; see below).

It was necessary to assess the possibility that sodium dithionite might induce changes in pH_i via mechanisms unrelated to its O_2 scavenging property. To do so, HCO_3^-/CO_2-buffered medium was bubbled vigorously with 95% ultrahigh purity Ar/5% CO_2 for periods of 1 to ≥18 h. In samples obtained anaerobically from the recording chamber, the P_{O_2} in medium bubbled with

Ar for 1 h was 25.3 ± 0.8 mm Hg (n = 4) whereas, measured in 8 different samples, the P_{O_2} in medium bubbled with Ar for ≥18 h was <1 mm Hg, and was not significantly different from that measured in medium containing 1 or 2 mM sodium dithionite. When a 5 min period of anoxia was imposed by exposing neurons to HCO_3^-/CO_2-buffered medium that had been equilibrated with 5% CO_2/95% Ar for ≥18 h, the resultant steady-state pH_i changes were not significantly different to those observed when the P_{O_2} was reduced to <1 mm Hg by the addition of sodium dithionite under identical buffering conditions (Table 3.1; Fig. 3.1*B*). Thus, the steady-state pH_i changes evoked by exposure to media containing sodium dithionite reflect a reduction in P_{O_2} and are not secondary to any additional properties of the O_2 scavenger.

Next, to assess the potential contribution of HCO_3^- ions and HCO_3^--dependent pH_i regulating mechanisms to anoxia-evoked changes in steady-state pH_i, experiments were repeated under nominally HCO_3^-/CO_2-free, Hepes-buffered conditions. Neither the decrease in pH_i nor the subsequent rise in pH_i observed during anoxia were significantly different in the absence or presence of HCO_3^- (Table 3.1; also see Pirttilä & Kauppinen, 1994). The increase in pH_i observed following the return to normoxia was larger under Hepes- than under HCO_3^-/CO_2-buffered conditions; however, this effect failed to reach statistical significance (Table 3.1; also see Pirttilä & Kauppinen, 1994; Bevensee & Boron, 2000).

In a portion of neurons (13/51) examined under Hepes-buffered conditions, 5 min anoxia elicited a different pattern of pH_i changes to that described above. In these neurons, the fall in pH_i during anoxia was significantly smaller (0.03 ± 0.01 pH units) than the response observed in the majority of cells examined under identical buffering conditions, and the small acidification gave way to a marked internal alkalinization (0.50 ± 0.04 pH units) that started during anoxia and continued into the post-anoxic period (Fig. 3.2*A*). This 'atypical' pattern of pH_i changes was also

observed under HCO_3^-/CO_2-buffered conditions in 3/14 neurons and, interestingly, is reported to be the usual response of mouse hippocampal CA1 neurons to O_2 deprivation under Hepes-buffered conditions (Yao *et al.* 2001). It is noteworthy that neurons which exhibited this 'atypical' response had low resting pH_i values (under Hepes-buffered conditions, the average pre-anoxic resting pH_i value observed in neurons which exhibited the 'atypical' response was 6.95 ± 0.06 compared with 7.33 ± 0.04 in neurons which exhibited the more 'typical' response; $n = 13$ and 38, respectively; $P < 0.05$) and that the magnitudes of the fall in pH_i observed during anoxia and the increase in pH_i observed following anoxia appeared related to the pre-anoxic resting pH_i value of a given neuron (Fig. 3.2*B*, *C*). This finding is consistent with the possibility (Bevensee *et al.* 1996; Smith *et al.* 1998; Brett *et al.* 2002a) that a "low" pH_i population of mature rat hippocampal CA1 pyramidal neurons exists that exhibits a distinct pattern of pH_i regulation.

3.2.3. Contribution of changes in $[Ca^{2+}]_i$ to the changes in pH_i observed during anoxia

In adult CA1 neurons, anoxia leads to a disruption of internal ion homeostasis that is associated with energy failure and an abrupt depolarization of the plasma membrane (reviewed by Hansen, 1985; Lipton, 1999; also see Rader & Lanthorn, 1989; Silver & Erecińska, 1990; Tanaka *et al.* 1997). In the present study, anoxia evoked a 2.0 ± 0.4 ($n = 8$) unit increase in the fura-2 BI_{334}/BI_{380} ratio value, which commenced at approximately 2 min after the induction of anoxia (as did the rise in pH_i observed during anoxia; Fig. 3.3*A*) and which remained elevated after the return to normoxia for as long as stable recordings could be maintained (up to 25 min following the end of an anoxic insult; also see Friedman & Haddad, 1993; Kubo *et al.* 2001).

The potential contribution of changes in $[Ca^{2+}]_i$ to the changes in steady-state pH_i evoked by anoxia was assessed by imposing anoxia under external Ca^{2+}-free conditions. As shown in

Fig. 3.3*B*, exposure to Ca^{2+}-free medium caused a 0.30 ± 0.02 (n = 6) ratio unit decrease in resting BI_{334}/BI_{380} values and anoxia failed to induce the rapid and marked rise in BI_{334}/BI_{380} values that was observed in the presence of Ca^{2+} (the increase in the BI_{334}/BI_{380} value observed under external Ca^{2+}-free conditions was 0.02 ± 0.01 ratio units)[5]. In parallel experiments in BCECF-loaded neurons, exposure to Ca^{2+}-free medium evoked an increase in steady-state pH_i of 0.11 ± 0.04 pH units (n = 6), as previously reported (Smith *et al.* 1998). Once a new steady-state pH_i value had been reached, a 5 min period of anoxia induced a triphasic pH_i response, the individual components of which were not significantly different to those observed in the presence of 2 mM $Ca^{2+}{}_o$ (Table 3.1; Fig. 3.3*B*).

Following the initial fall in pH_i, the increase in pH_i that occurred during anoxia in the present study has been observed only relatively infrequently in neurons *in vivo* or in slice preparations *in vitro* (see Mabe *et al.* 1983; Fujiwara *et al.* 1992; Silver & Erecińska, 1992; Pirttilä & Kauppinen, 1992; Melzian *et al.* 1996). Considering that BCECF inhibits the plasmalemmal acid-extruding Ca^{2+},H^+-ATPase in erythrocytes (see Section 3.1.2), the possibility existed that the rises in pH_i measured with BCECF under the high $[Ca^{2+}]_i$ conditions that pertain during anoxia may be artifacts consequent upon reduced background acid loading. Measured in HPTS-loaded neurons, however, the increases in pH_i observed during and following 5 min anoxia were not significantly different to those observed in BCECF-loaded cells (Table 3.1; Fig. 3.4). Thus, in agreement with reports in which activity-dependent changes in pH_i have been recorded in BCECF-loaded neurons (e.g. Trapp *et al.* 1996a; Wu *et al.* 1999), these data led me

---

[5] Interestingly, in 4/6 neurons examined under Ca^{2+}-free conditions, a small 0.08 ± 0.02 ratio unit increase in BI_{334}/BI_{380} values was observed in the immediate post-anoxic period (Fig. 3.3*B*); although the basis for this transient increase was not investigated, it may reflect Ca^{2+} release from intracellular stores consequent upon anoxia-evoked changes in pH_i (see Ou-Yang *et al.* 1994b).

to conclude that BCECF is an appropriate pH indicator for use in the present experiments. Other factors that may, in part, contribute to the absence of observable rises in pH_i during periods of anoxia or ischemia *in vivo* and in slice preparations *in vitro* are the concomitant falls in pH_o observed in these multicellular preparations (*cf* the present experiments in which pH_o was maintained at 7.35 prior to, during and following anoxia; see Chapter 4).

These results indicate that the typical steady-state pH_i response of acutely isolated adult rat hippocampal CA1 pyramidal neurons to 5 min anoxia consists of an initial fall in pH_i upon the induction of anoxia, a subsequent rise in pH_i in the continued absence of O_2, and a further internal alkalinization upon the return to normoxia. Because all three phases were not significantly influenced by the presence of HCO_3^-, subsequent experiments were conducted in the nominal absence of HCO_3^-/CO_2 to examine the effects of anoxia on Na^+/H^+ exchange activity.

3.2.4. Na^+/H^+ exchange activity during anoxia

3.2.4.1. Steady-state pH_i measurements

As noted in Chapter 1, Na^+/H^+ exchange is the dominant acid extrusion mechanism in rat hippocampal neurons under HCO_3^-/CO_2-free conditions but, unusually, this transport mechanism is insensitive to amiloride, amiloride derivatives and benzoylguanidinium compounds (Raley-Susman *et al.* 1991; Schwiening & Boron, 1994; Baxter & Church, 1996; Bevensee *et al.* 1996). To inhibit Na^+/H^+ exchange, therefore, neurons were perfused with reduced-Na^+, $NMDG^+$-substituted medium. In agreement with previous reports in rat hippocampal neurons (Baxter & Church, 1996; Bevensee *et al.* 1996; Smith *et al.* 1998), prolonged exposure to reduced-Na^+, $NMDG^+$-substituted medium was marked by an initial intracellular acidification which then slowly recovered over the following 20 - 30 min to a new steady-state pH_i value of 7.35 ± 0.04 (n = 20); this pH_i value was not significantly different either to the pH_i value observed prior to the

reduction in Na^+_o (7.34 ± 0.03; $P = 0.85$) or to the mean pH_i value typically observed prior to the induction of anoxia in the presence of normal $[Na^+]_o$ (7.33 ± 0.04; $n = 38$; $P = 0.77$). Under these reduced-Na^+_o, $NMDG^+$-substituted conditions, 5 min anoxia evoked an internal acidification, the magnitude of which was significantly reduced compared to the fall in pH_i observed in the presence of normal Na^+_o (Fig. 3.5*A*). Illustrated in Fig. 3.5*B*, the magnitude of the increase in pH_i observed during anoxia was not significantly influenced under $NMDG^+$-substituted conditions.

In contrast to $NMDG^+$, Li^+ can act as a substrate for Na^+/H^+ exchange (see Aronson, 1985; Jean *et al.* 1985). Consistent with previous reports in rat hippocampal neurons (Raley-Susman *et al.* 1991; Baxter & Church, 1996; Smith *et al.* 1998), exposure to reduced-Na^+_o, Li^+-substituted medium caused a transient fall in steady-state pH_i which recovered within 5 - 10 min to a pH_i value (7.40 ± 0.02; $n = 13$) which was not significantly different either to the pH_i value observed prior to the reduction of Na^+_o (7.38 ± 0.02) or to the pH_i value typically observed prior to the induction of anoxia in the presence of normal $[Na^+]_o$ (see above; $P = 0.36$ and 0.29, respectively). Under Li^+_o-substituted conditions, the magnitude of the fall in pH_i induced by 5 min anoxia was not significantly different from that observed in the presence of normal Na^+_o but was significantly greater than that observed after prolonged exposure to $NMDG^+$-substituted medium (Fig. 3.5*A*). The magnitude of the increase in pH_i observed during anoxia was not influenced under Li^+_o-substituted conditions (Fig. 3.5*B*). Similar results, under $NMDG^+$ and Li^+-substituted conditions, were obtained when anoxia was imposed in the presence of 5 mM, rather than 17.5 mM, glucose (not shown; see Sheldon & Church, 2004).

Taken together, these results suggest the possibility that Na^+/H^+ exchange activity in rat CA1 neurons becomes inhibited soon after the induction of anoxia. Under normoxic conditions, Na^+/H^+ exchange in rat hippocampal neurons is active at resting pH_i (see Raley-Susman *et al.*

1991; Schwiening & Boron, 1994; Baxter & Church, 1996; Bevensee *et al.* 1996) and, in the presence of normal Na^+_o or under Li^+_o-substituted conditions, reduced Na^+/H^+ exchange activity during anoxia would be expected to augment the internal acidosis produced during anoxia (also see Maduh *et al.* 1990; Chambers-Kersh *et al.* 2000). In contrast, under conditions where Na^+/H^+ exchange was blocked prior to the induction of anoxia by prolonged exposure to $NMDG^+$-substituted medium, inhibition of Na^+/H^+ exchange activity by anoxia is precluded and will not contribute to the fall in pH_i during anoxia; thus, the observed reduction in the magnitude of the anoxia-induced acidification when $NMDG^+$, as opposed to Li^+, was employed as an external Na^+ substitute. However, because blockade of Na^+/H^+ exchange failed to affect the magnitude of the rise in pH_i during anoxia, additional mechanism(s) must contribute to this phase of the anoxic pH_i response (see Chapter 4).

3.2.4.2. Recovery of pH_i from imposed internal acid loads

The steady-state pH_i measurements detailed above suggest that Na^+/H^+ exchange activity may decline soon after the onset of anoxia. To further investigate this possibility, I compared rates of pH_i recovery from intracellular acid loads imposed under HCO_3^-/CO_2-free, Hepes-buffered conditions prior to and during anoxia.

As illustrated in Fig. 3.6*A*, under control conditions pH_i recovery from an acid load imposed during anoxia was slowed, compared to that observed prior to anoxia in the same cell. Examined in a total of 9 neurons with a mean steady-state pH_i of 7.38 ± 0.04, instantaneous rates of pH_i recovery were reduced significantly during anoxia at all absolute values of pH_i (Fig. 3.6*B*); at a common test pH_i of 6.80, for example, there was a 47% decrease in the rate of pH_i recovery during anoxia. The increases in pH_i evoked by NH_4^+ (quantified by taking the difference

between the steady-state pH_i immediately prior to the application of NH_4^+ and the maximum pH_i observed during its application; see Smith *et al.* 1998) were similar prior to and during anoxia (0.25 ± 0.02 and 0.21 ± 0.04 pH units, respectively; $n = 9$ in each case; $P = 0.36$), suggesting that marked alterations in intracellular buffering power are unlikely to contribute to the reduction in rates of pH_i recovery observed during anoxia.

Next, internal acid loads were imposed prior to and during anoxia under reduced-$[Na^+]_o$, $NMDG^+$-substituted conditions (Na^+/H^+ exchange blocked). Consistent with previous reports in rat hippocampal neurons (Schwiening & Boron, 1994; Baxter & Church, 1996; Bevensee *et al.* 1996), rates of pH_i recovery prior to anoxia were significantly reduced, compared to rates of pH_i recovery established in the presence of normal Na^+_o (Fig. 3.6*C*, *D*). In contrast, rates of pH_i recovery during anoxia were not significantly different from those established during anoxia in the presence of normal Na^+_o (Fig. 3.6*D*). Also consistent with the possibility that functional Na^+/H^+ exchange activity is reduced during anoxia, plots of the differences between rates of pH_i recovery under normal Na^+_o-containing and reduced-Na^+_o, $NMDG^+$-substituted conditions both prior to and during anoxia (Fig. 3.6*E*) revealed a reduced contribution from Na^+_o-dependent mechanism(s) to pH_i recovery from acid loads during anoxia. Interestingly, under $NMDG^+$-substituted conditions, rates of pH_i recovery from internal acid loads imposed during anoxia were increased compared with rates observed prior to anoxia under $NMDG^+$-substituted conditions (Fig. 3.6*C*), suggesting that a Na^+_o- and HCO_3^--independent acid extrusion pathway is activated by anoxia. The potential mechanism(s) underlying the Na^+_o-independent recovery of pH_i observed during anoxia in rat hippocampal neurons are examined in Chapter 4.

Rates of pH_i recovery were also measured prior to and during anoxia in 3 "low" pH_i neurons (resting pH_i 7.05 ± 0.08) and these data are illustrated in Fig. 3.7. Consistent with

observations made by Bevensee and colleagues (1996), rates of pH_i recovery observed in "low" pH_i cells prior to anoxia were slower at given absolute values of pH_i than rates observed in "high" pH_i neurons prior to anoxia (compare Figs. 3.7*A, B* and 3.6*B, D*), a difference that reflects reduced Na^+_o-dependent acid extrusion at each pH_i value in "low" pH_i cells (and, therefore, is not apparent under $NMDG^+$-substituted conditions; see Bevensee *et al.* 1996). In "low" pH_i cells, rates of pH_i recovery from internal acid loads imposed prior to anoxia were not different from rates of pH_i recovery established during anoxia under Na^+_o-containing (Fig. 3.7*A*) or reduced Na^+_o, $NMDG^+$-substituted conditions (Fig. 3.7*B*). Illustrated in Fig. 3.7*C*, in "low" pH_i cells, the contribution of Na^+_o-dependent mechanism(s) to pH_i recovery from acid loads was nevertheless reduced during anoxia. However, this effect was less pronounced than observed in "high" pH_i cells, a difference which likely reflects the reduced activity of Na^+_o-dependent pH_i regulating mechanism(s) prior to anoxia in "low" *vs.* "high" pH_i cells (Bevensee *et al.* 1996). Thus, at a common test pH_i of 6.80, there were ~6 and 4-fold reductions in Na^+_o-dependent rates of pH_i recovery in "high" and "low" pH_i cells, respectively (compare Figs. 3.7*C* and 3.6*E*). Due to the limited number of "low" pH_i cells isolated, no attempt was made to characterize further the influence of anoxia on Na^+_o-dependent pH_i recovery in "low" pH_i neurons.

In light of the fact that Na^+/H^+ exchangers possess internal H^+ modifier site(s) that modulate transport activity, the observed functional reduction in the contribution of Na^+/H^+ exchange to pH_i recovery from acid loads imposed during anoxia may simply reflect the frequency of relatively "high" pH_i cells that were found at pH_o 7.35. Therefore, internal acid loads were imposed prior to anoxia at pH_o 7.35 and then during anoxia at pH_o 6.60, conditions that mimic the changes in pH_o that occur in response to anoxia *in vivo* (n = 9; Fig. 3.8*A*). Although the minimum pH_i values imposed by NH_4^+ prepulses during anoxia at pH_o 6.60 were lower than those observed at pH_o 7.35 (pH_i ~6.10 and ~6.80, respectively; also see Vornov *et al.*

1996), rates of pH_i recovery during anoxia at pH_o 6.60 were further reduced ($P < 0.05$), rather than increased, from those observed during anoxia at pH_o 7.35 (Fig. 3.8*C*). This result is consistent with the possibility that Na^+/H^+ exchange continues to be inhibited during anoxia at low pH_i values; however, the fact that rates of pH_i recovery during anoxia at pH_o 6.60 were slower than those observed during anoxia at pH_o 7.35 (Fig. 3.8*B, C*) suggests the possibility that low pH conditions might be affecting the activity of an additional mechanism that participates in acid extrusion during anoxia in rat CA1 neurons (e.g. the Na^+_o-independent, HCO_3^--independent H^+-efflux pathway referred to above; see Chapter 4).

To more rigorously assess the effects of anoxia on Na^+/H^+ exchange activity at low pH_o/pH_i, the Na^+_o-dependent component of pH_i recovery from internal acid loads was assessed by imposing acid loads prior to and during anoxia at pH_o 6.60, under both normal Na^+_o-containing ($n = 9$) and reduced-Na^+_o, $NMDG^+$-substituted ($n = 10$) conditions. As illustrated in Fig. 3.8*C*, rates of pH_i recovery prior to anoxia at pH_o 6.60 were significantly reduced, compared to those observed prior to anoxia at pH_o 7.35, consistent with the known effect of falls in pH_o to inhibit the activities of Na^+/H^+ exchangers (e.g. Jean *et al.* 1985; Wu & Vaughan-Jones, 1997). However, rates of pH_i recovery during anoxia at pH_o 6.60 were not significantly different to rates observed prior to anoxia at pH_o 6.60 (Fig. 3.8*C*; $P = 0.68$). In addition, although rates of pH_i recovery during anoxia at pH_o 6.60 were not significantly different under normal Na^+_o-containing *vs.* reduced-Na^+_o, $NMDG^+$-substituted conditions (Fig. 3.8*C*), plots of the differences between rates of pH_i recovery under Na^+_o-containing and $NMDG^+$-substituted conditions both prior to and during anoxia revealed a reduced contribution from Na^+_o-dependent mechanism(s) to pH_i recovery from acid loads during anoxia at pH_o 6.60 (Fig. 3.8*D*). The reduced rate of Na^+_o-dependent pH_i recovery during anoxia at pH_o 6.60 compared to pH_o 7.35 (compare Figs. 3.6*E*

and 3.8*D*) is consistent with a low pH_o-induced inhibition of residual Na^+/H^+ exchange activity during anoxia.

3.2.4.3. Role of internal ATP depletion

In all cell types studied to date, optimal Na^+/H^+ exchange activity requires the presence of normal physiological levels of intracellular ATP (Demaurex & Grinstein, 1994; Wu & Vaughan-Jones, 1994; Demaurex *et al.* 1997; Wakabayashi *et al.* 1997; Szabó *et al.* 2000). This raises the possibility that an anoxia-induced fall in internal ATP levels (see Erecińska & Silver, 1994) might contribute to the anoxia-evoked decline in Na^+/H^+ exchange activity. This was examined using a number of different approaches.

First, to assess whether rates of pH_i recovery from acid loads imposed in rat CA1 neurons in the nominal absence of HCO_3^- are sensitive to internal ATP depletion, microdissected CA1 regions were incubated with 2-DG and antimycin A under normoxic conditions. Consistent with previous reports (e.g. Kass & Lipton, 1982; Obrenovitch *et al.* 1990; Carter *et al.* 1995), resting ATP levels were 10.6 ± 3.5 μmol g^{-1} protein ($n = 6$), equivalent to ~4.4 mM assuming a cytosolic volume of 2.4 μl mg^{-1} protein (see Chinopoulos *et al.* 2000). After 10 min treatment with 2-DG and antimycin A, there was an $80 \pm 13\%$ fall in internal ATP levels to a value below the K_D of Na^+/H^+ exchange for ATP (see Discussion). At the time that ATP levels were reduced by 2-DG and antimycin A, rates of pH_i recovery from imposed acid loads were slowed, compared with rates measured prior to ATP depletion in the same neurons (Fig. 3.9*A*). At a common test pH_i of 7.00, for example, there was a 53% decrease in the rate of pH_i recovery ($P < 0.05$), which was not further slowed when the experiments were repeated under reduced-Na^+_o, $NMDG^+$-substituted conditions (Fig. 3.9*B*). However, plotting the difference between rates of pH_i recovery under

normal Na^+_o-containing and reduced-Na^+_o, $NMDG^+$-substituted conditions prior to and following treatment with 2-DG and antimycin A revealed a reduced contribution from Na^+_o-dependent mechanism(s) to pH_i recovery from imposed acid loads in the presence of 2-DG and antimycin A (Fig. 3.9*C*).

Next, I examined whether anoxia imposed under my experimental conditions results in intracellular ATP depletion. Consistent with previous reports (e.g. Obrenovitch *et al.* 1990; Erecińska & Silver, 1994; Fowler & Li, 1998; Lipton, 1999), after 3 min anoxia there was a 65 ± 4% (n = 3) fall in internal ATP levels, which declined further to 76 ± 4% (n = 2) after 5 min anoxia. Thus, pH_i recovery from acid loads imposed during anoxia was slowed at a time when cellular ATP was depleted.

Pretreatment of hippocampal slices with 10 mM creatine for ≥2 h has been shown to increase intracellular phosphocreatine levels in hippocampal neurons and delay the depletion of internal ATP during O_2 deprivation (e.g. Kass & Lipton, 1982; Lipton & Whittingham, 1982; Carter *et al.* 1995; Balestrino *et al.* 1999). Therefore, in the third series of experiments, I examined whether this maneuver could preserve internal ATP levels and concomitantly attenuate the anoxia-induced decline in rates of pH_i recovery from acid loads observed in untreated neurons. In creatine-treated slices, 3 min anoxia caused a 38 ± 6% (n = 4) fall in ATP levels, a reduction significantly less ($P < 0.05$) than that observed in untreated slices. In neurons isolated from creatine-treated slices, rates of pH_i recovery from acid loads imposed during anoxia were not significantly different from rates of pH_i recovery established in the same neurons prior to anoxia (Fig. 3.10*A*, *B*). Intracellular acid loads were then imposed in neurons isolated from creatine-treated slices both prior to and during anoxia under reduced-Na^+_o, $NMDG^+$-substituted conditions. At a common test pH_i of 7.00, rates of pH_i recovery from acid loads imposed under

$NMDG^+$-substituted conditions both prior to and during anoxia were slowed by ~60%, compared with rates of pH_i recovery observed in the presence of normal Na^+_o (Fig. 3.10*B*). Thus, Na^+_o-dependent acid extrusion mechanism(s) remain functional during anoxia in neurons isolated from creatine-treated slices. Indeed, plotting the difference between rates of pH_i recovery measured under normal Na^+_o-containing and reduced-Na^+_o, $NMDG^+$-substituted conditions prior to and during anoxia revealed that, in contrast to slices that had not been treated with creatine (see Fig. 3.6*E*), the contribution of Na^+_o-dependent mechanism(s) to pH_i recovery from acid loads during anoxia is preserved in neurons isolated from creatine-treated slices (Fig. 3.10*C*).

Recently, it has been suggested that the inhibitory effect of ATP depletion on Na^+/H^+ exchange activity is attributable, at least in part, to a decreased availability of plasmalemmal PIP_2 (Aharonovitz *et al.* 2000). Furthermore, reductions in plasmalemmal PIP_2 levels have been observed following chemical ATP depletion and periods of ischemia (Sun & Hsu, 1996; Aharonovitz *et al.* 2000). To start to examine the possibility that Na^+/H^+ exchange activity in rat hippocampal neurons is influenced by plasmalemmal PIP_2, cultured postnatal rat hippocampal neurons were incubated overnight with 5 mM neomycin and the effect of this treatment on rates of pH_i recovery from acid loads imposed under HCO_3^-/CO_2-free, normoxic conditions was examined. Neomycin interferes with the ability of PIP_2 to interact with membrane and cytoskeletal proteins, such as phospholipases C and D, actin and the Na^+/H^+ exchanger (see Abdul-Ghani *et al.* 1996; Castillo & Babson, 1998; Aharonovitz *et al.* 2000). Paired intracellular acid loads were not possible and rates of pH_i recovery in neuronal cultures that had or had not been treated with neomycin were compared in parallel experiments. At a common test pH_i of 6.90, rates of pH_i recovery from imposed intracellular acid loads were $7.63 \pm 2.6 \times 10^{-3}$ and $14.2 \pm 2.0 \times 10^{-3}$ pH units s^{-1} in the presence and absence of neomycin pretreatment, a 46% decrease

in the instantaneous rate of pH_i recovery following treatment with neomycin ($n = 6$ in both cases; $P < 0.05$).

3.3. DISCUSSION

3.3.1. Characterization of the changes in pH_i observed during and following anoxia in adult rat hippocampal CA1 pyramidal neurons

The typical steady-state pH_i response to anoxia in acutely isolated adult rat hippocampal CA1 pyramidal neurons consisted of an initial fall in pH_i, a subsequent rise in pH_i in the continued absence of O_2, and a further internal alkalinization upon the return to normoxia. In ~25% of neurons examined, and almost exclusively in neurons with resting pH_i values < 7.20 ("low" pH_i neurons), a small acidification was observed during anoxia that gave way to a marked internal alkalinization beginning during anoxia and continuing into the post-anoxic period. In both "low" and "high" pH_i neurons, the pH_i changes were observed under constant external conditions and, as such, represent the intrinsic pH_i response of the neurons to anoxia. A further discussion of the observations made in "high" *vs.* "low" pH_i neurons will be presented in Chapter 4.

Although studies in hippocampal slices have suggested that there are developmental changes in the neuronal pH_i response to anoxia (see Roberts & Chih, 1997), the typical pattern of pH_i changes observed in the present study was similar in most respects to that found in cultured postnatal rat hippocampal neurons (Diarra *et al.* 1999) and cultured fetal mouse neocortical neurons (Jørgensen *et al.* 1999). The major differences between the previous work in cultured postnatal hippocampal neurons (Diarra *et al.* 1999) and the present work in acutely isolated adult CA1 neurons are the relatively persistant increases in $[Ca^{2+}]_i$ and pH_i observed following 5 min

anoxia that, in cultured postnatal neurons, occur only after ≥ 10 min anoxia. These differences may reflect, at least in part, the more marked and more persistent membrane depolarization that occurs in adult, compared with fetal or postnatal, hippocampal neurons on withdrawal of metabolic substrates (Bickler *et al.* 1993; Isagai *et al.* 1999; Nabetani *et al.* 1997; Tanaka *et al.* 1997 and 1999).

In contrast to excitotoxin-evoked reductions in pH_i which, under normoxic conditions, are largely consequent upon increases in $[Ca^{2+}]_i$ and the subsequent activation of a plasmalemmal Ca^{2+},H^+-ATPase (e.g. Hartley & Dubinsky, 1993; Irwin *et al.* 1994; Trapp *et al.* 1996b; Wu *et al.* 1999), changes in $[Ca^{2+}]_i$ do not appear to be major determinants of anoxia-evoked changes in pH_i in hippocampal CA1 neurons. Thus, as previously reported in cultured postnatal rat hippocampal (Diarra *et al.* 1999) and fetal mouse neocortical (Jørgensen *et al.* 1999) neurons, despite the marked reduction in the anoxia-evoked increase in $[Ca^{2+}]_i$ observed in the absence of $Ca^{2+}{}_o$, the pH_i response to anoxia was not significantly affected. Experiments in which HPTS was employed as the pH_i indicator did not support the possibility that inhibition of the plasmalemmal Ca^{2+},H^+-ATPase by BCECF might account for the increases in pH_i observed during (or after) anoxia in the presence of external Ca^{2+}. Rather, my findings are consistent with the possibility that Ca^{2+},H^+-ATPase activity may be inhibited by metabolic insults (Kass & Lipton, 1989; Pereira *et al.* 1996; Castilho *et al.* 1998; Wu *et al.* 1999; Zaidi & Michaelis, 1999; Chinopoulos *et al.* 2000) and therefore contribute little to background acid loading despite the marked increase in $[Ca^{2+}]_i$ evoked by anoxia in adult CA1 neurons.

3.3.2. Reduced contribution from Na^+/H^+ exchange to acid extrusion during anoxia

Anoxia induces a marked decline in HCO_3^--independent, Na^+_o-dependent acid extrusion from adult rat hippocampal CA1 neurons. The only established HCO_3^--independent, Na^+_o-dependent acid extrusion mechanism that supports Na^+ and Li^+, but not $NMDG^+$, transport in this cell type is Na^+/H^+ exchange. As such, the results of the present study are consistent with the possibility that Na^+/H^+ exchange activity in adult rat CA1 pyramidal neurons declines soon after the onset of anoxia. The present finding is consistent with extensive studies in cardiac myocytes (e.g. Bond *et al.* 1993; Park *et al.* 1999; Satoh *et al.* 2001) and supports previous suggestions, made largely on the basis of pH_o measurements *in vivo* and in slice preparations *in vitro*, that Na^+/H^+ exchange activity in brain tissue is compromised during anoxia (Pirttilä & Kauppinen, 1992; Taylor *et al.* 1996; Chambers-Kersh *et al.* 2000; but see Yao *et al.* 2001). However, it contrasts with the fact that Na^+/H^+ exchange is the primary mechanism whereby pH_i recovers from the internal acidosis imposed by the application of excitotoxins under normoxic conditions (e.g. Hartley & Dubinsky, 1993; Koch & Barish, 1994), highlighting a further difference between the effects of excitotoxins and anoxia on central neuronal function (see Chow & Haddad, 1998).

Given that the majority of the experiments in the present study were performed under constant extracellular conditions, the reduction in observable Na^+/H^+ exchange activity during anoxia is not secondary to anoxia-evoked changes in the composition of the microenvironment. In particular, although reductions in pH_o (as occur during anoxia *in vivo* and in slices *in vitro*; Mutch & Hansen, 1984; Obrenovich *et al.* 1990; Erecińska & Silver, 1994) are known to inhibit Na^+/H^+ exchange activity (e.g. Jean *et al.* 1985; Vaughan-Jones & Wu, 1990; Wakabayashi *et al.* 1997; Wu & Vaughan-Jones, 1997), the present results indicate that a fall in pH_o is not an absolute requirement for reduced antiport activity during anoxia in rat CA1 neurons. In addition, although anoxia-evoked increases in $[Na^+]_i$ (Chapters 5 and 6; also see Chen *et al.* 1999) would

act to reduce the thermodynamic driving force for Na^+/H^+ exchange (see Vaughan-Jones & Wu, 1990; Wu & Vaughan-Jones, 1997), calculations indicate that the quotient $[Na^+]_o/[Na^+]_i$ remains greater than $[H^+]_o/[H^+]_i$ during anoxia at either pH_o 7.35 or pH_o 6.60, thereby favoring net H^+ efflux (a further discussion of the thermodynamics of Na^+/H^+ exchange activity is presented in Chapter 6). This is in agreement with studies in guinea pig neocortical slices (Pirttilä & Kauppinen, 1992) as well as cardiac myocytes (e.g. Park *et al.* 1999; Moor *et al.* 2001) and indicates that factor(s) other than changes in transmembrane H^+ and/or Na^+ gradients must contribute to the lack of observable Na^+/H^+ exchange activity in rat CA1 neurons during anoxia. Rather, the present results are consistent with the possibility that the decline in Na^+/H^+ exchange activity during anoxia might, at least in part, be consequent upon the fall in internal ATP levels which occurs rapidly after the induction of anoxia in adult rat CA1 neurons (also see Obrenovitch *et al.* 1990; Lipton, 1999).

In all cases studied to date, physiological levels of internal ATP are required for optimal Na^+/H^+ exchange activity (Demaurex & Grinstein, 1994; Wakabayashi *et al.* 1997; Szabó *et al.* 2000). In AP-1 cells transfected with Na^+/H^+ exchanger isoform 1 (NHE1), for example, half-maximal activation of the antiporter occurs at ~5 mM ATP (Demaurex *et al.* 1997). In the present study, rates of pH_i recovery from acid loads imposed during anoxia were slowed at a time when internal ATP levels were reduced from ~4.4 mM under resting conditions to ~1.5 mM, consistent with the established ATP dependence of not only NHE1 but also NHE5 (a candidate for the relatively amiloride-resistant Na^+/H^+ exchanger found in rat CA1 neurons; Szabó *et al.* 2000). Both the reduced slope of the rate of Na^+_o-dependent pH_i recovery *vs.* pH_i relationship and the acidic shift in the pH_i dependence of the rate of Na^+_o-dependent pH_i recovery from acid loads observed during anoxia (Figs. 3.6*E* and 3.7*C*) are also consistent with previous findings that internal ATP depletion decreases the affinities of Na^+/H^+ exchangers for internal protons and

lowers their maximum transport velocities (Demaurex & Grinstein, 1994; Wakabayashi *et al.* 1997; Szabó *et al.* 2000). The involvement of internal ATP depletion in the decline in Na^+/H^+ exchange activity during anoxia is also suggested by the present findings that: *a)* incubation with 2-DG and antimycin A under normoxic conditions produced not only a similar fall in internal ATP levels to that observed during anoxia but also reduced rates of Na^+_o-dependent pH_i recovery from internal acid loads to a similar extent; and *b)* creatine pretreatment not only limited anoxia-evoked reductions in ATP levels but also attenuated anoxia-induced reductions in rates of Na^+_o-dependent pH_i recovery from imposed acid loads.

Although depletion of cellular ATP reduces the activities of all known Na^+/H^+ exchanger isoforms, it is also apparent that Na^+/H^+ exchange transport activity is not necessarily dependent on the direct hydrolysis of ATP (reviewed by Demaurex & Grinstein, 1994; Fliegel, 2001). In this regard, recent evidence indicates that the effect of acute ATP depletion to decrease NHE1 transport activity is in large part consequent upon the depletion of plasmalemmal PIP_2, rapid reductions in which occur not only following chemical ATP depletion (Aharonovitz *et al.* 2000) but also in response to short (e.g. 3 min) periods of cerebral ischemia (Sun & Hsu, 1996). Indeed, in initial experiments, sequestration of PIP_2 by pretreatment with neomycin (see Aharonovitz *et al.* 2000) was associated with slowed rates of pH_i recovery from internal acid loads imposed under normoxic conditions, raising the possibility that Na^+/H^+ exchange activity in rat CA1 neurons might also be regulated by the availability of PIP_2. Although additional experiments are required to substantiate or refute this possibility, these experiments would provide novel insights into the second-messenger control of Na^+/H^+ exchange activity in rat hippocampal neurons. In addition, the apparent relationship between Na^+/H^+ exchange activity and internal ATP (and/or PIP_2) levels would act to link the activity of the exchanger with the metabolic state of the cell. A reduction in antiport activity during a period of metabolic stress

may, for example, limit its contribution to potentially detrimental elevations in $[Na^+]_i$ and (via reverse Na^+/Ca^{2+} exchange) $[Ca^{2+}]_i$, albeit at the expense of a reduced rate of acid extrusion.

The observation that the increase in pH_i observed during anoxia was not inhibited under reduced Na^+_o conditions indicates that Na^+/H^+ exchange does not make a major contribution to this phase of the pH_i response, as expected if exchange activity is reduced shortly following the onset of anoxia. Similar findings have been made in rat central neurons in slice preparations (Pirttilä & Kauppinen, 1992) and in primary culture (Diarra *et al.* 1999), although it appears contrary to a recent report in mouse hippocampal neurons (Yao *et al.* 2001). In the present study, it was observed that, under $NMDG^+$-substituted conditions, rates of pH_i recovery from internal acid loads imposed during anoxia were *increased* compared with rates observed prior to anoxia under $NMDG^+$-substituted conditions (Fig. 3.6*C*), suggesting that a Na^+_o- and HCO_3^--independent acid extrusion pathway is activated by anoxia. In the following Chapter, I will examine further the contribution of this alternate acid extrusion pathway to the neuronal pH_i response to anoxia.

In conclusion, the present study suggests that Na^+/H^+ exchange activity in adult rat hippocampal CA1 pyramidal neurons is reduced during anoxia. These findings suggest that, as in cardiac myocytes (Bond *et al.* 1993; Park *et al.* 1999), the neuroprotective effects of selective Na^+/H^+ exchange inhibitors (e.g. Vornov *et al.* 1996; Phillis *et al.* 1999; Horikawa *et al.* 2001a and b) are unlikely to be exerted during anoxia.

Table 3.1: Anoxia-evoked changes in steady-state pH_i

Buffering condition	*n*	Magnitude (pH units) of:		
		pH_i decrease during anoxia	pH_i increase during anoxia	pH_i increase after anoxia
HCO_3^-/CO_2	14	0.17 ± 0.02	0.07 ± 0.01	0.15 ± 0.05$^{N.S.}$
HCO_3^-/CO_2 (Ar)*	4	0.14 ± 0.01	0.08 ± 0.01	0.18 ± 0.07
Hepes	38	0.15 ± 0.01	0.05 ± 0.01	0.21 ± 0.02
Hepes, Ca^{2+}_o-free	6	0.18 ± 0.03	0.06 ± 0.01	0.18 ± 0.04
Hepes (HPTS)†	4	0.08 ± 0.02	0.06 ± 0.03	0.23 ± 0.07

Experiments were performed at 37°C, pH_o 7.35. Unless otherwise noted, 5 min anoxia was induced with sodium dithionite and BCECF was employed as the pH indicator. * 5 min anoxia was induced by exposure to medium equilibrated with 5% CO_2/95% Ar for ≥18 h. † HPTS was the pH indicator. N.S. indicates no statistically significant difference between the corresponding parameter obtained in response to 5 min anoxia under HCO_3^-/CO_2-free, Hepes-buffered conditions (unpaired, two-tailed Student's *t*-test; $P = 0.19$). The pH_i decrease during anoxia is the difference between the pre-anoxic steady-state pH_i value and the lowest pH_i value observed during anoxia. The pH_i increases during and after anoxia are, respectively, the difference between the pH_i value observed immediately prior to the return to normoxia and the minimum pH_i value observed during anoxia, and the difference between the highest pH_i value observed after anoxia and the pre-anoxic steady-state pH_i value.

Fig. 3.1. Steady-state pH_i changes evoked by transient periods of anoxia. *A*, shown are the steady-state pH_i changes evoked by 5 min anoxia in a single acutely isolated adult rat hippocampal CA1 pyramidal neuron. Anoxia was imposed under HCO_3^-/CO_2-buffered conditions by exposure to medium containing sodium dithionite. Beneath the pH_i trace is shown the BI_{452} values (filled circles) employed in the measurement of pH_i. The stability of the BI_{452} values indicates that the relatively persistent nature of the increase in pH_i observed after anoxia is not an artifact produced by a decline in BI_{452} values consequent upon a deterioration of membrane integrity (see Chapter 2; Bevensee *et al.* 1995). *B*, a 5 min period of anoxia was imposed by exposure to HCO_3^-/CO_2-buffered medium that had been bubbled vigorously with 5% CO_2/95% ultrahigh purity Ar for 20 hours. In *A* and *B*, records were obtained at 37°C and pH_o was 7.35 throughout.

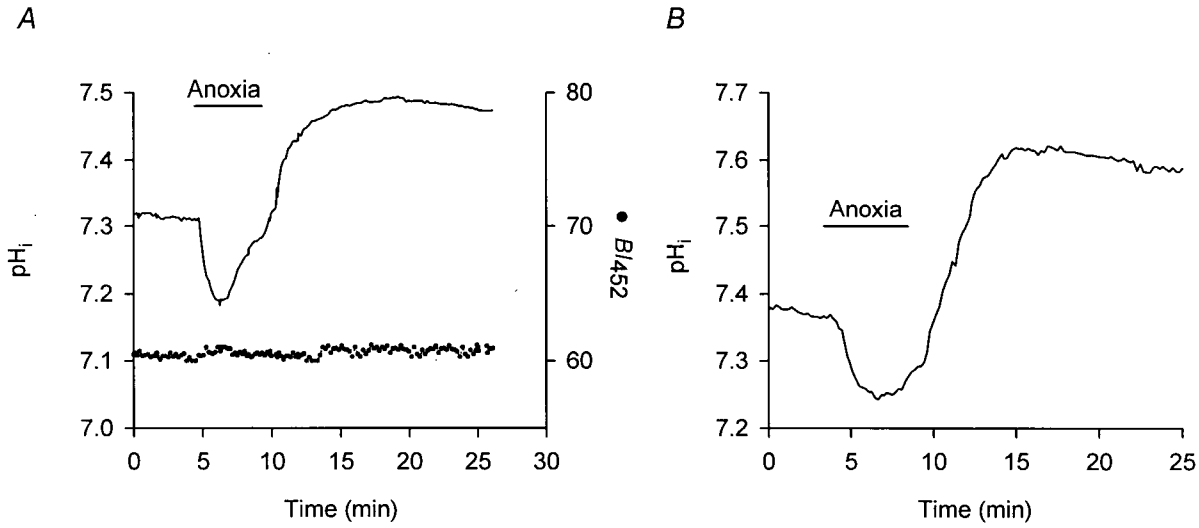
A
Anoxia
7.5
7.4
7.3
7.2
7.1
7.0
pHi
80
70
60
● Bi/452
0
5
10
15
20
25
30
Time (min)
B
Anoxia
7.7
7.6
7.5
7.4
7.3
7.2
pHi
0
5
10
15
20
25
Time (min)

Fig. 3.2. Relationship between pre-anoxic resting pH_i values and anoxia-evoked changes in steady-state pH_i. *A*, comparison of the 'typical' (solid line) and 'atypical' (open circles) pH_i responses to 5 min anoxia in two different BCECF-loaded neurons exposed to sodium dithionite-containing, Hepes-buffered medium. Note the low resting pH_i value in the neuron which responded to anoxia with a small reduction in pH_i that gave way to a large internal alkalinization that started during anoxia and continued into the post-anoxic period. *B*, scatter plot relating magnitude of the fall in pH_i observed during anoxia to pre-anoxic resting pH_i values under HCO_3^-/CO_2-(open circles) and Hepes-(filled circles) buffered conditions (n = 14 and 51, respectively). Solid and dashed lines represent linear regression fits to data obtained under HCO_3^-/CO_2- and Hepes-buffered conditions, respectively (correlation coefficient = 0.80 and 0.67, respectively; $P < 0.0005$ in each case). *C*, scatter plot relating magnitude of the rise in pH_i observed following anoxia to pre-anoxic resting pH_i values under HCO_3^-/CO_2-(open circles) and Hepes-(filled circles) buffered conditions (n = 14 and 51, respectively). Solid and dashed lines represent linear regression fits to data obtained under HCO_3^-/CO_2- and Hepes-buffered conditions, respectively (in each case, correlation coefficient = 0.63; $P < 0.02$ in each case).

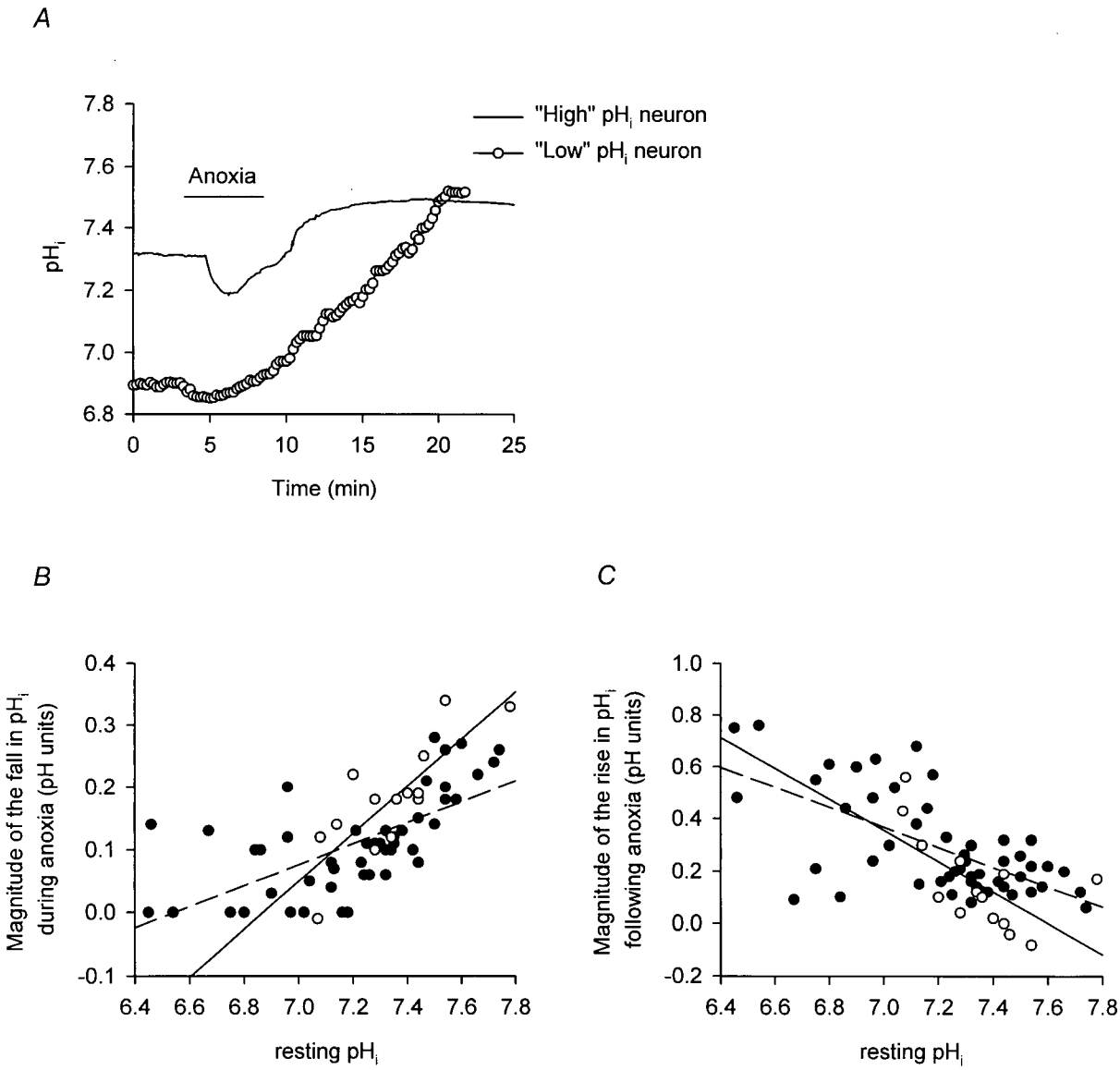
A
7.8
7.6
7.4
7.2
7.0
6.8
pHi
Anoxia
"High" pHi neuron
"Low" pHi neuron
0
5
10
15
20
25
Time (min)
B
0.4
0.3
0.2
0.1
0.0
-0.1
Magnitude of the fall in pHi during anoxia (pH units)
6.4
6.6
6.8
7.0
7.2
7.4
7.6
7.8
resting pHi
C
1.0
0.8
0.6
0.4
0.2
0.0
-0.2
Magnitude of the rise in pHi following anoxia (pH units)
6.4
6.6
6.8
7.0
7.2
7.4
7.6
7.8
resting pHi

Fig. 3.3. Effects of anoxia on steady-state pH_i and fura-2-derived BI_{334}/BI_{380} ratio values in the presence and absence of external Ca^{2+}. *A*, in the presence of 2 mM external Ca^{2+}, 5 min anoxia imposed under Hepes-buffered conditions induced a typical pattern of pH_i changes (filled circles). Compare with Fig. 3.1*A*, the same experiment conducted under HCO_3^-/CO_2-buffered conditions in a neuron with a similar resting pH_i prior to anoxia. The open circles illustrate the changes in fura-2-derived BI_{334}/BI_{380} ratio values (representing changes in $[Ca^{2+}]_i$) evoked by 5 min anoxia in a parallel experiment under identical conditions employing a sister neuron. *B*, upon exposure to Ca^{2+}-free medium, pH_i (filled circles) increased to a new steady-state value. The break in the pH_i trace indicates a 2 min gap in the recording. When a new steady-state pH_i value had been reached, 5 min anoxia induced a triphasic pattern of pH_i changes, none of the components of which were significantly different from those observed in the presence of 2 mM $Ca^{2+}{}_o$. In contrast, measured in a sister neuron in a parallel experiment under identical conditions, the rise in BI_{334}/BI_{380} ratio values (open circles) was significantly attenuated (note the change of scale for the BI_{334}/BI_{380} axis between *A* and *B*). There was also a small, reversible rise in BI_{334}/BI_{380} ratio values in the immediate post-anoxic period (see text). All records were obtained at 37°C under Hepes-buffered conditions at pH_o 7.35.

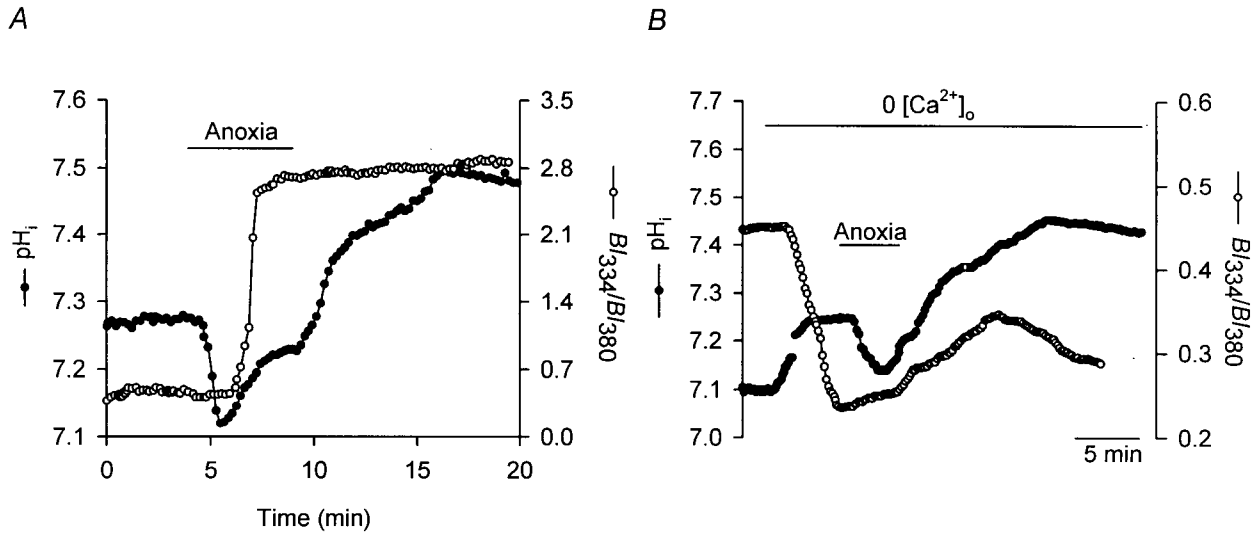
A
B
Anoxia
0 [Ca2+]o
pHi
BI334/BI380
Time (min)
5 min
7.6
7.5
7.4
7.3
7.2
7.1
7.0
7.7
3.5
2.8
2.1
1.4
0.7
0.0
0.6
0.5
0.4
0.3
0.2
0
5
10
15
20

Fig. 3.4. Anoxia-evoked changes in pH_i measured with HPTS. A representative record of the pH_i changes evoked by 5 min anoxia (sodium dithionite) in a neuron in which HPTS was employed as the pH_i indicator. The experiment was performed under HCO_3^--free, Hepes-buffered conditions at 37°C and pH_o 7.35 (see Table 3.1).

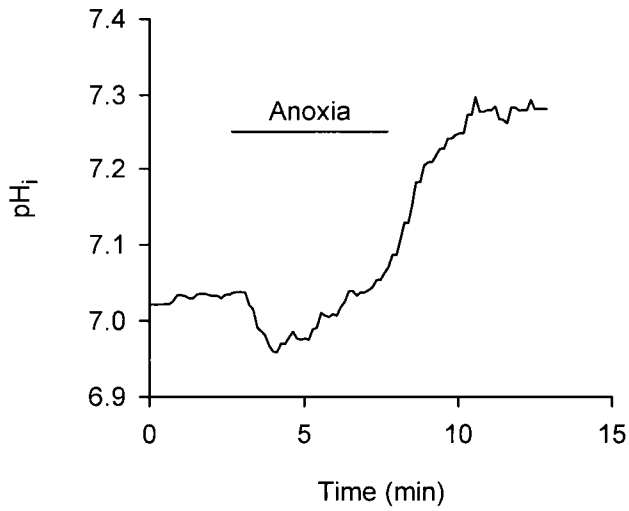
7.4
7.3
7.2
7.1
7.0
6.9
pHi
Anoxia
0
5
10
15
Time (min)

Fig. 3.5. The effects of external Na^+ substitutions on the magnitudes of the fall (*A*) and rise (*B*) in pH_i observed during anoxia under HCO_3^--free, Hepes-buffered conditions (pH_o 7.35, 37°C). Data were obtained under control conditions (normal Na^+_o-containing; open bars); under reduced-Na^+_o, $NMDG^+$-substituted conditions (hatched bars); and under reduced-Na^+_o, Li^+-substituted conditions (cross-hatched bars). * indicates $P < 0.05$ compared to control or Li^+-substituted conditions. N.S. indicates no significant difference ($P = 0.20$) between the fall in pH_i evoked by anoxia under normal Na^+_o-containing compared to Li^+_o-substituted conditions.

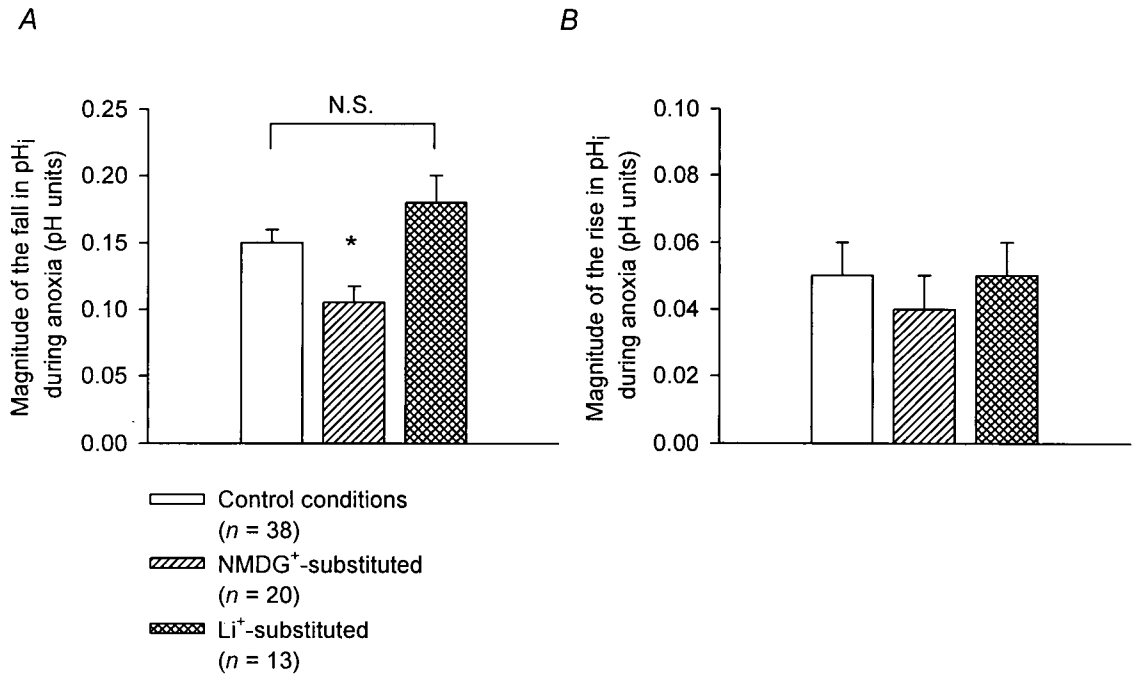
A
B
N.S.
*
Magnitude of the fall in pHi during anoxia (pH units)
0.25
0.20
0.15
0.10
0.05
0.00
Magnitude of the rise in pHi during anoxia (pH units)
0.10
0.08
0.06
0.04
0.02
0.00
Control conditions
(n = 38)
NMDG+-substituted
(n = 20)
Li+-substituted
(n = 13)

Fig. 3.6. Rates of pH_i recovery from internal acid loads are reduced during anoxia. All experiments were performed under Hepes-buffered conditions at pH_o 7.35, 37°C. *A*, following the first NH_4^+-induced intracellular acid load, pH_i was allowed to recover. A second acid load was then imposed after the start of anoxia. *Inset*, superimposed records of the recoveries of pH_i from acid loads imposed prior to (filled circles) and during (open circles) anoxia; the rate of recovery of pH_i was reduced during anoxia. *B*, the pH_i dependencies of rates of pH_i recovery prior to (filled circles) and during (open circles) anoxia under control conditions (normal $[Na^+]_o$). Continuous lines represent the weighted nonlinear regression fits to the data points indicated for each experimental condition (n = 9 in each case). *C*, the pH_i dependencies of rates of pH_i recovery prior to (filled squares) and during (open squares) anoxia under reduced Na^+_o, $NMDG^+$-substituted conditions. Continuous lines represent the weighted nonlinear regression fits to the data points indicated for each experimental condition (n = 5 in each case). *D*, rates of pH_i recovery from internal acid loads imposed prior to anoxia under normal Na^+_o-containing conditions (black bar) were faster than those observed prior to anoxia under reduced-Na^+_o, $NMDG^+$-substituted conditions (hatched bar) and during anoxia, under both normal Na^+_o-containing (open bar) and reduced-Na^+_o, $NMDG^+$-substituted conditions (cross-hatched bar) (P < 0.05 in each case). There was no significant difference (N.S., P = 0.50) between rates of pH_i recovery from acid loads imposed during anoxia under normal Na^+_o-containing and reduced-Na^+_o, $NMDG^+$-substituted conditions. Rates of pH_i recovery shown were determined at a common test pH_i of 6.80. *E*, the Na^+_o-dependent component of pH_i recovery prior to (filled circles) and during (open circles) anoxia, revealed by plotting the differences between the regression fits of pH_i *vs.* dpH_i/dt plots obtained under normal Na^+_o-containing conditions and reduced-Na^+_o, $NMDG^+$-substituted conditions.

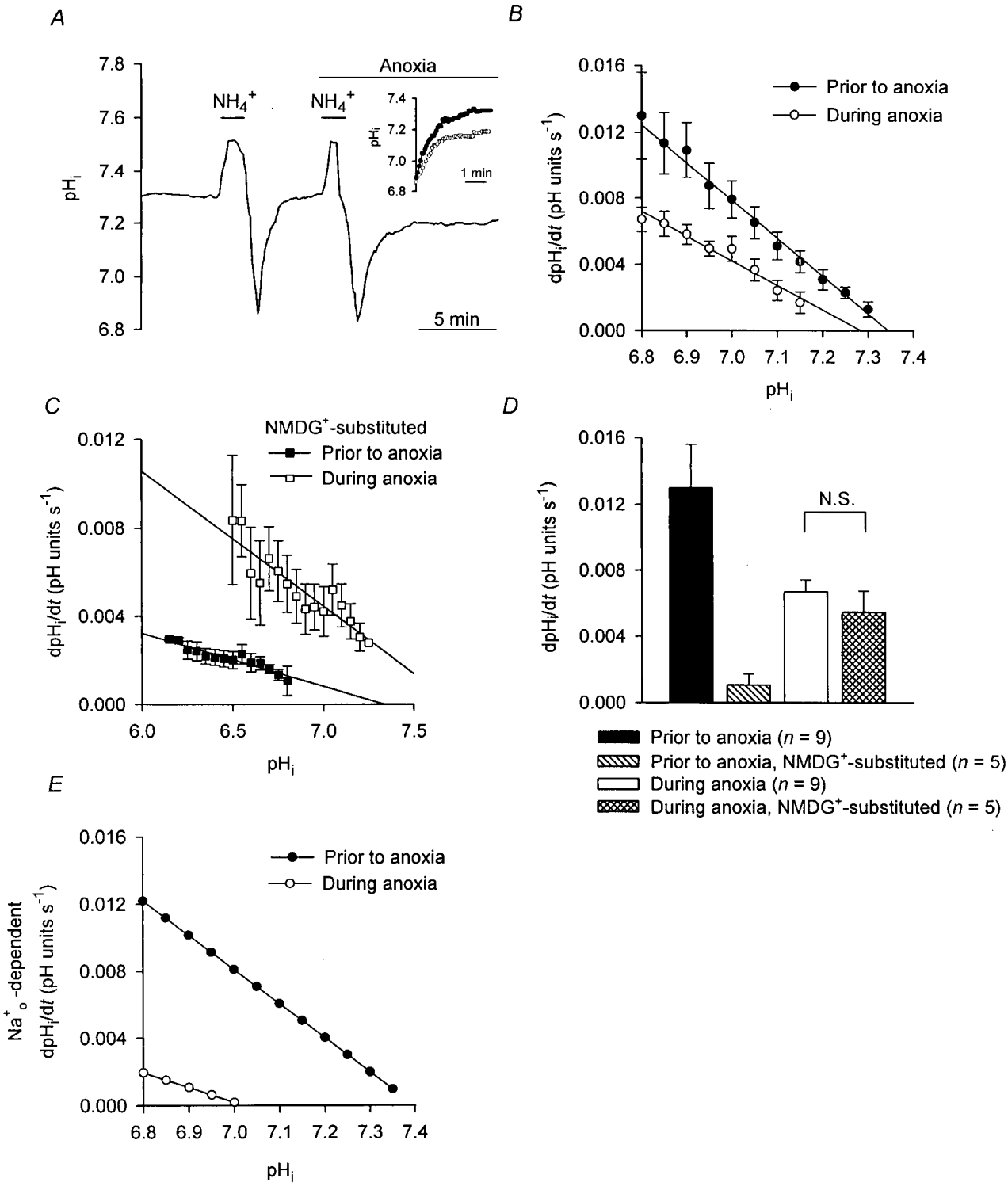
A
Anoxia
NH4+
NH4+
pHi
7.8
7.6
7.4
7.2
7.0
6.8
5 min
1 min
B
Prior to anoxia
During anoxia
dpHi/dt (pH units s-1)
0.016
0.012
0.008
0.004
0.000
6.8 6.9 7.0 7.1 7.2 7.3 7.4
pHi
C
NMDG+-substituted
Prior to anoxia
During anoxia
dpHi/dt (pH units s-1)
0.012
0.008
0.004
0.000
6.0 6.5 7.0 7.5
pHi
D
N.S.
dpHi/dt (pH units s-1)
0.016
0.012
0.008
0.004
0.000
Prior to anoxia (n = 9)
Prior to anoxia, NMDG+-substituted (n = 5)
During anoxia (n = 9)
During anoxia, NMDG+-substituted (n = 5)
E
Prior to anoxia
During anoxia
Na+o-dependent dpHi/dt (pH units s-1)
0.016
0.012
0.008
0.004
0.000
6.8 6.9 7.0 7.1 7.2 7.3 7.4
pHi

Fig. 3.7. Rates of pH_i recovery from internal acid loads prior to and during anoxia in neurons with "low" resting pH_i values. All experiments were performed under Hepes-buffered conditions at pH_o 7.35, 37°C. *A*, the pH_i dependencies of rates of pH_i recovery prior to (filled circles) and during (open circles) anoxia under control conditions (normal $[Na^+]_o$) were determined in 3 neurons in experiments of the type illustrated in Fig. 3.6*A*. Continuous lines represent the weighted nonlinear regression fits to the data points indicated for each experimental condition. *B*, rates of pH_i recovery from internal acid loads imposed prior to anoxia under normal Na^+_o-containing conditions (black bar) were faster than those observed prior to anoxia under reduced-Na^+_o, $NMDG^+$-substituted conditions (hatched bar; $P < 0.05$). There was no significant difference (N.S., $P = 0.56$) between rates of pH_i recovery from acid loads imposed during anoxia under normal Na^+_o-containing and reduced-Na^+_o, $NMDG^+$-substituted conditions (compare with Fig. 3.6*D*, the same finding in "high" pH_i neurons). Rates of pH_i recovery are illustrated at a common test pH_i of 6.80. *D*, the Na^+_o-dependent component of pH_i recovery prior to (filled circles) and during (open circles) anoxia, revealed by plotting the differences between the regression fits of pH_i *vs.* dpH_i/dt plots obtained under normal Na^+_o-containing conditions and reduced-Na^+_o, $NMDG^+$-substituted conditions (compare with Fig. 3.6*E*, the similar finding in "high" pH_i neurons).

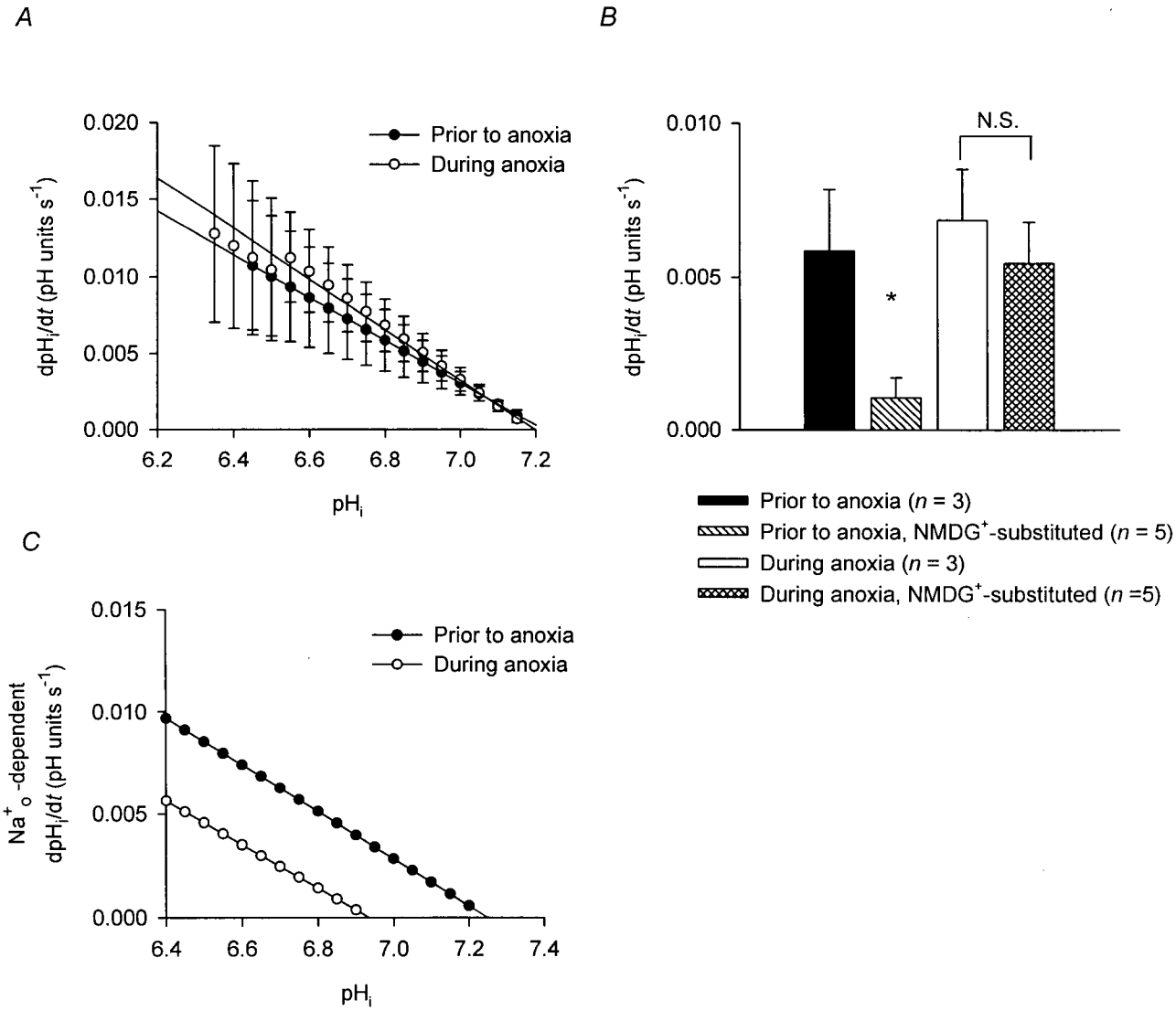
A
0.020
0.015
0.010
0.005
0.000
6.2
6.4
6.6
6.8
7.0
7.2
pHi
dpHi/dt (pH units s-1)
Prior to anoxia
During anoxia
B
0.010
0.005
0.000
N.S.
*
dpHi/dt (pH units s-1)
Prior to anoxia (n = 3)
Prior to anoxia, NMDG+-substituted (n = 5)
During anoxia (n = 3)
During anoxia, NMDG+-substituted (n =5)
C
0.015
0.010
0.005
0.000
6.4
6.6
6.8
7.0
7.2
7.4
pHi
Na+o-dependent dpHi/dt (pH units s-1)
Prior to anoxia
During anoxia

Fig. 3.8. pH_i recovery from acid loads imposed prior to and during anoxia under reduced pH_o conditions. Experiments were performed under Hepes-buffered conditions at 37°C. *A*, an initial acid load was imposed prior to anoxia at pH_o 7.35. After the recovery of pH_i, pH_o was reduced to 6.60 and, when pH_i had stabilized at a new resting level (pH 6.80 ± 0.05, $n = 9$), a second acid load was imposed during anoxia. *B*, the pH_i dependencies of rates of pH_i recovery from internal acid loads imposed during anoxia under normal Na^+_o-containing conditions at pH_o 6.60 (open squares). Also illustrated are the pH_i dependencies of rates of pH_i recovery from internal acid loads imposed prior to (filled circles) and during (open circles) anoxia under normal Na^+_o-containing conditions at pH_o 7.35 (see Fig. 3.6*B*). A comparison for overall coincidence of the regression fits representing the pH_i dependencies of rates of pH_i recovery under pH_o 7.35 and pH_o 6.60 conditions indicated that the rate of pH_i recovery from acid loads imposed during anoxia at pH_o 6.60 was significantly slower ($P < 0.05$) than the rate established during anoxia at pH_o 7.35. *C*, rates of pH_i recovery from internal acid loads imposed prior to and during anoxia under the conditions shown on the figure, measured at a common test pH_i of 6.40. Rates of pH_i recovery from acid loads imposed prior to (black bar) and during (open bar) anoxia under normal Na^+_o-containing conditions at pH_o 7.35 were estimated by extrapolating the weighted nonlinear regression fits relating absolute pH_i values to the rates of pH_i recovery obtained under each experimental condition (see *B*). At pH_o 6.60, there was no significant difference (N.S., $P = 0.35$) between rates of pH_i recovery from internal acid loads imposed during anoxia under Na^+_o-containing or reduced-Na^+_o, $NMDG^+$-substituted conditions. *D*, the Na^+_o-dependent component of pH_i recovery prior to and during anoxia at pH_o 6.60, revealed by plotting the difference between the regression fits of pH_i *vs.* dpH_i/dt plots obtained under normal Na^+_o-containing

conditions and reduced-Na^+_o, $NMDG^+$-substituted conditions (note the change in scale of the *y*-axis from *C*). Rates were measured at a common test pH_i of 6.40.

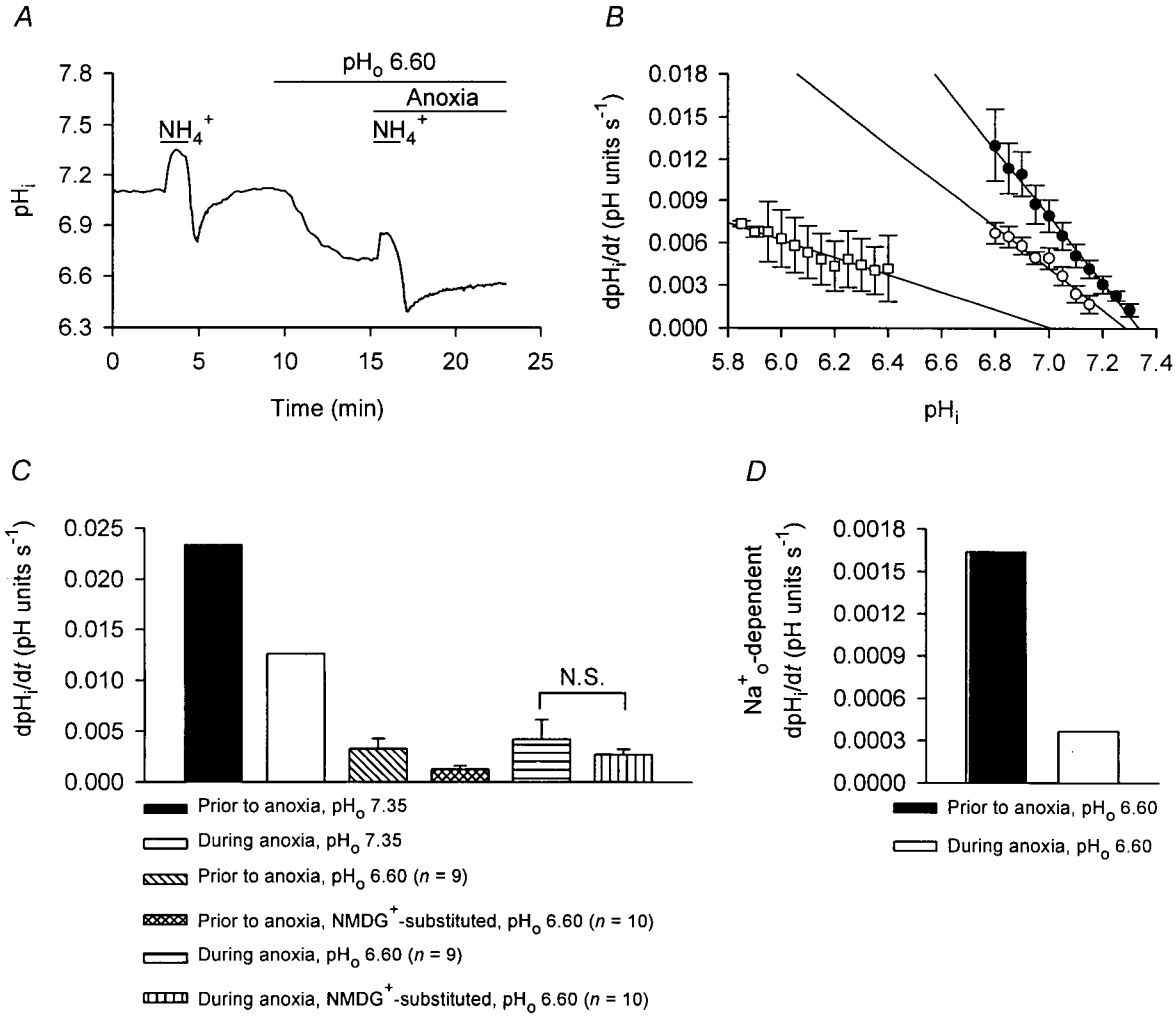
A
pH$_o$ 6.60
Anoxia
NH$_4^+$
NH$_4^+$
pH$_i$
7.8
7.5
7.2
6.9
6.6
6.3
0
5
10
15
20
25
Time (min)
B
dpH$_i$/dt (pH units s^{-1})
0.018
0.015
0.012
0.009
0.006
0.003
0.000
5.8
6.0
6.2
6.4
6.6
6.8
7.0
7.2
7.4
pH$_i$
C
dpH$_i$/dt (pH units s^{-1})
0.025
0.020
0.015
0.010
0.005
0.000
N.S.
Prior to anoxia, pH$_o$ 7.35
During anoxia, pH$_o$ 7.35
Prior to anoxia, pH$_o$ 6.60 (n = 9)
Prior to anoxia, NMDG$^+$-substituted, pH$_o$ 6.60 (n = 10)
During anoxia, pH$_o$ 6.60 (n = 9)
During anoxia, NMDG$^+$-substituted, pH$_o$ 6.60 (n = 10)
D
Na^+_o-dependent dpH$_i$/dt (pH units s^{-1})
0.0018
0.0015
0.0012
0.0009
0.0006
0.0003
0.0000
Prior to anoxia, pH$_o$ 6.60
During anoxia, pH$_o$ 6.60

Fig. 3.9. Treatment with 2-DG and antimycin A under normoxic conditions slows the rates of pH_i recovery from internal acid loads. *A*, superimposed records of the recoveries of pH_i from acid loads imposed in a CA1 neuron prior to and following 10 min incubation with 2-DG and antimycin A (2-DG + A). The rate of recovery of pH_i was reduced following ATP depletion. *B*, rates of pH_i recovery following 10 min incubation with 2-DG + A (open bar) were significantly slower than those observed in the same neurons prior to ATP depletion (black bar). No significant difference (N.S., $P = 0.49$) was observed between rates of pH_i recovery from acid loads imposed following exposure to 2-DG + A under normal Na^+_o-containing and reduced-Na^+_o, $NMDG^+$-substituted conditions. *C*, the Na^+_o-dependent component of pH_i recovery prior to (black bar) and following (open bar) 10 min exposure to 2-DG + A, revealed by plotting the difference between the regression fits of pH_i *vs.* dpH_i/dt plots obtained under normal Na^+_o-containing and reduced-Na^+_o, $NMDG^+$-substituted conditions. In *B* and *C*, rates of pH_i recovery were determined at a common test pH_i of 7.00.

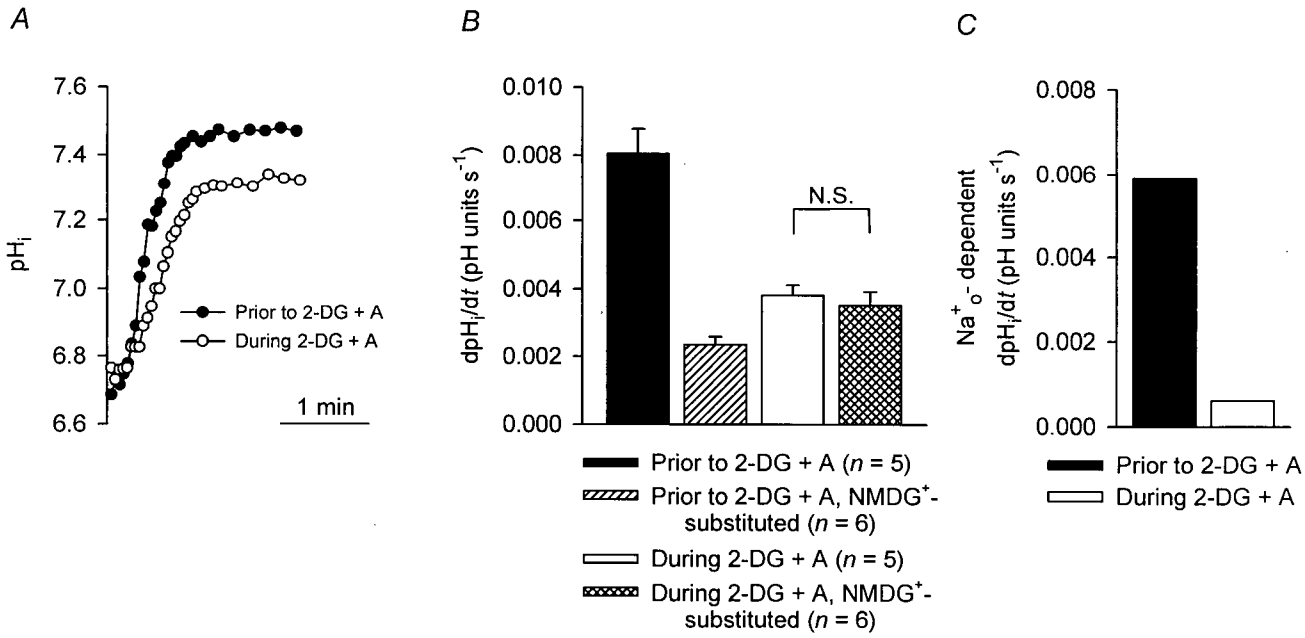
A
7.6
7.4
7.2
7.0
6.8
6.6
pHi
Prior to 2-DG + A
During 2-DG + A
1 min
B
0.010
0.008
0.006
0.004
0.002
0.000
dpHi/dt (pH units s-1)
N.S.
Prior to 2-DG + A (n = 5)
Prior to 2-DG + A, NMDG+-substituted (n = 6)
During 2-DG + A (n = 5)
During 2-DG + A, NMDG+-substituted (n = 6)
C
0.008
0.006
0.004
0.002
0.000
Na+o- dependent dpHi/dt (pH units s-1)
Prior to 2-DG + A
During 2-DG + A

Fig. 3.10. pH_i recovery from internal acid loads in creatine-pretreated neurons. *A*, superimposed records of the recoveries of pH_i from acid loads imposed prior to and during anoxia in a CA1 pyramidal neuron isolated from a hippocampal slice pretreated for 2 h with 10 mM creatine. In contrast to untreated neurons (see Fig. 3.6*A*), the rate of pH_i recovery from the acid load imposed during anoxia was not slowed. *B*, in neurons pretreated with 10 mM creatine, rates of pH_i recovery measured at ~3 min after the start of anoxia under normal Na^+_o-containing conditions (open bar) were not significantly different to those observed in the same neurons prior to anoxia (black bar; N.S., $P = 0.84$). Reducing Na^+_o ($NMDG^+$-substitution) slowed rates of pH_i recovery from acid loads imposed both prior to and during anoxia (hatched and cross-hatched bars, respectively; *, $P < 0.05$ in each case). *C*, the Na^+_o-dependent component of pH_i recovery prior to (black bar) and during (open bar) anoxia in neurons isolated from creatine-treated slices, revealed by plotting the difference between the regression fits to pH_i *vs.* dpH_i/dt plots obtained under normal Na^+_o-containing conditions and reduced-Na^+_o, $NMDG^+$-substituted conditions. In *B* and *C*, rates of pH_i recovery were determined at a common test pH_i of 7.00.

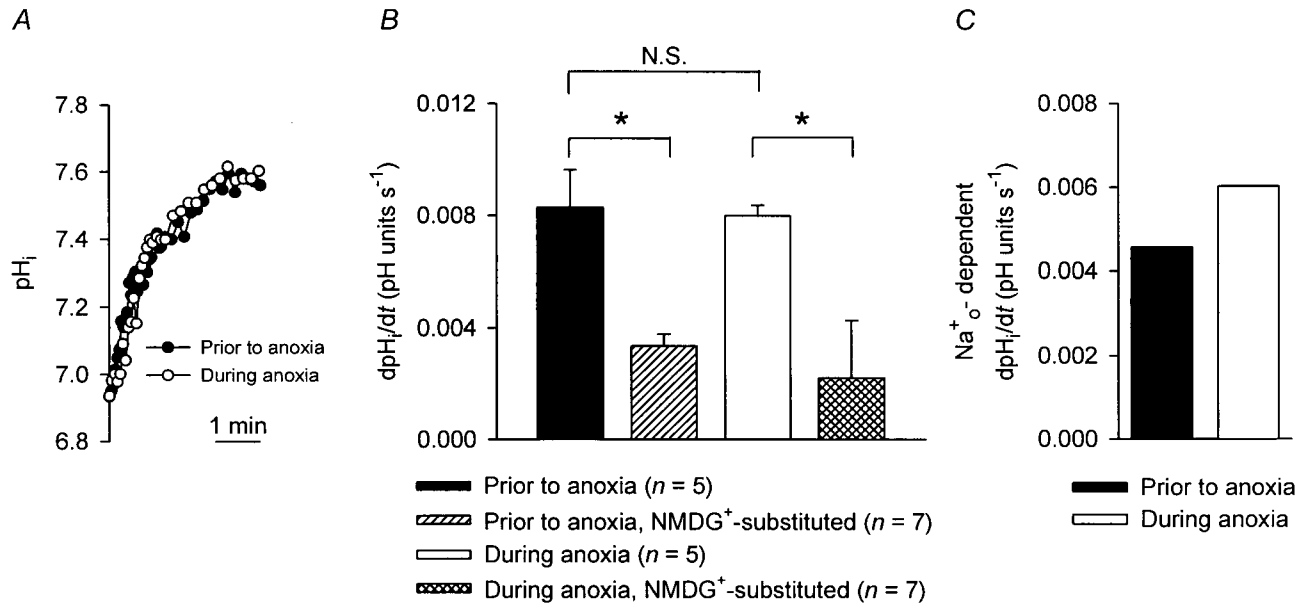
A
7.8
7.6
7.4
7.2
7.0
6.8
pHi
Prior to anoxia
During anoxia
1 min
B
N.S.
*
*
0.012
0.008
0.004
0.000
dpHi/dt (pH units s-1)
Prior to anoxia (n = 5)
Prior to anoxia, NMDG+-substituted (n = 7)
During anoxia (n = 5)
During anoxia, NMDG+-substituted (n = 7)
C
0.008
0.006
0.004
0.002
0.000
Na+o- dependent dpHi/dt (pH units s-1)
Prior to anoxia
During anoxia

CHAPTER FOUR

INTRACELLULAR pH RESPONSE TO ANOXIA IN ACUTELY ISOLATED ADULT RAT HIPPOCAMPAL CA1 PYRAMIDAL NEURONS: INCREASED Na^+/H^+ EXCHANGE ACTIVITY AFTER ANOXIA[6]

4.0. INTRODUCTION

The potential importance of Na^+/H^+ exchange activity to ischemic neuropathology is suggested by findings that pharmacological blockers of Na^+/H^+ exchange exert a protective effect in neurons in which the antiport is sensitive to such compounds (e.g. Vornov *et al.* 1996; Kuribayashi *et al.* 1999; Phillis *et al.* 1999); however, the timing of these neuroprotective actions is uncertain. The results presented in Chapter 3 suggested that Na^+/H^+ exchange activity in acutely isolated adult rat hippocampal CA1 pyramidal neurons is reduced shortly following the onset of anoxia. In the present Chapter, the possibility that Na^+/H^+ exchange activity may become activated following anoxia was investigated. Na^+/H^+ exchange inhibitors have been shown to limit post-ischemic amino acid release (Phillis *et al.* 1998), free fatty acid efflux (Pilitsis *et al.* 2001) and cerebral Na^+ and water content (Kuribayashi *et al.* 1999; also see Chapters 5 and 6), suggesting that Na^+/H^+ exchange may be active during reperfusion. Thus, the *first* aim of this study was to examine Na^+/H^+ exchange activity in acutely isolated adult rat hippocampal CA1 pyramidal neurons in the immediate post-anoxic period.

In addition to Na^+/H^+ exchange, studies in cultured postnatal rat hippocampal (Diarra *et al.* 1999) and fetal mouse neocortical (Jørgensen *et al.* 1999) neurons point to the involvement of

---

[6] A version of this chapter has been published. Sheldon C. and Church J. (2002) Intracellular pH response to anoxia in acutely dissociated adult rat hippocampal CA1 neurons. J. Neurophysiol 87: 2209-2224.

a Zn^{2+}-sensitive acid extrusion mechanism in the neuronal pH_i response to anoxia. Indeed, results presented in Chapter 3 illustrated that a Na^+_o- and HCO_3^--independent mechanism(s) contributes to the increase in pH_i observed during anoxia. Therefore, the *second* aim of this study was to further examine the activity of this additional acid extrusion mechanism during and following periods of anoxia in acutely isolated adult rat hippocampal CA1 pyramidal neurons.

4.1. MATERIALS AND METHODS

4.1.1. Experimental preparation

In all experiments presented in this Chapter, BCECF-loaded acutely isolated adult rat hippocampal CA1 pyramidal neurons were used. Nominally HCO_3^-/CO_2-free, Hepes-buffered media were employed in all experiments, which were conducted at 37°C and pH_o 7.35 (unless otherwise noted).

4.1.2. Experimental maneuvers

The effects of transient periods of anoxia were examined on both steady-state pH_i and on rates of pH_i recovery from internal acid loads imposed by the NH_4^+ prepulse technique. To compare the steady-state pH_i changes evoked by anoxia under the various experimental conditions, the magnitudes of the increases in pH_i observed during and after anoxia were measured (as described in Chapter 3, Section 3.1.3). In experiments in which rates of pH_i recovery were examined, internal acid loads were imposed immediately following 5 min anoxia. In experiments where the composition of the external medium was altered during the recovery of pH_i from an intracellular

acid load (see Figs. 4.6 and 4.7), individual portions of the recovery were fit to a linear equation, as described by Raley-Susman *et al.* (1991).

Data are reported as mean ± S.E.M. with the accompanying *n* value referring to the number of neurons from which data were obtained. Statistical analyses were performed with Student's two-tailed paired or unpaired *t* tests, as appropriate. Significance was assumed at the 5% level.

4.2. RESULTS

4.2.1. Na^+/H^+ exchange activity in the immediate post-anoxic period

The following series of experiments were designed to examine Na^+/H^+ exchange activity in the immediate post-anoxic period. I first examined whether inhibiting Na^+/H^+ exchange activity influenced the magnitude of the increase in steady-state pH_i observed following anoxia (described in Chapter 3, Section 3.2.2; Fig. 4.1*A*). To inhibit Na^+/H^+ exchange activity, neurons were perfused with reduced-Na^+, $NMDG^+$-substituted medium prior to, during and following anoxia. Under these conditions, the increase in pH_i observed following anoxia was significantly reduced compared to the increase in pH_i observed following anoxia in the presence of normal Na^+_o (Fig. 4.1*A*, *B*). Under reduced-Na^+_o, Li^+-substituted conditions, conditions which support Na^+/H^+ exchange activity (see Raley-Susman *et al.* 1991; Baxter & Church, 1996), the increase in pH_i observed after anoxia was restored to control levels (Fig. 4.1*A*, *B*). The results are consistent with the possibility that Na^+/H^+ exchange becomes active after anoxia and contributes to the internal alkalinization observed at this time.

To further examine Na^+/H^+ exchange activity in the immediate post-anoxic period, I compared rates of pH_i recovery from internal acid loads imposed prior to and immediately following anoxia. Examined in 17 neurons with a mean resting pH_i of 7.34 ± 0.02, instantaneous rates of pH_i recovery were increased significantly after anoxia at all absolute values of pH_i (Fig. 4.2*A*, *B*). The increases in pH_i evoked by NH_4^+ (quantified by taking the difference between the steady-state pH_i immediately prior to the application of NH_4^+ and the maximum pH_i observed during its application; see Smith *et al.* 1998) were similar prior to and after anoxia (0.24 ± 0.02 and 0.21 ± 0.02 pH unit increases, respectively; $n = 17$ in each case; $P = 0.16$), suggesting that marked alterations in intracellular buffering power are unlikely to underlie the changes in the rates of pH_i recovery observed after anoxia. Next, internal acid loads were imposed under reduced-Na^+_o, $NMDG^+$-substituted conditions ($n = 5$); rates of pH_i recovery after anoxia were significantly slower than the corresponding rates observed in the presence of Na^+_o (Fig. 4.2*B*). Consistent with the possibility that Na^+/H^+ exchange activation was occurring in the immediate post-anoxic period, plots of the differences between rates of pH_i recovery under Na^+_o-containing and reduced-Na^+_o ($NMDG^+$-substituted) conditions both prior to and after anoxia (Fig. 4.2*C*) revealed an increased contribution from a Na^+_o-dependent mechanism to pH_i recovery from acid loads imposed in the immediate post-anoxic period.

Rates of pH_i recovery prior to and following anoxia were also determined in 5 "low" pH_i neurons (average resting pH_i 6.89 ± 0.03) and these data are illustrated in Fig. 4.3. As detailed in Chapter 3 (Section 3.2.4.2), rates of pH_i recovery observed in "low" pH_i cells prior to anoxia were slower than rates observed in "high" pH_i cells prior to anoxia (compare Fig. 4.3*A* with Fig. 4.2*B*). Nevertheless, consistent with observations made in "high" pH_i cells, in "low" pH_i cells, rates of pH_i recovery from internal acid loads imposed immediately following anoxia were faster

than rates of pH_i recovery observed prior to anoxia (Fig. 4.3*A* and *B*). As illustrated in Fig. 4.3*B*, compared to rates of pH_i recovery observed in "low" pH_i cells in the presence of normal Na^+_o, reducing external $[Na^+]_o$ ($NMDG^+$-substitution) had only a minor effect on rates of pH_i recovery observed prior to anoxia, but significantly slowed rates of pH_i recovery observed following anoxia. Thus, analogous with findings made in "high" pH_i neurons, the contribution of Na^+_o-dependent mechanism(s) to pH_i recovery from acid loads imposed immediately following anoxia was enhanced in "low" pH_i neurons (Fig. 4.3*C*). According to Bevensee *et al.* (1996) and Smith *et al.* (1998), "low" and "high" pH_i adult rat CA1 neurons appear to represent neurons with "low" and "high" levels of Na^+/H^+ exchange activity, respectively. As outlined in Chapter 3, Na^+/H^+ exchange activity was reduced during anoxia and, accordingly, the magnitude of this reduction was larger in "high" *vs.* "low" pH_i neurons. The present results suggest that Na^+/H^+ exchange activity is increased following anoxia in both "high" and "low" pH_i neurons; however, this effect is more marked in "low" pH_i neurons, presumably reflecting the lower level of Na^+/H^+ exchange activity prior to anoxia in this group of neurons (at a common test pH_i of 6.80, rates of Na^+_o-dependent pH_i recovery immediately following anoxia were increased by ~8.5 and 1.3-fold in "low" and "high" pH_i neurons, respectively; compare Figs. 4.2*C* and 4.3*C*).

Of particular interest is the finding that the apparent activation of Na^+/H^+ exchange in the immediate post-anoxic period occurred even though external pH was held at a constant value (i.e. pH_o 7.35). Thus, a return to normal pH_o values from an external acidification, as would occur after anoxia *in vivo*, is not an absolute requirement for the post-anoxic activation of Na^+/H^+ exchange activity in isolated rat hippocampal neurons. One mechanism that could contribute to the activation of Na^+/H^+ exchange after anoxia is an anoxia-induced change in the activity of intracellular second messenger system(s) which, in turn, act to regulate Na^+/H^+ exchange activity. In hippocampal neurons, the intracellular concentration of cAMP rises rapidly in the immediate

post-anoxic period (e.g. Whittingham *et al.* 1984; Domanska-Janik, 1996; Small *et al.* 1996), and our laboratory has shown previously that increases in $[cAMP]_i$, acting via PKA, activate Na^+/H^+ exchange in acutely isolated rat CA1 neurons under normoxic conditions (Smith *et al.* 1998). Therefore, I investigated the effect of modulating the activity of the cAMP/PKA system on the rise in steady-state pH_i observed after anoxia.

As previously reported (Smith *et al.* 1998), the selective PKA inhibitor *R*p-cAMPS (50 μM) failed to affect steady-state pH_i under Hepes-buffered, normoxic conditions. However, as illustrated in Fig. 4.4*A*, the magnitude of the internal alkalinization observed after anoxia was significantly reduced in the presence of *R*p-cAMPS. In contrast, 50 μM *R*p-cAMPS failed to significantly affect the increase in pH_i observed after anoxia under reduced-Na^+_o ($NMDG^+$-substituted) conditions (Fig. 4.4*B*; also see Fig. 4.5*B* for the effects of $NMDG^+$-substitution on the increase in pH_i observed after anoxia in the absence of *R*p-cAMPS). Similar results were obtained following pretreatment with the adenylate cyclase inhibitor DDA (100 μM), which reduced the magnitude of the increase in pH_i seen after anoxia under normal Na^+_o-containing conditions to 0.11 ± 0.03 pH units ($n = 9$; $P < 0.05$ for the difference to the increase in pH_i observed in the absence of DDA).

The action of β adrenergic agonists to increase $[cAMP]_i$ is potentiated after ischemia (Lin *et al.* 1983; Domanska-Janik, 1996). Therefore, to further assess the role of the cAMP/PKA pathway in the regulation of Na^+/H^+ exchange activity in the immediate post-anoxic period, the effects of β adrenergic agonists on anoxia-evoked changes in pH_i were examined. Stimulation of the cAMP/PKA pathway with the β-adrenoceptor agonist isoproterenol (10 μM) significantly increased the magnitude of the post-anoxic alkalinization, an effect that was attenuated by pretreatment with the full β adrenoceptor antagonist propranolol (20 μM) or *R*p-cAMPS (50 μM; Fig. 4.4*B*). Furthermore, the

isoproterenol-evoked increase in the magnitude of the post-anoxic alkalinization was attenuated significantly under reduced-Na^+_o ($NMDG^+$-substituted) conditions and was restored to control values when Li^+ was employed as the Na^+-substitute (Fig. 4.4*B*). Taken together, the results are consistent with the possibility that anoxia-induced changes in the activity of the cAMP/PKA second messenger system may contribute to the activation of Na^+/H^+ exchange in adult rat hippocampal CA1 pyramidal neurons immediately after anoxia.

4.2.2. Contribution of a Na^+_o- and HCO_3^--independent mechanism to acid extrusion during and following anoxia

A number of lines of evidence presented in this and the preceding Chapter suggests that mechanisms other than Na^+/H^+ exchange must contribute to acid extrusion during and following anoxia in adult rat CA1 neurons. Despite marked reductions in Na^+/H^+ exchange activity shortly following the onset of anoxia, increases in pH_i, in the presence and absence of Na^+_o, were often observed during anoxia (Fig. 3.5). In addition, under conditions that inhibit Na^+/H^+ exchange activity ($NMDG^+$-substitution), the increase in pH_i observed immediately following anoxia was not fully eliminated (Fig. 4.1*B*). In fact, under $NMDG^+$-substituted, Hepes-buffered conditions, rates of pH_i recovery from internal acid loads were increased during *and* following anoxia, compared to rates established prior to anoxia under the same conditions (see Fig 3.6*C* and 4.2*B*), suggesting that a Na^+_o- and HCO_3^--independent acid extrusion pathway is activated by anoxia. The Na^+_o-independent internal alkalinizations that occurred during and following anoxia appeared to be associated temporally with marked and persistent increases in $[Ca^{2+}]_i$ (see Fig. 3.3*A*), raising the possibility that they may reflect H^+ efflux through a H^+-conductive pathway activated by membrane depolarization. In all cell types studied to date, voltage-activated H^+

conductances (g_{H^+}s) are blocked by micromolar concentrations of Zn^{2+} (for reviews see DeCoursey & Cherny, 1994a and 2000; Eder & DeCoursey, 2001; also see Cherny & DeCoursey, 1999). Therefore, the following series of experiments examined the potential contribution of a Zn^{2+}-sensitive, voltage-activated H^+ efflux pathway to the increases in pH_i observed during and following anoxia in isolated rat hippocampal CA1 neurons.

First, I examined the effects of 100 - 500 μM Zn^{2+} on the rises in pH_i observed during and following anoxia. While the application of Zn^{2+} did not change resting pH_i prior to anoxia, there was a significant reduction in the magnitudes of the rises in pH_i observed during and following anoxia (Fig. 4.5*A*, *B*). When Zn^{2+} was applied under reduced-$[Na^+]_o$, $NMDG^+$-substituted conditions, the magnitudes of the rises in pH_i observed during and following anoxia were reduced to values significantly less than those observed under reduced-$[Na^+]_o$, $NMDG^+$-substituted, conditions alone (Fig. 4.5*A*, *B*).

Next, internal acid loads were applied during or immediately after anoxia and pH_i recovery was allowed to proceed in the presence of 100 - 500 μM Zn^{2+} and/or under reduced-Na^+_o, $NMDG^+$-substituted conditions. The recovery of pH_i from internal acid loads imposed during anoxia was markedly inhibited under reduced-Na^+_o conditions in the presence of Zn^{2+}, and there was an increase in the rate of pH_i recovery when Zn^{2+} was removed from the low-Na^+ medium. Rates of pH_i recovery were estimated by linear regression fits to pH_i data obtained under reduced Na^+_o, $NMDG^+$-substituted conditions in the presence of Zn^{2+} and under reduced Na^+_o, $NMDG^+$-substituted conditions upon the removal of Zn^{2+} (for ~120 s after its removal): the slopes of the fitted lines approximated the rates of pH_i recovery (pH units s^{-1}) and, in order to provide estimates of the pH_i values at which rates of pH_i recovery were measured, the pH_i values at the mid-point of the lines ($pH_{0.5}$) were also determined. Rates of pH_i recovery were 1.08 ± 1.0

x 10^{-3} and 2.84 ± 1.20 x 10^{-3} pH units s^{-1} under reduced Na^+_o, $NMDG^+$-substituted conditions in the presence and absence of 250 μM Zn^{2+}, respectively (n = 4 in both cases). Thus, there was an increase in the rate of pH_i recovery when Zn^{2+} was removed from the low-Na^+ medium, although this did not reach statistical significance (P = 0.46), likely reflecting both the limited number of neurons that could tolerate this experimental series and the different pH_i values at which rates were measured (the $pH_{0.5}$ values at which rates were estimated under reduced Na^+_o, $NMDG^+$-substituted conditions in the presence and absence of Zn^{2+} were ~6.4 and 6.7, respectively).

The recovery of pH_i from an internal acid load imposed immediately following anoxia was also markedly inhibited under reduced-Na^+_o conditions in the presence of Zn^{2+}. As illustrated in Fig. 4.6*A*, there was a significant increase in the rate of pH_i recovery when Zn^{2+} was removed from the low-Na^+ medium, and the rate of recovery increased further upon the reintroduction of normal external Na^+. Similar results were obtained in experiments in which pH_i recovery from an acid load imposed following anoxia was allowed to proceed initially under control conditions (i.e. in the presence of normal $[Na^+]_o$ and absence of Zn^{2+}); in these experiments, reducing external Na^+ and/or adding Zn^{2+} also slowed the rate at which pH_i recovered. The pooled results from these series of experiments are presented in Fig. 4.6*B*. Taken together, the results are entirely consistent with the possibilities, raised in light of the steady-state pH_i data, that a Na^+_o- and HCO_3^--independent, Zn^{2+}-sensitive mechanism contributes to acid extrusion during and after anoxia in acutely isolated adult rat CA1 pyramidal neurons.

To assess the possibility that the Zn^{2+}-sensitive component of the recovery of pH_i from acid loads imposed during or following anoxia might be activated by membrane depolarization, internal acid loads were applied during normoxia under Na^+_o-free conditions (i.e. Na^+/H^+ exchange blocked). As illustrated in Fig. 4.7, pH_i recovery in the absence of external Na^+ (see

Bevensee *et al.* 1996; Smith *et al.* 1998) was >2-fold faster under depolarizing (139.5 mM K^+_o) than under control (3 mM K^+_o) conditions ($n \geq 5$ in each case). Furthermore, whereas 100 μM Zn^{2+} failed to affect pH_i recovery under control conditions, the rate of pH_i recovery under high-$[K^+]_o$ conditions was reduced upon the application of Zn^{2+}. In contrast, as illustrated in Fig. 4.8, the effect of high-$[K^+]_o$ to increase rates of pH_i recovery from acid loads imposed under normoxic conditions (in the absence of Na^+_o) was not affected by the P-type H^+,K^+-ATPase inhibitors omeprazole (50 μM; Wu & Delamere, 1997) or SCH-28080 (500 μM; Petrovic *et al.* 2002), or the V-type H^+-ATPase inhibitor bafilomycin A_1 (2 μM; Wu & Delamere, 1997).

4.2.3 Effects of changes in pH_o

Anoxia and ischemia *in vivo* and in slice preparations *in vitro* lead to reductions in pH_o (e.g. Obrenovitch *et al.* 1990; Silver & Erecińska, 1990 and 1992; Roberts & Chih, 1997 and 1998). In addition, the activities of Na^+/H^+ exchangers and g_{H^+}s are reduced by falls in pH_o (Green *et al.* 1988; Vaughan-Jones & Wu, 1990; Wu & Vaughan-Jones, 1997; Ritucci *et al.* 1998; DeCoursey & Cherny, 2000). Therefore, I examined the effects of lowering pH_o on the magnitudes of the increases in pH_i observed during and after anoxia, and compared the anoxia-evoked changes in pH_i observed at pH_o 6.60 with those changes observed under conditions that inhibit Na^+/H^+ exchange activity and/or g_{H^+}s. Lowering pH_o from 7.35 to 6.60 caused a 0.49 ± 0.03 pH unit fall in pH_i ($n = 19$; see Church *et al.* 1998) and, once pH_i had stabilized at a new resting level, anoxia evoked an internal acidification followed by increases in pH_i during and after anoxia that were significantly smaller than those observed at pH_o 7.35 (Fig. 4.5*A*, *B*). Because Na^+/H^+ exchange activity is reduced during anoxia (Chapter 3, Section 3.2.4.2), the attenuation of the rise in pH_i observed during anoxia at pH_o 6.60 is consistent with the suggestion that a putative g_{H^+}

contributes to the rise in pH_i observed during anoxia (see Section 4.2.2). Indeed, there was no difference between the increase in pH_i observed during anoxia in the presence of Zn^{2+} *vs.* at pH_o 6.60 ($P = 0.51$; Fig. 4.5*A*). The effect of pH_o to reduce the increase in pH_i observed after anoxia may reflect an inhibitory effect on Na^+/H^+ exchange activity and/or a g_{H^+} active in the post-anoxic period. In support, there was no difference between the rise in pH_i observed after anoxia at pH_o 6.60 compared with the rise in pH_i observed after anoxia under reduced Na^+_o, NMDG-substituted, conditions in the presence of Zn^{2+} ($P = 0.43$; Fig. 4.5*B*).

Next, intracellular acid loads were imposed prior to and following anoxia at pH_o 6.60 (Fig. 4.9*A*; see Chapter 3, Section 3.2.4.2 for the effect of pH_o 6.60 on rates of pH_i recovery from internal acid loads imposed prior to and during anoxia). Consistent with observations made in Chapter 3, rates of pH_i recovery prior to anoxia were decreased at pH_o 6.60, compared to rates of pH_i recovery observed at the same absolute values of pH_i under control (pH_o 7.35) conditions (Fig. 4.9*B*). When acid loads were imposed immediately after anoxia, rates of pH_i recovery increased, compared to rates of recovery established prior to anoxia also at pH_o 6.60 ($n = 9$; Fig. 4.9*A, B*; $P < 0.05$ at each absolute value of pH_i). Nevertheless, plots of the pH_i dependence of the rates of pH_i recovery obtained at pH_o 6.60 (Fig. 4.9*B*) indicated that rates of pH_i recovery after anoxia were reduced at pH_o 6.60, compared to rates established after anoxia at pH_o 7.35. Qualitatively opposite results were obtained under pH_o 7.60 conditions (not shown; see Sheldon & Church, 2002a). Taken together, the results are consistent with contributions from Na^+/H^+ exchange activity and a putative g_{H^+} to the rises in pH_i observed in rat hippocampal neurons immediately following anoxia. The data also indicate that, even at pH_o 6.60, an increase in pH_i still occur after anoxia, albeit slowly.

4.3. DISCUSSION

4.3.1. Na^+/H^+ exchange activity after anoxia

In contrast to the decline in observable Na^+/H^+ exchange activity that occurs in adult rat hippocampal CA1 pyramidal neurons during anoxia (see Chapter 3), the present results suggest that activation of Na^+/H^+ exchange occurs in this cell type immediately upon reoxygenation. Thus, pH_i 'overshoots' following anoxia were reduced either when $NMDG^+$ (but not Li^+) was employed as a Na^+_o substitute or when pH_o was lowered; in contrast to $NMDG^+$, Li^+ can act as a substrate for Na^+/H^+ exchange, and it is established that Na^+/H^+ exchange activity can be reduced by falls in pH_o (Green *et al.* 1988; Vaughan-Jones & Wu, 1990; Baxter & Church, 1996; Wu & Vaughan-Jones, 1997; Ritucci *et al.* 1998). It is important to note that while pH_i 'overshoots' immediately after anoxia (as well as increases in pH_i during anoxia) have occasionally been observed in hippocampal slice preparations (see Mabe *et al.* 1983; Fujiwara *et al.* 1992; Pirttilä & Kauppinen, 1992; Melzian *et al.* 1996), the more usual response in these preparations comprises a fall in pH_i during anoxia and a gradual restoration of pH_i towards normal resting levels in the period following the return to normoxia (e.g. Silver & Erecińska, 1992; Roberts & Chih, 1997). In the present study, when anoxia was imposed under pH_o 6.60 conditions, the increases in pH_i during and after anoxia were greatly reduced and, similar to the changes in pH_i observed in response to anoxia *in vivo* and in slice preparations *in vitro*, pH_i fell during anoxia and gradually recovered upon the return to normoxia. Thus, the apparent differences in the steady-state pH_i changes observed in response to anoxia in isolated neurons compared to more complex multicellular preparations are likely, in part, consequent upon the lower pH_o values (along with concurrent changes in $[K^+]_o$ and neurotransmitter release) that are associated with the

latter preparations and can reduce the activities of the Na^+/H^+ exchanger and other pH_i regulating mechanisms (including the Zn^{2+}-sensitive, putative g_{H^+}; see below).

Consistent with the steady-state pH_i results, rates of pH_i recovery from acid loads increased in the period immediately following the return to normoxia, and these increases were attenuated either when $NMDG^+$ was employed as an external Na^+ substitute or when pH_o was reduced. The increase in the Na^+_o-dependent component of pH_i recovery from acid loads observed after anoxia (Figs. 4.2*C* and 4.3*C*) is also consistent with the activation of Na^+/H^+ exchange in the immediate post-anoxic period. Although it remains unknown what influence cellular ATP levels and/or post-anoxic changes in $[Na^+]_i$ may have on Na^+/H^+ exchange activity following anoxia (see Chapters 5 and 6), the present results are consistent with previous reports not only in cultured postnatal rat hippocampal neurons (Diarra *et al.* 1999) but in other isolated neuronal preparations in which an involvement of Na^+/H^+ exchange in the restoration of pH_i following anoxia has been demonstrated with selective pharmacological inhibitors (Vornov *et al.* 1996; Jørgensen *et al.* 1999; Yao *et al.* 2001). The results of the present study also support previous suggestions, made on the basis of pH_o measurements, that Na^+/H^+ exchange activity may contribute to the acidotic $[H^+]_o$ shift which occurs *in vivo* and in slice preparations during early reperfusion (Ohno *et al.* 1989; Obrenovitch *et al.* 1990).

In cardiac myocytes, it has been proposed that Na^+/H^+ exchange activity is inhibited during anoxia/ischemia by the extracellular acidosis which occurs at this time, and that the rapid normalization of pH_o immediately upon reperfusion relieves this inhibition, thereby contributing to the activation of Na^+/H^+ exchange in the immediate post-anoxic period (Lazdunski *et al.* 1985). In the present study, however, stimulation of Na^+/H^+ exchange activity occurred after anoxia even when pH_o was maintained at a constant value throughout the anoxic and post-anoxic

periods and even when pH_i immediately prior to the return to normoxia may not have been markedly decreased from the resting level observed prior to anoxia. Thus, neither a decrease in pH_i during anoxia nor a return to normal pH_o values in the immediate post-anoxic period are absolute requirements for the rapid post-anoxic activation of Na^+/H^+ exchange in adult rat CA1 neurons. In cardiac myocytes, PKC activation also contributes to the rapid activation of Na^+/H^+ exchange activity during reperfusion (Ikeda *et al.* 1988; Yasutake & Avkiran, 1995), and the present study points to an analogous contribution from anoxia-evoked changes in the activity of the cAMP/PKA second messenger system in mediating the activation of Na^+/H^+ exchange in hippocampal neurons in the immediate post-anoxic period. Thus, not only do rapid increases in $[cAMP]_i$ occur in hippocampal neurons immediately upon reperfusion but these increases can be maintained for up to 60 min (reviewed by Tanaka, 2001; also see Kobayashi *et al.* 1977; Whittingham *et al.* 1984; Blomqvist *et al.* 1985; Domanska-Janik 1996; Small *et al.* 1996). In addition, our laboratory has shown previously that, under normoxic conditions, β-adrenoceptor activation, acting via cAMP and PKA, evokes a sustained increase in Na^+/H^+ exchange activity in acutely isolated adult rat CA1 neurons by producing an alkaline shift in the pH_i dependence of the transport mechanism (Smith *et al.* 1998; also see Connor & Hockberger, 1984 where intracellular injections of cAMP into invertebrate neurons evoked increases in pH_i). Consistent with these previous findings, in the present study there was an alkaline shift in the pH_i dependence of Na^+_o-dependent acid extrusion following anoxia (see Figs. 4.2*C* and 4.3*C*). Furthermore, inhibition of adenylate cyclase or PKA reduced the magnitude of the Na^+_o-dependent component of the pH_i 'overshoot' after anoxia (also see Yao *et al.* 2001) whereas β-adrenoceptor activation augmented the post-anoxic rise in pH_i (an effect that was blocked by propranolol, *R*p-cAMPS and under conditions where $NMDG^+$, but not Li^+, was employed as a

Na^+_o substitute). The effects of modulating the activity of the cAMP/PKA system on the increase in pH_i observed immediately after anoxia are not only consistent with a contribution from Na^+/H^+ exchange to the post-anoxic increase in pH_i but also provide an example of the potential importance of the regulation of neuronal Na^+/H^+ exchange activity by second messenger systems.

4.3.2. Potential contribution of a g_{H^+} to the increases in pH_i during and after anoxia

In contrast to the effects of inhibiting Na^+/H^+ exchange which reduced the rise in pH_i observed following anoxia, micromolar concentrations of Zn^{2+} attenuated the increases in pH_i observed both during *and* following anoxia. Although concurrent pH_i imaging and electrophysiological recordings will be required to substantiate or refute the possibility that the effects of Zn^{2+} may be due to the inhibition of H^+ efflux through a H^+-conductive pathway activated as a consequence of membrane depolarization, there is precedence for external Na^+- and HCO_3^--independent H^+ extrusion from hippocampal neurons under anoxic conditions (Ohno *et al.* 1989; Pirttilä & Kauppinen, 1994; Diarra *et al.* 1999), and the possible contribution of a g_{H^+} to the rises in pH_i observed during and immediately after anoxia in the present experiments is suggested by a number of lines of evidence.

First, inhibition by Zn^{2+} is an identifying characteristic of g_{H^+}s (for reviews see DeCoursey & Cherny, 1994a and 2000; Eder & DeCoursey, 2001) and although Zn^{2+} failed to affect steady-state pH_i under normoxic conditions, it attenuated the increases in pH_i that occurred during and after anoxia under both Na^+_o-containing and reduced-Na^+_o ($NMDG^+$ substituted) conditions. The effect of Zn^{2+} to reduce the magnitudes of the alkalinizations observed during anoxia under $NMDG^+$-substituted conditions may reflect the established coupling between Na^+/H^+ exchange activity and g_{H^+}s (Fig. 4.5; DeCoursey & Cherny, 1994b; Demaurex *et al.*

1995). Thus, inhibition of Na^+/H^+ exchange activity under $NMDG^+$-substituted conditions would potentially act to increase the relative contribution of the Zn^{2+}-sensitive g_{H^+} to acid extrusion under the depolarizing conditions that occur during anoxia. It is important to note that although Zn^{2+} ions modulate the activities of a variety of ion channels (for reviews see Harrison & Gibbons, 1994; Smart *et al.* 1994), under the constant perfusion conditions employed in the present experiments, the pH_i changes evoked by anoxia are unaffected by NMDA, AMPA or $GABA_A$ receptor antagonists, or organic inhibitors of high voltage-activated Ca^{2+} channels (A. Diarra, C. Sheldon, and J. Church, unpublished observations; also see Chapters 5 and 7). Zn^{2+} has also been shown to induce falls in pH_i in cultured cortical neurons in a manner dependent on $Ca^{2+}{}_o$ (Dineley *et al.* 2002); however, in the present study (Chapter 3), the removal of $Ca^{2+}{}_o$ failed to alter anoxia-evoked changes in pH_i. *Second*, consistent with the steady-state pH_i results, Zn^{2+} decreased rates of pH_i recovery from acid loads imposed during and after anoxia, both under control conditions and under conditions where Na^+/H^+ exchange was inhibited by the substitution of $NMDG^+$ for external Na^+. *Third*, the fact that the Zn^{2+}-sensitive increases in pH_i observed during and after anoxia were inhibited by a reduction in pH_o is consistent with the established sensitivity of voltage-activated H^+-conducting pathways to the transplasmalemmal pH gradient (DeCoursey & Cherny, 1994a and 2000). *Fourth*, the Zn^{2+}-inhibitable internal alkalinizations that occurred during and after anoxia were associated temporally with marked and persistent increases in $[Ca^{2+}]_i$ that, in turn, are known to occur in adult CA1 neurons in response to membrane depolarization (Rader & Lanthorn, 1989; Silver & Erecińska, 1990; Tanaka *et al.* 1997). In this regard, I found not only that the recovery of pH_i from internal acid loads imposed during normoxia in the absence of external Na^+ was faster under depolarizing (139.5 mM $K^+{}_o$) than under control (3 mM $K^+{}_o$) conditions, but also that Zn^{2+} only slowed the rate of recovery of

pH_i in the former case. Arguing against the possibility that the Zn^{2+}-sensitive acid extrusion mechanism might be a H^+-conductive pathway is the fact that Zn^{2+}-sensitive increases in pH_i after anoxia could occur even when the proton gradient across the plasma membrane was not apparently outwardly directed (i.e. $pH_i > pH_o$). However, this observation is tempered by the facts that membrane depolarization occurs during and following anoxia in rat hippocampal neurons (see Chapter 7; also Tanaka *et al.* 1997) and that the local $[H^+]$ in the vicinity of presumed H^+-conducting channels may greatly exceed that monitored in bulk cytoplasm. Indeed, as noted by DeCoursey and Cherny (1994a) '... spatial or temporal pH fluctuations may activate the g_{H^+} in situations not predictable from time-averaged, bulk pH measurements, for example, by fluorescent dyes.'

4.3.3. Synthesis of Chapters 3 and 4

Data presented in Chapters 3 and 4 have examined the contribution of alterations in the activities of pH_i regulating mechanisms to the changes in pH_i observed during and following transient periods of anoxia in acutely isolated adult rat hippocampal CA1 pyramidal neurons. Thus, Na^+/H^+ exchange, a major acid-extruding mechanism under normoxic conditions in rat hippocampal neurons, becomes inhibited shortly following the onset of anoxia. In contrast, a Zn^{2+}-sensitive alkalinizing mechanism, possibly a g_{H^+}, appears to be activated during anoxia as a consequence of membrane depolarization and contributes to acid extrusion at this time. These findings do not preclude contributions from other mechanism(s) to the rises in pH_i that sometimes occurred during anoxia, such as a decreased rate of internal acid loading following the onset of anoxic depolarization (see Erecińska *et al.* 1991; Sánchez-Armass *et al.* 1994).

Following the return to normoxia, the presumed g_{H^+} continues to contribute to acid extrusion. The activity of the putative g_{H^+} may be maintained by the persistant membrane depolarization observed in mature hippocampal neurons in response to anoxia or ischemia. Na^+/H^+ exchange activity is enhanced following anoxia, an effect which may be mediated, at least in part, by an anoxia-induced activation of the cAMP/PKA second messenger pathway. This finding is consistent with the possibility that the neurotoxic effects associated with post-ischemic activation of the cAMP/PKA pathway (e.g. Shibata *et al.* 1992; Small *et al.* 1996) may, in part, reflect an activation of Na^+/H^+ exchange upon reoxygenation. These results do not, however, eliminate the possibility that Na^+/H^+ exchange activity in the post-anoxic period may be regulated concurrently by more than one signaling pathway. Indeed, in mouse hippocampal CA1 neurons, anoxia-induced activation of Na^+/H^+ exchange can be reduced by inhibiting either PKC or PKA (Yao *et al.* 2001) and, in recent studies, Na^+/H^+ exchange activity in brainstem neurons has been found to be regulated by reactive oxygen species (the production of which is enhanced following periods of anoxia or ischemia; Lipton, 1999; Mulkey *et al.* 2004; also see Wei *et al.* 2001 in cardiac myocytes). In addition, it is noteworthy that g_{H^+}s can couple to Na^+/H^+ exchange (DeCoursey & Cherny, 1994b; Demaurex *et al.* 1995), such that the activation of a g_{H^+} during anoxia would act as an 'acid-relief valve' to limit the potentially detrimental activation of forward Na^+/H^+ exchange occurs in the immediate post-anoxic period (Vornov *et al.* 1996). Conversely, the neurotoxic effects associated with micromolar concentrations of Zn^{2+} (e.g. Choi & Koh, 1998; Weiss *et al.* 2000; Dineley *et al.* 2003) may, in part, reflect an inhibition of g_{H^+}s and augmented Na^+/H^+ exchange activity upon reoxygenation. Indeed, the activation of Na^+/H^+ exchange activity following anoxia may act to increase the internal Na^+ load in the period immediately after anoxia (see Chapter 5) and thereby, for example, worsen cellular energy state

(Fried *et al.* 1995; Chinopoulos *et al.* 2000), potentiate NMDA receptor-mediated responses (Yu & Salter, 1998; Manzerra *et al.* 2001), and/or promote the reversal of plasmalemmal Na^+/Ca^{2+} exchange (Kiedrowski *et al.* 1994).

Originally described by Bevensee *et al.* (1996), CA1 pyramidal neurons can be classified into those exhibiting "high" and "low" levels of Na^+/H^+ exchange activity under steady-state conditions (also see Smith *et al.* 1998; Brett *et al.* 2002a), a finding which supports previous illustrations of intrinsic variations between CA1 pyramidal neurons (e.g. subtle morphological differences and differences in the expression of calcium-binding proteins; Amaral & Witter, 1995; Morris *et al.* 1995). Notably, however, anoxia-induced changes in Na^+/H^+ exchange activity were observed in both "high" and "low" pH_i cells. It was apparent that neurons expressing "high" levels of Na^+/H^+ exchange activity prior to anoxia (i.e. "high" pH_i neurons; see Bevensee *et al.* 1996) were more sensitive to the actions of anoxia to reduce Na^+/H^+ exchange activity than were "low" pH_i neurons (which have low levels of Na^+/H^+ exchange activity). Conversely, following anoxia, activation of Na^+/H^+ exchange activity was more marked in "low" pH_i neurons that exhibit relatively "low" levels of Na^+/H^+ exchange activity prior to anoxia. Although the potential functional significance of these findings is unclear, a number of events that are known to occur in response to anoxia appear dependent on pH_i. For example, neurons with pre-anoxic pH_i values greater than ~ 7.20 are more likely to undergo hypoxia-induced depolarizations (*vs.* hyperpolarizations; Cowan & Martin, 1995).

There is a growing body of evidence that pharmacological inhibition of Na^+/H^+ exchange effectively protects against anoxia- and ischemia-induced neuronal injury (e.g. Vornov *et al.* 1996; Kuribayashi *et al.* 1999; Phillis *et al.* 1999). The results presented in Chapters 3 and 4 suggest that any neuroprotective actions of Na^+/H^+ exchange inhibitors would likely be realized in the period immediately following anoxia or ischemia. Whether a similar benefit might be

conferred in mature rat hippocampal CA1 pyramidal neurons awaits the identification of pharmacological inhibitors of Na^+/H^+ exchange in this highly vulnerable cell type.

Fig. 4.1. Effects of external Na^+ substitutions on the increase in pH_i observed following 5 min anoxia. *A*, the magnitude of the internal alkalinization observed following 5 min anoxia under control conditions (solid line) was reduced under $NMDG^+_o$-(open circles) but not Li^+_o-(filled circles) substituted conditions. Records shown were obtained under Hepes-buffered conditions (pH_o 7.35) at 37°C from three different neurons with similar resting pH_i values immediately prior to the induction of anoxia. *B*, effects of changes in perfusate composition on the increase in pH_i observed following 5 min anoxia. All experiments were conducted under HCO_3^-/CO_2-free, Hepes-buffered conditions (pH_o 7.35, 37°C); error bars are S.E.M. * denotes a statistically significant difference ($P < 0.05$) compared to control or Li^+_o-substituted conditions. N.S. indicates no significant difference ($P = 0.76$) between the increase in pH_i observed following anoxia under Na^+_o-containing compared with Li^+_o-substituted conditions.

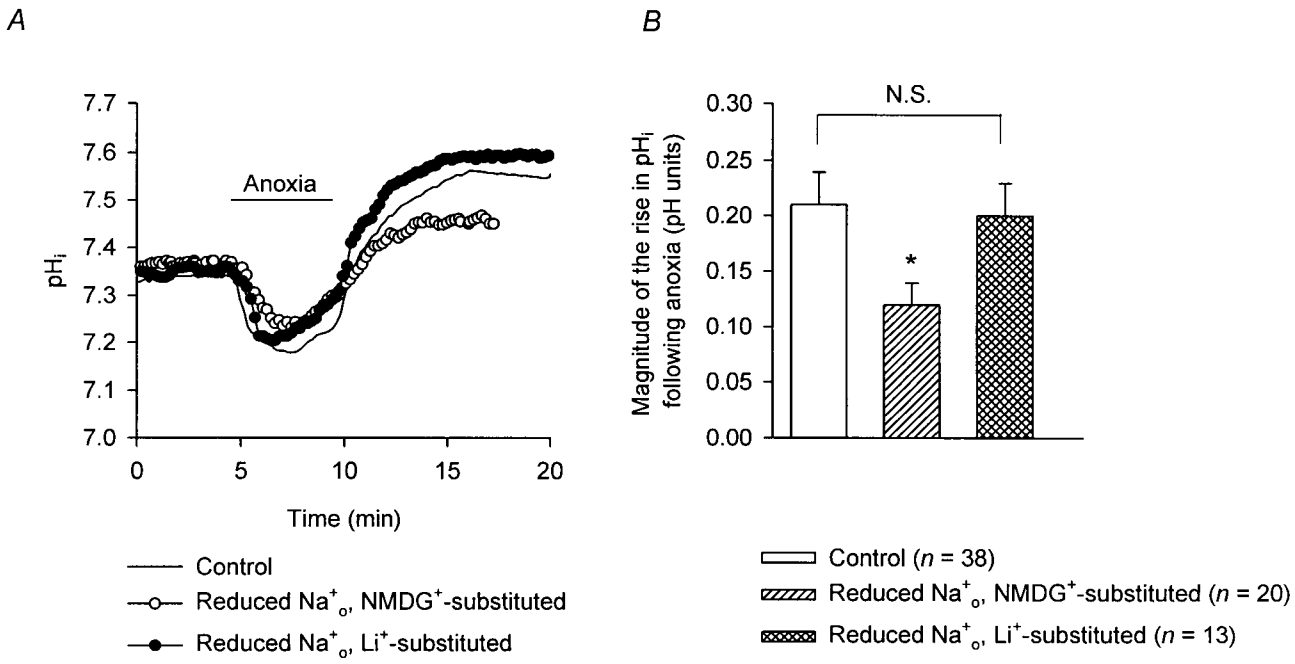
A
B
7.7
7.6
7.5
7.4
7.3
7.2
7.1
7.0
pHi
Anoxia
0
5
10
15
20
Time (min)
Control
Reduced Na+o, NMDG+-substituted
Reduced Na+o, Li+-substituted
N.S.
0.30
0.25
0.20
0.15
0.10
0.05
0.00
Magnitude of the rise in pHi following anoxia (pH units)
*
Control (n = 38)
Reduced Na+o, NMDG+-substituted (n = 20)
Reduced Na+o, Li+-substituted (n = 13)

Fig. 4.2. Recovery of pH_i from internal acid loads imposed immediately after anoxia. *A*, following the first NH_4^+-induced intracellular acid load, pH_i was allowed to recover. A second acid load was then applied after 5 min anoxia. The rate of recovery of pH_i was increased in the post-anoxic period, compared to the rate of pH_i recovery observed prior to anoxia. *B*, rates of pH_i recovery prior to (filled symbols) and immediately after (open symbols) 5 min anoxia under control (Na^+_o-containing; circles) and reduced-Na^+_o, $NMDG^+$-substituted (triangles) conditions. Under both conditions, rates of pH_i recovery were increased following anoxia ($P < 0.05$ at each absolute value of pH_i); data points were obtained from 17 and 5 experiments, respectively, of the type shown in *A*. Continuous lines represent the weighted non-linear regression fits to the data points indicated for each experimental condition. Where missing, standard error bars lie within the symbol areas. *C*, the Na^+_o-dependent component of pH_i recovery prior to (filled circles) and after (open circles) anoxia revealed by plotting the differences between the regression fits (shown in *B*) obtained under Na^+_o-containing and reduced-Na^+_o ($NMDG^+$-substituted) conditions. In *A* - *C*, data were obtained at 37°C during perfusion with Hepes-buffered media at pH_o 7.35.

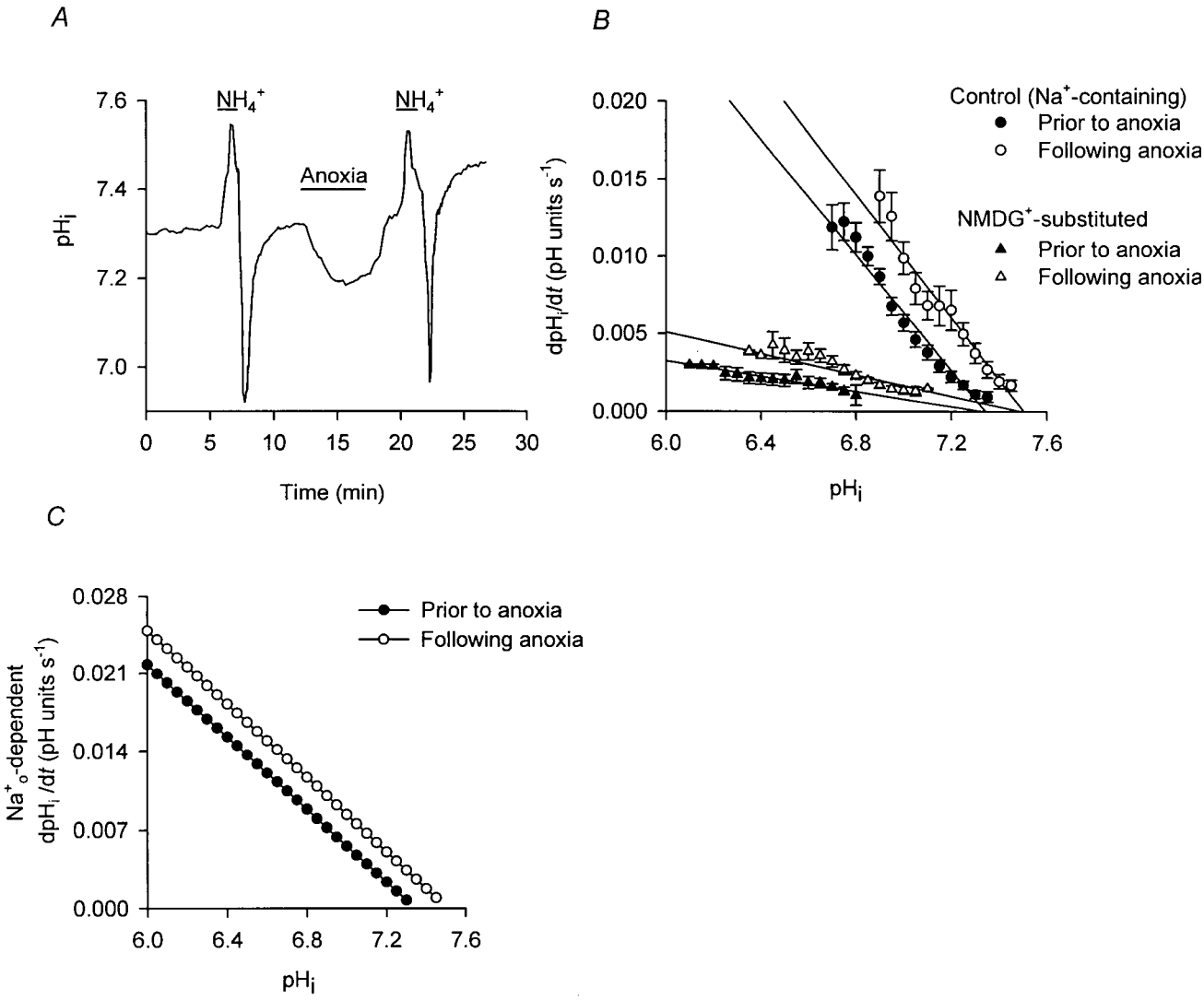
A
B
C
NH4+
NH4+
Anoxia
pHi
Time (min)
Control (Na+-containing)
Prior to anoxia
Following anoxia
NMDG+-substituted
Prior to anoxia
Following anoxia
dpHi/dt (pH units s-1)
pHi
Prior to anoxia
Following anoxia
Na+o-dependent
dpHi /dt (pH units s-1)
pHi

Fig. 4.3. Recovery of pH_i from internal acid loads imposed immediately after anoxia in "low" pH_i neurons. *A*, the pH_i dependencies of rates of pH_i recovery prior to (filled circles) and after (open circles) 5 min anoxia under control conditions (normal $[Na^+]_o$). Continuous lines represent the weighted nonlinear regression fits to the data points indicated for each experimental condition (n = 5 in each case). *B*, rates of pH_i recovery from internal acid loads imposed following anoxia under normal Na^+_o-containing conditions (open bar) were faster than those observed prior to anoxia under normal Na^+_o-containing conditions (filled bar). Also shown are rates of pH_i recovery observed prior to (hatched bar) and following (cross-hatched bar) anoxia under reduced-Na^+_o, $NMDG^+$-substituted conditions. Rates of pH_i recovery shown were determined at a common test pH_i of 6.80. * denotes a statistically significant difference ($P < 0.05$). *C*, the Na^+_o-dependent component of pH_i recovery prior to (filled circles) and after (open circles) anoxia revealed by plotting the differences between the regression fits to pH_i *vs.* dpH_i/dt plots obtained under Na^+_o-containing and reduced-Na^+_o ($NMDG^+$-substituted) conditions. In *A* - *C*, data were obtained at 37°C during perfusion with Hepes-buffered media at pH_o 7.35.

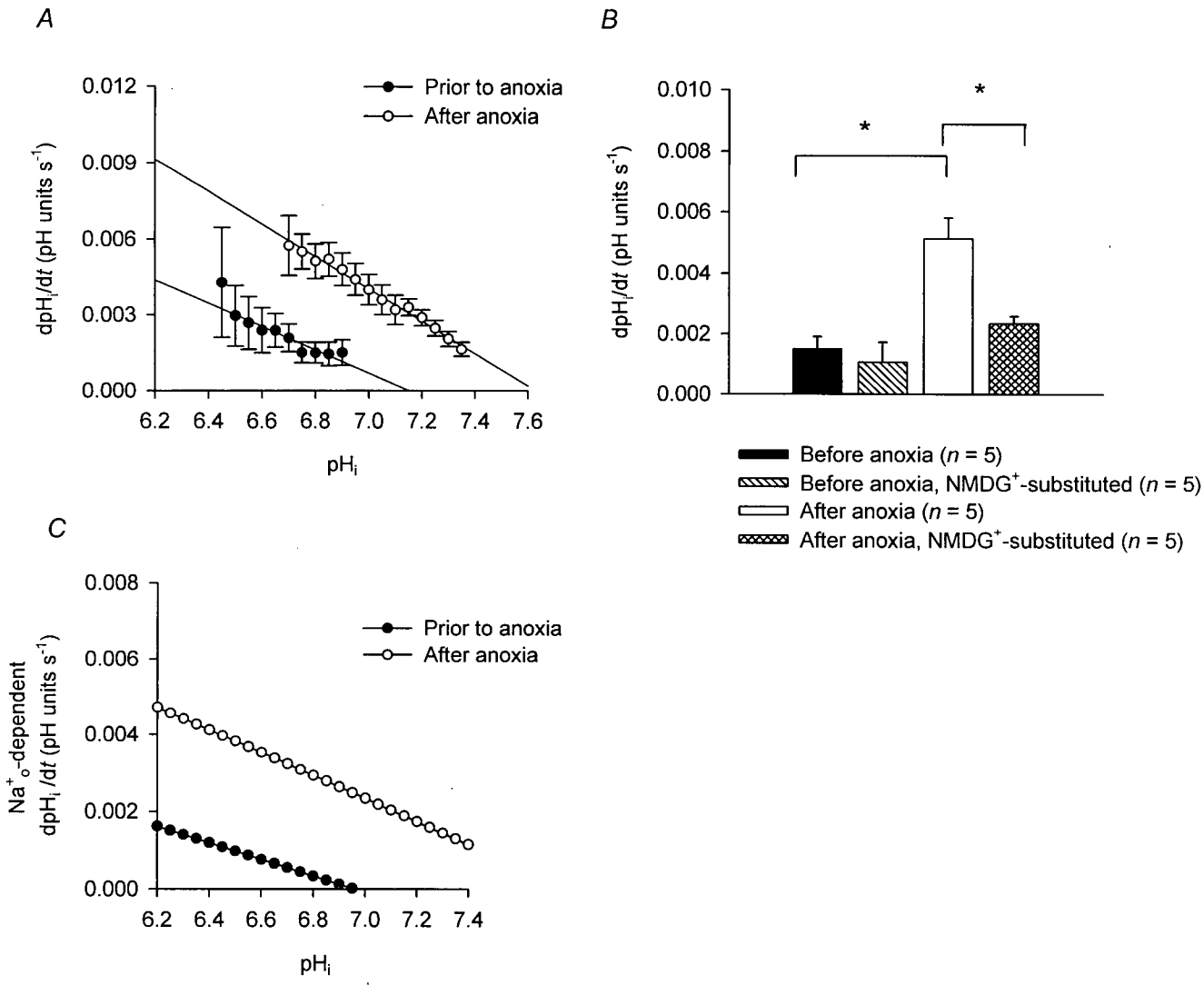
A
0.012
0.009
0.006
0.003
0.000
dpHi/dt (pH units s-1)
6.2 6.4 6.6 6.8 7.0 7.2 7.4 7.6
pHi
Prior to anoxia
After anoxia
B
0.010
0.008
0.006
0.004
0.002
0.000
dpHi/dt (pH units s-1)
*
*
Before anoxia (n = 5)
Before anoxia, NMDG+-substituted (n = 5)
After anoxia (n = 5)
After anoxia, NMDG+-substituted (n = 5)
C
0.008
0.006
0.004
0.002
0.000
Na+o-dependent dpHi /dt (pH units s-1)
6.2 6.4 6.6 6.8 7.0 7.2 7.4
pHi
Prior to anoxia
After anoxia

Fig. 4.4. Effects of modulating the activity of the cAMP/PKA pathway on the pH_i response to anoxia. *A*, the magnitude of the internal alkalinization observed following 5 min anoxia under control conditions (filled circles) was increased in the presence of the β-adrenoceptor agonist isoproterenol (10 μM; open circles) and reduced in the presence of the PKA inhibitor *R*p-cAMPS (50 μM; open triangles). The records shown were obtained under Hepes-buffered conditions (pH_o 7.35) at 37°C from three different neurons with similar resting pH_i values immediately prior to the induction of anoxia. Pharmacological treatments were applied for ≥10 min prior to the induction of anoxia and were maintained throughout the records shown. *B*, effects of the test conditions shown in the figure on the increase in pH_i observed after 5 min anoxia. All experiments were performed under nominally HCO_3^-/CO_2-free, Hepes-buffered conditions at 37°C, pH_o 7.35; error bars are S.E.M. * denotes a statistically significant difference ($P < 0.05$) compared to control (shown in the first column). † denotes a statistically significant difference ($P < 0.05$) compared to the value obtained in the presence of 10 μM isoproterenol (shown in the fourth column).

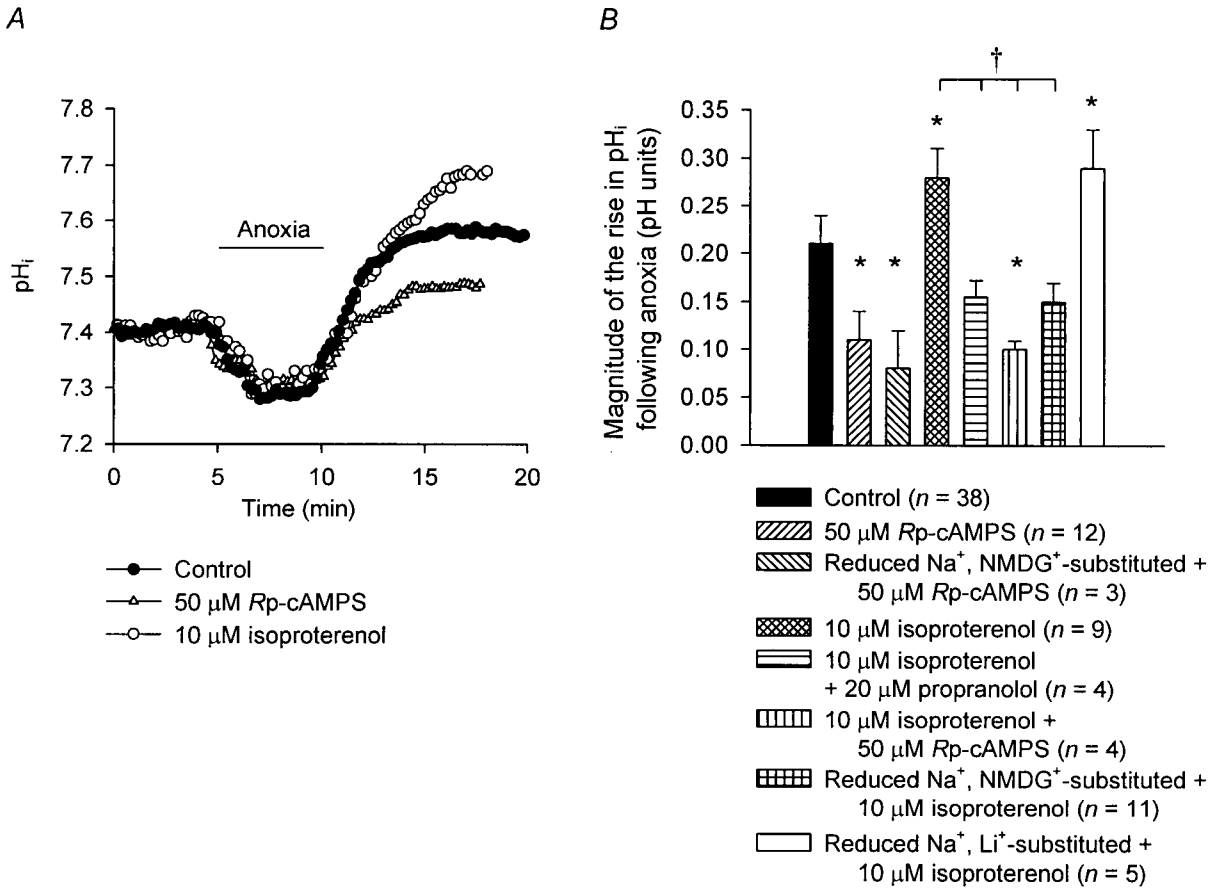
A
7.8
7.7
7.6
7.5
7.4
7.3
7.2
pHi
Anoxia
0
5
10
15
20
Time (min)
Control
50 μM Rp-cAMPS
10 μM isoproterenol
B
Magnitude of the rise in pHi following anoxia (pH units)
0.35
0.30
0.25
0.20
0.15
0.10
0.05
0.00
†
*
Control (n = 38)
50 μM Rp-cAMPS (n = 12)
Reduced Na+, NMDG+-substituted + 50 μM Rp-cAMPS (n = 3)
10 μM isoproterenol (n = 9)
10 μM isoproterenol + 20 μM propranolol (n = 4)
10 μM isoproterenol + 50 μM Rp-cAMPS (n = 4)
Reduced Na+, NMDG+-substituted + 10 μM isoproterenol (n = 11)
Reduced Na+, Li+-substituted + 10 μM isoproterenol (n = 5)

Fig. 4.5. Effects of changes in perfusate composition on the increases in pH_i observed during (*A*) and following (*B*) 5 min anoxia. All experiments were performed under nominally HCO_3^-/CO_2-free, Hepes-buffered conditions at 37°C; error bars are S.E.M. * denotes a statistically significant difference ($P < 0.05$) compared to control, normal Na^+_o-containing conditions at pH_o 7.35 (shown in the first column in both *A* and *B*). † denotes a statistically significant difference ($P < 0.05$) compared to the value obtained under reduced-Na^+_o, $NMDG^+$-substituted conditions (shown in the second column in both *A* and *B*).

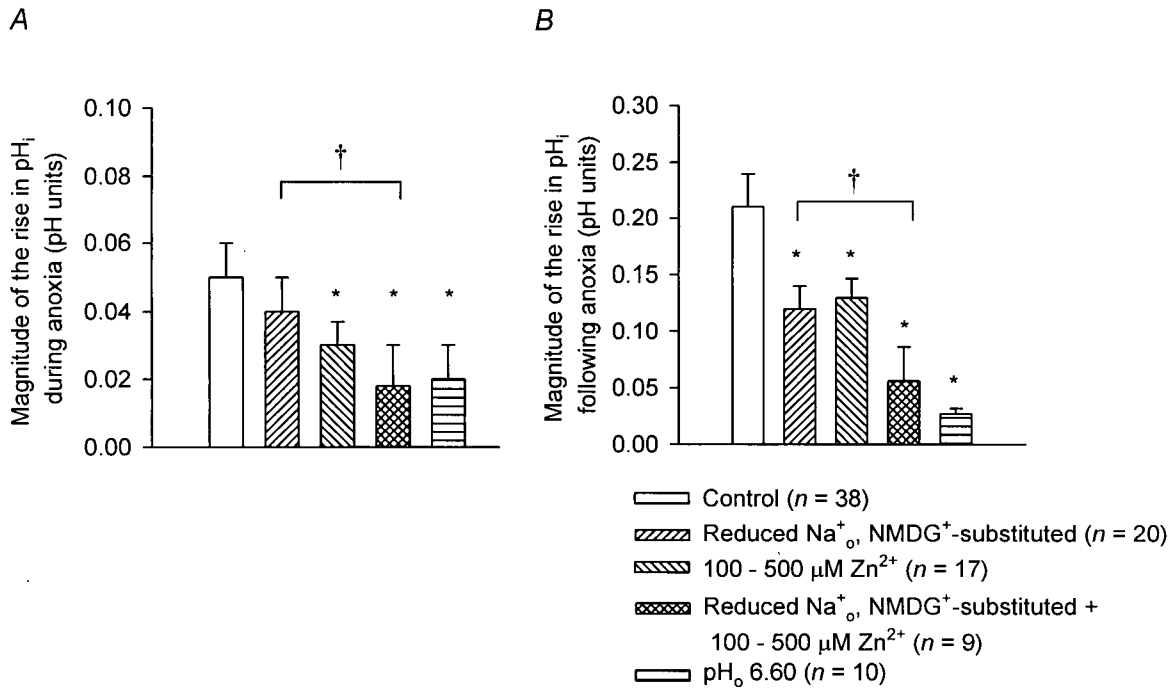
A
B
Magnitude of the rise in pHi during anoxia (pH units)
0.10
0.08
0.06
0.04
0.02
0.00
†
*
Magnitude of the rise in pHi following anoxia (pH units)
0.30
0.25
0.20
0.15
0.10
0.05
0.00
Control (n = 38)
Reduced Na+o, NMDG+-substituted (n = 20)
100 - 500 μM Zn2+ (n = 17)
Reduced Na+o, NMDG+-substituted + 100 - 500 μM Zn2+ (n = 9)
pHo 6.60 (n = 10)

Fig. 4.6. Influence of Zn^{2+} on the recovery of pH_i from internal acid loads imposed immediately after anoxia. *A*, following a 5 min period of anoxia, an internal acid load was imposed under control (Zn^{2+}-free, Na^+_o-containing) conditions. At the peak of the acidification, the perfusate was changed to a reduced-Na^+, $NMDG^+$-substituted medium containing 100 μM Zn^{2+} (a to b). From b to c, Zn^{2+} was removed and pH_i recovery was allowed to proceed under reduced-Na^+, $NMDG^+$-substituted conditions. At c, the neuron was reperfused with control medium. *B*, rates of pH_i recovery from internal acid loads imposed immediately after anoxia during perfusion with reduced-Na^+, $NMDG^+$-substituted medium containing 100 μM Zn^{2+} (open bar); reduced-Na^+, $NMDG^+$-substituted medium (diagonal hatching); Na^+-containing medium in the presence of 100 μM Zn^{2+} (cross hatching); and control (Zn^{2+}-free, Na^+-containing) medium (filled bar). The $pH_{0.5}$ values at which rates of pH_i recovery were determined were ~ 6.7, 6.9, 7.1 and 7.2, respectively; error bars are S.E.M. † denotes a statistically significant difference ($P < 0.05$) compared to control (Zn^{2+}-free, normal Na^+_o). * denotes a statistically significant difference ($P < 0.05$) compared to the value obtained under reduced-Na^+_o, $NMDG^+$-substituted conditions in the presence of 100 μM Zn^{2+}. In *A* and *B*, data were obtained at 37°C during perfusion with Hepes-buffered media at pH_o 7.35.

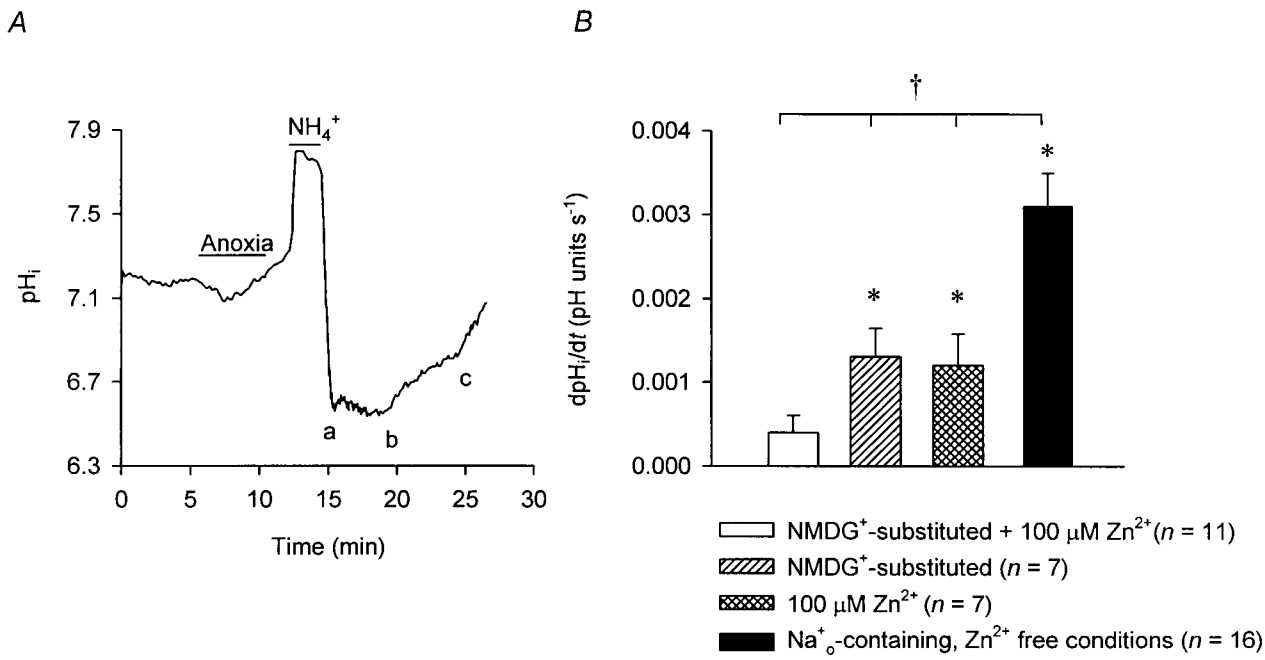
A
B
7.9
7.5
7.1
6.7
6.3
pHi
NH4+
Anoxia
a
b
c
0
5
10
15
20
25
30
Time (min)
†
0.004
0.003
0.002
0.001
0.000
dpHi/dt (pH units s-1)
*
*
*
NMDG+-substituted + 100 μM Zn2+(n = 11)
NMDG+-substituted (n = 7)
100 μM Zn2+ (n = 7)
Na+o-containing, Zn2+ free conditions (n = 16)

Fig. 4.7. Effect of high-$[K^+]_o$ on pH_i recovery from intracellular acid loads imposed under normoxic Na^+_o-free, nominally HCO_3^--free, Hepes-buffered conditions (pH_o 7.35). *A*, under control conditions (3 mM KCl; solid line), an internal acid load was applied by the NH_4^+ prepulse technique and pH_i recovered. The rate of pH_i recovery was faster under high-$[K^+]_o$ conditions (139.5 mM KCl; open circles) compared to control, and the brief application of 100 μM Zn^{2+} slowed the rate of pH_i recovery under high K^+_o-conditions (filled circles) but had no effect at normal $[K^+]_o$ (filled triangles). Records were obtained from four different neurons which exhibited similar minimum pH_i values in response to the NH_4^+ prepulse (with the exception of the control response, NH_4^+ prepulses have been omitted for clarity). *B*, rates of pH_i recovery (± S.E.M.) from internal acid loads imposed during perfusion with reduced-Na^+, $NMDG^+$-substituted medium containing 3 mM K^+ either in the absence (open bar) or presence (diagonal hatched bar) of 100 μM Zn^{2+}, and under reduced-Na^+_o, 139.5 mM K^+ substituted conditions in the absence (filled bar) or presence (cross-hatched bar) of 100 μM Zn^{2+}. The $pH_{0.5}$ values at which rates of pH_i recovery were estimated were ~ 6.6, 6.8, 6.8 and 6.9, respectively. * denotes a statistically significant difference ($P < 0.05$) compared to the value obtained in the presence of 100 μM Zn^{2+}.

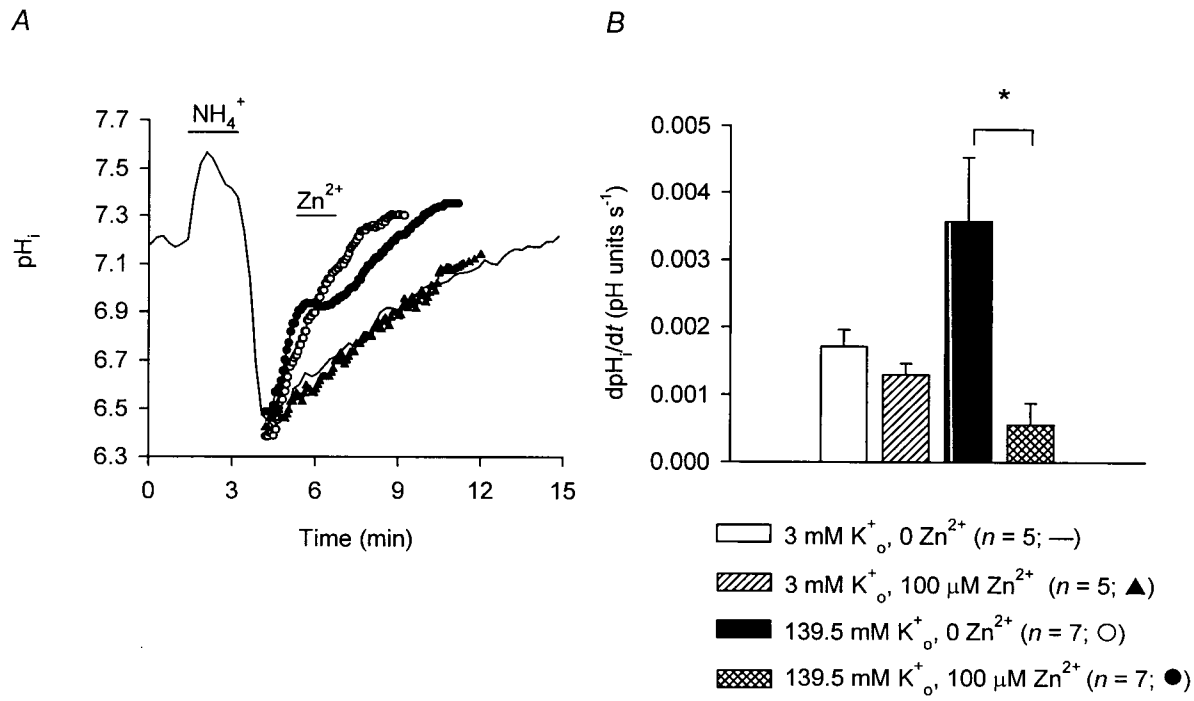
A
B
NH4+
Zn2+
pHi
7.7
7.5
7.3
7.1
6.9
6.7
6.5
6.3
0
3
6
9
12
15
Time (min)
*
dpHi/dt (pH units s-1)
0.005
0.004
0.003
0.002
0.001
0.000
3 mM K+o, 0 Zn2+ (n = 5; —)
3 mM K+o, 100 μM Zn2+ (n = 5; ▲)
139.5 mM K+o, 0 Zn2+ (n = 7; ○)
139.5 mM K+o, 100 μM Zn2+ (n = 7; ●)

Fig. 4.8. Representative traces of the effects of inhibitors of P-type H^+,K^+-ATPase and V-type H^+-ATPase activity on pH_i recovery from intracellular acid loads imposed under high-$[K^+]_o$ conditions (pH_o 7.35). *A*, an internal acid load was imposed using the NH_4^+ prepulse technique and 50 μM omeprazole was added to the perfusate during the recovery of pH_i. *B* and *C*, 500 μM SCH-28080 (*B*) or 2 μM bafilomycin A_1 (*C*) were added to the perfusate immediately upon the removal of NH_4^+. Neither omeprazole, SCH 28080 nor bafilomycin A_1 had any effect on the recovery of pH_i from internal acid loads imposed under the high-$[K^+]_o$ (139.5 mM KCl), Na^+_o-free ($NMDG^+$-substituted) nominally HCO_3^--free, Hepes-buffered conditions (pH_o 7.35) employed throughout all the traces shown.

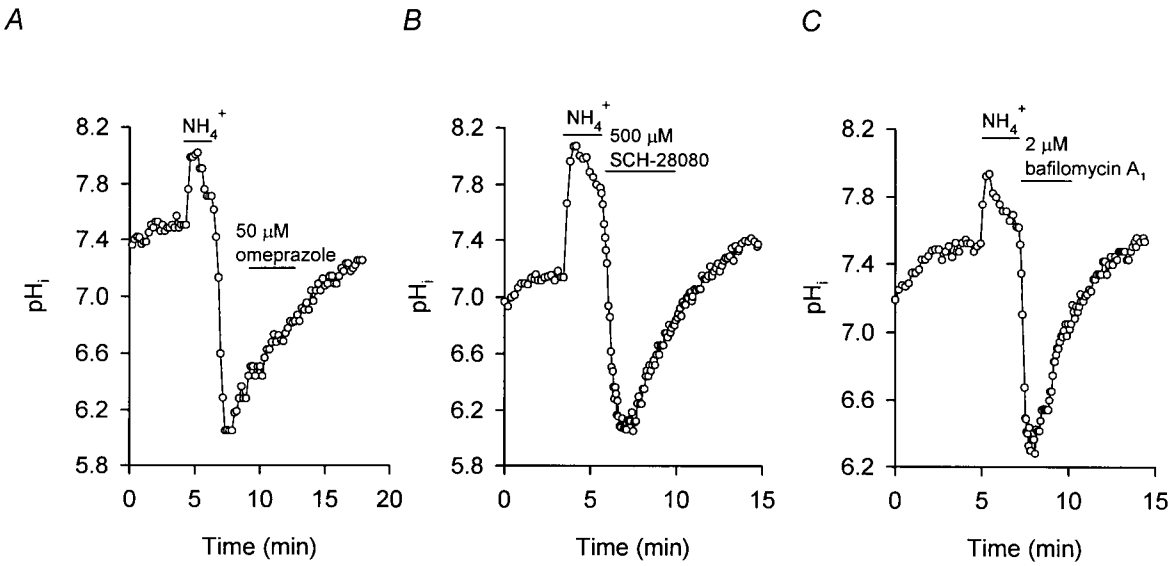
A
B
C
NH_4^+
50 μM
omeprazole
500 μM
SCH-28080
2 μM
bafilomycin A_1
pH_i
Time (min)
8.2
7.8
7.4
7.0
6.6
6.2
5.8
0
5
10
15
20

Fig. 4.9. Effects of reduced pH_o on rates of pH_i recovery from acid loads imposed in the immediate post-anoxic period. *A*, an initial acid load was imposed at pH_o 6.60 and pH_i was allowed to recover. The neuron was then exposed to anoxia for 5 min and a second acid load was applied after the return to normoxia. *B*, rates of pH_i recovery from acid loads imposed prior to (filled symbols) and immediately after (open symbols) anoxia at pH_o 6.60 (squares) and pH_o 7.35 (circles). Continuous lines represent the weighted non-linear regression fits to the data points indicated for each experimental condition. Data collected at pH_o 6.60 were obtained from 9 experiments of the type shown in *A*; where missing, standard error bars lie within the symbol areas.

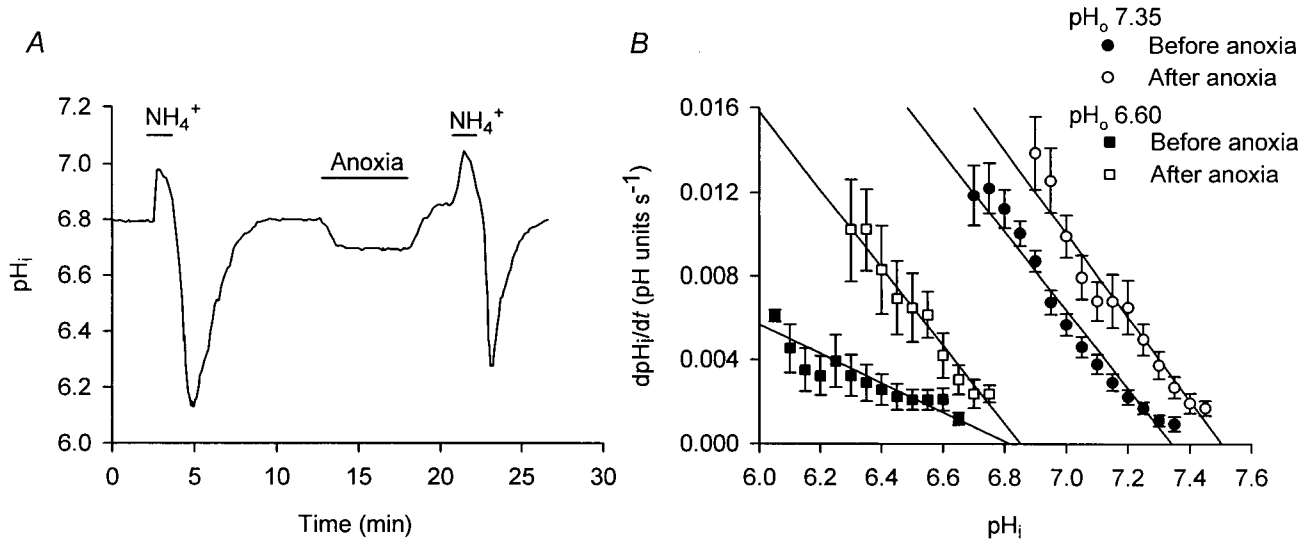
A
B
NH4+
Anoxia
NH4+
pHi
Time (min)
pHo 7.35
Before anoxia
After anoxia
pHo 6.60
Before anoxia
After anoxia
dpHi/dt (pH units s-1)
pHi

CHAPTER FIVE

CHANGES IN $[Na^+]_i$ INDUCED BY ANOXIA IN ISOLATED RAT HIPPOCAMPAL NEURONS: ROLE OF Na^+/H^+ EXCHANGE ACTIVITY

5.0. INTRODUCTION

The contribution of Na^+/H^+ exchange to the increases in $[Na^+]_i$ that occur under conditions of metabolic inhibition has been most extensively established in cardiac myocytes (see Pike *et al.*1993; Wu & Vaughan-Jones, 1994). In response to a marked intracellular acidosis and the accumulation regulatory factors, such as catecholamines and lysophosphatidlycholine, Na^+/H^+ exchange activity is activated by periods of ischemia (Avkiran & Haworth, 1999; Karmazyn *et al.*, 1999). Although this acts to restore pH_i, there is a concomitant rise in internal Na^+ that, in turn, leads to reversal of the Na^+/Ca^{2+} exchanger and a subsequent elevation of $[Ca^{2+}]_i$ (e.g. Tani & Neely, 1989; An *et al.* 2001). While pharmacological inhibition of Na^+/H^+ exchange reduces the extent of ischemic damage in cardiac myocytes, it remains unclear whether the cardioprotective effects result from a reduction in acid extrusion, Na^+_i accumulation or Ca^{2+} entry, or through additional so far unidentified mechanism(s) (see Schäfer *et al.* 2000; Avkiran, 2001). Recent studies have also suggested that Na^+_o and HCO_3^--dependent pH_i regulating mechanisms, specifically Na^+/HCO_3^- cotransport, may act alongside Na^+/H^+ exchange to promote cell damage in cardiac cells in response to ischemia (e.g. Khandoudi *et al.* 2001; Lemars, 2001).

The results presented in Chapters 3 and 4 suggest that Na^+/H^+ exchange activity in rat hippocampal neurons, while inhibited during anoxia, is increased in the immediate post-anoxic period, raising the possibility that Na^+/H^+ exchange may contribute to the increases in $[Na^+]_i$ observed previously in response to anoxia in isolated neurons (Friedman & Haddad, 1994a; Chen *et al.* 1999; Diarra *et al.* 2001). In support, changes in Na^+/H^+ exchange activity under normoxic conditions (e.g.

in response to imposed internal acid loads) are associated with transient increases in $[Na^+]_i$ in neurons (Moody, 1981; Chesler, 1986; Schwiening & Thomas, 1992; also see Chapter 6). In addition, following transient focal ischemia, Kuribayashi *et al.* (1999) attributed the neuroprotective effects of Na^+/H^+ inhibitors to reductions in tissue Na^+ and water content. Although less well-characterized, Na^+-dependent Cl^-/HCO_3^- exchange is similarly capable of eliciting small increases in $[Na^+]_i$ in rat hippocampal neurons (Rose & Ransom, 1997; also see Thomas, 1977 for similar findings in snail neurons). Thus, the activities of these transport mechanisms may contribute to the potentially detrimental increases in $[Na^+]_i$ observed in hippocampal neurons in response to anoxia.

In the present study, the Na^+-sensitive fluorophore, SBFI, was used to: *i)* characterize the changes in $[Na^+]_i$ observed during and following anoxia in isolated rat hippocampal neurons; and *ii)* examine the potential contribution of pH_i regulating mechanisms to the observed increases in $[Na^+]_i$.

5.1. MATERIALS AND METHODS

5.1.1. Experimental preparation

Unless otherwise noted, primary cultures of hippocampal neurons obtained from 2 - 4 day postnatal Wistar rats were used.

5.1.2. Recording techniques

The methods used to load acutely isolated adult rat hippocampal CA1 neurons with SBFI were presented in Chapter 2. To load cultured postnatal hippocampal neurons with SBFI, coverslips with neurons attached were incubated with 10 μM SBFI-AM (in the presence of 0.10% Pluronic

F-127 and 5 mg ml^{-1} of bovine serum albumin) for 120 - 180 min at 32°C. Following loading, coverslips with neurons attached were mounted into a temperature-controlled perfusion chamber so as to form the base of the chamber and neurons were superfused at a rate of 2 ml min^{-1} for 15 min with the initial experimental solution (at 37°C) before the start of an experiment.

Anoxia-evoked changes in $[Na^+]_i$ were measured using the dual-excitation ratiometric technique, as detailed in Chapter 2. Neurons loaded with SBFI were alternately excited at 334 and 380 nm and fluorescence emissions were collected from ROIs placed on individual neuronal somata. Raw emission intensity data at each excitation wavelength were corrected for background fluorescence prior to calculation of the ratio (BI_{334}/BI_{380}). A one-point calibration technique ($[Na^+]_i$ = 10 mM) was employed to convert BI_{334}/BI_{380} ratio values into $[Na^+]_i$ values as described (Chapter 2; also see Diarra *et al.* 2001). It is important to note that, loaded into rat hippocampal neurons, SBFI possesses a negligible sensitivity to K^+ (Rose & Ransom, 1997) and a slight sensitivity to changes in pH_i, with intracellular acidifications and alkalinizations resulting in apparent decreases and increases in $[Na^+]_i$, respectively (see Rose & Ransom, 1997; Nett & Deitmer, 1998). A formal assessment of the pH-sensitivity of SBFI, conducted during the course of this thesis (Diarra *et al.* 2001) established that the effects of $[Na^+]_i$ values estimated with SBFI are unlikely to affect the interpretation of results presented here.

5.1.3. Internal ATP determination

Cellular ATP content was measured using the Molecular Probes ATP determination kit (see Chapter 3 for details). Transient periods of anoxia were induced in cultured neurons under conditions identical to those used for the microspectrofluorimetric measurements of $[Na^+]_i$ (i.e. conditions of constant perfusion, 37°C, pH_o 7.35). Prior to and at given time intervals during or

following anoxia, neurons were lysed by the addition of 40 μl of a solution containing 10 mM Tris buffer (pH 7.5), 0.1 M NaCl, 1 mM EDTA and 0.01% Triton X-100 in the presence of a cocktail of protease inhibitors (Roche Diagnostic Canada, Laval, QB) and homogenized with a cell scraper. Ten microlitre aliquots were then removed and used to measure ATP. ATP levels are reported as a percentage decline compared to paired pre-anoxic measurements.

5.1.4. Experimental procedures and data analysis

Changes in $[Na^+]_i$ observed during anoxia ($\Delta[Na^+]_{i(during)}$) were measured as the difference between the pre-anoxic resting $[Na^+]_i$ value and the peak $[Na^+]_i$ value observed during a 5 min period of anoxia (see Fig. 5.1). Changes in $[Na^+]_i$ occurring after anoxia were examined in separate experiments. As illustrated in Fig. 5.3*A*, neurons were exposed to 5 min anoxia and, upon the return to normoxia, Na^+,K^+-ATPase activity was inhibited for 7 min (by perfusion with $[K^+]$-free medium or the application of 500 μM ouabain), revealing continued Na^+ entry at this time. The magnitude of the increase in $[Na^+]_i$ observed after anoxia under these conditions ($\Delta[Na^+]_{i(after)}$) was measured as the difference between the $[Na^+]_i$ value observed at the end of 5 min anoxia and the $[Na^+]_i$ value observed at the end of the 7 min exposure to 0 $[K^+]_o$ or 500 μM ouabain.

Data are reported as mean ± S.E.M. with the accompanying *n* value referring to the number of neuronal populations (i.e. coverslips) from which data were obtained. As detailed in the Results, the magnitudes of the rises in $[Na^+]_i$ observed during and after anoxia were related to the number of days neurons had been maintained in culture. Therefore, experiments were routinely performed on cultures maintained for 6 - 10 days *in vitro* (DIV) and, where noted, were repeated using 11 - 14 DIV neuronal cultures. Measurements of anoxia-evoked increases in

$[Na^+]_i$ observed under a given test condition were normalized to the corresponding $[Na^+]_i$ measurement made in experiments performed in the absence of a test condition using age-matched sister cultures (yielding Normalized $\Delta[Na^+]_{i(during)}$ and $\Delta[Na^+]_{i(after)}$ values; see Tables 5.1 and 5.2). Statistical comparisions were performed by comparing absolute $[Na^+]_i$ measurements (i.e. not normalized $\Delta[Na^+]_{i(during)}$ and $\Delta[Na^+]_{i(after)}$ values) made under a given test condition to measurements made in age-matched sister cultures under control conditions using Student's two-tailed unpaired *t*-tests. Where appropriate, additional statistical analysis was performed with one-way ANOVA. Significance was assumed at the 5% level.

5.2. RESULTS

5.2.1. Anoxia-induced increases in $[Na^+]_i$ in acutely isolated adult rat hippocampal CA1 pyramidal neurons

Initially, I explored the feasibility of using acutely isolated adult rat hippocampal CA1 pyramidal neurons to examine the contribution of Na^+/H^+ exchange to the changes in $[Na^+]_i$ evoked by anoxia. Although 5 min anoxia induced an increase in $[Na^+]_i$ of 22 ± 16 mM ($n = 4$), resting $[Na^+]_i$ in these cells was elevated (27 ± 7 mM) and $[Na^+]_i$ failed to recover to pre-anoxic values upon the return to normoxia. A similar pattern of changes has been observed by others in acutely isolated hippocampal neurons using the non-ratiometric Na^+-sensitive fluorophore, Sodium Green (Friedman & Haddad, 1994a) and may reflect, at least in part, the limited viability of acutely isolated adult neurons and the difficulty with which sufficient SBFI-derived fluorescent signals could be obtained. Therefore all subsequent experiments were performed using postnatal hippocampal neurons in primary culture. Importantly, the pH_i response to anoxia in these

cultured neurons is similar in nearly all respects to the response in acutely isolated adult rat CA1 neurons described in Chapters 3 and 4: thus, in cultured postnatal hippocampal neurons, Na^+/H^+ exchange activity is reduced during and activated immediately following anoxia and a Zn^{2+}-sensitive, putative g_{H^+} appears to contribute to acid extrusion during and after anoxia (Diarra *et al.* 1999).

5.2.2. Anoxia-induced increases in $[Na^+]_i$ in cultured postnatal rat hippocampal neurons

Prior to anoxia, resting $[Na^+]_i$ was 11 ± 1 mM, (n = 444), a value similar to those previously reported by others in either isolated neuronal (Pinelis *et al.* 1994; Rose & Ransom, 1997; Silver *et al.* 1997; Chen *et al.* 1999; Diarra *et al.* 2001) or brain slice (Guatteo *et al.* 1998; Calabresi *et al.* 1998) preparations. As illustrated in Fig. 5.1*A*, a 5 min period of anoxia induced a ~15 - 40 mM increase in $[Na^+]_i$ that began ~ 90 s into the anoxic insult and recovered to pre-anoxic levels within ~6 - 10 min after the return to normoxia. There was a positive correlation between the magnitude of the anoxia-evoked increase in $[Na^+]_i$ and the length of time hippocampal neurons had been maintained in culture (Fig. 5.1*B*). When anoxia was imposed under reduced $[Na^+]_o$, $NMDG^+$-substituted conditions, the increase in $[Na^+]_i$ was inhibited (n = 8; Fig. 5.1*C*), indicating a requirement for Na^+ entry.

In Chapters 2 and 3, I reported that media containing 1 - 2 mM sodium dithionite have P_{O_2} values <1 mm Hg and that the pH_i changes observed during exposure to these media reflect reductions in P_{O_2} and are not secondary to any additional properties of the O_2 scavenger. In the present series of experiments, the possibility that dithionite-containing solutions may induce changes in $[Na^+]_i$ via mechanisms unrelated to its O_2 scavenging property was assessed in two ways. First, solutions containing 1 or 2 mM sodium dithionite were bubbled vigorously with air

for 20 - 30 min, which elevated P_{O_2} in these solutions from <1 mm Hg to 152 ± 6 mm Hg (n = 5), as measured with an oxygen electrode (ISO_2; World Precision Instruments Inc., Sarasota, FL; also see Carpenter *et al.* 2000). The increase in $[Na^+]_i$ observed during exposure to dithionite-containing media equilibrated with air was 3 ± 1 mM (n = 7), significantly ($P < 0.05$) less than the 23 ± 3 mM (n = 23) increase observed in age-matched cultures exposed to dithionite-containing media equilibrated with 100% Ar (Fig. 5.1*A*). As an additional control, standard Hepes-buffered medium was bubbled vigorously with ultra-pure Ar for >18 h, reducing P_{O_2} in the medium to <1 mM Hg (see Chapter 3; Section 3.2.2). The resultant increase in $[Na^+]_i$ observed upon exposure to this medium was not different to that observed when P_{O_2} was reduced to <1 mM Hg by the addition of sodium dithionite (Fig. 5.1*B*). Thus, the $[Na^+]_i$ changes evoked by exposure to media containing 1 - 2 mM sodium dithionite largely reflect reductions in P_{O_2} and are not secondary to any additional properties of the O_2 scavenger.

As previously described (see Silver *et al.* 1997), the accumulation of Na^+_i in neurons during anoxia in part reflects reduced Na^+,K^+-ATPase activity. In agreement, 5 min applications of standard Hepes-buffered media containing 500 μM ouabain or $[K^+]_o$-free medium under normoxic conditions evoked increases in $[Na^+]_i$ of 27 ± 4 mM (n = 7) and 26 ± 5 mM (n = 7), respectively (Fig. 5.2*A*; also see Rose & Ransom, 1997)[7]. In addition, Na^+_i accumulation during anoxia occurred at times at which cellular ATP levels were reduced. After 3 min anoxia, internal ATP had fallen to 34 ± 7%, with a further decrease to 24 ± 8% of pre-anoxic values at the end of

[7] Five min applications of 1 μM ouabain evoked an increase in $[Na^+]_i$ that was significantly smaller than that observed in response to 500 μM ouabain (the magnitude of the increase in $[Na^+]_i$ observed after 5 min 1 μM ouabain was 4 ± 1 mM; n = 5; $P < 0.05$ compared to the increase in $[Na^+]_i$ observed after 5 min 500 μM ouabain), consistent with the possibility that the maintenance of resting $[Na^+]_i$ in rat hippocampal neurons relies on the activity of a Na^+,K^+-ATPase isoform which possesses a low-affinity ouabain binding site (Juhaszuva & Blaustein, 1997).

5 min anoxia (Fig. 5.2*B*; also see Gleitz *et al.* 1996). Neuronal cultures were then incubated with 10 mM creatine for >2 h to increase intracellular phosphocreatine levels and delay anoxia-induced falls in ATP (see Chapter 3, Section 3.2.4.3; also see Balestrino *et al.* 2002). In creatine pretreated neurons, there was a significant attenuation of the fall in ATP observed after 3 min anoxia under control conditions (Fig. 5.2*B*). Furthermore, the magnitude of the increase in $[Na^+]_i$ observed after 3 min anoxia was reduced by ~55% compared to the increase observed in age-matched sister cultures not treated with creatine (Fig. 5.2*C*). Following 5 min anoxia, creatine pretreatment failed to limit significantly either the fall in internal ATP or the increase in $[Na^+]_i$ (Fig. 5.2*B, C*). For each of the experimental series described above, similar effects were observed in neurons maintained for 11 - 14 DIV (not shown). These results suggest that the maintenance of resting $[Na^+]_i$ in cultured rat hippocampal neurons is dependent upon the activity of the Na^+,K^+-ATPase and that the accumulation of $[Na^+]_i$ during anoxia likely reflects, at least in part, a reduced activity of the pump consequent upon decreases in internal ATP.

As illustrated in Figure 5.1*A*, $[Na^+]_i$ recovered to pre-anoxic values within ~6 - 10 min following the return to normoxia. This recovery likely reflects the resumption of Na^+,K^+-ATPase activity following anoxia (see Ekholm *et al.* 1993; van Emous *et al.* 1998). Thus, 5 min after the return to normoxia, internal ATP levels increased by ~10% from values measured at the end of anoxia (to 33 ± 7% of pre-anoxic values; n = 4). In addition, inhibition of Na^+,K^+-ATPase activity ($[K^+]_o$-free conditions for a 7 min duration) prevented the recovery of $[Na^+]_i$ and revealed a secondary post-anoxic increase in $[Na^+]_i$ that, as in the case of the rise in $[Na^+]_i$ observed during anoxia, was related to the length of time that neurons had been maintained in culture (Fig. 5.3*A*, *B*). Similar results were observed if Na^+,K^+-ATPase activity was blocked after anoxia with 500 μM ouabain (see Fig. 5.3*B*). Once Na^+,K^+-ATPase activity was re-established by perfusion with

standard medium containing 3 mM $[K^+]_o$, $[Na^+]_i$ recovered to pre-anoxic values (Fig. 5.3*A*). The secondary post-anoxic increase in $[Na^+]_i$ observed during Na^+,K^+-ATPase inhibition was blocked when $NMDG^+$ was substituted for external Na^+ ($n = 4$; Fig. 5.3*A*), indicating continued Na^+ entry in the immediate post-anoxic period.

Taken together, these results suggest that: *i)* the accumulation of Na^+_i during anoxia in cultured postnatal rat hippocampal neurons likely reflects, in part, reduced Na^+,K^+-ATPase activity, consequent upon decreases in internal ATP; *ii)* upon the return to normoxia, the resumption of Na^+,K^+-ATPase activity mediates the recovery of $[Na^+]_i$ to pre-anoxic levels, and *iii)* the increases in $[Na^+]_i$ observed during *and* after anoxia are strongly dependent on the influx of Na^+ from the extracellular space. The pH_i measurements described in Chapters 3 and 4 indicated that Na^+/H^+ exchange activity in rat hippocampal neurons is inhibited during anoxia and activated in the immediate post-anoxic period. In the following section, I examined the potential contribution of Na^+/H^+ exchange activity to the increases in $[Na^+]_i$ observed during and following anoxia. As described by van Emous *et al.* (1998), by inhibiting Na^+,K^+-ATPase activity, the contribution of Na^+/H^+ exchange activity to Na^+ entry occurring following anoxia could be examined effectively.

5.2.3. Role of Na^+/H^+ exchange activity

The examination of the contribution of Na^+/H^+ exchange to anoxia-evoked changes in $[Na^+]_i$ in rat hippocampal neurons is complicated by the lack of a selective pharmacological inhibitor (see Section 1.4.1; Raley-Susman *et al.* 1991; Schwiening & Boron, 1994; Baxter & Church, 1996). In Chapters 3 and 4, the effects of anoxia on Na^+/H^+ exchange activity, and the contribution of these changes in transport activity to the pH_i changes observed during and after anoxia, were inferred by determining the Na^+_o- (and Li^+_o-) dependency of the anoxia-evoked changes in steady-state pH_i and the Na^+_o-

dependency of rates of pH_i recovery from imposed internal acid loads. Because this approach was not feasible in the present study, I sought to indirectly assess the role of Na^+/H^+ exchange activity in the production of anoxia-evoked changes in $[Na^+]_i$ by testing a number of maneuvers that have previously been found to influence Na^+/H^+ exchange activity in rat hippocampal neurons.

Harmaline is reported to be a non-selective inhibitor of Na^+/H^+ exchange activity in rat hippocampal neurons (Raley-Susman *et al.* 1991). In agreement, examined under HCO_3^--free, Hepes-buffered normoxic conditions, harmaline pretreatment (200 μM) reduced rates of pH_i recovery from internal acid loads imposed using the NH_4^+ prepulse technique (see Fig. 5.4*A, inset*). However, consistent with the findings presented in Chapter 3 and 4 which, on the basis of pH_i measurements, suggested that Na^+/H^+ exchange activity was inhibited during anoxia and stimulated immediately following anoxia, pretreatment with harmaline failed to reduce the rise in $[Na^+]_i$ observed during 5 min anoxia in either 6 - 10 or 11 - 14 DIV neurons (Table 5.1; Fig. 5.4*A*) but reduced the increase in $[Na^+]_i$ observed following anoxia in both 6 - 10 and 11 - 14 DIV neuronal cultures (Table 5.2; Fig. 5.4*A*).

The pH_i measurements presented in Chapter 4 suggested that the activation of Na^+/H^+ exchange activity in the immediate post-anoxic period can be inhibited by an extracellular acidosis or inhibition of the cAMP/PKA pathway and, conversely, that exchange activity can be further enhanced by an external alkalosis (see Diarra *et al.* 1999; Sheldon & Church, 2002a). Consistent with a contribution of Na^+/H^+ exchange to Na^+ influx in the immediate post-anoxic period, exposure of neurons to pH_o 6.60 conditions or 50 μM *R*p-cAMPS reduced the magnitude of the increase in $[Na^+]_i$ observed at this time by 25 - 40% (Table 5.2; Fig. 5.4*A*). Conversely, an extracellular alkalosis enhanced the increase in $[Na^+]_i$ observed following anoxia (Table 5.2; Fig. 5.4*A*).

The pH_i measurements presented in Chapters 3 and 4 also suggested that a Zn^{2+}-sensitive voltage-activated H^+ conductance (g_{H^+}) may contribute to the dissipation of the internal acid load imposed by 5 min anoxia in rat hippocampal neurons (also see Diarra *et al.* 1999). It has previously been suggested that inhibition of g_{H^+}s (e.g. with Zn^{2+}) may increase the contribution of Na^+/H^+ exchange to acid extrusion in non-neuronal cell types (Demaurex *et al.* 1995). In the present study, Zn^{2+} might therefore be expected to promote Na^+ influx at a time when Na^+/H^+ exchange is active (i.e. in the immediate post-anoxic period) but have no effect during anoxia (i.e. at a time when Na^+/H^+ exchange is inhibited). Indeed, exposure of neurons to 100 μM Zn^{2+} failed to affect significantly the increase in $[Na^+]_i$ during anoxia (Table 5.1); in contrast, applied immediately after anoxia under K^+_o-free conditions, Zn^{2+} significantly enhanced the increase in $[Na^+]_i$ (Table 5.2; Fig. 5.4*B*). The ability of Zn^{2+} to augment the increase in $[Na^+]_i$ observed following anoxia was blocked under pH_o 6.60 conditions (Table 5.2; Fig. 5.4*B*), consistent with Zn^{2+} indirectly enhancing Na^+ influx through Na^+/H^+ exchange.

5.2.4. Role of HCO_3^--dependent mechanisms

The potential contribution of HCO_3^--dependent pH_i regulating mechanisms to anoxia-evoked increases in $[Na^+]_i$ was examined by measuring the changes in $[Na^+]_i$ observed during and after anoxia under HCO_3^-/CO_2-buffered conditions. As reported previously (Rose & Ransom, 1997), the transition from a HCO_3^--free, Hepes-buffered medium to a HCO_3^-/CO_2-buffered medium (pH_o constant at 7.35) caused a small (~3 mM) increase in $[Na^+]_i$, consistent with the activation of Na^+-dependent Cl^-/HCO_3^- exchange. Under HCO_3^-/CO_2-buffered conditions, however, the increase in $[Na^+]_i$ observed during anoxia was not significantly different to that observed in age-matched sister cultures under HCO_3^--free, Hepes-buffered conditions (Table 5.1). The addition

of 200 μM DIDS under HCO_3^-/CO_2-buffered conditions failed to limit the rise in $[Na^+]_i$ seen during anoxia (Table 5.1), further suggesting that HCO_3^--dependent pH_i regulating mechanisms do not contribute significantly to the increase in $[Na^+]_i$ observed during anoxia in rat hippocampal neurons.

In contrast, the magnitude of the increase in $[Na^+]_i$ observed after anoxia was consistently greater under HCO_3^-/CO_2-buffered conditions than under nominally HCO_3^--free, Hepes-buffered conditions in 11 - 14, but not 6 - 10, DIV neuronal cultures (Fig. 5.5*A*, *B*); in neurons 11 - 14 DIV, the magnitude of the increase in $[Na^+]_i$ observed following anoxia was 27 ± 2 and 50 ± 13 mM under Hepes- and HCO_3^-/CO_2-buffered conditions, respectively (n = 5 in each case). The HCO_3^--dependent increase in $[Na^+]_i$ observed after anoxia in 11 - 14 DIV neurons was blocked by 200 μM DIDS (Fig. 5.5*A*, *B*). Although DIDS is commonly employed as an inhibitor of HCO_3^--dependent pH_i regulating mechanisms, it can also inhibit a variety of cellular events potentially associated with anoxia (e.g. mitochondrial free radical production; see Cabantchik & Greger, 1992; Han *et al.* 2003; Tauskela *et al.* 2003). Indeed, 200 μM DIDS reduced slightly, albeit significantly, the increase in $[Na^+]_i$ observed following anoxia under nominally HCO_3^--free, Hepes-buffered conditions; there was no significant difference between the rise in $[Na^+]_i$ seen after anoxia in the presence of DIDS under HCO_3^--containing compared to HCO_3^--free conditions (Fig. 5.5*B*; $P = 0.15$).

Taken together, the results are consistent with the possibility that Na^+/H^+ exchange activity contributes to Na^+ influx immediately following, but not during, 5 min anoxia in 6 - 10 and 11 - 14 DIV rat hippocampal neuronal cultures. HCO_3^--dependent mechanisms also appear to contribute to Na^+ influx following anoxia, but only in neurons maintained in culture for 11 - 14 DIV.

5.3. DISCUSSION

5.3.1. Resting $[Na^+]_i$ under normoxic conditions

Resting $[Na^+]_i$ in cultured postnatal rat hippocampal neurons was ~11 mM, a value that is in good agreement with earlier studies in hippocampal neurons (Pinelis *et al.* 1994; Rose & Ransom, 1997; Diarra *et al.* 2001). The maintenance of a low resting $[Na^+]_i$ in the face of a steep inwardly directed electrochemical gradient for Na^+ is a common feature of vertebrate and invertebrate neurons (e.g. Thomas, 1972; Deitmer & Schlue, 1983; Chen *et al.* 1999). In the present study, under normoxic conditions, the application of ouabain or the removal of K^+_o caused increases in $[Na^+]_i$ of ~ 6.0 mM min^{-1} (estimated from the slope of linear fits to $[Na^+]_i$ measurements obtained during the first 3 min of 0 $[K^+]_o$ or ouabain application). As outlined by Rose & Ransom (1997), these rates approximate, in rat hippocampal neurons, a resting molar flux density for Na^+ of ~ 16 x 10^{-12} mol cm^{-2} s^{-1} (assuming a spherical cell body and cell body diameter of 25 μM). Similar flux values have been estimated in squid axons and snail neurons (Hodgkin & Keynes, 1955; Thomas, 1972; also see Pinelis *et al.* 1994) and, while they may be influenced by a slowly developing (min) ouabain-induced depolarization sometimes observed in neurons (Thomas, 1972; Fujiwara *et al.* 1987), they are larger than those observed in non-neuronal cell types (e.g. MacLeod, 1989; Wu & Vaughan-Jones, 1994; Despa *et al.* 2002). It is apparent that maintenance of resting $[Na^+]_i$ in rat hippocampal neurons under normoxic conditions reflects a balance between Na^+,K^+-ATPase activity and ongoing Na^+ influx.

5.3.2. Anoxia-evoked increases in $[Na^+]_i$

The changes in $[Na^+]_i$ observed during anoxia similarly reflect a balance between reduced Na^+,K^+-ATPase activity and ongoing/increased Na^+ influx. At the end of 5 min anoxia, I

observed an increase in $[Na^+]_i$ of ~15 (6 DIV neurons) to ~40 (14 DIV neurons) mM that was dependent on the presence of external Na^+ and was reduced when anoxia-induced falls in internal ATP levels were attenuated by creatine pretreatement. The increases in $[Na^+]_i$ observed in the present study are consistent with those observed previously in a variety of mammalian central neurons in response to anoxia or oxygen-glucose deprivation, not only in culture and slice preparations *in vitro* (Friedman & Haddad, 1994a; Pisani *et al.* 1998a; Calabresi *et al.* 1999b; Diarra *et al.* 2001) but also in CA1 neurons *in vivo* in response to 8 min low-flow global ischemia (under which conditions $[Na^+]_i$ increased by ~50 mM; Erecińska & Silver, 2001). In contrast, the changes in $[Na^+]_i$ observed immediately following anoxia have remained poorly defined (e.g. Taylor *et al.* 1999; LoPachin *et al.* 2001). In the present study, the recovery of $[Na^+]_i$ to resting levels after anoxia reflected a resumption of Na^+,K^+-ATPase activity in spite of ongoing/increased Na^+ influx. Thus, when the Na^+/K^+-ATPase was inhibited in the immediate post-anoxic period, a further increase in $[Na^+]_i$ of ~30 (6 DIV) to ~60 (14 DIV neurons) mM was observed and was blocked in the absence of external Na^+. By inhibiting Na^+,K^+-ATPase activity, the contribution of Na^+ influx pathways (e.g. Na^+/H^+ exchange) to Na^+ entry occurring following anoxia could be identified; these routes of entry may be of importance under conditions in which the recovery Na^+,K^+-ATPase activity occurs more slowly and/or by creating local changes in $[Na^+]_i$.

That the magnitudes of the increases in $[Na^+]_i$ observed during and after anoxia were related to the number of days that neurons had been maintained in culture may in part account for the previous finding (Jiang *et al.* 1992) that anoxia-induced falls in $[Na^+]_o$ are smaller in brainstem slices taken from neonatal *vs.* adult rats and may reflect developmental increase in the expression and/or activities of the mechanisms involved in their production (e.g. Bevensee *et al.* 1996; Sakaue *et al.* 2000;

Douglas *et al.* 2001; Gibney *et al.* 2002); this finding is considered further below (see Section 5.3.5 and Chapter 7).

5.3.3. Contribution of Na^+/H^+ exchange activity

As noted earlier, the examination of the contribution of Na^+/H^+ exchange to anoxia-evoked changes in $[Na^+]_i$ in rat hippocampal neurons is complicated by the lack of a specific pharmacological inhibitor. Therefore, only an indirect assessment of the role of Na^+/H^+ exchange activity to the increases in $[Na^+]_i$ observed during and following anoxia could be made by testing a number of maneuvers that have previously been shown to influence exchange activity in rat hippocampal neurons. Thus, harmaline (a non-selective inhibitor of Na^+/H^+ exchange activity in rat hippocampal neurons; see Raley-Susman *et al.* 1991), while decreasing rates of pH_i recovery from internal acid loads imposed under normoxic, Hepes-buffered conditions, had no influence on Na^+ influx occurring during anoxia. In contrast, harmaline limited significantly the increase in $[Na^+]_i$ observed following anoxia. These observations are consistent with the pH_i measurements presented in Chapters 3 and 4 which suggested that, in rat hippocampal neurons, Na^+/H^+ exchange activity is reduced during anoxia and becomes activated in the immediate post-anoxic period. Additional maneuvers which were found, on the basis of pH_i measurements, to inhibit Na^+/H^+ exchange activity in the post-anoxic period (i.e. pH_o 6.60 and *R*p-cAMPS; see Chapter 4) similarly limited the increase in $[Na^+]_i$ observed following anoxia. Furthermore, the increase in $[Na^+]_i$ observed following anoxia was enhanced by maneuvers which stimulate Na^+/H^+ exchange activity in the immediate post-anoxic period (i.e. pH_o 7.80).

In response periods of ischemia, extensive studies have pointed to Na^+/H^+ exchange as an important mechanism that contributes to the increase in $[Na^+]_i$ seen in cardiac myocytes during reperfusion (reviewed by Karmazyn, 1999; Avkiran, 2001). The present results point to an

analogous contribution from Na^+/H^+ exchange activity to the increase in $[Na^+]_i$ observed immediately following anoxia in rat hippocampal neurons. In a similar manner, following periods of oxygen-glucose deprivation, cortical astrocytes deficient in NHE1 do not demonstrate the internal Na^+ loading typically observed in astrocytes expressing functional NHE1 activity (Kintner *et al.* 2004). The contribution of Na^+/H^+ exchange to the increase in $[Na^+]_i$ observed following anoxia may provide a mechanistic explanation for the neuroprotective effects of Na^+/H^+ exchange inhibitors in *in vivo* models of cerebral ischemia. Indeed, in one study, the protective effect of Na^+/H^+ exchange inhibitors was attributed to a reduction in cerebral Na^+ content (Kuribayashi *et al.* 1999; also see Matusmoto *et al.* 2003; Yamamoto *et al.* 2003).

That Na^+/H^+ exchange activity can lead to elevations in $[Na^+]_i$ is not without precedence. Na^+/H^+ exchange activity causes increases in $[Na^+]_i$ under normoxic conditions in many cell types (see Chapter 6; also Moody, 1981; Kaila & Vaughan-Jones, 1987) and it has been suggested that Na^+/H^+ exchanger-induced increases in $[Na^+]_i$ may play key roles in regulating Na^+/Ca^{2+} exchange activity and/or the activities of intracellular signaling cascades (e.g. Hayasaki-Kajiwara *et al.* 1999; Trudeau *et al.* 1999; Mukhin *et al.* 2004). In these, and possibly other, ways, increased Na^+/H^+ exchange appears to underlie the increase in presynaptic quantal glutamate release that occurs during the recovery of pH_i from imposed internal acidification in hippocampal neurons (Trudeau *et al.* 1999; also see Nordmann & Stuenkel, 1991; Bouron & Reuter, 1996). The contribution of Na^+/H^+ exchange activity in the increase in $[Na^+]_i$ observed following anoxia is considered further in Chapter 6.

As detailed in Chapter 4, a Zn^{2+}-sensitive H^+ efflux pathway (a putative g_{H^+}) also contributes to acid extrusion following anoxia in rat hippocampal neurons (also see Diarra *et al.* 1999), and it has been suggested previously by others that inhibition of g_{H^+}s may increase the

demand placed on Na^+/H^+ exchange for acid extrusion (see Chapter 4; Demaurex *et al.* 1995). Consistent with this idea, Zn^{2+} had no effect on the increase in $[Na^+]_i$ observed during anoxia but enhanced Na^+ influx in the post-anoxic period, an effect that was blocked under pH_o 6.60, conditions that are known to inhibit functional Na^+/H^+ exchange (Jean *et al.* 1985; Vaughan-Jones & Wu, 1990; Diarra *et al.* 1999). Although Zn^{2+} can modulate the activities of several ion channels and transport mechanisms (see Chapter 4), under the constant perfusion conditions employed in the present study, anoxia-evoked changes in $[Na^+]_i$ are unaffected by NMDA or AMPA receptor antagonists or blockers of voltage-activated Ca^{2+} channels (see Chapter 7) and the effects of Zn^{2+} on the increase in $[Na^+]_i$ observed following anoxia were observed when the Na^+,K^+-ATPase was already inhibited. It is of note that Zn^{2+}-induced increases in $[Na^+]_i$ have been observed previously in cultured cortical neurons and may contribute to a post-ischemic upregulation of NMDA receptor activity (Manzerra *et al.* 2001).

5.3.4. Contribution of HCO_3^--dependent mechanisms

In the majority of cells, HCO_3^--dependent pH_i regulating mechanisms act in concert with Na^+/H^+ exchange to regulate pH_i and some of these HCO_3^--dependent mechanisms (i.e. Na^+-dependent Cl^-/HCO_3^- exchange and electrogenic Na^+/HCO_3^- cotransport) also transport Na^+ ions. In the present study, I found no evidence to suggest that HCO_3^--dependent mechanisms contribute to Na^+ influx during anoxia in rat hippocampal neurons (possibly a result of a decline in internal ATP levels; e.g. Boron *et al.* 1988).

In contrast, HCO_3^--dependent mechanism(s) appear to contribute to Na^+ influx following anoxia. Given the multiple HCO_3^--dependent processes in rat hippocampal neurons, the identity of those mechanism(s) that contribute to enhanced Na^+ influx after anoxia in neurons 11 - 14 DIV remains unclear. On the one hand, Na^+-dependent Cl^-/HCO_3^- exchange contributes to acid

extrusion in this cell type (Schwiening & Boron, 1994; Baxter & Church, 1996; Brett *et al.* 2002a) and a post-anoxic activation of exchange activity may account for the HCO_3^--dependent, DIDS-sensitive Na^+ influx observed following anoxia. On the other hand, in non-neuronal cell types, electrogenic Na^+/HCO_3^- cotransport has been found to contribute to Na^+-dependent acid extrusion both during and following periods of ischemia (Lamers, 2001; Khandoudi *et al.* 2001; also see Giffard *et al.* 2000). Na^+/HCO_3^- cotransporters are expressed in discrete populations of central neurons (see Bevensee *et al.* 2000; Giffard *et al.* 2000; Schmitt *et al.* 2000); however, there is little functional evidence for their participation in pH_i regulation in rat hippocampal neurons, at least under normoxic conditions (Schwiening & Boron, 1994; Baxter & Church, 1996), although inward (i.e. acid-extruding) Na^+/HCO_3^- cotransport activity could be activated in response to membrane depolarizations observed during anoxia. The possibility that Na^+_o- and HCO_3^--dependent acid extrusion (either Na^+-dependent Cl^-/HCO_3^- exchange or Na^+/HCO_3^- cotransport) might contribute to an increase in $[Na^+]_i$ immediately following anoxia in rat hippocampal neurons is at variance with the previous observation that HCO_3^--dependent mechanisms appear to *limit* the magnitude of the internal alkalinization observed in the immediate post-anoxic period (see Chapter 3 for data in isolated adult hippocampal neurons and Diarra *et al.* 1999 for similar findings in cultured postnatal rat hippocampal neurons). Rather, the observation that the magnitude of the increase in pH_i observed following anoxia appears smaller in the presence *vs.* the absence of HCO_3^- is consistent to observations made in mouse hippocampal neurons wherein an acid-loading Na^+/HCO_3^- cotransporter is activated during and following transient periods of anoxia (Yao *et al.* 2003); however, this mechanism would act to extrude Na^+ ions. Finally, it is also possible that the complex modulation of voltage-dependent Na^+ currents by HCO_3^- ions (e.g. Gu *et al.* 2000; Bruehl & Witte, 2003) could contribute to the

differences in Na^+ influx observed after anoxia under HCO_3^--containing compared with HCO_3^--free conditions.

Although the ability of DIDS to limit the increase in $[Na^+]_i$ following anoxia under HCO_3^-/CO_2-buffered conditions is consistent with its ability to inhibit HCO_3^--dependent pH_i regulating mechanisms present in rat hippocampal neurons, DIDS also reduced the increase in $[Na^+]_i$ observed following anoxia under HCO_3^--free, Hepes-buffered conditions, albeit to a much lesser extent. The latter observation may reflect residual activities of HCO_3^--dependent, Na^+-transporting mechanisms in the nominal absence of HCO_3^- (see Wu *et al.* 1994; Deitmer & Schneider, 1998) or the recognized effects of DIDS on HCO_3^--independent processes, which include the inhibition of chloride channels, K^+/Cl^- transport and mitochondrial release of free radicals (see Han *et al.* 2003; Malek *et al.* 2003; Tauskela *et al.* 2003).

5.3.5. Summary

This present study in rat hippocampal neurons is consistent with previous findings, made in a variety of non-neuronal cell types, that Na^+/H^+ exchange and HCO_3^--dependent mechanism(s) contribute to potentially injurious Na^+ influx in the vulnerable period immediately after anoxia. Thus, in isolated rat hippocampal cultures, Na^+/H^+ exchange activity appears to contribute to post-anoxic increases in $[Na^+]_i$. Although developmental changes in neuronal Na^+/H^+ exchange expression and/or activity have been observed (see Bevensee *et al.* 1996; Ma & Haddad, 1997; Douglas *et al.* 2001; Nottingham *et al.* 2001), the contribution of Na^+/H^+ exchange to the increases in $[Na^+]_i$ observed following anoxia was observed in neurons both 6 - 10 and 11 - 14 DIV. In light of the evidence that pharmacological inhibitors of Na^+/H^+ exchange effectively protect against anoxia- and ischemia-induced neuronal injury, the results presented in Chapters 3 - 5 are consistent with the possibilities that the neuroprotective actions of Na^+/H^+ exchange

inhibitors may result from reductions in the rises in pH_i *and/or* $[Na^+]_i$ that occur during early reperfusion (this is considered further in Chapter 6).

HCO_3^--dependent mechanisms also appear to contribute to the increase in $[Na^+]_i$ observed following anoxia, although this effect was restricted to neuronal cultures 11 - 14 DIV. Developmental upregulation of the expression of HCO_3^--dependent pH_i regulating mechanisms has been reported in the central nervous system (Raley-Susman *et al.* 1993; Kobayashi *et al.* 1994; Ma & Haddad, 1997; Douglas *et al.* 2001; Giffard *et al.* 2003) and, thus, may account for this difference. However, given the presence of multiple HCO_3^--dependent mechanisms that may contribute to this observed response, together with the complexities of the regulation of such mechanisms in rat hippocampal neurons (see Brett *et al.* 2002a), further experiments are required to clarify the potential contribution of HCO_3^--dependent pH_i regulating mechanisms to anoxia-evoked increases in $[Na^+]_i$ in rat hippocampal neurons.

Despite the findings summarized above, there are two important limitations of the present study. *First*, although it is established that Na^+/H^+ exchange activity is a major acid-extruding mechanism in rat hippocampal neurons under nominally HCO_3^--free conditions, firm conclusions regarding the contribution of Na^+/H^+ exchange activity to anoxia-induced changes in $[Na^+]_i$ (and pH_i) are limited by the non-selective maneuvers that had to be employed to modulate exchange activity. Thus, to more precisely establish the contribution of Na^+/H^+ exchange to anoxia-evoked changes in pH_i and $[Na^+]_i$, in the following Chapter (Chapter 6), I developed a microspectrofluorimetric technique for the concurrent measurement of both ions in isolated hippocampal neurons. *Second,* it is clear that the activities of pH_i regulating mechanisms can account for neither the increase in $[Na^+]_i$ observed during anoxia nor all of the Na^+ entry that takes place in the immediate post-anoxic period. Thus, in Chapter 7, a study examining additional

mechanism(s) that might potentially contribute to the increases in $[Na^+]_i$ observed during *and* following anoxia will be presented.

Table 5.1: Contribution of pH_i regulating mechanisms to the increase in $[Na^+]_i$ observed during anoxia

	Normalized $\Delta[Na^+]_{i(during)}$	
	6 – 10 DIV	11 – 14 DIV
Treatment		
200 μM harmaline[1]	0.91 ± 0.22 (7)	0.98 ± 0.26 (5)
100 μM Zn^{2+}	1.03 ± 0.18 (12)	1.17 ± 0.15 (15)
HCO_3^-/CO_2-buffered medium	1.11 ± 0.13 (8)	0.77 ± 0.15 (5) N.S.
HCO_3^-/CO_2-buffered medium + 200 μM DIDS	1.28 ± 0.28 (3)	0.78 ± 0.31 (4) N.S.

To generate Normalized $\Delta[Na^+]_{i(during)}$ values, measurements of $\Delta[Na^+]_{i(during)}$ under experimental test conditions were normalized to measurements made in experiments performed on age-matched sister cultures under control conditions. Statistical comparisons were performed by comparing absolute $\Delta[Na^+]_{i(during)}$ measurements made under experimental test conditions to measurements made in age-matched sister cultures under control conditions. Numbers in brackets denote the number of neuronal populations (i.e. coverslips) from which the data were generated. [1]Neurons were treated with 200 μM harmaline for 120 - 180 min prior to the start of an experiment. DIV, days *in vitro*. N.S. indicates no significant difference between the increase in $[Na^+]_i$ observed during anoxia under HCO_3^-/CO_2-buffered conditions, either in the presence or absence of 200 μM DIDS, and the increase in $[Na^+]_i$ observed during anoxia in age-matched sister cultures under control (HCO_3^--free, Hepes-buffered) conditions (P = 0.51 and 0.78, respectively).

Table 5.2: Contribution of pH_i regulating mechanisms to the increase in $[Na^+]_i$ observed following anoxia under 0 $[K^+]_o$ conditions

	Normalized $\Delta[Na^+]_{i(after)}$	
	6 – 10 DIV	11 – 14 DIV
Treatment		
200 μM harmaline[1]	0.48 ± 0.11 (7)*	0.76 ± 0.08 (7)*
pH_o 6.60	0.56 ± 0.10 (6)*	0.79 ± 0.05 (7)*
50 μM *R*p-cAMPS[2]	0.69 ± 0.09 (5)*	0.77 ± 0.08 (4)*
pH_o 7.80	1.27 ± 0.06 (10)*	1.57 ± 0.41 (4)*
100 μM Zn^{2+}	1.87 ± 0.27 (7)*	1.38 ± 0.16 (8)*
100 μM Zn^{2+}, pH_o 6.60	0.81 ± 0.28 (3)	n.d.

To generate Normalized $\Delta[Na^+]_{i(after)}$ values, measurements of $\Delta[Na^+]_{i(after)}$ under experimental test conditions were normalized to measurements made in experiments performed on age-matched sister cultures under control conditions. Statistical comparisons were performed by comparing absolute $\Delta[Na^+]_{i(after)}$ measurements made under experimental test conditions to measurements made in age-matched sister cultures under control conditions. Numbers in brackets denote the number of neuronal populations (i.e. coverslips) from which the data were generated. [1]Neurons were treated with 200 μM harmaline for 120 - 180 min prior to the start of an experiment. [2]*R*p-cAMPS was present in the perfusate during and following anoxia. Alterations in pH_o and exposure to Zn^{2+} began at the start of perfusion with K^+-free media. * indicates statistical significance ($P < 0.05$) compared with measurements of made in age-matched sister cultures in the absence of treatment. DIV, days *in vitro*; n.d., not determined.

Fig. 5.1. Anoxia-evoked changes in $[Na^+]_i$ in rat hippocampal neurons. *A*, 5 min anoxia was imposed under nominally HCO_3^--free, Hepes-buffered conditions by exposure to medium containing 1 - 2 mM sodium dithionite and bubbled vigorously with 100% Ar (filled circles). Also shown are the changes in $[Na^+]_i$ evoked by anoxia in a sister culture exposed to medium containing 1 - 2 mM sodium dithionite and bubbled vigorously with air (open circles). *B*, relationship between the magnitude of the increase in $[Na^+]_i$ observed during 5 min anoxia ($\Delta[Na^+]_{i(during)}$) and the number of days that neurons were maintained in culture (DIV, days *in vitro*). Anoxia was imposed under Hepes-buffered conditions either by the addition of 1 - 2 mM sodium dithionite to medium bubbled with 100% Ar (filled circles; n = 21 - 54 for each datum point) or by exposure to medium that had been bubbled vigorously with 100% ultrapure Ar for >18 h (open circles; $n \geq 2$ for each datum point). The solid line represents a linear regression fit to the data points obtained when anoxia was imposed by the addition of sodium dithionite (correlation coefficient = 0.96; $P<0.0001$ by one-way ANOVA). Error bars are S.E.M. *C*, under normal Na^+_o-containing conditions, anoxia induced an increase in $[Na^+]_i$ that recovered upon the return to normoxia (filled circles). When anoxia was imposed under reduced Na^+_o, $NMDG^+$-substituted conditions, the increase in $[Na^+]_i$ was abolished (open circles).

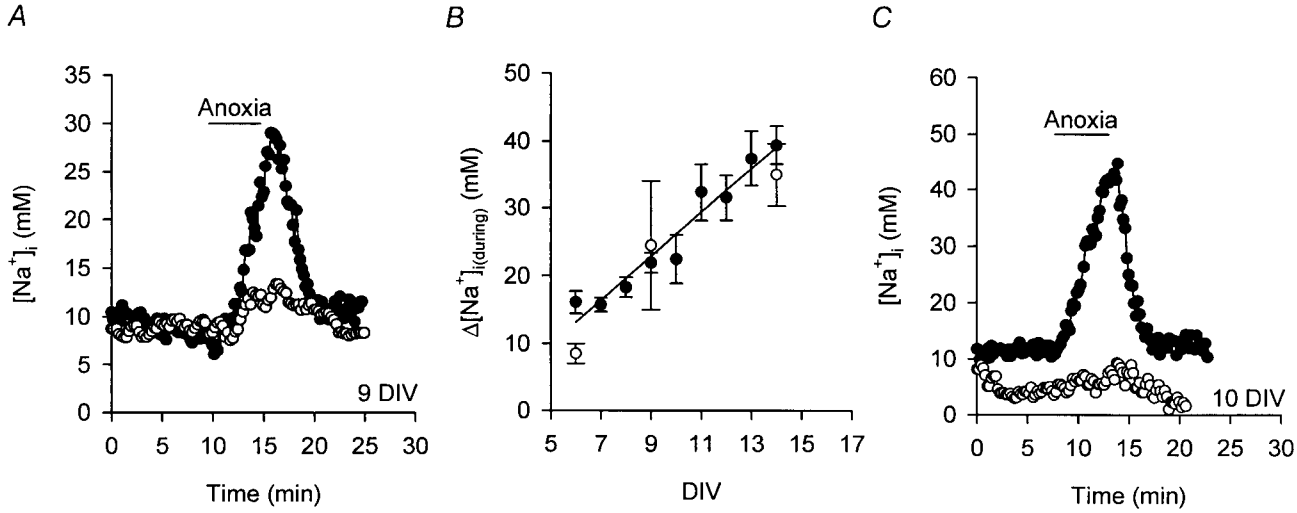
A
B
C
Anoxia
9 DIV
10 DIV
[Na+]i (mM)
Time (min)
Δ[Na+]i(during) (mM)
DIV

Fig. 5.2. Contribution of reduced Na^+,K^+-ATPase activity to the increase in $[Na^+]_i$ observed during anoxia. *A,* superimposed records of the changes in $[Na^+]_i$ observed in response to 5 min exposure to $[K^+]$-free medium (filled symbols) or 500 μM ouabain (open symbols), as indicated by the bar above the traces (compare with Fig. 5.1*A*). $[Na^+]_i$ failed to show complete recovery following ouabain application. *B,* intracellular ATP levels were determined after 3 or 5 min anoxia induced by exposure to sodium dithionite-containing medium in neurons with (open symbols) or without (filled symbols) pretreatment with 10 mM creatine for ≥2 h. Measurements were made using neuronal cultures 8 - 10 DIV and were normalized to values obtained prior to anoxia in age-matched sister cultures in each experimental group. The fall in ATP levels evoked by 3 min anoxia under control conditions was significantly attenuated by creatine pretreatment (*, $P < 0.05$). Numbers in brackets indicate the number of neuronal populations from which data were obtained. *C,* in 6 - 10 DIV neurons pretreated with 10 mM creatine for ≥2 h (open bars), the increase in $[Na^+]_i$ measured 3 min after the start of anoxia was significantly less than that observed in age-matched sister cultures under control neurons (filled bar; *; $P < 0.05$). There was no statistical difference between the increase in $[Na^+]_i$ measured following 5 min anoxia in creatine-treated and untreated cultures ($P = 0.57$).

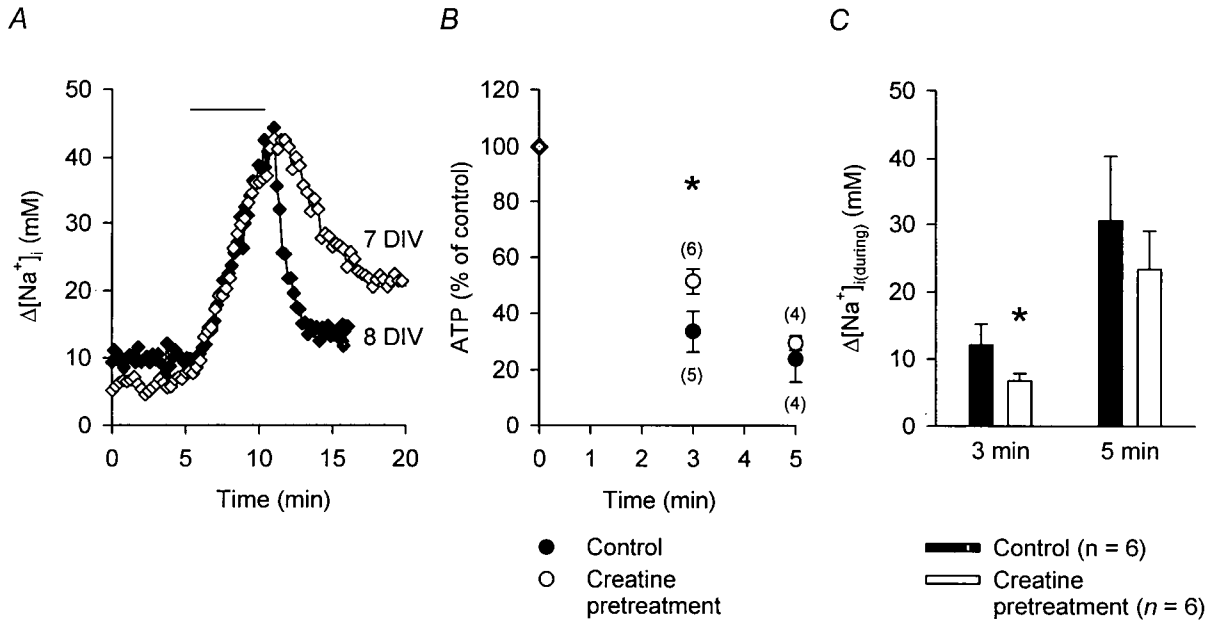
A
B
C
50
40
30
20
10
0
Δ[Na+]i (mM)
7 DIV
8 DIV
0
5
10
15
20
Time (min)
120
100
80
60
40
20
0
ATP (% of control)
*
(6)
(5)
(4)
(4)
0
1
2
3
4
5
Time (min)
Control
Creatine pretreatment
50
40
30
20
10
0
Δ[Na+]i(during) (mM)
*
3 min
5 min
Control (n = 6)
Creatine pretreatment (n = 6)

Fig. 5.3. Changes in $[Na^+]_i$ observed after anoxia during inhibition of Na^+,K^+-ATPase activity. *A*, Na^+,K^+-ATPase activity was inhibited by perfusion with K^+-free medium at the end of 5 min anoxia (filled circles), revealing a secondary rise in $[Na^+]_i$ in the immediate post-anoxic period. Neurons on a different coverslip were exposed to K^+- and Na^+-free medium immediately after 5 min anoxia (open circles). In the absence of external Na^+ ($NMDG^+$-substitution), the increase in $[Na^+]_i$ following anoxia was abolished. *B*, the relationship between the magnitude of the increase in $[Na^+]_i$ observed after anoxia ($\Delta[Na^+]_{i(after)}$) and the number of days neurons were maintained in culture (filled circles; n = 7 - 31 for each datum point). The solid line represents a linear regression fit to the data points indicated (correlation coefficient = 0.88; $P<0.0001$ by one-way ANOVA). Also shown are $\Delta[Na^+]_{i(after)}$ values measured during inhibition of the Na^+,K^+-ATPase with 500 μM ouabain (open circles; $n = 3$ for each datum point).

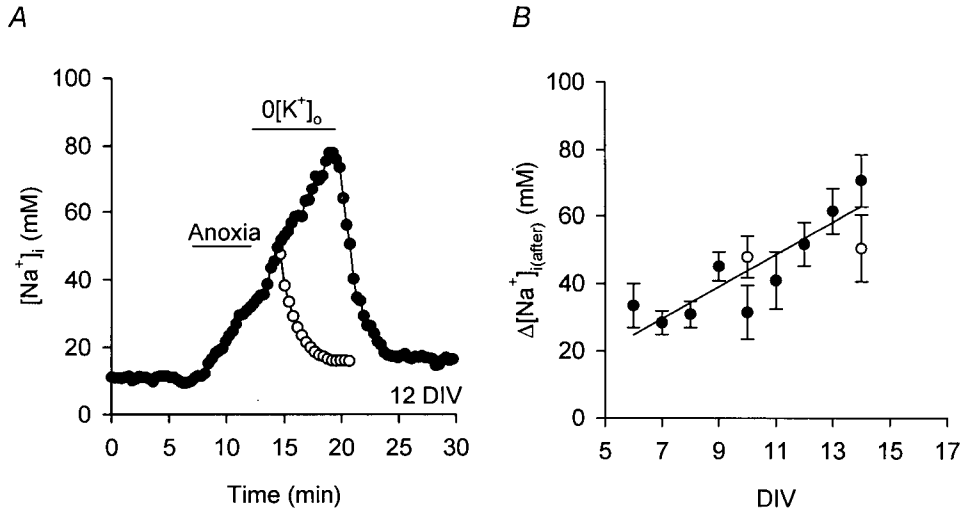
A
B
100
80
60
40
20
0
$[Na^+]_i$ (mM)
$0[K^+]_o$
Anoxia
12 DIV
0
5
10
15
20
25
30
Time (min)
$\Delta[Na^+]_{i(after)}$ (mM)
5
7
9
11
13
15
17
DIV

Fig. 5.4. Effects of modulating Na^+/H^+ exchange activity on the increase in $[Na^+]_i$ observed after anoxia (Na^+,K^+-ATPase inhibited). *A,* at the end of 5 min anoxia, neurons were exposed to K^+-free medium for 7 min. Compared with changes observed under control conditions (filled circles), the magnitude of the increase in $[Na^+]_i$ observed after anoxia under K^+-free conditions was reduced by pretreatment with harmaline (200 μM for 120 - 180 min; open circles), at pH_o 6.60 (open diamonds), or in the presence of the PKA inhibitor, *R*p-cAMPS (50 μM, applied at the beginning of anoxia; cross-hairs). In contrast, the magnitude of the increase in $[Na^+]_i$ observed following anoxia was enhanced at pH_o 7.80 (open triangles). Alterations in pH_o began immediately at the start of superfusion with K^+-free medium and continued for the duration of the records shown. *Inset,* examined under normoxic HCO_3^--free, Hepes-buffered conditions, internal acid loads were imposed using the NH_4^+ pre-pulse technique in age-matched sister cultures pretreated (open symbols; $n = 6$) or not pretreated (filled symbols; $n = 10$) with 200 μM harmaline. Harmaline pretreatment reduced rates of pH_i recovery. *B,* exposure to 100 μM Zn^{2+} (open squares) immediately following anoxia under under $[K^+]_o$-free conditions enhanced the increase in $[Na^+]_i$ observed at this time, compared with that observed following anoxia in an age-matched sister culture in the absence of Zn^{2+} (filled circles). In another age-matched sister culture, this effect was abolished when 100 μM Zn^{2+} was applied at pH_o 6.60 (filled squares). Exposure to Zn^{2+} with or without alterations in pH_o began at the start of perfusion with K^+-free medium and continued for the duration of the records shown.

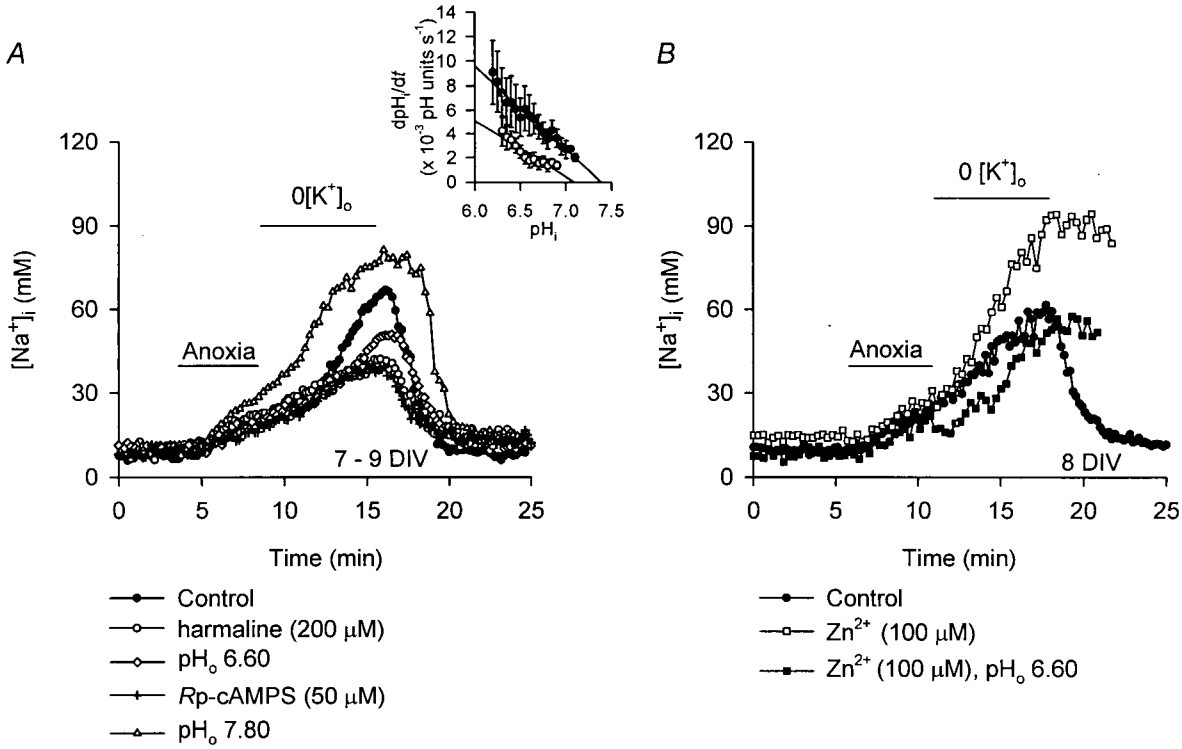
A
B
0[K+]o
Anoxia
7 - 9 DIV
[Na+]i (mM)
Time (min)
dpHi/dt (x 10-3 pH units s-1)
pHi
0 [K+]o
8 DIV
Control
harmaline (200 μM)
pHo 6.60
Rp-cAMPS (50 μM)
pHo 7.80
Zn2+ (100 μM)
Zn2+ (100 μM), pHo 6.60

Fig. 5.5. Contribution of HCO_3^--dependent mechanisms to the increase in $[Na^+]_i$ observed after anoxia (Na^+,K^+-ATPase inhibited). *A*, under HCO_3^--free, Hepes-buffered (filled circles) or HCO_3^-/CO_2-buffered (open circles) conditions, neurons were exposed to 5 min anoxia followed by 7 min perfusion with K^+-free medium. 200 μM DIDS reduced the augmented increase in $[Na^+]_i$ observed after anoxia under HCO_3^-/CO_2-buffered conditions (open diamonds; DIDS was added to anoxic media and was present throughout the rest of the record). *B*, summary of the effects of external buffering conditions and DIDS on the increase in $[Na^+]_i$ observed after anoxia in neurons 6 - 10 and 11 - 14 DIV. Neither the addition of HCO_3^- nor the presence of 200 μM DIDS under HCO_3^-/CO_2-buffered or Hepes-buffered conditions, influenced significantly the increase in $[Na^+]_i$ observed after anoxia in neuronal cultures 6 - 10 DIV, compared to the increase in $[Na^+]_i$ observed after anoxia in the absence of HCO_3^-. In contrast, in neuronal cultures 11 - 14 DIV, the increase in $[Na^+]_i$ after anoxia was enhanced in the presence of HCO_3^-/CO_2 and, under HCO_3^-/CO_2-buffered conditions, DIDS reduced the magnitude of the rise in $[Na^+]_i$ to a value similar to that observed under control conditions (i.e. Hepes-buffered media in the absence of DIDS; $P = 0.66$). † indicates statistical significance ($P < 0.05$) compared to measurements made in age-matched sister cultures under HCO_3^-/CO_2-buffered conditions in the absence of DIDS. * indicates statistical significance ($P < 0.05$) compared to measurements made in age-matched sister neurons under nominally HCO_3^--free, Hepes-buffered conditions in the absence of DIDS. Error bars are S.E.M.

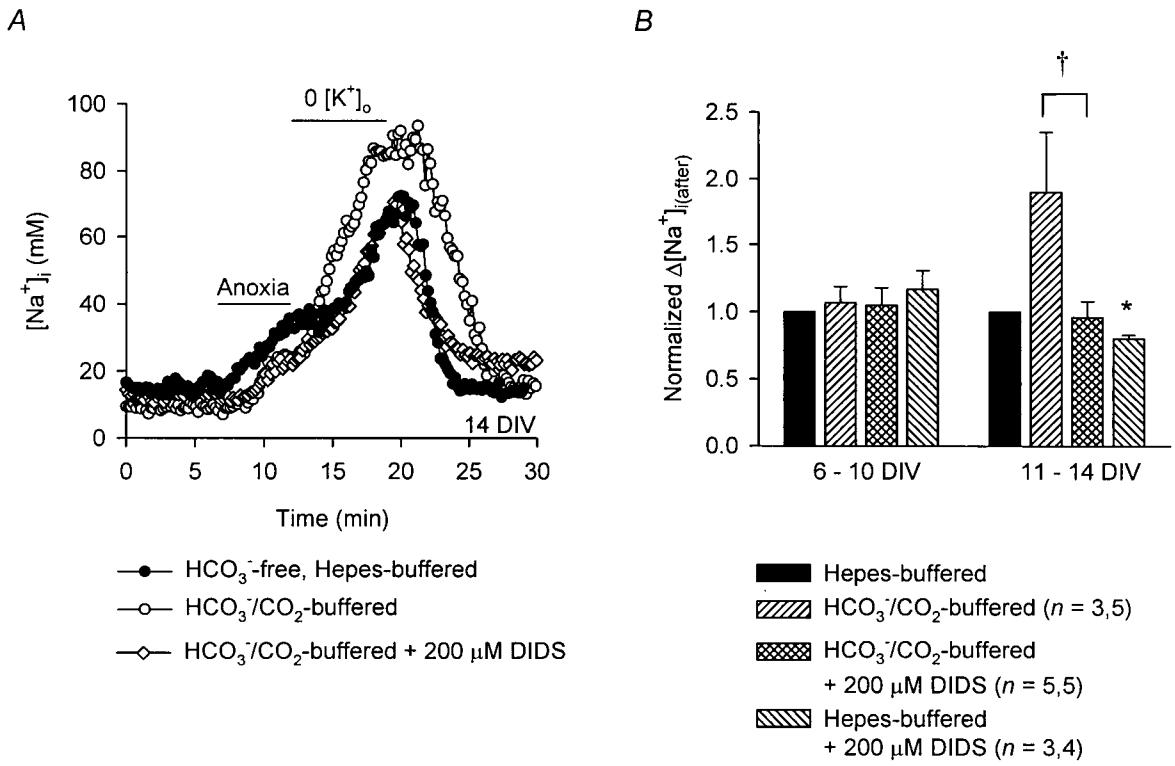
A
B
0 [K+]o
Anoxia
14 DIV
[Na+]i (mM)
Time (min)
HCO3-free, Hepes-buffered
HCO3-/CO2-buffered
HCO3-/CO2-buffered + 200 μM DIDS
Normalized Δ[Na+]i(after)
6 - 10 DIV
11 - 14 DIV
Hepes-buffered
HCO3-/CO2-buffered (n = 3,5)
HCO3-/CO2-buffered + 200 μM DIDS (n = 5,5)
Hepes-buffered + 200 μM DIDS (n = 3,4)

CHAPTER SIX

CONCURRENT MEASUREMENT OF pH_i AND $[Na^+]_i$ WITH FLUORESCENT INDICATORS: A FURTHER EVALUATION OF THE ROLE OF Na^+/H^+ EXCHANGE TO ANOXIA-EVOKED CHANGES IN $[Na^+]_i$ AND pH_i[8]

6.0. INTRODUCTION

In the absence of a selective pharmacological agent to inhibit Na^+/H^+ exchange activity in rat hippocampal neurons, in Chapters 3 - 5, the contribution of Na^+/H^+ exchange activity to the changes in pH_i and $[Na^+]_i$ observed during and following anoxia was inferred, under HCO_3^--free conditions, by determining the Na^+_o- (and Li^+_o-) dependencies of the anoxia-evoked changes in pH_i (Chapters 3 and 4) and by examining the effects of non-selective maneuvers that influence Na^+/H^+ exchange activity on anoxia-evoked changes in $[Na^+]_i$ (Chapter 5). The results were consistent with the possibility that Na^+/H^+ exchange activity is stimulated immediately following anoxia in rat hippocampal neurons and contributes to the regulation of both pH_i and $[Na^+]_i$ at this time. Nevertheless, in the studies presented in Chapters 3 - 5, fluorescent probe-based measurements of pH_i and $[Na^+]_i$ were conducted separately in experiments performed in parallel, an approach that limits attempts to understand the interrelationships that exist between $[H^+]_i$ and $[Na^+]_i$. It is apparent that concurrent measurements of pH_i and $[Na^+]_i$ would provide further insight into the presumed relationship between anoxia-evoked changes in $[H^+]_i$ and $[Na^+]_i$, particularly in the post-anoxic period, and would strengthen conclusions made regarding the role of Na^+/H^+ exchange activity in the genesis of these ionic changes.

---

[8] A version of this chapter has been published. Sheldon C., Cheng Y.M. and Church J. (2004) Concurrent measurements of the free cytosolic concentrations of H^+ and Na^+ ions with fluorescent indicators. Pflügers Arch. Epub.

Changes in pH_i and $[Na^+]_i$ may be linked directly through mechanisms as diverse as Na^+/H^+ exchange (e.g. Kaila & Vaughan-Jones, 1987), Na^+-dependent Cl^-/HCO_3^- exchange (e.g. Rose & Ransom, 1997) and electrogenic Na^+/HCO_3^- cotransport (e.g. Bers *et al.* 2003; Deitmer & Schlue, 1989), or indirectly via the coordinated activities of two or more transport mechanisms. In a number of cell types, for example, a rise in $[Na^+]_i$ promotes reverse-mode Na^+/Ca^{2+} exchange and the subsequent rise in $[Ca^{2+}]_i$ can cause a fall in pH_i by activating the acid-loading Ca^{2+},H^+-ATPase (e.g. Kiedrowksi, 1999). Furthermore, changes in pH_i and $[Na^+]_i$ can influence the activities of not only pH_i regulating transporters (Green *et al.* 1988; Kaila & Vaughan-Jones, 1987) but also mechanisms that contribute to Na^+ flux across biological membranes, including Na^+/Ca^{2+} exchange and $Na^+/K^+/2Cl^-$ cotransport (Blaustein & Lederer, 1999; Russell, 2000). This complex relationship between changes in $[H^+]_i$ and $[Na^+]_i$, and the recognized importance of both of these ions as determinants of cell function under a variety of physiological and pathophysiological conditions, further highlights the need for concurrent quantitative measurements of both ions.

Thus, in the *first* part of this study I developed and characterized a novel technique for the near-simultaneous measurement of $[Na^+]_i$ and pH_i in rat hippocampal neurons using, respectively, the dual excitation Na^+ indicator SBFI (Minta & Tsien, 1989) and the dual emission seminaphthorhodafluor pH indicators carboxy SNARF-1 (Whitaker *et al.* 1991) or SNARF-5F (Liu *et al.* 2001). Although SNARF-5F retains the spectral properties of other SNARF derivatives, it displays a lower pK_a value under cell-free *in vitro* conditions (pK_a ~7.2) that may make it more suitable than carboxy SNARF-1 (pK_a ~7.5) for measuring changes in pH_i below ~6.5, as may occur, for example, in mammalian central neurons during anoxia or ischemia. Next, in the *second* part of this study, I used the technique developed in the first part of the study to perform concurrent measurements of pH_i and $[Na^+]_i$ to further examine the involvement of

Na^+/H^+ exchange activity in the anoxia-evoked changes in pH_i and $[Na^+]_i$ observed in cultured rat hippocampal neurons.

6.1. MATERIALS AND METHODS

6.1.1. Experimental preparation

Primary cultures of hippocampal neurons prepared from 2 - 4 day old postnatal Wistar rats were employed in all experiments presented in this Chapter.

6.1.2. Dye loading and recording techniques

In the majority of experiments, changes in pH_i were measured with either carboxy SNARF-1 or SNARF-5F carboxylic acid. The acetoxymethyl esters of carboxy SNARF-1 and SNARF-5F (carboxy SNARF-1-AM and SNARF-5F-AM, respectively) were prepared as 10 and 5 mM stock solutions in DMSO, respectively. In a limited number of experiments, BCECF was used to measure anoxia-evoked changes in pH_i.

Cultured postnatal rat hippocampal neurons were loaded with SBFI in the manner described in Chapter 5. To load SNARF derivatives, either individually or following SBFI-AM incubation, coverslips with neurons attached were placed in standard loading medium containing 0.10% Pluronic acid and either 10 μM carboxy SNARF-1-AM or SNARF-5F-AM for 30 min at 32°C. In experiments in which BCECF was employed as the pH_i indicator, coverslips with neurons attached were placed in standard loading medium containing 2 μM BCECF-AM for 30 min at 22°C (Baxter & Church, 1996). Following loading, coverslips were placed in standard loading medium for 20 min to ensure de-esterification of the fluorophore(s) and then mounted in a temperature-controlled perfusion chamber to form the base of the chamber. Neurons were

superfused at a rate of 2 ml min^{-1} for 15 min with the initial experimental solution at 37°C (unless otherwise noted) before the start of an experiment.

Details of the recording techniques used to measure pH_i in neurons loaded only with BCECF are provided in Chapter 2. In neurons loaded with SBFI and/or a SNARF-based derivative, measurements of $[Na^+]_i$ and/or pH_i were performed using the dual-excitation and dual-emission ratio methods, respectively. The same imaging system employed in studies described in Chapters 3 - 5 to measure pH_i or $[Na^+]_i$ in neurons single-loaded with BCECF or SBFI, respectively, was used to measure pH_i and $[Na^+]_i$ concurrently but with a different filter set and the addition of a second intensified charge coupled device camera. A schematic diagram of the optical equipment used for measurements of $[Na^+]_i$ and pH_i in neurons loaded with SBFI and/or carboxy SNARF-1 or SNARF-5F in the present series of experiments is presented in Fig. 6.1. Filter selection was based upon the published *in vitro* spectra of SBFI, carboxy SNARF-1 and SNARF-5F (Minta & Tsein, 1989; Martínez-Zaguilán *et al.* 1991; Liu *et al.* 2001). In experiments in which SBFI alone was employed, neurons were excited alternately at 334 ± 5 and 380 ± 5 nm and fluorescence emissions at 550 ± 40 nm were detected sequentially by a single camera (Camera 2 in Fig. 6.1). In experiments in which carboxy SNARF-1 or SNARF-5F alone were employed, neurons were excited at 488 ± 5 nm and fluorescence emissions at 550 ± 40 and 640 ± 20 nm were detected simultaneously by two cameras (Cameras 1 and 2, respectively, in Fig. 6.1), the registration of which was confirmed prior to every experiment. In experiments in which neurons were co-loaded with SBFI and either carboxy SNARF-1 or SNARF-5F, ratio pairs were collected continuously by alternating between the excitation and emission modes; each automated cycle took ~1.5 s to complete, including a ~0.5 s delay between collecting SBFI- and SNARF-derived ratio pairs, and was repeated every 2 - 15 s during the course of an experiment.

6.1.3. Calculation of $[Na^+]_i$ and pH_i

As described in Chapter 2, a one-point calibration technique was employed to convert background-corrected BCECF ratio values to absolute pH_i values. Similarly, a one-point calibration technique was employed to convert background-corrected SBFI (BI_{334}/BI_{380}) and SNARF-derived (BI_{550}/BI_{640}) ratio values into $[Na^+]_i$ and pH_i values, respectively. At the end of an experiment, neurons loaded with SBFI were exposed to a pH 7.35 medium containing 10 mM Na^+ and 4 μM gramicidin D (Table 2.3; Diarra *et al.* 2001) whereas neurons loaded with carboxy SNARF-1 or SNARF-5F were exposed to a high-$[K^+]$, pH 7.00 solution containing 10 μM nigericin (Table 2.3; Baxter & Church, 1996); in neurons loaded with both SBFI and a SNARF derivative, the SBFI and SNARF one-point calibrating media were applied sequentially. The resulting background-corrected ratio values at $[Na^+]_i$ = 10 mM (for SBFI) and at pH_i = 7.00 (for carboxy SNARF-1 or SNARF-5F) were used as normalization factors for experimentally-derived background-subtracted SBFI (BI_{334}/BI_{380}) and SNARF (BI_{550}/BI_{640}) ratio values, respectively. At the end of some experiments conducted at 37°C, I was unable to obtain stable normalizing ratio values for carboxy SNARF-1 or SNARF-5F during the one-point calibration at pH 7.00. In these cases, the one-point calibration was either repeated at pH 7.50 or the experimental data were normalized with ratio values obtained under identical experimental and optical conditions from a fresh sister culture loaded with the appropriate dye(s) and exposed to SNARF calibrating medium at pH 7.00. A similar instability of carboxy SNARF-1 and SNARF-5F ratio values, characterized by anomalous increases and decreases in background-subtracted 550 and 640 nm emission intensities, respectively, was also sometimes experienced during full calibration experiments conducted at 37°C when pH values were ≤7.00. The reasons for these atypical behaviours, which could occur in neurons loaded with carboxy SNARF-1 or SNARF-5F in the absence or presence of SBFI, remain unclear, although

similar difficulties have been experienced by others (e.g. Bassnett *et al.* 1990; Martínez-Zaguilán *et al.* 1991; Seksek *et al.* 1991; Blank *et al.* 1992; Boyarsky *et al.* 1996a; Seksek & Bolard, 1996). Nevertheless, reproducible calibration parameters for carboxy SNARF-1 and SNARF-5F at 37°C *in situ* were obtained and, in the case of carboxy SNARF-1, are consistent with those reported by others (see Section 6.3.1.1).

Details regarding the conversion of normalized SBFI ratio values into $[Na^+]_i$ values are provided in Chapter 2. Normalized carboxy SNARF-1 or SNARF-5F ratio values were converted into pH_i values using the equation

$$pH = pK_a + \log F640_{min/max} - \log[(R_n - R_{n(min)}) / (R_{n(max)} - R_n)] \qquad \textit{(Equation 6.1)}$$

where R_n is the background-subtracted carboxy SNARF-1 or SNARF-5F fluorescence intensity ratio (BI_{550}/BI_{640}) normalized to pH 7.00 (or pH 7.50; see above); pK_a is the -log of the dissociation constant of the fluorophore; and $F640_{min/max}$ is the ratio of fluorescence measured at 640 nm for low pH (pH 5.5) to that for high pH (pH 8.5; see Buckler & Vaughan-Jones, 1990). The parameters fitting Equation 6.1 were derived from full *in situ* calibration experiments, as described in Section 6.2.2.

6.1.4. Data Analysis

In contrast to the anoxia-evoked changes in pH_i observed in acutely isolated adult rat hippocampal CA1 pyramidal neurons, in which pH_i rose during anoxic transients and increased further in the post-anoxic period to values above pre-anoxic resting pH_i values (see Chapters 3 and 4), in experiments in which SNARF-5F, carboxy SNARF-1 or BCECF were used as pH_i indicators, pH_i increases during anoxia and pH_i 'overshoots' following anoxia were infrequently

observed in the cultured postnatal rat hippocampal neurons employed in the present studies. Thus, in experiments in which the changes in pH_i observed after periods of anoxia (Na^+,K^+-ATPase inhibited) were measured, the magnitude of the increase in pH_i observed after anoxia was measured as the difference between the pH_i value observed at the end of anoxia and the pH_i value observed at the end of a 7 min exposure to 0 $[K^+]_o$ media (see Table 6.2; Fig. 6.8 *D, F*). In a similar manner, the magnitude of the increase in $[Na^+]_i$ observed after anoxia was measured as the difference between the $[Na^+]_i$ value observed at the end of anoxia and the $[Na^+]_i$ value observed at the end of 7 min exposure to 0 $[K^+]_o$ media (as described in Chapter 5). The differences between the anoxia-evoked changes in pH_i observed in acutely isolated adult *vs.* cultured rat hippocampal neurons is discussed further in Chapter 8.

Results are reported as mean ± S.E.M. In experiments in which internal acid loads were imposed by the NH_4^+ prepulse technique or neurons were exposed to transient periods of anoxia, experiments were performed on at least three coverslips obtained from 2 – 5 different batches of cultures and the accompanying *n* value refers to the number of neurons from which data were analyzed. For all other experiments, including full calibration experiments, the accompanying *n* value refers to the number of cell populations (i.e. number of coverslips) analyzed. Statistical comparisons were carried out using Student's two-tailed t-test, paired or unpaired as appropriate, with a 95% confidence limit.

6.2. RESULTS

6.2.1. Separation of SBFI and SNARF fluorescence emissions *in situ*

With the optical filters specified in the Methods, the excitation and emission characteristics of SBFI, carboxy SNARF-1 and SNARF-5F *in vitro* appear sufficiently distinct to permit the discrimination of Na^+_i- and pH_i-dependent signals from dual dye-loaded cells. However, the spectral properties of many fluorescent probes, including SBFI (see Negulescu & Machen, 1990; Diarra *et al.* 2001) and carboxy SNARF-1 (see Seksek *et al.* 1991; Martínez-Zaguilán *et al.* 1996), may differ *in situ* compared to *in vitro*. Initially, therefore, I examined whether the behaviours of SBFI, carboxy SNARF-1 and SNARF-5F in hippocampal neurons *in situ* would allow the isolation of signals coming from the respective dyes under the experimental conditions employed. To do so, the intensities of emitted fluorescence relative to background fluorescence values under a variety of conditions were measured.

In neurons single-loaded with SBFI, excitation at 334 and 380 nm (emissions collected at 550 nm) elicited fluorescence signals respectively ~20 and ~11 times greater than those originating from neurons single-loaded with carboxy SNARF-1, and ~16 and ~14 times greater than those originating from neurons single-loaded with SNARF-5F (Fig. 6.2*A* & *C*). In neurons single-loaded with carboxy SNARF-1 or SNARF-5F, excitation at 488 nm (emissions collected at 550 nm and 640 nm) elicited fluorescence signals respectively ~8 (at 550 nm) and ~7 (at 640 nm) times greater than those obtained from neurons single-loaded with SBFI (Fig. 6.2*B* & *C*). When neurons were co-loaded with SBFI and either carboxy SNARF-1 or SNARF-5F, fluorescence emissions originating from SBFI and carboxy SNARF-1 or SNARF-5F continued to be adequately resolved (Fig. 6.2*A* - *C*). Nevertheless, emission intensities measured at 550 nm following excitation at 334 or 380 nm in neurons co-loaded with SBFI and either carboxy SNARF-1 or SNARF-5F were significantly reduced, compared to those measured in neurons

single-loaded with SBFI (Fig. 6.2*A*). In addition, following excitation at 488 nm, fluorescence emissions at 550 nm, but not 640 nm, were reduced by ~25% in neurons co-loaded with SBFI and either carboxy SNARF-1 or SNARF-5F compared to those measured in neurons single-loaded with carboxy SNARF-1 or SNARF-5F (Fig. 6.2*B*).

These observations are consistent with the possibility that SNARF derivatives may quench SBFI fluorescence, and vice versa. When neurons were single-loaded with SBFI and subsequently loaded with carboxy SNARF-1 or SNARF-5F (n = 3 in each case), BI_{334} and BI_{380} values were reduced by 61 ± 2 and 63 ± 1% (carboxy SNARF-1; not shown) and by 60 ± 13 and 60 ± 10% (SNARF-5F; Fig. 6.3*A*), respectively. However, because BI_{334} and BI_{380} values were reduced to a proportionately similar extent, SBFI-derived BI_{334}/BI_{380} ratio values were minimally affected by the presence of either carboxy SNARF-1 (not shown) or SNARF-5F (Fig. 6.3*A*). Due to the length of time required for SBFI loading, I was unable to further examine the apparent effect of SBFI to quench carboxy SNARF-1 and SNARF-5F 550 nm emissions in a manner similar to that shown in Fig. 6.3*A*. Therefore, I measured fluorescence emission intensities at 550 and 640 nm (excitation at 488 nm) in neurons single-loaded with either carboxy SNARF-1 or SNARF-5F at pH 6.0, 7.0 and 8.5, and compared these intensities to those obtained in neurons from sister cultures co-loaded with SBFI and carboxy SNARF-1 or SNARF-5F. Neither carboxy SNARF-1 (not shown) nor SNARF-5F (Fig. 6.3*B*) emission intensities at 550 and 640 nm were significantly influenced by the addition of SBFI, indicating that SBFI does not significantly reduce fluorescence emissions from SNARF-based dyes at any of the pH values examined.

Quenching between fluorophores requires intracellular co-localization. Exposure of neurons co-loaded with SBFI and carboxy SNARF-1 or SNARF-5F to 0.005 - 0.01% saponin (n = 3 in each case) reduced emission intensities measured at 550 nm (following excitation at 334,

380 or 488 nm) and at 640 nm (following excitation at 488 nm) by >85% (Fig. 6.3*A*; also see Blank *et al.* 1992; Rose & Ransom, 1997). Similar findings, which also indicate that SBFI- and SNARF-derived fluorescence emissions originate largely from the cytosolic compartment, were made when co-loaded neurons were exposed to 20 μM digitonin ($n = 3$ in each case; not shown).

6.2.2. Full calibrations of SBFI, carboxy SNARF-1 and SNARF-5F ratio values *in situ*

Next, full *in situ* calibrations of SBFI, carboxy SNARF-1 and SNARF-5F in single-loaded neurons and in neurons co-loaded with SBFI and carboxy SNARF-1 or SNARF-5F were performed.

As illustrated in Fig. 6.4*A*, full SBFI calibrations were performed at 37°C by exposing neurons to pH 7.35 media containing 4 μM gramicidin D at eight different $[Na^+]$ values (range, 0 – 130 mM). The resulting plot of the data points relating $[Na^+]$ to R_n in neurons single-loaded with SBFI is shown in Fig. 6.4*B* and the resulting fitted SBFI calibration parameters are presented in Table 6.1. Importantly, when neurons single-loaded with SBFI were illuminated at 488 nm (i.e. the excitation wavelength employed for carboxy SNARF-1 and SNARF-5F), fluorescence emissions measured at 550 and 640 nm (i.e. the emission wavelengths of the SNARF dyes) remained small and stable as $[Na^+]$ was altered from 0 to 130 mM (Fig. 6.4*A*). Finally, when full SBFI calibrations were performed in neurons co-loaded with SBFI and either carboxy SNARF-1 or SNARF-5F, there were no significant differences between the resulting SBFI calibration parameters and those computed from neurons loaded with SBFI alone (Table 6.1; Fig. 6.4*B*). Thus, carboxy SNARF-1 and SNARF-5F do not influence the *in situ* sensitivity of SBFI to changes in $[Na^+]_i$.

Full *in situ* calibrations of carboxy SNARF-1 are presented in Figure 6.5. As described by others (e.g. Buckler & Vaughan-Jones, 1990; Martínez-Zaguilán *et al.* 1991; Blank *et al.* 1992), exposing neurons single-loaded with carboxy SNARF-1 to 10 μM nigericin-containing high-K^+ solutions at a variety of pH values influenced both BI_{550} and BI_{640} emission intensities (Fig. 6.5*A*). The resulting plots of the data points relating R_n and pH, at both 22°C and 37°C, are shown in Fig. 6.5*B* and the fitted carboxy SNARF-1 calibration parameters are presented in Table 6.1. Interestingly, the carboxy SNARF-1 $F640_{min/max}$ value was significantly reduced at 37°C compared to 22°C (Table 6.1) and, in agreement with Ch'en *et al.* (2003), the dynamic range of the dye's fluorescence ratio increased with increasing temperature (Table 6.1; Fig. 6.5*B*). As noted in the Introduction, SNARF-5F displays a lower pK_a value *in vitro* than carboxy SNARF-1. Therefore, full *in situ* calibrations (at 37°C) of SNARF-5F single-loaded into hippocampal neurons were performed. The fitted calibration parameters (Table 6.1) confirmed that SNARF-5F also possesses a lower pK_a value than carboxy SNARF-1 *in situ*. Carboxy SNARF-1 and SNARF-5F calibration parameters were then determined at 37°C in neurons also loaded with SBFI (see Fig. 6.5*B*). There were no significant differences between the values of the calibration parameters obtained from neurons loaded with carboxy SNARF-1 or SNARF-5F alone and those obtained from neurons co-loaded with SBFI and carboxy SNARF-1 or SNARF-5F (Table 6.1). Together, the results indicate that SBFI does not influence the *in situ* sensitivities of carboxy SNARF-1 or SNARF-5F to changes in pH_i.

6.2.3. Effects of changes in $[Na^+]$ on pH_i measurements with carboxy SNARF-1 and SNARF-5F *in situ*

The effects of changes in pH_i on $[Na^+]_i$ estimated with SBFI *in situ* have been well characterized (see Negulescu & Machen, 1990; Rose & Ransom, 1997; Diarra *et al.* 2001). To examine the effects of changes in $[Na^+]_i$ on SNARF-based pH_i measurements, neurons were single-loaded with carboxy SNARF-1 or SNARF-5F and $[Na^+]$ was varied from 0 to 10 to 130 mM at four different pH values (6.00, 6.50, 7.00 and 7.50) in the presence of 4 μM gramicidin D at 37°C (see Diarra *et al.* 2001). As illustrated in Fig. 6.6*A*, increasing $[Na^+]$ from 0 to 10 to 130 mM at a constant pH had minimal effects on carboxy SNARF-1 ratio measurements. Moreover, plots of R_n as a function of pH at each $[Na^+]$ (Fig. 6.6*B*) indicated that changes in $[Na^+]$ did not alter the computed $pK_a + \log F640_{min/max}$, $R_{n(min)}$ or $R_{n(max)}$ values for carboxy SNARF-1. Thus, neither carboxy SNARF-1-derived R_n nor pH_i measurements were influenced significantly by changes in $[Na^+]$ in the range 0 - 130 mM ($P \geq 0.32$ at each pH value). Similar findings were made in neurons single-loaded with SNARF-5F ($n \geq 3$ at each pH value; not shown). These results indicate that the effects of changes in $[Na^+]_i$ on SNARF-based pH_i measurements are unlikely to affect the interpretation of results under most experimental conditions.

6.2.4. Concurrent measurements of pH_i and $[Na^+]_i$ in rat hippocampal neurons

Consistent with previous measurements in cultured rat hippocampal neurons (Chapters 3 - 4; also see Baxter & Church, 1996), resting pH_i values in cells single-loaded with carboxy SNARF-1 or SNARF-5F were 7.37 ± 0.03 (n = 13) and 7.39 ± 0.02 (n = 57), respectively. Also consistent with previous reports, resting $[Na^+]_i$ values in cells single-loaded with SBFI were 12 ± 1 mM (n = 44; see Chapter 5 and Rose & Ransom, 1997; Diarra *et al.* 2001). These values were not

different to those obtained in neurons co-loaded with carboxy SNARF-1 and SBFI (resting pH_i 7.40 ± 0.02; resting $[Na^+]_i$ 10 ± 1 mM; n = 51) or neurons co-loaded with SNARF-5F and SBFI (resting pH_i 7.36 ± 0.05; resting $[Na^+]_i$ 10 ± 1 mM; n = 76).

To demonstrate the utility of concurrent measurements of $[Na^+]_i$ and pH_i in cells co-loaded with SBFI and a SNARF derivative, rat hippocampal neurons were subjected to internal acid loads imposed by the NH_4^+ prepulse technique. Under the nominally HCO_3^--free, Hepes-buffered conditions employed in the present experiments, the recovery of pH_i from NH_4^+-induced internal acid loads in rat hippocampal neurons is mediated in large part by Na^+/H^+ exchange (e.g. Raley-Susman *et al.* 1991; Baxter & Church, 1996; Bevensee *et al.* 1996). In light of its lower pK_a value, SNARF-5F was employed in these experiments in preference to carboxy SNARF-1. As expected, in neurons loaded with SNARF-5F alone, pH_i increased during NH_4^+ application, fell to below resting levels upon NH_4^+ washout and then recovered (Table 6.2; Fig. 6.7*A*). In neurons loaded with SBFI alone, the washout of NH_4^+ was associated with an increase in $[Na^+]_i$ that subsequently recovered towards resting levels (Table 6.2; Fig. 6.7*B*). When cells were co-loaded with SNARF-5F and SBFI, the magnitudes of the decrease in pH_i and increase in $[Na^+]_i$ observed upon NH_4^+ washout were not significantly different from those seen in neurons loaded with either SBFI or SNARF-5F alone (Table 6.2; Fig. 6.7*C*) and were comparable to the changes measured concurrently with ISMs in crayfish neurons (see Fig. 4 in Moody, 1981). Further, as shown in Fig. 6.7*D*, rates of pH_i recovery from NH_4^+-induced internal acid loads were similar in neurons loaded with either SBFI and SNARF-5F or SNARF-5F alone. Finally, measurements in neurons co-loaded with SNARF-5F and SBFI revealed a positive relationship between the magnitude of the recovery of pH_i and the increase in $[Na^+]_i$ seen after NH_4^+ washout (Fig. 6.7*E*).

Taken together, these findings support the feasibility of using either carboxy SNARF-1 or SNARF-5F in conjunction with SBFI to concurrently and accurately measure pH_i and $[Na^+]_i$. Therefore, in the next series of experiments, I used this technique to further examine the contribution of Na^+/H^+ exchange activity to anoxia-evoked changes in pH_i and $[Na^+]_i$.

6.2.5. Contribution of Na^+/H^+ exchange activity to anoxia-evoked changes in pH_i and $[Na^+]_i$

First, I assessed the validity using a SNARF-based fluorophore and SBFI in combination to measure the changes in pH_i and $[Na^+]_i$ evoked by anoxia in cultured rat hippocampal neurons. Similar to the findings presented in Chapters 3 - 5 (also see Diarra *et al.* 1999), in cultured neurons loaded only with SNARF-5F (Table 6.2; Fig. 6.8*A*) or SBFI (Table 6.2; Fig. 6.8*B*), 5 min anoxia produced falls in pH_i and increases in $[Na^+]_i$, respectively, with recoveries toward resting values upon the return to normoxia. Comparable changes in pH_i and $[Na^+]_i$ were observed in neurons co-loaded with SNARF-5F and SBFI (Table 6.2; Fig. 6.8*C*) or in neurons co-loaded with carboxy SNARF-1 and SBFI (Table 6.2). Next, I used the 0 $[K^+]_o$ protocol (Chapter 5) to examine pH_i and/or $[Na^+]_i$ in the immediate post-anoxic period. In rat hippocampal neurons loaded only with SNARF-5F (Fig. 6.8*D*) or SBFI (Fig. 6.8*E*), perfusion with $[K^+]_o$-free medium for 7 min immediately after the end of 5 min anoxia did not influence the rise in pH_i observed following anoxia (compare Fig. 6.8*A* and 6.8*D*) and, as discussed in Chapter 5, revealed further Na^+ influx occurring at this time (compare Fig. 6.8*B* and 6.8*E*). Comparable changes in pH_i and $[Na^+]_i$, which increased in parallel after anoxia (Na^+,K^+-ATPase inhibited; Fig. 6.8*F*), were observed in neurons co-loaded with either SNARF-5F or carboxy SNARF-1 and SBFI (Table 6.2). These results support the feasibility of using either carboxy SNARF-1 or SNARF-5F in conjunction with SBFI to measure concurrently and accurately the changes in pH_i and $[Na^+]_i$ evoked by anoxia in rat hippocampal neurons.

If Na^+/H^+ exchange activity contributes to the increases in pH_i and $[Na^+]_i$ observed in the immediate post-anoxic period (Na^+,K^+-ATPase blocked), both events should be dependent on external Na^+, and the rates at which pH_i and $[Na^+]_i$ increase after anoxia should exhibit an inverse dependency on pH_i (see Lazdunski *et al.* 1985). Indeed, reducing Na^+_o ($NMDG^+$-substitution) prevented the rises in pH_i and $[Na^+]_i$ normally observed after 5 min anoxia (compare Figs. 6.9*A* and *B*). As illustrated in Fig. 6.9*B*, when Na^+_o was returned to normal (in the continued absence of $[K^+]_o$), both pH_i and $[Na^+]_i$ rapidly increased. In addition, when rates at which pH_i and $[Na^+]_i$ increased after anoxia were plotted as functions of absolute pH_i (Fig. 6.10), both parameters were faster at lower pH_i values.

Finally, in neurons co-loaded with either carboxy SNARF-1 or SNARF-5F and SBFI, I examined the effects of maneuvers that have previously been found to influence Na^+/H^+ exchange activity in rat hippocampal neurons (see Chapters 4 and 5) on anoxia-evoked changes in pH_i and $[Na^+]_i$. Consistent with previous suggestions that Na^+/H^+ exchange activity is reduced during and activated immediately following 5 min anoxia, pretreatment with 200 μM harmaline failed to influence the magnitudes of the fall in pH_i or increase in $[Na^+]_i$ observed during anoxia but reduced significantly the magnitudes of the increases in pH_i *and* $[Na^+]_i$ observed following anoxia (Fig. 6.11). The activation of Na^+/H^+ exchange activity in the immediate post-anoxic period can be inhibited by an extracellular acidosis or inhibition of the cAMP/PKA pathway (Chapters 4 and 5). Conversely, as illustrated in Chapter 3, anoxia-evoked changes in pH_i are not influenced by the removal of Ca^{2+}_o prior to, during and following anoxia. Lowering pH_o to 6.60 or the application of 50 μM *R*p-cAMPS, but not perfusion with Ca^{2+}-free medium, reduced significantly the magnitudes of the increases in pH_i and $[Na^+]_i$ observed after anoxia (Na^+,K^+-ATPase inhibited; Fig. 6.11). Taken together, the results obtained in neurons co-loaded with a SNARF-based

fluorophore and SBFI strengthen previous suggestions that Na^+/H^+ exchange activity in rat hippocampal neurons is increased in the immediate post-anoxic period and contributes to not only the recovery of pH_i but also to Na^+ influx at this time.

6.3. DISCUSSION

There were two distinct objectives of the present study: in the *first* part of this study, I developed and characterized a technique for the near-simultaneous measurement of $[Na^+]_i$ and pH_i in rat hippocampal neurons, and; in the *second* part of this study, I employed this technique to further examine the contribution of Na^+/H^+ exchange activity to the anoxia-evoked changes in pH_i and $[Na^+]_i$ in cultured rat hippocampal neurons.

6.3.1. Part 1: The development of microspectrofluorimetric methods for the concurrent measurement of pH_i and $[Na^+]_i$

The dual excitation ratiometric indicator SBFI has been used to measure $[Na^+]_i$ in a large number of cell types; the ion selectivity of the probe has been assessed, methods for its *in situ* calibration have been developed and a one-point technique for the conversion of SBFI-derived ratio measurements into $[Na^+]_i$ has been validated (Diarra *et al.* 2001). Similarly, the dual emission ratiometric dye, carboxy SNARF-1, has gained wide acceptance as a pH indicator, in part because of its wide dynamic range and good signal-to-noise ratio (see Buckler & Vaughan-Jones, 1990). Nevertheless, its relatively high pK_a may limit the accuracy of low pH_i measurements, a potential disadvantage that prompted me to assess the utility of SNARF-5F as a pH_i indicator in hippocampal neurons. I confirmed that the pK_a of SNARF-5F *in situ* is lower than that of carboxy SNARF-1 but that it behaves in an otherwise similar manner to carboxy SNARF-1.

To date, concurrent single cell measurements of $[Na^+]_i$ (or intracellular Na^+ activity) and pH_i have been obtained with ISMs, sometimes in conjunction with an ion-sensitive fluorescent probe (e.g. Thomas, 1977; Moody, 1981; Kaila & Vaughan-Jones, 1987; Deitmer & Schlue, 1989; Munsch & Deitmer, 1997; Kilb & Schlue, 1999). Although ISMs offer some advantages over fluorescent probes (see Nett & Deitmer, 1996; Voipio, 1998), they cannot easily be applied to small cells (e.g. mammalian central neurons). In contrast, SBFI and SNARF derivatives offer means for measuring $[Na^+]_i$ and pH_i, respectively, in small cells that are not amenable to stable impalements with ISMs, but heretofore they have only been employed separately[9], precluding a clear understanding of the temporal and other relationships between cytosolic Na^+ and H^+ homeostasis and the role of either ion in the regulation of specific physiological responses. As noted in the Introduction, $[H^+]_i$ and $[Na^+]_i$, like $[H^+]_i$ and $[Ca^{2+}]_i$ (and also $[Na^+]_i$ and $[Ca^{2+}]_i$), are related by a variety of mechanisms; indeed, an appreciation of the latter relationships has led to the development of techniques for the concurrent measurement of pH_i and $[Ca^{2+}]_i$ with carboxy SNARF-1 and fura-2 (Martínez-Zaguilán *et al.* 1991 and 1996) or indo-1 (Wiegmann *et al.* 1993; Austin *et al.* 1996), and $[Na^+]_i$ and $[Ca^{2+}]_i$ with SBFI and fluo-3 (Satoh *et al.* 1994 and 1995) or fluo-4 (Grant *et al.* 2002).

6.3.1.1. Part 1: Technical considerations

A number of conditions must be satisfied for the accurate measurement of the concentrations of two ions simultaneously with fluorescent probes (see Wiegmann *et al.* 1993; Martínez-Zaguilán *et al.* 1996): *i)* a lack of spectral overlap between the probes; *ii)* minimal interactions between

[9] Jung *et al.* (1995) employed SBFI and carboxy SNARF-1 simultaneously in isolated heart mitochondria but few details were given and the behaviours of the fluorophores when co-loaded were not systematically examined.

the probes; *iii)* a lack of differential compartmentalization between the probes; *iv)* binding affinities in the physiological range; *v)* distinct ion selectivities; and *vi)* lack of toxicity. In the present study, the combination of SBFI and carboxy SNARF-1 or SNARF-5F fulfilled each of these criteria. First, using the optical equipment specified, the fluorescence signals originating from the fluorophores *in situ* could be adequately resolved (Fig. 6.2). Second, although carboxy SNARF-1 and SNARF-5F quenched the fluorescence of SBFI (Figs. 6.2 and 6.3), SBFI-derived ratio values and the Na^+-sensitivity of SBFI were minimally affected (Figs. 6.3 and 6.4). Third, in agreement with previous reports (e.g. Martínez-Zaguilán *et al.* 1996; Rose & Ransom, 1997), SBFI- and SNARF-derived fluorescence emissions emanated largely from the same (i.e. cytosolic) compartment (Fig. 6.3). Fourth, the calibration parameters obtained in neurons single-loaded with SBFI or carboxy SNARF-1 were consistent with previous *in situ* estimates (e.g. Buckler & Vaughan-Jones, 1990; Blank *et al.* 1992; Diarra *et al.* 2001; Ch'en *et al.* 2003) and were not significantly influenced by the presence of a second fluorophore (Table 6.1; Figs. 6.4 and 6.5); similarly, the pK_a of SNARF-5F was not affected by the presence of SBFI (Table 6.1). Fifth, carboxy SNARF-1 and SNARF-5F *in situ* are effectively insensitive to changes in $[Na^+]$ (Fig. 6.6); previously, SBFI *in situ* has been found to be weakly sensitive to changes in pH (Negulescu & Machen, 1990; Rose & Ransom, 1997; Diarra *et al.* 2001). Sixth, although it is well-established that fluorescent probes employed for ratiometric $[ion]_i$ determinations may, under some conditions, exert toxic effects (see Nett & Deitmer, 1996; Voipio, 1998 and references therein), resting $[Na^+]_i$ and pH_i values (and rates of pH_i recovery from NH_4^+-induced internal acid loads) obtained in neurons co-loaded with SBFI and either carboxy SNARF-1 or SNARF-5F were not significantly different from the respective values obtained in neurons single-loaded with either dye (Fig. 6.7) and are consistent with previous measurements in cultured rat hippocampal neurons (see Raley-Susman *et al.* 1991; Baxter & Church, 1996; Rose

& Ransom, 1997; Diarra *et al.* 2001). In addition, in initial experiments using perforated patch electrophysiological recordings, our laboratory has observed that cultured rat hippocampal neurons co-loaded with SBFI and SNARF-5F have normal resting membrane potentials, exhibit a stable input resistance over time and generate trains of overshooting action potentials in response to membrane depolarization (T. Kelly and C. Sheldon, unpublished observations). These findings suggest that co-loading neurons with SBFI and SNARF-5F does not, at least in the short-term, adversely affect neuronal viability.

6.3.1.2. Part 1: Summary

Together, these findings support the feasibility of using SBFI in conjunction with either carboxy SNARF-1 or SNARF-5F to concurrently and accurately measure $[Na^+]_i$ and pH_i. Indeed, no significant differences were observed in the changes in $[Na^+]_i$ and pH_i evoked by NH_4^+-induced internal acid loads (Table 6.2; Fig. 6.7) in neurons single-loaded with SBFI or SNARF-5F or co-loaded with both probes. Concurrent measurements of pH_i and $[Na^+]_i$ will help to resolve the interplay between changes in $[Na^+]_i$ and pH_i under various experimental conditions. Thus, the records shown in Fig. 6.7*C* and *E* demonstrate that the recovery of pH_i from NH_4^+-induced internal acid loads in rat hippocampal neurons is accompanied by a transient rise in $[Na^+]_i$, a finding that provides further evidence for Na^+/H^+ exchange (see Thomas, 1977; Moody, 1981; Kaila & Vaughan-Jones, 1987; Munsch & Deitmer, 1997) in a cell type in which the transport mechanism is insensitive to known pharmacological inhibitors (Raley-Susman *et al.* 1991; Schwiening & Boron, 1994; Baxter & Church, 1996). Concurrent measurements of $[Na^+]_i$ and pH_i also provide the data required to correct, on a region-by-region basis, $[Na^+]_i$ values estimated with SBFI for changes in pH_i. Using the methods developed during the course of this thesis and detailed in Diarra *et al.* (2001), the magnitude of the increase in $[Na^+]_i$ observed in response to

NH_4^+ washout increased from 12 ± 2 mM (uncorrected) to 16 ± 3 mM (corrected) ($P < 0.05$ by paired Student's *t*-tests). The ability to correct apparent $[Na^+]_i$ values measured with SBFI for the prevailing pH_i is another advantage offered by the simultaneous use of SBFI and carboxy SNARF-1 or SNARF-5F.

In summary, I have developed a method for the near-simultaneous measurement of $[Na^+]_i$ and pH_i in cells co-loaded with SBFI and carboxy SNARF-1 or SNARF-5F, a technique that offers a useful alternative to the use of ISMs in experiments employing small cells in which information is required on both $[Na^+]_i$ and pH_i and the relationship between these two ions. It is my hope that the method described will serve as a useful reference point for other investigators who wish to study the interrelationships between $[Na^+]_i$ and pH_i regulation in other cell types.

6.3.2. Part 2: Anoxia-evoked changes in pH_i and $[Na^+]_i$

The results obtained from neurons single-loaded with BCECF (Chapters 3 and 4) or SBFI (Chapter 5) suggested that, although Na^+/H^+ exchange activity is inhibited shortly following the onset of anoxia, exchange activity is increased in the post-anoxic period and appears to contribute the increases in pH_i and $[Na^+]_i$ observed immediately upon the return to normoxia. These suggestions are strengthened by the results of the present study in which anoxia-evoked changes in pH_i and $[Na^+]_i$ were measured concurrently. *First*, harmaline pretreatment (which inhibits Na^+/H^+ exchange activity in rat hippocampal neurons; see Chapter 5) had no influence on either the fall in pH_i or the increase in $[Na^+]_i$ observed during anoxia[10] but reduced significantly

[10] The inability of harmaline to reduce the magnitude of the fall in pH_i observed during anoxia (as was observed when Na^+/H^+ exchange activity was inhibited in acutely isolated adult rat hippocampal neurons under reduced Na^+_o, $NMDG^+$-substituted conditions; see Chapter 3) may reflect either the inability of harmaline pretreatment to fully inhibit Na^+/H^+ exchange activity or differences in the extent to which Na^+/H^+ exchange activity contributes to the maintenance of resting pH_i in acutely isolated adult *vs.* cultured postnatal hippocampal neurons.

the increases in both pH_i and $[Na^+]_i$ observed in the immediate post-anoxic period (Na^+,K^+-ATPase inhibited). *Second,* consistent with the pH_i-dependency of Na^+/H^+ exchange activity, the rates at which pH_i and $[Na^+]_i$ increased following anoxia (Na^+,K^+-ATPase inhibited) were both inversely dependent on pH_i. *Third,* maneuvers that have previously been found to inhibit Na^+/H^+ exchange activity in rat hippocampal neurons reduced significantly the post-anoxic increases in both pH_i and $[Na^+]_i$. Although previous studies have illustrated that PKA regulates the activity of plasmalemmal Na^+/Ca^{2+} exchange in rat hippocampal neurons under normoxic conditions (e.g. He *et al.* 1998), in the present study, the prolonged removal of external Ca^{2+} (i.e. prior to, during and following anoxia, a maneuver which inhibits forward- and reverse-mode Na^+/Ca^{2+} exchange activity) failed to influence the increases in pH_i or $[Na^+]_i$ observed following anoxia and the ability of *R*p-cAMPS to reduce post-anoxic Na^+ influx was associated with a parallel reduction in the post-anoxic rise in pH_i, suggesting that *R*p-cAMPS is likely acting to inhibit Na^+/H^+ exchange activity in the post-anoxic period in rat hippocampal neurons. Finally, concurrent measurements of anoxia-evoked changes in pH_i and $[Na^+]_i$ in the same cells confirmed that the interpretation of the anoxia-evoked changes in $[Na^+]_i$, measured in neurons single-loaded with SBFI, are unlikely to be influenced by the pH-sensitivity of the dye. In fact, at a time when SBFI-derived $[Na^+]_i$ values would be expected to be most influenced by changes in pH_i (i.e. when pH_i and $[Na^+]_i$ values were reduced and elevated, respectively; see Diarra *et al.* 2001), the magnitude of the increase in $[Na^+]_i$ at the end of 5 min anoxia was underestimated by < 4 mM (the magnitude of the increase in $[Na^+]_i$ observed at the end of 5 min anoxia in 7 - 10 DIV neurons loaded with SBFI and SNARF-5F was 18 ± 4 mM and 21 ± 4 mM, before and after correcting the SBFI-derived $[Na^+]_i$ value for the 0.44 pH units decrease in pH_i, respectively; $P < 0.05$ by paired Student's *t*-tests).

In cardiac tissue, post-ischemic increases in pH_i and $[Na^+]_i$ aggravate myocyte damage and the abilities of pharmacological Na^+/H^+ exchange inhibitors to slow both the recovery of pH_i and Na^+ entry upon reperfusion may, together, underlie their cardioprotective actions (reviewed by Avkiran, 2001). Analogous mechanism(s) may underlie the neuroprotective effects of Na^+/H^+ exchange inhibitors. Indeed, Na^+/H^+ exchange inhibitors limit the increases in pH_i observed following periods of anoxia or metabolic inhibition *in vitro* (e.g. Pirtillä & Kauppinen, 1992; Vornov *et al.* 1996; also see Ohno *et al.* 1989; Taylor *et al.* 1996) and reduce Na^+ accumulation and water content during reperfusion *in vivo* (e.g. Kuribayashi *et al.* 1999; Horikawa *et al.* 2001a and b). Although the findings of the present study are consistent with an activation of Na^+/H^+ exchange activity in the immediate post-anoxic period and its subsequent contribution to the increases in pH_i and $[Na^+]_i$ observed at this time, it remains unclear whether the neuroprotective actions of Na^+/H^+ exchange inhibitors arise from a reduction in H^+ extrusion and/or Na^+ entry (see Chapter 8).

It is notable that exposure of neurons to K^+-free medium immediately following anoxia (in the presence of normal Na^+_o) had minimal effects on the increases in pH_i observed at this time. In non-neuronal cell types, inhibition of Na^+,K^+-ATPase activity has been reported to reduce (e.g. Kimura & Aviv, 1993) or not influence (e.g. Aickin & Thomas, 1977) the rate of pH_i recovery from imposed internal acid loads. When it has been observed, the slowing of Na^+/H^+ exchange has been, in part, attributed to a reduction in the thermodynamic driving force for Na^+/H^+ exchange activity (see Wu & Vaughan-Jones, 1997). Vaughan-Jones & Wu (1990) estimated the "thermodynamic driving force" (DF) of Na^+/H^+ exchange as follows

$$\text{DF (RT units)} = 2.3\ RT(\log([Na^+]_o/[Na^+]_i) + (pH_o - pH_i)) \qquad \textit{(Equation 6.2)}$$

where, under the conditions of the present study, $[Na^+]_o$ and pH_o are 148 mM and 7.35, respectively, and R and T have their usual meanings. In the present experiments in rat hippocampal neurons in which pH_i and $[Na^+]_i$ were measured concurrently, there was an ~ 45% reduction in the driving force for forward Na^+/H^+ exchange during exposure to K^+-free medium (DF = 3.1 ± 0.1 and 1.7 ± 0.1 RT units at the end of 5 min anoxia and the subsequent 7 min K^+-free medium, respectively; n = 49 neurons 7 - 10 DIV). On the other hand, these calculations indicate that even at end of a 7 min exposure to K^+-free medium, Na^+/H^+ exchange will continue to mediate acid extrusion (i.e. the values for DF are positive). Moreover, calculated rates of pH_i recovery following anoxia under K^+_o-free conditions were similar to rates observed following anoxia under control conditions (measured at a common test pH_i of 6.95, rates of pH_i recovery from anoxia-induced falls in pH_i were $1.58 \pm 0.29 \times 10^{-3}$ and $2.38 \pm 0.88 \times 10^{-3}$ pH units s^{-1} in the presence and absence of external K^+; n = 6 and 7, respectively; P = 0.35; data obtained from neurons 7 - 10 DIV). It is apparent that, in the present study, despite reductions in its thermodynamic driving force, Na^+/H^+ exchange activity is enhanced in the immediate post-anoxic period, suggesting that the rate of Na^+/H^+ exchange activity in the period following anoxia is likely regulated by a variety of intracellular events, including anoxia-evoked changes in the activity of the cAMP/PKA pathway, although other mechanisms may be involved (e.g. the restoration of internal ATP levels and/or regulation by free radicals; Yao *et al.* 2001; Mulkey *et al.* 2004).

In non-neuronal cell types, under conditions of Na^+,K^+-ATPase inhibition, the ratio between the net flux of H^+ *vs.* Na^+ ions has previously provided reasonable estimates of the coupling ratio of Na^+/H^+ exchange (e.g. Grinstein *et al.* 1984; Aronson, 1985; Kaila & Vaughan-Jones, 1987). However, from the present study, I am unable to provide similar estimates of the stoichiometry of Na^+/H^+ exchange in rat hippocampal neurons: intrinsic H^+ buffering power cannot be assessed

accurately in rat hippocampal neurons (because of the inability to completely inhibit the activities of all pH_i regulating mechanisms in rat hippocampal neurons) and it is apparent from the results presented in this study that the increases in pH_i and $[Na^+]_i$ observed following anoxia do not simply reflect only changes in Na^+/H^+ exchange activity. Rather, as detailed in Chapters 4 and 7, the increases in pH_i and $[Na^+]_i$ observed following anoxia in rat hippocampal neurons reflect co-ordinated changes in the activities of multiple pH_i regulating mechanisms and Na^+ influx pathways.

In summary, the results of the present study, in which anoxia-evoked changes in pH_i and $[Na^+]_i$ were measured concurrently in the same neurons, have strengthened the previous suggestion that Na^+/H^+ exchange activity in rat hippocampal neurons is inhibited during anoxia and is increased in the immediate post-anoxic period, at which time it contributes to potentially detrimental increases in pH_i and $[Na^+]_i$.

Table 6.1: Calibration parameters for SBFI, carboxy SNARF-1 and SNARF-5F in single dye- and dual dye-loaded hippocampal neurons

A, SBFI calibration

Neurons loaded with	Temp	K_d	β	$R_{n(min)}$	$R_{n(max)}$	*n*
SBFI	37°C	21.7 ± 2.1	4.5 ± 0.7	0.77 ± 0.01	3.2 ± 0.4	21
SBFI + carboxy SNARF-1	37°C	17.6 ± 3.5	5.4 ± 1.3	0.77 ± 0.03	3.2 ± 0.4	5
SBFI + SNARF-5F	37°C	22.7 ± 4.8	4.5 ± 1.3	0.78 ± 0.03	3.3 ± 0.5	8

B, carboxy SNARF-1 and SNARF-5F calibrations

Neurons loaded with	Temp	pK_a	$F640_{min/max}$	$R_{n(min)}$	$R_{n(max)}$	*n*
Carboxy SNARF-1	22°C	7.40 ± 0.06	0.83 ± 0.06	0.34 ± 0.05	1.3 ± 0.04	7
Carboxy SNARF-1	37°C	7.59 ± 0.13	0.62 ± 0.05*	0.18 ± 0.04*	1.4 ± 0.07	19
Carboxy SNARF-1 + SBFI	37°C	7.62 ± 0.09	0.46 ± 0.07	0.19 ± 0.05	1.3 ± 0.06	9
SNARF-5F	37°C	7.25 ± 0.12	0.45 ± 0.05	0.29 ± 0.06	1.7 ± 0.19	12
SNARF-5F + SBFI	37°C	7.30 ± 0.09	0.58 ± 0.11	0.27 ± 0.06	1.8 ± 0.17	12

Values are means ± S.E.M. *, $P < 0.05$ compared to the corresponding value at 22°C.

Table 6.2: NH_4^+ prepulse- and anoxia-evoked changes in pH_i and $[Na^+]_i$ in hippocampal neurons loaded with a SNARF-based fluorophore and/or SBFI

A, NH_4^+ prepulse

Neurons loaded with	Decrease in pH_i on NH_4^+ washout (pH units)	Increase in $[Na^+]_i$ on NH_4^+ washout (mM)	*n*
SNARF-5F	0.81 ± 0.08		39
SBFI		12 ± 1	25
SBFI + SNARF-5F	0.87 ± 0.12	13 ± 2	14

B, During anoxia

Neurons loaded with	Decrease in pH_i (pH units)	Increase in $[Na^+]_i$ (mM)	*n*
SNARF-5F	0.40 ± 0.02		18
SBFI		18 ± 1	19
SBFI + SNARF-5F	0.44 ± 0.03	18 ± 4	8
SBFI + carboxy SNARF-1	0.37 ± 0.04	16 ± 4	15

C, After anoxia (Na^+,K^+-ATPase blocked by perfusion with K^+-free medium)

Neurons loaded with	Increase in pH_i (pH units)	Increase in $[Na^+]_i$ (mM)	*n*
carboxy SNARF-1	0.18 ± 0.02		13
SBFI		20 ± 5	11
SBFI + carboxy SNARF-1	0.25 ± 0.03	22 ± 2	27
SBFI + SNARF-5F	0.20 ± 0.02	23 ± 2	22

Values are mean ± S.E.M. In *A* and *B*, the changes in pH_i and $[Na^+]_i$ shown are with respect to pre-stimulus resting values (data obtained from neuronal cultures 10 - 14 and 7 - 10 DIV, respectively). In *C*, measurements of the increases in pH_i and $[Na^+]_i$ observed following anoxia (Na^+,K^+-ATPase inhibited) were measured as the differences between the pH_i and $[Na^+]_i$ values observed at the end of 5 min anoxia and the pH_i and $[Na^+]_i$ values observed at the end of 7 min exposure to 0 $[K^+]$ medium; data were obtained from neuronal cultures 7 - 10 DIV.

Fig. 6.1. A schematic representation of the optical equipment used to measure $[Na^+]_i$ and pH_i in hippocampal neurons loaded with SBFI and/or carboxy SNARF-1 or SNARF-5F (adapted from Buckler & Vaughan-Jones, 1990). Fluorophores loaded into neurons were excited with light provided by a 100 W Hg lamp and band-pass filtered at 488 ± 5 nm (for SNARF dyes) or alternately at 334 ± 5 and 380 ± 5 nm (for SBFI). Filtered excitation light was reflected off a 505 nm long-pass dichroic mirror (Dichroic 1), passed through a x40 LD Achroplan objective (0.6 N.A.) and illuminated neurons loaded with fluorophore(s). SBFI fluorescence emissions passed through Dichroic 1, reflected off a long-pass dichroic mirror centred at 605 nm (Dichroic 2), passed through a 550 ± 40 nm band-pass emission filter and were detected by Camera 2. Fluorescence emissions from carboxy SNARF-1 or SNARF-5F passed through Dichroic 1, were split by Dichroic 2 and passed through 640 ± 20 nm or 550 ± 40 nm band-pass emission filters before being detected by Cameras 1 and 2, respectively. Optical filters, including Dichroic mirrors 1 (505dcxru) and 2 (605drlpxr), were obtained from Chroma Technology Corp. (Rockingham, VT).

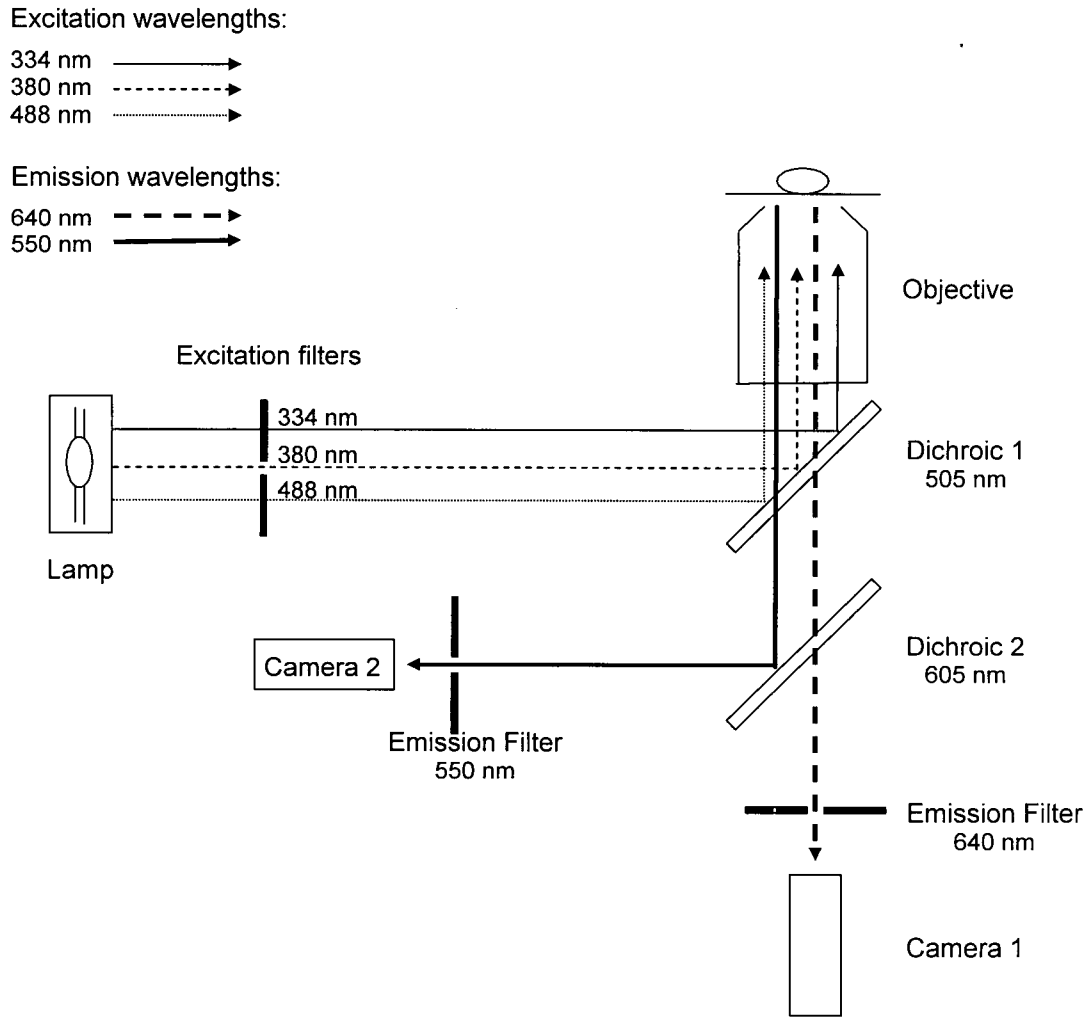
Excitation wavelengths:
334 nm
380 nm
488 nm
Emission wavelengths:
640 nm
550 nm
Objective
Excitation filters
334 nm
380 nm
488 nm
Lamp
Dichroic 1
505 nm
Camera 2
Dichroic 2
605 nm
Emission Filter
550 nm
Emission Filter
640 nm
Camera 1

Fig. 6.2. Fluorescence emissions from single and dual dye-loaded hippocampal neurons. Neurons were single- or co-loaded with fluorophores, as shown on the Figure, and illuminated at the indicated excitation wavelengths (λ_{ex}). The intensities of emitted fluorescence were measured at either 550 nm or 640 nm (λ_{em}) and, in *A* and *B*, are reported as percentages above background fluorescence values (± S.E.M.). *A*, in contrast to neurons single-loaded with either carboxy SNARF-1 or SNARF-5F, neurons single-loaded with SBFI exhibited large fluorescence emissions (measured at 550 nm) during excitation at 334 or 380 nm. Emission intensities from neurons single-loaded with carboxy SNARF-1 were 5% (excitation at 334 nm) and 9% (excitation at 380 nm) of those observed in neurons single-loaded with SBFI and excited at the same wavelengths. In neurons single-loaded with SNARF-5F and excited at 334 and 380 nm, emission intensities were, respectively, 6% and 7% of those observed in neurons single-loaded with SBFI (compare the appropriate images in the left-hand and middle panels in *C*). Also shown are fluorescence emission intensities (measured at 550 nm) during 334 and 380 nm excitation of neurons co-loaded with SBFI and either carboxy SNARF-1 or SNARF-5F (see text and the right-hand panel in *C*). *B*, in neurons single-loaded with either carboxy SNARF-1 or SNARF-5F, excitation at 488 nm evoked fluorescence emissions at both 550 and 640 nm. In neurons single-loaded with SBFI and also excited at 488 nm, fluorescence emissions measured at 550 and 640 nm were, respectively, 11% and 15% of those observed in neurons single-loaded with carboxy SNARF-1 and 13% and 13% of those observed in neurons single-loaded with SNARF-5F (compare the appropriate images in the left-hand and middle panels in *C*). Also shown are fluorescence emission intensities (measured at 550 and 640 nm) during 488 nm excitation of neurons co-loaded with SBFI and either carboxy SNARF-1 or SNARF-5F (see text and the right-hand panel in *C*). *, $P < 0.05$ between the indicated measurements in single- and

dual dye-loaded neurons. *C*, representative pseudocoloured fluorescence emission images from neurons loaded with SBFI (left-hand panel), SNARF-5F (middle panel) or SBFI and SNARF-5F (right-hand panel); each panel consists of four images, captured at the excitation and emission wavelengths indicated on each image in the left-hand panel.

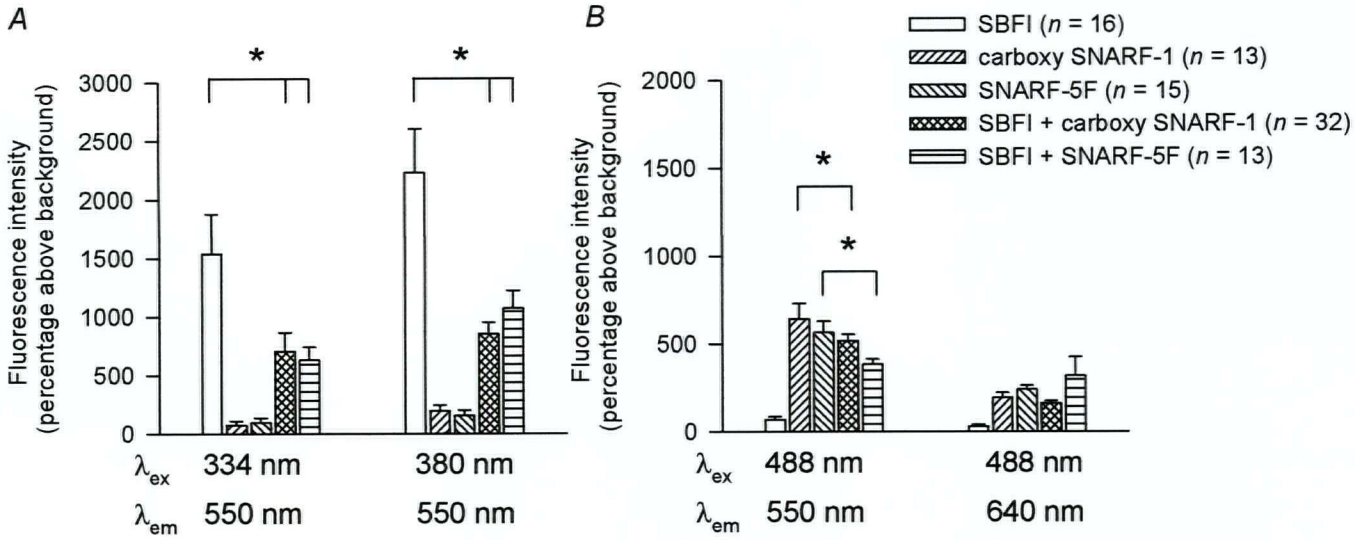

C

SBFI-loaded

SNARF-5F-loaded

SBFI + SNARF-5F-loaded

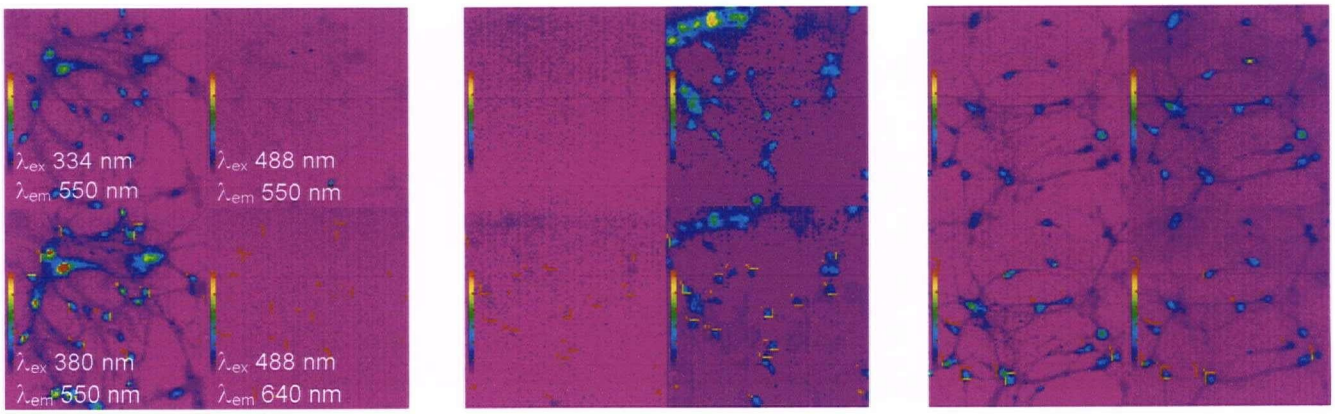

Fig. 6.3. Quenching effects between SBFI and SNARF-based fluorophores. *A*, in a population of 19 neurons single-loaded with SBFI, background-subtracted emission intensities were measured at 550 nm during excitation at 334 nm (BI_{334}, open circles) and 380 nm (BI_{380}, open diamonds). Perfusion and data collection were then interrupted and 10 μM SNARF-5F-AM was added to the recording chamber. After loading with SNARF-5F, SBFI-derived BI_{334} and BI_{380} values were reduced to a proportionately similar extent, resulting in little change in SBFI BI_{334}/BI_{380} ratio values (filled circles). Data collection was then interrupted again, during which time the gain of camera 2 was adjusted to increase emission intensities measured during excitation at 334 and 380 nm. Finally, the addition of 0.005% saponin (arrow) caused rapid decreases in BI_{334} and BI_{380} values. Also measured throughout the experiment were background-subtracted emission intensities at 550 nm (BI_{550}, open squares) and 640 nm (BI_{640}, open triangles) during excitation at 488 nm; BI_{550} and BI_{640} values increased after neurons were loaded with SNARF-5F and fell rapidly upon the subsequent addition of saponin. Temperature was 37°C throughout. *B*, neurons single-loaded with SNARF-5F (filled symbols) or co-loaded with SBFI and SNARF-5F (open symbols) were exposed to SNARF calibration media at pH 6.0, 7.0 or 8.5. The intensities of emitted fluorescence (excitation at 488 nm) were measured at 550 (circles) and 640 (squares) nm and are reported as percentages above background fluorescence values ($n \geq 12$ for each data point). Compared with measurements made in neurons single-loaded with SNARF-5F, emission intensities at 550 and 640 nm were not significantly different ($P \geq 0.20$ at each pH value) in the presence of SBFI at any of the pH values tested. Error bars are S.E.M.

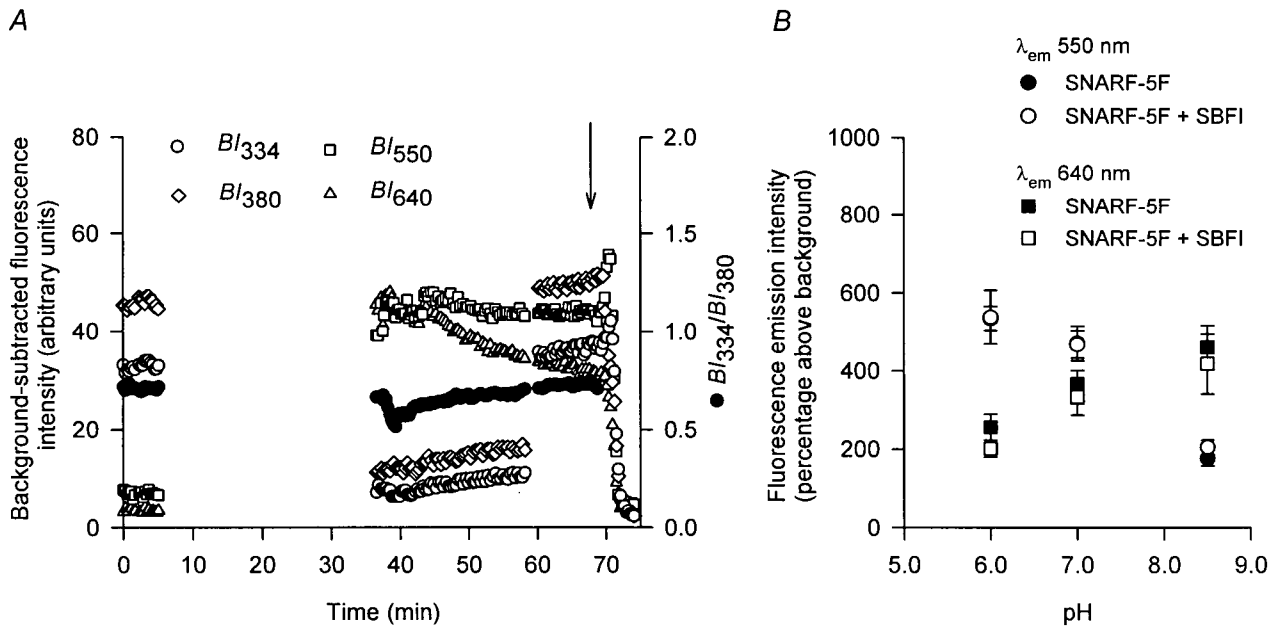
A
Background-subtracted fluorescence intensity (arbitrary units)
80
60
40
20
0
BI_{334}
BI_{380}
BI_{550}
BI_{640}
2.0
1.5
1.0
0.5
0.0
BI_{334}/BI_{380}
0
10
20
30
40
50
60
70
Time (min)
B
λ_{em} 550 nm
SNARF-5F
SNARF-5F + SBFI
λ_{em} 640 nm
SNARF-5F
SNARF-5F + SBFI
Fluorescence emission intensity (percentage above background)
1000
800
600
400
200
0
5.0
6.0
7.0
8.0
9.0
pH

Fig. 6.4. *In situ* calibration of SBFI at 37°C, pH_o 7.35. *A*, a full calibration experiment in which 20 neurons single-loaded with SBFI were exposed to 4 μM gramicidin D-containing solutions at the $[Na^+]$ values (in mM) indicated above the traces. Shown are the mean changes in emitted background-subtracted fluorescence intensities measured at 550 nm during excitation at 334 nm (BI_{334}, open circles) and 380 nm (BI_{380}, open diamonds) and the mean normalized BI_{334}/BI_{380} ratio values (R_n, filled circles), which increased as $[Na^+]$ increased. Also shown are the background-subtracted fluorescence emission intensities measured at 550 nm (BI_{550}, open squares) and 640 nm (BI_{640}, open triangles) during excitation at 488 nm (i.e. the excitation and emission wavelengths used for SNARF measurements); note the change of scale. *B*, plots of $[Na^+]$ vs. R_n obtained from experiments of the type shown in *A*. Data points fitted by the continuous line were obtained from four experiments conducted on sister cultures in which neurons were loaded with SBFI alone. Data points fitted by the dashed line were obtained from four experiments conducted on sister cultures in which neurons were co-loaded with SBFI and SNARF-5F. In both cases, error bars are S.E.M. As detailed in Chapter 2, the curves are the result of at fit to a three-parameter hyperbola (Equation 2.4) to the respective data points indicated and were used to determine the values of the SBFI calibration parameters (i.e. K_d, β, $R_{n(min)}$ and $R_{n(max)}$) under the different dye loading conditions (Table 6.1; also see Diarra *et al.* 2001).

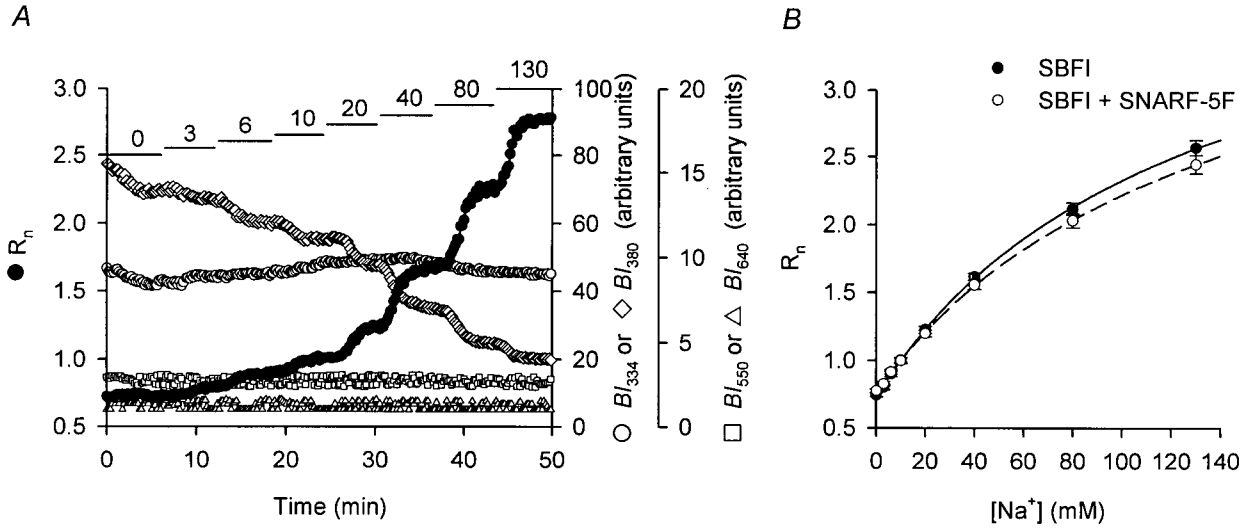
A
B
0
3
6
10
20
40
80
130
Rn
Time (min)
○ BI334 or ◇ BI380 (arbitrary units)
□ BI550 or △ BI640 (arbitrary units)
SBFI
SBFI + SNARF-5F
[Na+] (mM)

Fig. 6.5. *In situ* calibration of carboxy SNARF-1. *A*, a full calibration experiment performed at 22°C in which 18 neurons single-loaded with carboxy SNARF-1 were exposed to high-[K^+], 10 μM nigericin-containing solutions at the pH values shown above the records. Background-subtracted fluorescence emissions measured at 550 nm (BI_{550}, open squares) increased upon protonation of the dye while background-subtracted emissions measured at 640 nm (BI_{640}, open triangles) decreased; thus, the resulting background-subtracted BI_{550}/BI_{640} ratio values normalized to 1.00 at pH 7.00 (R_n, filled circles) increased as pH_i fell. Also shown are the background-subtracted fluorescence emission intensities measured at 550 nm during excitation at 334 nm (BI_{334}, open circles) and 380 nm (BI_{380}, open diamonds) (i.e. the excitation and emission wavelengths used for SBFI measurements); BI_{334} and BI_{380} emissions from carboxy SNARF-1 (and SNARF-5F; not shown) remained small as pH was altered (note the change of scale). *B*, plots of pH vs. R_n obtained from experiments of the type shown in A. In neurons single-loaded with carboxy SNARF-1, data points obtained from experiments performed at 22°C and 37°C (n = 3 experiments conducted on sister cultures in each case) were fitted using non-linear least squares regression (dashed and continuous lines, respectively). Also shown are data points obtained from three experiments performed on sister cultures in which neurons were co-loaded with carboxy SNARF-1 and SBFI; these are fitted by the dotted line. In all cases, error bars are S.E.M. The curves were used to determine the values of the carboxy SNARF-1 calibration parameters (i.e. pK_a, $\log F640_{min/max}$, $R_{n(min)}$ and $R_{n(max)}$) under the different dye loading conditions (see Table 6.1).

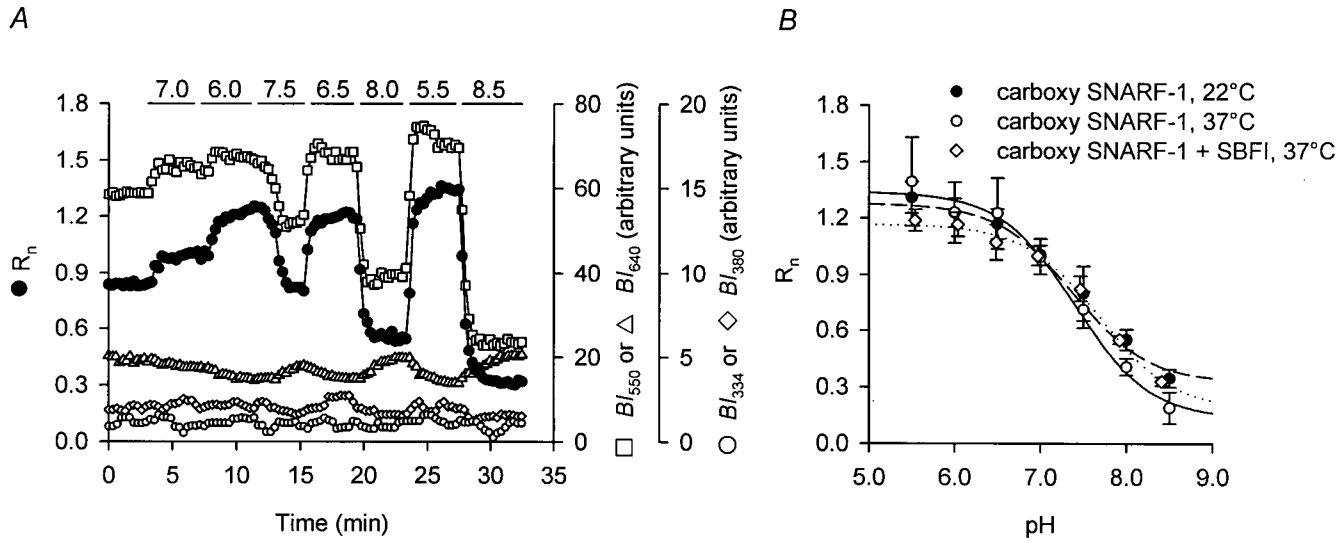
A
7.0 6.0 7.5 6.5 8.0 5.5 8.5
● R_n
□ BI_{550} or △ BI_{640} (arbitrary units)
○ BI_{334} or ◇ BI_{380} (arbitrary units)
Time (min)
B
● carboxy SNARF-1, 22°C
○ carboxy SNARF-1, 37°C
◇ carboxy SNARF-1 + SBFI, 37°C
R_n
pH

Fig. 6.6. Sodium sensitivity of carboxy SNARF-1 *in situ*. *A*, neurons loaded with carboxy SNARF-1 were exposed at 37°C to calibration media containing 4 μM gramicidin at pH 6.00 (open squares), 6.50 (open circles), 7.00 (filled circles) or 7.50 (open diamonds). At each pH, $[Na^+]$ was changed from 0 to 10 to 130 mM as indicated above the records. BI_{550}/BI_{640} ratio values (R_n) were normalized to unity at pH = 7.00 and $[Na^+]$ = 10 mM. *Inset*, to quantify the effects of changes in $[Na^+]$ on R_n values measured with carboxy SNARF-1, apparent changes in R_n (ΔR_n) were calculated as $R_{n(x)}$ - $R_{n(10)}$ (where x = 0, 10 or 130) for each pH value indicated and plotted as a function of $[Na^+]$. *B*, R_n values at a given $[Na^+]$ were plotted as a function of pH (n = 3 at pH 6.50, 7.00 and 7.50; n = 1 at pH 6.00) and data points were fitted using non-linear least squares regression (continuous, dotted and dashed curves for data obtained at 0, 10 and 130 mM $[Na^+]$, respectively). The $pK_a + \log F640_{min/max}$, $R_{n(min)}$ and $R_{n(max)}$ values for carboxy SNARF-1 did not change significantly as $[Na^+]$ was increased from 0 to 10 to 130 mM ($pK_a + \log F640_{min/max}$, $R_{n(min)}$ and $R_{n(max)}$ values were, respectively, 7.35, 0.44 and 1.25 at 0 mM $[Na^+]$; 7.32, 0.47 and 1.26 at 10 mM $[Na^+]$; and 7.28, 0.46 and 1.30 at 130 mM $[Na^+]$). *Inset*, R_n values were converted into pH_i and apparent changes in pH_i (ΔpH_i) were then calculated as $pH_{i(x)}$ - $pH_{i(10)}$ (where x = 0, 10 or 130) for each pH value indicated and plotted as a function of $[Na^+]$. In the insets in *A* and *B*, each datum point represents measurements made in 3 separate experiments; error bars are S.E.M. and the continuous lines represent linear regression fits to the data points indicated for each pH value.

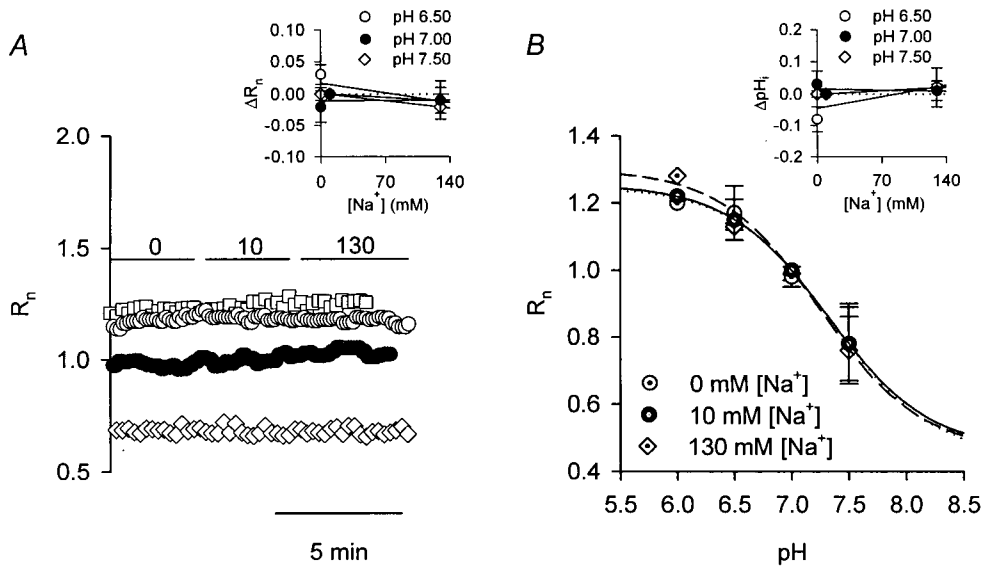
A
pH 6.50
pH 7.00
pH 7.50
ΔRn
[Na+] (mM)
Rn
0
10
130
5 min
B
ΔpHi
0 mM [Na+]
10 mM [Na+]
130 mM [Na+]
pH

Fig. 6.7. Changes in pH_i and $[Na^+]_i$ observed in rat hippocampal neurons in response to intracellular acid loads imposed by the NH_4^+ prepulse technique. *A*, in a neuron single-loaded with SNARF-5F, washout of NH_4^+ evoked a fall in pH_i which gradually returned to the resting level. *B*, in a neuron single-loaded with SBFI, an increase in $[Na^+]_i$ occurred upon the washout of NH_4^+. *C*, in a neuron co-loaded with SNARF-5F and SBFI, the changes in pH_i (filled circles) observed on NH_4^+ washout were temporally associated with a transient increase in $[Na^+]_i$ (open circles). *D*, rates of pH_i recovery from NH_4^+-induced internal acid loads measured in neurons either single-loaded with SNARF-5F (solid circles; n = 39) or co-loaded with SNARF-5F and SBFI (open circles; n = 14). Error bars are S.E.M. and continuous lines represent weighted nonlinear regression fits to the data points indicated for each experimental condition. Rates of pH_i recovery in neurons single-loaded with SNARF-5F were not significantly different from those in neurons co-loaded with SNARF-5F and SBFI ($P > 0.05$ at each absolute pH_i value). *E*, scatter plot demonstrating the relationship between the magnitude of the recovery of pH_i (measured as the difference between the minimum pH_i value attained after NH_4^+ washout and the steady-state pH_i value reached after recovery) and the increase in $[Na^+]_i$ observed after NH_4^+ washout in 14 neurons co-loaded with SNARF-5F and SBFI. The continuous line is a linear regression fit to the data points shown (correlation coefficient = 0.68; $P < 0.05$).

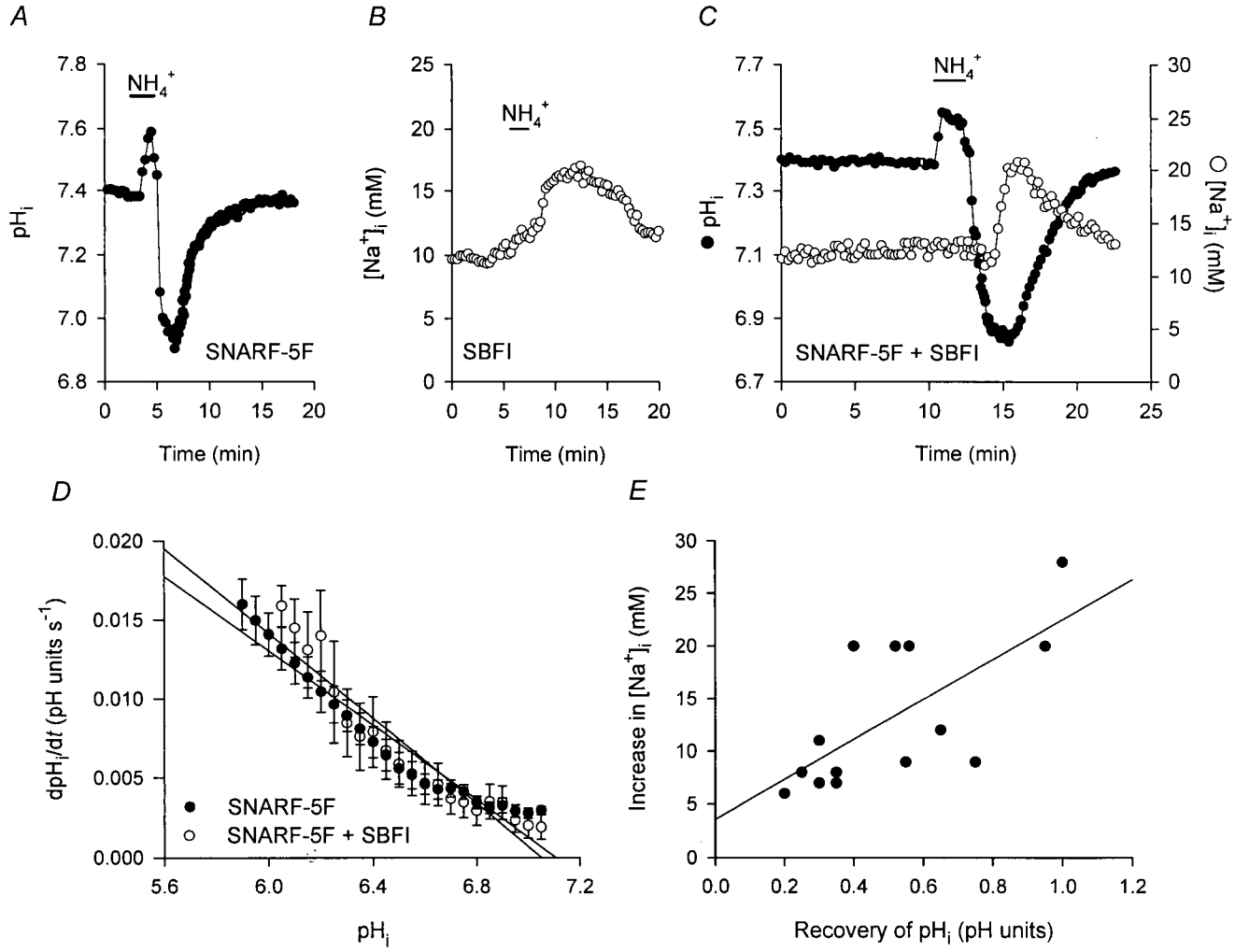
A
B
C
D
E
NH4+
SNARF-5F
SBFI
SNARF-5F + SBFI
pHi
[Na+]i (mM)
Time (min)
dpHi/dt (pH units s-1)
Increase in [Na+]i (mM)
Recovery of pHi (pH units)

Fig. 6.8. Changes in pH_i and $[Na^+]_i$ induced by anoxia in rat hippocampal neurons. *A*, in a neuron single-loaded with SNARF-5F, 5 min anoxia evoked a fall in pH_i that recovered towards the resting value upon the return to normoxia. *B*, in a neuron single-loaded with SBFI, 5 min anoxia induced an increase in $[Na^+]_i$ that recovered to the resting value upon the return to normoxia. *C*, in a neuron co-loaded with SNARF-5F and SBFI, 5 min anoxia induced a fall in pH_i (solid circles) and an increase in $[Na^+]_i$ (open circles). Upon the return to normoxia, both pH_i and $[Na^+]_i$ recovered toward pre-anoxic values. *D*, in a neuron single-loaded with SNARF-5F, inhibition of Na^+,K^+-ATPase activity (by perfusion with K^+-free medium) for 7 min following 5 min anoxia did not influence the recovery of pH_i (compare with *A*). *E*, in a neuron single-loaded with SBFI, inhibition of Na^+,K^+-ATPase activity following 5 min anoxia revealed a secondary increase in $[Na^+]_i$ in the post-anoxic period (compare with *B*). Once Na^+,K^+-ATPase activity was re-established (i.e. 3 mM $[K^+]_o$), $[Na^+]_i$ recovered to pre-anoxic values. *F*, in a neuron co-loaded with SNARF-5F and SBFI, both pH_i and $[Na^+]_i$ increased during the period of Na^+,K^+-ATPase inhibition after anoxia. In *A* - *F*, traces were obtained from neurons 7 - 10 DIV.

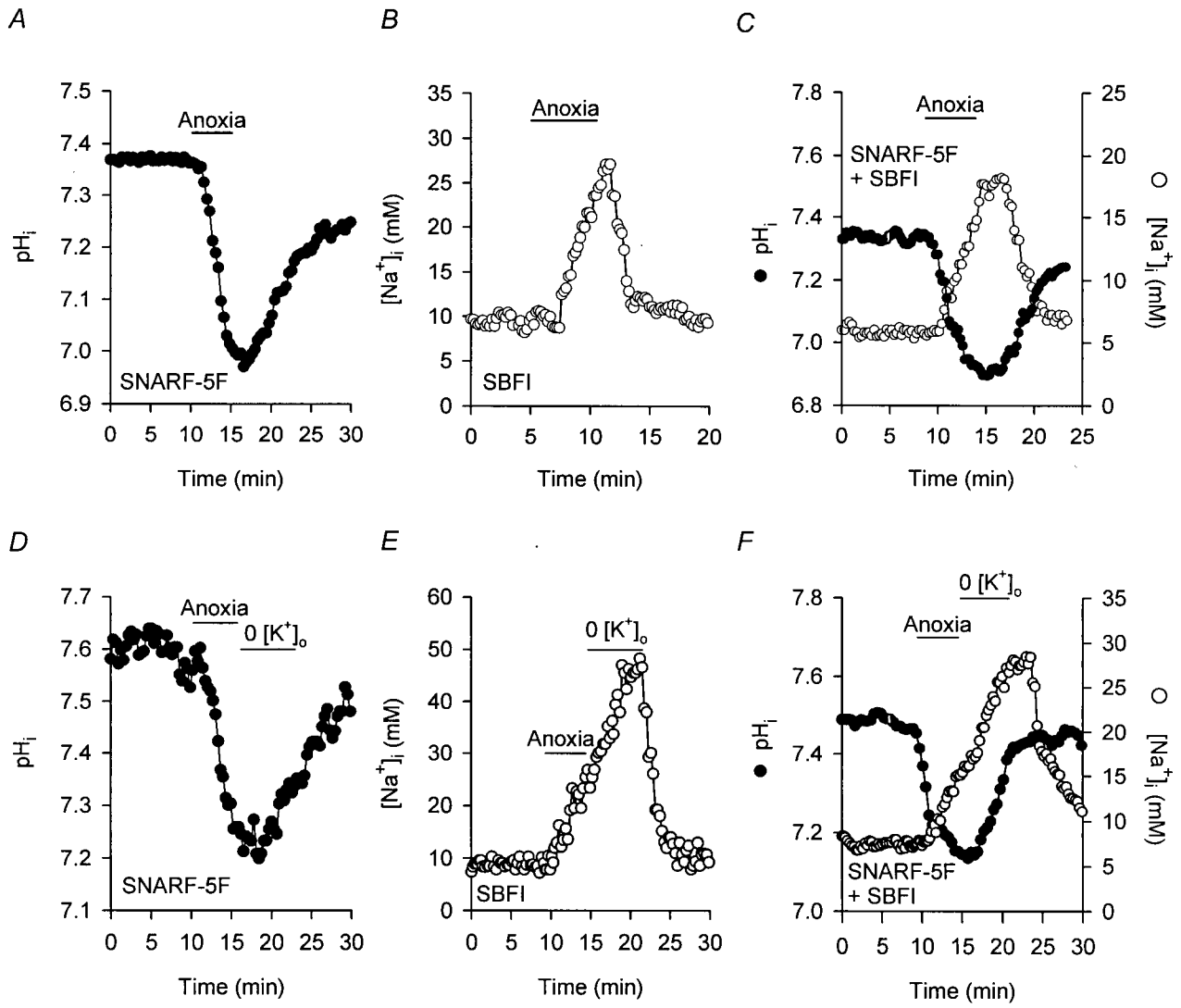
A
B
C
D
E
F
Anoxia
0 [K+]o
SNARF-5F
SBFI
SNARF-5F + SBFI
pHi
[Na+]i (mM)
Time (min)

Fig. 6.9. Reducing $[Na^+]_o$ limits the increases in pH_i and $[Na^+]_i$ observed immediately after anoxia. *A,* during 5 min anoxia, pH_i fell and $[Na^+]_i$ increased. Upon the return to normoxia (Na^+,K^+-ATPase inhibited), both pH_i (filled circles) and $[Na^+]_i$ (open circles) increased (compare with Fig. 6.8*F*, an identical experiment performed in a neuron 7 DIV). *B*, during 5 min anoxia, in the presence of normal Na^+_o, pH_i (filled squares) fell and $[Na^+]_i$ (open squares) increased. Following anoxia, neurons were perfused with K^+- and Na^+-free medium. Reducing Na^+_o ($NMDG^+$-substitution) prevented the rises in pH_i and $[Na^+]_i$ observed after anoxia in the presence of normal Na^+_o (compare with *A*). Upon the return to normal Na^+_o (in the continued absence of $[K^+]_o$; arrow), both pH_i and $[Na^+]_i$ increased. This trace is representative of data obtained from 6 additional neurons co-loaded with SBFI and SNARF-5F.

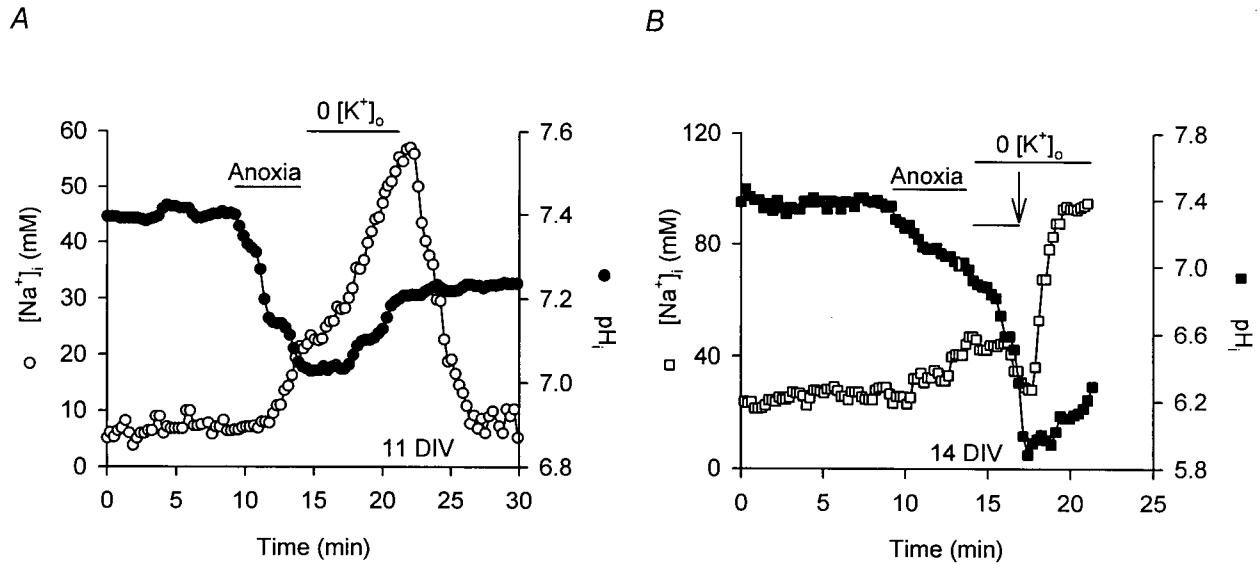
A
0 [K+]o
Anoxia
11 DIV
○ [Na+]i (mM)
● pHi
Time (min)
B
0 [K+]o
Anoxia
14 DIV
□ [Na+]i (mM)
■ pHi
Time (min)

Fig. 6.10. Relationships between changes in pH_i and $[Na^+]_i$ observed in the period immediately after anoxia (Na^+,K^+-ATPase inhibited). *A,* measured in 20 neurons 7 - 10 DIV (co-loaded with SNARF-5F and SBFI), rates at which pH_i (open circles) and $[Na^+]_i$ (filled circles) increase in the immediate post-anoxic period (Na^+,K^+-ATPase blocked) show an inverse dependence on absolute pH_i values. Similar results were observed in neuronal cultures 11 - 14 DIV (*B*; $n = 10$). Rates at which pH_i and $[Na^+]_i$ increased following anoxia under $[K^+]_o$-free conditions were determined by fitting the pH_i and $[Na^+]_i$ records obtained under $[K^+]_o$-free conditions to single exponential functions. The first derivatives of these functions were used to determine rates of pH_i recovery and $[Na^+]_i$ rise as functions of time. Rates of pH_i and $[Na^+]_i$ rises were determined at 0.05 pH unit and 5 mM intervals, respectively. The pH_i values at which rates of $[Na^+]_i$ rises were measured were determined from obtained curve-fitted parameters. Error bars represent S.E.M.

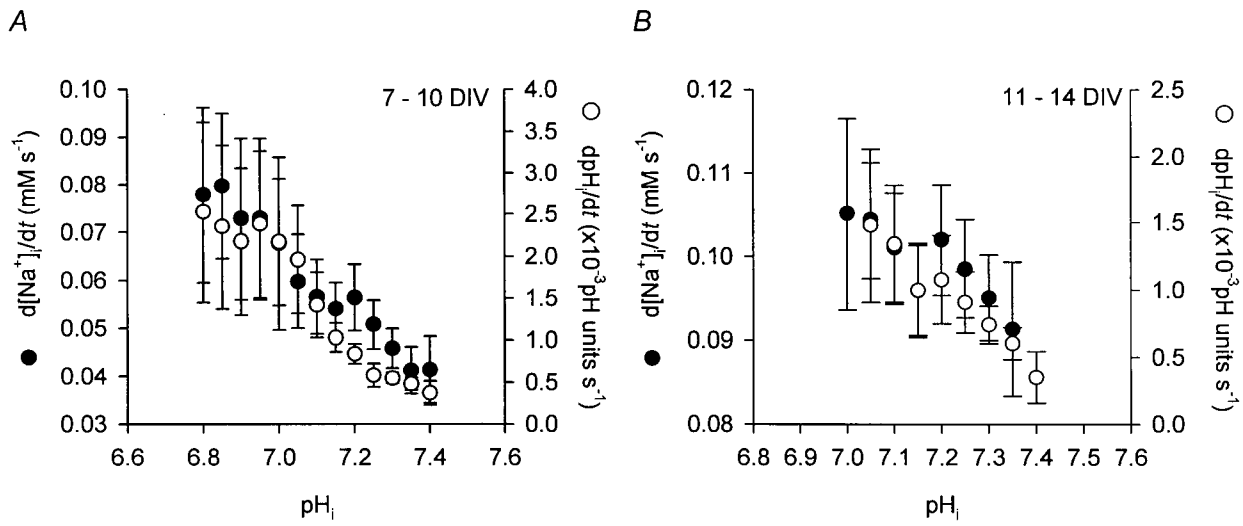
A
7 - 10 DIV
● d[Na+]i/dt (mM s-1)
○ dpHi/dt (x10-3 pH units s-1)
pHi
B
11 - 14 DIV
● d[Na+]i/dt (mM s-1)
○ dpHi/dt (x10-3 pH units s-1)
pHi

Fig. 6.11. The influence of maneuvers which inhibit Na^+/H^+ exchange activity on anoxia-evoked changes in pH_i and $[Na^+]_i$ measured concurrently in individual cells co-loaded with either carboxy SNARF-1 or SNARF-5F and SBFI. The magnitudes of the falls in pH_i (bars with horizontal lines) and increases in $[Na^+]_i$ (cross-hatched bars) observed *during* anoxia were measured as the difference between the minimum pH_i and maximum $[Na^+]_i$ observed at the end of 5 min anoxia and the pre-anoxic resting pH_i and $[Na^+]_i$ values, respectively. The magnitudes of the increase in pH_i (filled bars) and $[Na^+]_i$ (open bars) observed *after* anoxia (Na^+,K^+-ATPase inhibited) were measured as the difference between the pH_i and $[Na^+]_i$ values observed at the end of anoxia and the pH_i and $[Na^+]_i$ values observed at the end of 7 min 0 $[K^+]_o$, respectively. Measurements under an experimental test condition were normalized to measurements made in experiments performed on age-matched sister cultures under control conditions. Statistical comparisons were performed by comparing the absolute measurements of the anoxia-evoked changes in pH_i and $[Na^+]_i$ (i.e. not normalized) made under experimental test conditions to corresponding measurements made in age-matched sister cultures under control conditions. * indicates statistical significance ($P < 0.05$) compared with measurements made in sister cultures under control conditions. All data were obtained from neuronal cultures 7 - 10 DIV.

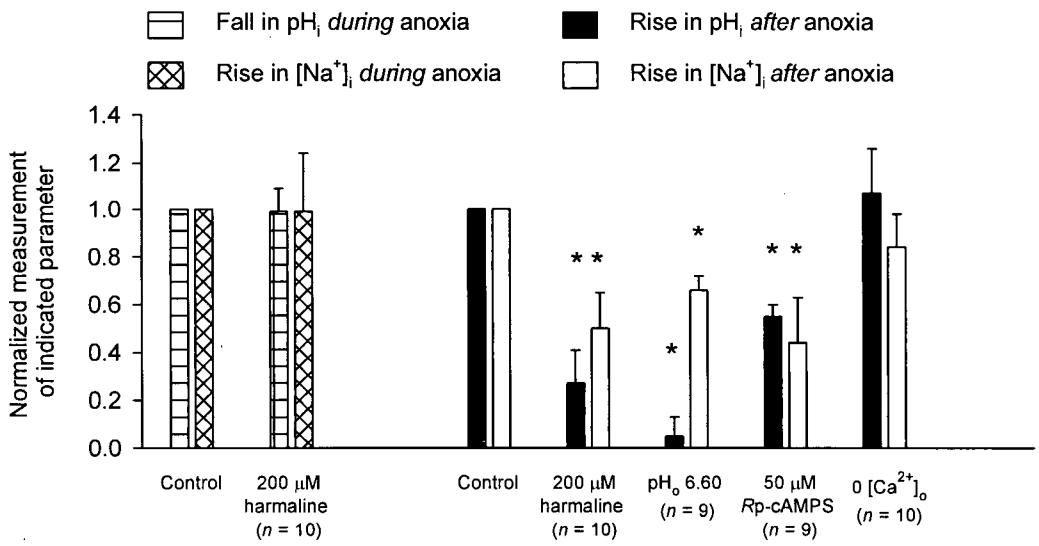
Fall in pH$_i$ *during* anoxia
Rise in [Na$^+$]$_i$ *during* anoxia
Rise in pH$_i$ *after* anoxia
Rise in [Na$^+$]$_i$ *after* anoxia
Normalized measurement of indicated parameter
1.4
1.2
1.0
0.8
0.6
0.4
0.2
0.0
Control
200 μM harmaline (*n* = 10)
Control
200 μM harmaline (*n* = 10)
pH$_o$ 6.60 (*n* = 9)
50 μM *R*p-cAMPS (*n* = 9)
0 [Ca^{2+}]$_o$ (*n* = 10)

CHAPTER SEVEN

ADDITIONAL MECHANISMS CONTRIBUTING TO ANOXIA-EVOKED INCREASES IN $[Na^+]_i$ IN CULTURED POSTNATAL RAT HIPPOCAMPAL NEURONS

7.0. INTRODUCTION

The detrimental effects of increases in $[Na^+]_i$ evoked by anoxia or ischemia are well-established; however, in contrast to non-neuronal cell types (e.g. cardiac myocytes; Carmeliet, 1999) and myelinated central nervous system axons (Stys, 1998), the mechanisms which mediate Na^+ influx in response to anoxia or ischemia in mammalian central neurons remain relatively poorly defined. Although Na^+ influx through glutamate receptor-operated channels has received some attention (Müller & Somjen, 2000a, LoPachin *et al.* 2001), few studies have examined the potential contributions of mechanisms integral to the cell to the increases in $[Na^+]_i$ observed during anoxia or ischemia (e.g. Chen *et al.* 1999 for $[Na^+]_i$ measurements in cerebellar granule cells during metabolic inhibition; also see Guatteo *et al.* 1998; Pisani *et al.* 1998a; Calabresi *et al.* 1999b for studies in slice preparations). In addition, despite indications that continued Na^+ influx upon reperfusion may be more damaging than Na^+ entry during anoxia or ischemia (Lipton, 1999; also discussed in Chapter 8), the pathways that mediate Na^+ entry immediately after anoxia/ischemia have not been characterized and it remains unknown whether these pathways might differ from those active during an insult, as reported for Ca^{2+} (e.g. Silver & Erecińska, 1990 and 1992; Stys & LoPachin, 1998).

As detailed in Chapters 5 and 6, postnatal rat hippocampal neurons responded to 5 min anoxia with an increase in $[Na^+]_i$ of ~15 - 40 mM that, upon the return to normoxia, recovered to pre-anoxic values despite continued Na^+ entry. Under conditions which inhibit the Na^+,K^+-ATPase following anoxia (perfusion with K^+_o-free medium or the application of ouabain), a

further elevation in $[Na^+]_i$ of ~30 - 60 mM was revealed. The increases in $[Na^+]_i$ observed during and following anoxia were related to the duration that neurons had been maintained in culture (within the examined range of 6 - 14 DIV) and, in all neurons examined, were dependent on the influx of external Na^+ ions. The results presented in Chapters 5 and 6 also indicated that Na^+/H^+ exchange contributes to Na^+ influx immediately after, but not during, anoxia; thus, it is apparent that other mechanisms must contribute to the Na^+ influx occurring during and following anoxia in rat hippocampal neurons.

In this study, I assessed the potential contribution of intrinsic mechanisms other than Na^+/H^+ exchange to the rises in $[Na^+]_i$ that occur during and following 5 min anoxia in postnatal rat hippocampal neurons.

7.1. MATERIALS AND METHODS

7.1.1. Experimental preparation and solutions

Primary cultures of hippocampal neurons prepared from 2 - 4 day old postnatal Wistar rats were employed in all experiments presented in this Chapter. Hyperosmolar solutions were prepared by adding 50 or 100 mM mannitol to standard, Hepes-buffered solutions: the osmolalities of these solutions were measured with an μOsmette osmometer (Precision Systems, Inc., Natick, MA), calibrated before use. The osmolalities of standard Hepes-buffered media in the absence of mannitol and of standard Hepes-buffered media to which 50 and 100 mM mannitol had been added were 296 ± 2 (n = 4), 345 ± 1 (n = 2) and 392 ± 2 mOsm kg H_2O^{-1} (n = 4), respectively.

7.1.2. Recording techniques

Details of the techniques used to load cultured postnatal rat hippocampal neurons with SBFI-AM are presented in Chapter 5. Details of the techniques used to measure SBFI-derived emission intensity ratios and the conversion of these ratio values to $[Na^+]_i$ are described in Chapter 2.

7.1.3. Experimental procedures and data analysis

As described in Chapter 5, changes in $[Na^+]_i$ observed during anoxia ($\Delta[Na^+]_{i(during)}$) were measured as the difference between the pre-anoxic resting $[Na^+]_i$ value and the $[Na^+]_i$ value observed at the end of 5 min anoxia. Changes in $[Na^+]_i$ observed following anoxia ($\Delta[Na^+]_{i(after)}$) were measured as the difference between the $[Na^+]_i$ value observed at the end of 5 min anoxia and the $[Na^+]_i$ value observed at the end of a 7 min exposure to 0 $[K^+]_o$ or 500 μM ouabain.

Data are reported as mean ± S.E.M. with the accompanying *n* value referring to the number of neuronal populations (i.e. coverslips) from which data were obtained. In light of the findings presented in Chapter 5 that the increases in $[Na^+]_i$ observed during and after anoxia were related to the duration of time that neurons had been maintained in culture, measurements of anoxia-evoked increases in $[Na^+]_i$ observed under a given test condition were normalized to $[Na^+]_i$ measurements made in control experiments performed on the same day using age-matched sister cultures (see Tables 7.1 and 7.2). Statistical comparisons were performed by comparing absolute $[Na^+]_i$ measurements (i.e. not normalized $\Delta[Na^+]_{i(during)}$ and $\Delta[Na^+]_{i(after)}$) made under a given test condition to the corresponding measurements made in age-matched sister cultures under control conditions using Student's two-tailed unpaired *t*-tests. Significance was assumed at the 5% level.

7.2. RESULTS

7.2.1. Increases in $[Na^+]_i$ *during* anoxia

7.2.1.1. Role of ionotropic glutamate receptor-operated channels

Ionotropic glutamate receptor activation did not contribute to the increase in $[Na^+]_i$ induced by anoxia under the constant superfusion conditions of the present experiments. Thus, in neurons maintained for either 6 - 10 or 11 - 14 DIV, the addition of 2 μM MK-801 and/or 20 μM CNQX failed to influence significantly the magnitude of the increase in $[Na^+]_i$ observed during anoxia (Table 7.1; Fig. 7.1). In contrast, the same concentrations of MK-801 and CNQX together abolished the increase in $[Na^+]_i$ evoked by 30 s applications of 20 μM NMDA and 20 μM AMPA under normoxic conditions (Fig. 7.1, *inset*).

7.2.1.2. Role of voltage-activated Na^+ channels

In whole-cell recordings obtained using the perforated patch (amphotericin B) configuration (courtesy of T. Kelly), the average resting membrane potential of cultured postnatal rat hippocampal neurons prior to anoxia was -62 ± 1 mV and 5 min anoxia evoked a depolarization of 21 ± 2 mV (n = 3), similar to the depolarizations observed by others in a variety of isolated mammalian central neurons in reponse to 5 min anoxia (e.g. Haddad & Jiang, 1993) or 30 min metabolic inhibition (e.g. Pisani *et al.* 1997; Aarts *et al.* 2003). Despite the anoxia-induced membrane depolarization, 1 μM TTX failed to affect the increase in $[Na^+]_i$ observed during anoxia in neurons maintained either for 6 - 10 or 11 - 14 DIV (Table 7.1; Fig. 7.2*A*). In contrast, 1 μM tetrodotoxin (TTX) reduced the increases in $[Na^+]_i$ evoked by 60 s applications of 50 mM

K^+_o under normoxic conditions from 12 ± 3 (n = 5) to 3 ± 1 (n = 6) mM (Fig. 7.2*A*, *inset*; $P < 0.05$).

7.2.1.3. Role of plasmalemmal Na^+/Ca^{2+} exchange and $Na^+/K^+/2Cl^-$ cotransport

While the increase in $[Ca^{2+}]_i$ observed in cultured postnatal rat hippocampal neurons during 5 min anoxia (see Diarra *et al.* 1999) could activate forward mode Na^+/Ca^{2+} exchange and thereby contribute to the influx of Na^+ during anoxia, a rise in $[Na^+]_i$ could promote reverse-mode operation of the exchange mechanism and, thus, Na^+ efflux (Blaustein & Lederer, 1999). Forward- and reverse-mode operation of the plasmalemmal Na^+/Ca^{2+} exchanger can be inhibited by bepridil (50 μM) and KB-R7943 (1 μM), respectively, while elevated concentrations of KB-R7943 (10 μM) have been reported to inhibit both forward- and reverse-mode Na^+/Ca^{2+} exchange activity in hippocampal neurons (Breder *et al.* 2000). Neither bepridil (50 μM) nor KB-R7943 (1 or 10 μM) influenced the magnitude of the increase in $[Na^+]_i$ observed during anoxia (Table 7.1; Fig. 7.2*B*). In addition, neither CGP-37157 (25 μM), an inhibitor of plasmalemmal Na^+/Ca^{2+} exchange in cerebellar granule cells (Czyż & Kiedrowski, 2003; but see Zhang & Lipton, 1999 for an illustration of CGP-37157 acting to inhibit mitochondrial Na^+/Ca^{2+} exchange in rat hippocampal slices) nor the removal of external Ca^{2+} prior to and during anoxia, influenced the increase in $[Na^+]_i$ observed during anoxia (Table 7.1).

Inhibition of $Na^+/K^+/2Cl^-$ cotransport with bumetanide reduces infarct volume and brain edema following focal cerebral ischemia (Yan *et al.* 2001 and 2003). Given that $Na^+/K^+/2Cl^-$ cotransport protein expression and transport activity increases with time in cultured neocortical neurons (Sun & Murali, 1999; Beck *et al.* 2003), the effects of bumetanide were examined in 6 - 10 and 11 - 14 DIV cultured neurons. Exposure to 50 - 100 μM bumetanide did not affect resting

$[Na^+]_i$ in either 6 - 10 (n = 5) or 11 - 14 (n = 9) DIV neuronal cultures (also see Rose & Ransom, 1997) and failed to influence the magnitude of the increase in $[Na^+]_i$ observed during anoxia in 6 - 10 DIV cultures (Table 7.1). In contrast, in neurons 11 - 14 DIV, bumetanide caused a significant reduction in the rise in $[Na^+]_i$ observed during anoxia (Table 7.1; Fig. 7.2*C*).

7.2.1.4. Role of non-selective cation channels

Non-selective cation channels (NSCCs) can be activated during anoxia or ischemia as a result of membrane stretching, increases in $[Ca^{2+}]_i$ or free radical production (e.g. Chen *et al.* 1999; Barros *et al.* 2001; Aarts *et al.* 2003) and have been found to participate in the production of a variety of events that occur in response to anoxia or ischemia in isolated neurons (e.g. Chen *et al.* 1997; Chen *et al.* 1998a; El-Sherif *et al.* 2001; Aarts *et al.* 2003; Limbrick *et al.* 2003; Smith *et al.* 2003). To examine the potential contribution of Na^+ influx through NSCCs to the rise in $[Na^+]_i$ observed during anoxia, I applied Gd^{3+}, an established blocker of stretch-activated and other types of NSCCs (see Caldwell *et al.* 1998).

In the presence of 30 or 100 μM Gd^{3+}, the anoxia-induced increase in $[Na^+]_i$ was reduced by ~40 % (Fig. 7.3*A*, *D*). When neurons were exposed to 50 or 100 mM mannitol to limit anoxia-induced cell swelling (see Alojado *et al.* 1996; Hasbani *et al.* 1998), the increase in $[Na^+]_i$ observed during anoxia was enhanced, not reduced, when compared to measurements made under control conditions (Fig. 7.3*B*, *D*), an effect which may reflect the activation of Na^+ influx pathways under these conditions (e.g. Shrode *et al.* 1997; Bevensee *et al.* 1999b; Gosmanov *et al.* 2003). Nevertheless, applied in the presence of 100 mM mannitol, Gd^{3+} continued to reduce the magnitude of the increase in $[Na^+]_i$ observed during anoxia (Fig. 7.3*C,D*), suggesting that the ability of Gd^{3+} to significantly reduce the increase in $[Na^+]_i$ observed during anoxia cannot

simply reflect its ability to inhibit stretch-activated NSCCs. Similarly, the finding presented above that the increase in $[Na^+]_i$ during anoxia is not reduced in the absence of external Ca^{2+} suggests that the ability of Gd^{3+} to reduce the increase in $[Na^+]_i$ during anoxia is not likely mediated via an inhibition of NSCCs activated by increases in $[Ca^{2+}]_i$ (we were unable to examine the effects of flufenamate, an inhibitor of $Ca^{2+}{}_i$-activated NSCCs in hippocampal neurons, on the increases in $[Na^+]_i$ during anoxia because it evoked variable increases in resting $[Na^+]_i$; also see Partridge & Valenzuela, 2000). In addition, neither the broad-spectrum Ca^{2+} channel blockers, Ni^{2+} and verapamil, nor the L-type Ca^{2+} channel blocker, nifedipine, influenced significantly the increase in $[Na^+]_i$ during anoxia (Fig. 7.3*D*). These findings, together with those presented above that the increase in $[Na^+]_i$ during anoxia is not influenced significantly by CNQX, indicate that the effect of Gd^{3+} to limit Na^+ influx during anoxia is likely independent of its ability to block voltage-activated Ca^{2+} channels (e.g. Boland *et al.* 1991; Elinder & Århem, 1994; Caldwell *et al.* 1998) or AMPA/kainate receptors (e.g. Huettner *et al.* 1998; Lei & MacDonald, 2001).

To examine the potential role of reactive oxygen species (ROS) in activating Gd^{3+}-sensitive Na^+ influx through NSCCs, neuronal cultures were pretreated with the antioxidant, trolox (1 mM for 2 - 3 h prior to anoxia; see Papadopoulos *et al.* 1998; Vergun *et al.* 2001). Following pretreatment, the magnitude of the increase in $[Na^+]_i$ during anoxia was reduced by ~40% (Fig. 7.4) and 30 μM Gd^{3+} failed to exert an additional inhibitory effect on the increase in $[Na^+]_i$ observed during anoxia (Fig. 7.4). Although these results support the possibility that NSCCs activated by ROS may contribute to the increases in $[Na^+]_i$ observed during anoxia, neither 15 - 30 μM $AACOCF_3$ nor 500 μM L-NAME had a significant effect on the increases in $[Na^+]_i$ during anoxia (Fig. 7.4*B*), suggesting a lack of involvement of cytosolic phospholipase A_2

(PLA_2) and nitric oxide synthase (NOS) in the generation of the reactive oxygen species involved (also see Vergun *et al.* 2001). I was unable to examine the potential effects of manganese (III) tetrakis (4-benzoic acid) porphyrin (MnTBAP, an O_2^- scavenger; see Patel *et al.* 1996) or mepacrine (a non-specific PLA_2 inhibitor; see Chen *et al.* 1999), which were highly fluorescent during excitation at both 334 and 380 nm.

7.2.2. Increases in $[Na^+]_i$ *after* anoxia

7.2.2.1. Role of ionotropic glutamate receptor-operated channels, voltage-activated Na^+ channels and $Na^+/K^+/2Cl^-$ cotransport

Analogous with their inability to influence Na^+ influx during anoxia, the addition of 2 μM MK-801 and 20 μM CNQX failed to significantly influence the magnitude of the increase in $[Na^+]_i$ observed after anoxia (Na^+,K^+-ATPase inhibited; Table 7.2). Similarly, the magnitude of the increase in $[Na^+]_i$ observed following anoxia was not different in the presence or absence of 1 μM TTX (Table 7.2). One hundred micromolar TTX (n = 3 neuronal cultures at 9 DIV; not shown) and 250 μM lidocaine (Table 7.2) were also without significant effects, suggesting that Na^+ influx via TTX-resistant persistent Na^+ channels are not major contributors to the continued Na^+ influx found to occur immediately after 5 min anoxia. Finally, in contrast to the ability of bumetanide to limit the rise in $[Na^+]_i$ observed during anoxia in neurons maintained in culture for 11 - 14 DIV, 100 μM bumetanide did not reduce the magnitude of the increase in $[Na^+]_i$ observed following anoxia in 6 - 10 or 11 - 14 DIV neuronal cultures (Table 7.2).

7.2.2.2. Role of plasmalemmal Na^+/Ca^{2+} exchange

The plasmalemmal Na^+/Ca^{2+} exchanger, operating in forward mode, has been suggested to contribute, at least in part, to Ca^{2+} efflux following depolarization-induced increases in $[Ca^{2+}]_i$ (e.g. Koch & Barish, 1994; Verdru *et al.* 1997). This mechanism may thereby contribute to the rise in $[Na^+]_i$ seen after anoxia under conditions where the Na^+,K^+-ATPase is blocked. Conversely, the present experimental conditions (in which $[Na^+]_i$ after anoxia was maintained at a relatively high level) could favor reverse-mode operation of the exchange mechanism and, thus, Na^+ efflux (e.g. Czyż *et al.* 2002; also see Blaustein & Lederer, 1999). Applied immediately after anoxia under conditions where Na^+,K^+-ATPase activity was inhibited (0 $[K^+]_o$), 50 μM bepridil significantly reduced the magnitude of the increase in $[Na^+]_i$, suggesting that forward-mode Na^+/Ca^{2+} exchange contributes to Na^+ influx immediately after anoxia (Table 7.2; Fig 7.5). In contrast, KB-R7943 (1 μM) enhanced the magnitude of the increase in $[Na^+]_i$ observed after anoxia, suggesting that reverse-mode Na^+/Ca^{2+} exchange may contribute to Na^+ efflux at this time (Table 7.2; Fig 7.5). The removal of external Ca^{2+} immediately after anoxia under $[K^+]_o$-free conditions, which would also inhibit reverse-mode Na^+/Ca^{2+} exchange, appeared to similarly enhance Na^+ influx at this time, although this effect did not reach statistical significance ($n = 4$; $P = 0.35$). In contrast, when applied at 10 μM (to inhibit both forward- and reverse-mode Na^+/Ca^{2+} exchange), KB-R7943 reduced the increase in $[Na^+]_i$ observed after anoxia compared to those observed in age-matched sister cultures under control conditions (Table 7.2; Fig. 7.5). Together, these results are consistent with those of White & Reynolds (1995), who reported considerable variability in the contribution of forward-mode Na^+/Ca^{2+} exchange to the recovery of $[Ca^{2+}]_i$ following glutamate stimulation in cultured rat forebrain neurons (also see Sidky & Baimbridge, 1997; Verdru *et al.* 1997), and those of Yu & Choi (1997), who found that Na^+/Ca^{2+} exchangers

in neocortical neurons can operate concurrently in forward and reverse directions. These issues are considered further in the Discussion.

7.2.2.3. Role of non-selective cation channels

As detailed above, 30 μM Gd^{3+} significantly reduced the increase in $[Na^+]_i$ observed during anoxia via a mechanism that appeared dependent on the production of ROS. Because ROS production is enhanced upon reoxygenation (see Lipton, 1999), Gd^{3+} was applied immediately after anoxia under K^+_o-free conditions. As illustrated in Fig. 7.6, 30 μM Gd^{3+} significantly reduced the magnitude of the increase in $[Na^+]_i$ seen after anoxia in neurons 6 - 10 DIV. Similar effects were observed in neurons maintained in culture 11 - 14 DIV (Normalized $\Delta[Na^+]_{i(after)}$ = 0.73 ± 0.11; $n = 5$; $P < 0.05$). Analogous to findings made during anoxia (see above), the effect of Gd^{3+} to reduce the magnitude of the increase in $[Na^+]_i$ observed after anoxia was not affected by perfusion with 100 mM mannitol but was occluded by pretreatment with 1 mM trolox (Fig. 7.6*B*). Although 500 μM L-NAME was without effect, in contrast to observations made during anoxia, 15 - 30 μM $AACOCF_3$ significantly reduced the magnitude of the increase in $[Na^+]_i$ observed after anoxia (Fig. 7.6*B*), suggesting that ROS derived via the PLA_2/arachidonic acid pathway may play a role in regulating Na^+ influx in the immediate post-anoxic period, possibly by influencing the activity of a Gd^{3+}-sensitive NSCC.

7.3. DISCUSSION

In isolated rat hippocampal neurons, $[Na^+]_i$ increases during 5 min anoxia and, shortly following the return to normoxia, recovers to resting values. As detailed in Chapters 5 and 6, the increase in $[Na^+]_i$ observed during anoxia reflects both reduced efflux, consequent upon an inhibition of

Na^+,K^+-ATPase activity, and ongoing/increased entry of Na^+ ions. Similarly, the change in $[Na^+]_i$ observed in the period immediately following anoxia reflects a balance between re-established Na^+,K^+-ATPase activity and continued Na^+ influx. Although Na^+/H^+ exchange activity (and, possibly, the activities of HCO_3^--dependent pH_i regulating mechanisms) contributes to Na^+ influx immediately following anoxia, it cannot account for all Na^+ entry at this time and, in addition, does not appear to contribute to Na^+ influx during anoxia. In the present Chapter, I considered other mechanisms that might potentially account for Na^+ entry occurring during and/or immediately after anoxia. Given that there is no *a priori* reason that the mechanism(s) contributing to Na^+ entry during and following anoxia are the same, the study provided novel insights into the similarities and differences of $[Na^+]_i$ regulation between these two vulnerable periods (see Lipton, 1999 and Silver & Erecińska, 1990 and 1992, for similar comments concerning the regulation of $[Ca^{2+}]_i$ during and following transient ischemia *in vivo*). Moreover, during the course of these studies, it was also found that the increases in $[Na^+]_i$ observed during and following anoxia were related to the duration of time neurons were maintained in culture (within the examined range 6 - 14 DIV).

7.3.1. The role of ionotropic glutamate receptor-operated channels

Although the application of glutamate receptor agonists under normoxic conditions evoked increases in $[Na^+]_i$ (see Fig. 7.1; also see Rose, 2002; also see Lasser-Ross & Ross, 1992; Knöpfel *et al.* 2000), the increases in $[Na^+]_i$ observed during or following (Na^+,K^+-ATPase blocked) anoxia under the constant perfusion conditions of the present experiments were not dependent on the activation of ionotropic glutamate receptor-operated channels. Glutamate-dependent increases in $[Na^+]_i$ have been observed during oxygen-glucose deprivation (e.g. Müller & Somjen, 2000a; LoPachin *et al.* 2001); however, this is not a consistent finding. For example,

Guatteo *et al.* (1998) and Pisani *et al.* (1998a) observed that a combination of ionotropic and metabotropic glutamate receptor antagonists failed to limit the increases in $[Na^+]_i$ observed during periods of hypoxia in midbrain neurons and periods of oxygen-glucose deprivation in cortical neurons, respectively. In a similar manner, in a study employing isolated cerebellar granule cells, Chen *et al.* (1999) reported that ionotropic glutamate receptor-operated channels do not contribute to the increases in $[Ca^{2+}]_i$ observed during periods of metabolic inhibition. Thus, the present experimental conditions have allowed me to characterize those components of the $[Na^+]_i$ response to anoxia that are independent of glutamate receptor-operated channels and are intrinsic to the neuron itself.

7.3.2. <u>The role of voltage-activated Na^+ channels</u>

TTX-sensitive Na^+ channels did not contribute significantly to the increase in $[Na^+]_i$ observed during anoxia (*cf* prolonged hypoxia; Banasiak *et al.* 2004); TTX and lidocaine also failed to attenuate Na^+ influx in the immediate post-anoxic period. Other studies, employing isolated neuronal and brain slice preparations, have also suggested voltage-activated Na^+ channels are only minor contributors to anoxia-evoked increases in Na^+ (e.g. Pisani *et al.* 1998a; Chen *et al.* 1999; Müller & Somjen, 2000b; but see Fung *et al.* 1999; Raley-Susman *et al.* 2001). Indeed, it has been reported that anoxia inhibits whole-cell Na^+ currents in isolated hippocampal and neocortical neurons (Cummins *et al.* 1993; O'Reilly *et al.* 1997; Mironov & Richter, 1999; but see Hammarström & Gage, 2000 for data illustrating an hypoxia-induced activation of TTX-sensitive persistant sodium currents in hippocampal neurons). In light of the relatively small membrane depolarization observed during anoxia in the present studies, I may be underestimating the contribution of voltage-activated Na^+ channels to the anoxia-evoked increases in $[Na^+]_i$; however, even in studies in which more profound hypoxia- or ischemia-

induced membrane depolarizations were observed, TTX similarly had only minor influences on the extent of membrane depolarization (Calabresi *et al.* 1999b) and magnitude of Na^+ entry (Müller & Somjen, 2000b). As a result, our findings support suggestions that the neuroprotective actions of Na^+ channel blockers may be mediated at a presynaptic locus (e.g. Taylor *et al.* 1995; Gleitz *et al.* 1996; Strijbos *et al.* 1996; Probert *et al.* 1997; Kimura *et al.* 1998; Raley-Susman *et al.* 2001).

These present results do not, however, rule out potential contribution(s) from TTX- and/or lidocaine-insensitive voltage-activated mechanisms to the production of the increases in $[Na^+]_i$ observed during or following anoxia. Indeed, in preliminary experiments in SBFI-loaded hippocampal neurons voltage-clamped at -60 mV, 5 min anoxia evoked smaller increases in $[Na^+]_i$ than those recorded simultaneously from unpatched SBFI-loaded neurons present on the same coverslip (data obtained from neurons 13 DIV; C. Sheldon and T. Kelly, unpublished observations). The mechanism(s) underlying this apparent reduction remain to be determined.

7.3.3. The role of Na^+/Ca^{2+} exchange

I found no evidence to suggest that Na^+/Ca^{2+} exchange (forward- or reverse-mode) contributes to the changes in $[Na^+]_i$ observed during anoxia in rat hippocampal neurons. In a similar manner, the removal of $Ca^{2+}{}_o$ did not influence the increase in $[Na^+]_i$ observed during metabolic inhibition in rat cerebellar granule cells (Chen *et al.* 1999) and bepridil failed to influence the increase in $[Na^+]_i$ observed during periods of oxygen-glucose deprivation in rat cortical neurons (Pisani *et al.* 1998a). These findings may reflect the inhibitory effects of reductions in pH_i and/or internal ATP levels on Na^+/Ca^{2+} exchange activity (see Blaustein & Lederer, 1999).

Driven by the increase in $[Na^+]_i$ and membrane depolarization that occur during anoxia, reverse-mode Na^+/Ca^{2+} exchange activity may contribute to Na^+ efflux (and Ca^{2+} entry) in the

immediate post-anoxic period. Assuming a 3:1 stoichiometry, the reversal potential of Na^+/Ca^{2+} exchange (E_{NCX}) immediately upon the return to normoxia can be estimated by

$$E_{NCX} = 3\,E_{Na^+} - 2\,E_{Ca^{2+}} \qquad \textit{(Equation 7.1)}$$

where E_{Na^+} and $E_{Ca^{2+}}$ are the equilibrium potentials for Na^+ and Ca^{2+} and values of E_{NCX} more negative than membrane potential indicate reverse-mode Na^+/Ca^{2+} exchange (i.e. Na^+ efflux; Blaustein & Lederer, 1999). Employing $[Na^+]_i$ measurements made in this thesis (see Fig. 7.2*C*) and $[Ca^{2+}]_i$ measurements made in the same cultured postnatal rat hippocampal neurons under identical conditions (e.g. Diarra *et al.* 1999), $[Na^+]_i$ and $[Ca^{2+}]_i$ values at the end of 5 min anoxia were estimated as ~30 mM and ~500 nM, respectively. Using these values, E_{NCX} immediately upon the return to normoxia under the present experimental conditions was calculated as ~-90 mV (also see Yu & Choi, 1997; Blaustein & Lederer, 1999; Czyż *et al.* 2002), a value significantly more negative than that pertaining prior to anoxia (E_{NCX} was ~-50 mV assuming 10 mM $[Na^+]_i$, 80 nm $[Ca^{2+}]_i$, 148 mM $[Na^+]_o$ and 2 mM $[Ca^{2+}]_o$) and more negative than measurements of membrane potential made under the present experimental conditions at the end of 5 min anoxia (~-40 mV; see Section 7.2.1.2). These calculations suggest that Na^+/Ca^{2+} exchange is likely functioning in reverse-mode to extrude Na^+ ions immediately after anoxia. Consistent with this possibility, KB-R7943 (1 μM) enhanced the magnitude of the increase in $[Na^+]_i$ observed after anoxia (Na^+,K^+-ATPase inhibited). In hippocampal slices, KB-R7943 at higher concentrations (10 μM) non-selectively inhibits both forward- and reverse-mode Na^+/Ca^{2+} exchange (Breder *et al.* 2000; see also Iwamoto *et al.* 1996). In the present study, KB-R7943 (10 μM) no longer increased but, rather, significantly reduced the increase in $[Na^+]_i$ observed after anoxia and this inhibitory effect was similar to that evoked by the forward-mode Na^+/Ca^{2+}

exchange inhibitor, bepridil (50 μM). A previous study (Yu & Choi, 1997) illustrated that forward- and reverse-mode Na^+/Ca^{2+} exchange can operate concurrently in cortical neurons; in the same study, it was found that glutamate exposure, despite causing a negative-shift in E_{NCX} (which would promote reverse-mode Na^+/Ca^{2+} exchange) preferentially enhanced forward-mode Na^+/Ca^{2+} exchange. Similarly, the results of the present study suggest that while reverse-mode Na^+/Ca^{2+} exchange may be acting to extrude Na^+ ions immediately after anoxia, forward-mode Na^+/Ca^{2+} exchange may also be active at this time and contribute to concurrent Na^+ influx. Nevertheless, it should be noted that bepridil (30 - 50 μM) has also been reported to inhibit reverse-mode Na^+/Ca^{2+} exchange and, in this way, augments ischemia-induced depolarizations in striatal neurons (Calabresi *et al.* 1999a) and reduces anoxia-induced Ca^{2+} influx in rat optic nerve preparations (Brown *et al.* 2001).

The role of Na^+/Ca^{2+} exchanger-mediated increases and decreases in $[Na^+]_i$ (mediated by forward- and reverse-mode Na^+/Ca^{2+} exchange, respectively) to the pathogenesis of ischemic cell death is unclear. Arguing against their importance are the observations that inhibition of forward-mode Na^+/Ca^{2+} exchange (which would limit Na^+ entry) typically aggravates neuronal death while inhibition of reverse-mode Na^+/Ca^{2+} exchange (which would increase $[Na^+]_i$) typically limits neuronal death, in response to ischemia/reperfusion or hypoxia/hypoglycemia (e.g. Schröder *et al.* 1999; Breder *et al.* 2000; Matsuda *et al.* 2001; see also Hoyt *et al.* 1998 in which 10 μM KB-R7943 failed to have any effect on the viability of cultured cortical neurons following glutamate excitotoxicity). On the other hand, Calabresi and colleagues (1999a) have suggested that, in striatal neurons, reverse-mode Na^+/Ca^{2+} exchange may play a protective role by reducing internal Na^+ accumulation and promoting membrane repolarization following transient periods of oxygen-glucose deprivation.

In summary, in light of the relatively non-selective nature of the pharmacological agents available to assess forward- and reverse-mode Na^+/Ca^{2+} exchange activity and the fact that the direction of Na^+/Ca^{2+} exchange will be not only influenced by $[Na^+]_i$ and $[Ca^{2+}]_i$ but also membrane potential values attained during and following anoxia, the contribution of Na^+/Ca^{2+} exchange to the regulation of $[Na^+]_i$ (and $[Ca^{2+}]_i$) in rat hippocampal neurons during and immediately after anoxia under the present experimental conditions is difficult to determine precisely. Further investigation into anoxia-evoked changes in Na^+/Ca^{2+} exchange activity and the effects of these changes to anoxia-evoked changes in $[Na^+]_i$ and $[Ca^{2+}]_i$ will necessitate simultaneous measurements of not only $[Na^+]_i$ and $[Ca^{2+}]_i$ but also membrane potential (e.g. Ginsburg *et al.* 2002 in cardiac myocytes). Notably, the results of the present experiments do not exclude the possibility that, as in cardiac myocytes, Na^+/H^+ exchanger-induced increases in $[Na^+]_i$ in rat hippocampal neurons in the post-anoxic period might contribute to the reversal of Na^+/Ca^{2+} exchange activity at this time (see Chapters 5 and 6).

7.3.4. The role of $Na^+/K^+/2Cl^-$ cotransport

In the present study, the $Na^+/K^+/2Cl^-$ cotransport inhibitor, bumetanide, failed to affect resting $[Na^+]_i$ suggesting that, in agreement with Rose & Ransom (1997), $Na^+/K^+/2Cl^-$ cotransport does not mediate Na^+ entry in rat hippocampal neurons under resting conditions. In contrast, bumetanide reduced the rise in $[Na^+]_i$ observed during anoxia in 11 - 14, but not 6 - 10, neurons suggesting that $Na^+/K^+/2Cl^-$ cotransport contributes to Na^+ influx during anoxia in neurons expected to express significant levels of functional transporters (i.e. neurons maintained in culture for at least 11 DIV; Sun & Murali, 1999). In a similar manner, $Na^+/K^+/2Cl^-$ cotransport also contributes to the accumulation of internal Na^+ ions in cortical astrocytes in response to periods of oxygen-glucose deprivation (Lenart *et al.* 2003), though not in cerebellar granule neurons during metabolic inhibition (Chen *et al.* 1999). These results, however, contrast with the rapid

inactivation of $Na^+/K^+/2Cl^-$ cotransport reported in neocortical slices upon the initiation of oxygen-glucose deprivation (Yamada *et al.* 2001). Interestingly, $Na^+/K^+/2Cl^-$ cotransport contributes of Na^+ entry during ischemia in cardiac myocytes; immediately upon reperfusion, $Na^+/K^+/2Cl^-$ cotransport mediates Na^+ efflux in this cell type (Anderson *et al.* 1996), a finding that may account for the ability of bumetanide to enhance (albeit not significantly) the rise in $[Na^+]_i$ observed in the post-anoxic period in 11 - 14, but not 6 - 10, DIV neuronal cultures.

Previous studies have reported that bumetanide limits neuronal death observed in response to periods of oxygen-glucose deprivation *in vitro* (Beck *et al.* 2003) and reduces infarct size *in vivo* when applied during, but not following, ischemic episodes (Yan *et al.* 2001 and 2003). The present study suggests that these neuroprotective actions may reflect, in part, a reduction in Na^+ influx during these insults.

7.3.5. <u>The role of a Gd^{3+}-sensitive mechanism</u>

Gd^{3+}, a non-selective blocker of NSCCs, attenuated the increases in $[Na^+]_i$ observed during *and* following anoxia. From the other results presented in this study, the inhibitory effects of Gd^{3+} on the anoxia-evoked changes in $[Na^+]_i$ are unlikely to reflect the ability of Gd^{3+} to inhibit AMPA/kainate receptors or voltage-activated Ca^{2+} channels (Boland *et al.* 1991; Elinder & Århem, 1994; Huettner *et al.* 1998; Lei & MacDonald, 2001). Moreover, hyperosmolar conditions failed to reduce anoxia-evoked increases in $[Na^+]_i$ and did not occlude the effect of Gd^{3+} to limit the increases in $[Na^+]_i$ during and following anoxia, suggesting that mechanogated NSCCs are not major contributors to the increases in $[Na^+]_i$ seen under the present experimental conditions. In contrast, pretreatment of neuronal cultures with trolox occluded the effect of Gd^{3+} to limit anoxia-evoked increases in $[Na^+]_i$, suggesting that the inhibitory effects of Gd^{3+} on Na^+ influx during and following anoxia may be dependent on the production of reactive oxygen

species. Although Gd^{3+} reduces the increase in $[Ca^{2+}]_i$ observed during 5 min anoxia in 7 - 9 DIV cultured postnatal rat hippocampal neurons under conditions identical to those used in the present experiments (n = 7; A. Diarra & J. Church, unpublished observations), the pathway involved in the production of ROS in the present experiments appears to differ from that involved in the activation of the recently described Gd^{3+}-sensitive NSCC that contributes to Ca^{2+} influx during prolonged (>30 min) oxygen-glucose deprivation in cultured mouse cortical neurons (Aarts *et al.* 2003) in that it does not appear to depend on free radical production via the NOS/nitric oxide pathway. Although further investigation is required to identify the free radical species interacting with the Gd^{3+}-sensitive Na^+ influx pathway described in the present study, PLA_2 may be involved in the immediate post-anoxic period. PLA_2 activity, acting through a cascade of events that may involve the production of reactive oxygen species, has been shown to activate NSCCs in response to periods of metabolic inhibition in cerebellar granule cells (Chen *et al.* 1999). Interestingly, PLA_2 activity is enhanced with an increase in pH_i (such as that which occurs upon the return to normoxia; e.g. Harrison *et al.* 1991; Stella *et al.* 1995; Phillis & O'Regan, 2004) and is increased in the hippocampus immediately following oxygen-glucose deprivation (Arai *et al.* 2001), where it has been shown to maintain post-ischemic membrane depolarization (Tanaka *et al.* 2003) and contribute to neuronal death (Arai *et al.* 2001).

The results of the present study suggest that the established effects of Gd^{3+} to reduce neuronal death following periods of oxygen-glucose deprivation *in vitro* (Aarts *et al.* 2003) and to reduce brain edema following traumatic brain injury *in vivo* (Vaz *et al.* 1998) may reflect the ability of Gd^{3+} to limit not only Ca^{2+} but also Na^+ influx both during and immediately after these insults.

7.3.6. Age-dependence of the increases in $[Na^+]_i$ observed during and following anoxia

The results presented in Chapter 5 illustrated that the increases in $[Na^+]_i$ observed during and after anoxia displayed a clear dependence on length of time hippocampal neurons were maintained in culture. The larger magnitudes of the increases in $[Na^+]_i$ observed during and following anoxia in more phenotypically mature neuronal cultures may contribute to the enhanced vulnerability of these neurons to transient anoxic insults, an observation which has previously been ascribed to differences in $[Ca^{2+}]_i$ entry and/or the activities of 'Ca^{2+}-dependent lethal processes' (e.g. Rothman, 1983; Di Lorteo & Balestrino, 1997; Sattler *et al.* 1998; Keelan *et al.* 1999).

In both 6 - 10 and 11 - 14 DIV neurons, creatine incubation limited the increase in $[Na^+]_i$ during anoxia. In addition, a Gd^{3+}-sensitive pathway and $Na^+/K^+/2Cl^-$ cotransport contributed to the increase in 6 - 10 and 11- 14 DIV neurons, respectively. That $Na^+/K^+/2Cl^-$ cotransport fails to contribute to the increase in $[Na^+]_i$ observed during anoxia in 6 - 10 DIV neurons is consistent with the reported *in vivo* and *in vitro* developmental regulation of $Na^+/K^+/2Cl^-$ cotransport activity (Plotkin *et al.* 1997; Sun & Murali, 1999). Immediately after anoxia, continued Na^+ influx was mediated, in part, by Na^+/H^+ exchange activity (Chapters 5 and 6); in addition, a Gd^{3+}-sensitive pathway and Na^+/Ca^{2+} exchange activity were also found to contribute to Na^+ influx at this time. Although the potential contribution of Na^+/Ca^{2+} exchange activity to Na^+ influx after anoxia in 11 - 14 DIV neurons was not examined, given the developmental upregulation of Na^+/Ca^{2+} exchanger expression and activity (Sakaue *et al.* 2000; Gibney *et al.* 2002), anoxia-evoked changes in Na^+/Ca^{2+} exchange activity are likely to play a role in 11 - 14 DIV neurons as well. Indeed, the larger increases in $[Na^+]_i$ observed following anoxia in 11 - 14, compared to 6 - 10, DIV neurons may reflect the developmental regulation of the expression and/or activities of

Na^+/H^+ exchangers (e.g. Bevensee *et al.* 1996; Douglas *et al.* 2001) and/or Na^+/Ca^{2+} exchangers (e.g. Sakaue *et al.* 2000; Gibney *et al.* 2002).

7.3.7. Synthesis of Chapters 5, 6 and 7

Cultured postnatal rat hippocampal neurons respond to 5 min periods of anoxia with an increase in $[Na^+]_i$ of ~15 - 40 mM. The increase in $[Na^+]_i$ observed during anoxia is, in part, dependent on external Na^+ influx through a putative Gd^{3+}-sensitive NSCC in 6 - 10 DIV neurons and $Na^+/K^+/2Cl^-$ cotransport in 11 - 14 DIV neurons. In addition, in both 6 - 10 and 11 - 14 DIV cells, reduced Na^+,K^+-ATPase activity, consequent upon declining internal ATP levels, also contributes to the internal Na^+ accumulation during anoxia. It is of note that the activation of NSCCs and $Na^+/K^+/2Cl^-$ cotransport as well as Na^+,K^+-ATPase inhibition, can initiate and promote cell swelling (e.g. Chen & Simard, 2001; Xiao *et al.* 2002; Beck *et al.* 2003) and, in this way, their contributions to the increase $[Na^+]_i$ during anoxia may mediate, at least in part, the acute neurotoxic effects of anoxia. Upon the return to normoxia, Na^+,K^+-ATPase activity mediates the recovery of $[Na^+]_i$ in the face of continued Na^+ entry. In addition a putative Gd^{3+}-sensitive NSCC, Na^+/Ca^{2+} exchange and Na^+/H^+ exchange also contribute to the increase in $[Na^+]_i$ observed after anoxia.

In summary, the present study represents one of the first detailed descriptions of the changes in $[Na^+]_i$ observed in isolated mammalian central neurons during and after transient periods of anoxia. A number of mechanisms that contribute to the observed anoxia-evoked changes in $[Na^+]_i$ have also been identified and, as a result, these mechanisms may be important in regulation of anoxic/ischemic cell death.

Table 7.1: Potential mechanisms contributing to the increase in $[Na^+]_i$ observed during anoxia

	Normalized $\Delta[Na^+]_{i(during)}$	
Treatment	6 – 10 DIV	11 – 14 DIV
2 μM MK-801	1.14 ± 0.14 (8)	0.98 ± 0.12 (4)
20 μM CNQX	1.01 ± 0.03 (5)	1.17 ± 0.31 (3)
2 μM MK-801 + 20 μM CNQX	0.98 ± 0.18 (4)	0.96 ± 0.26 (7)
1 μM TTX	1.04 ± 0.11 (4)	0.91 ± 0.17 (5)
50 μM bepridil	0.94 ± 0.17 (7)	n.d.
1 μM KB-R7943	1.05 ± 0.28 (5)	n.d.
10 μM KB-R7943	1.02 ± 0.17 (6)	n.d.
25 μM CGP-37157	1.02 ± 0.28 (4)	n.d.
0 Ca^{2+}_o	0.92 ± 0.16 (5)	1.04 ± 0.20 (4)
50 - 100 μM bumetanide	1.12 ± 0.19 (5)	0.61 ± 0.05 (9)*

To generate Normalized $\Delta[Na^+]_{i(during)}$ values, measurements of $\Delta[Na^+]_{i(during)}$ under a given experimental test condition were normalized to $[Na^+]_i$ measurements made in age-matched sister cultures under control conditions. Statistical comparisons were performed by comparing absolute $\Delta[Na^+]_{i(during)}$ values (i.e. not normalized) made under a given experimental test condition to measurements made in age-matched sister cultures under control conditions. * indicates statistical significance ($P < 0.05$) compared to measurements made in age-matched sister neurons in the absence of treatment. Numbers in brackets denote number of neuronal populations (i.e. coverslips) from which the data were obtained. DIV, days *in vitro*; n.d., not determined.

Table 7.2: Potential mechanisms contributing to the increase in $[Na^+]_i$ observed after anoxia under 0 $[K^+]_o$ conditions

Treatment	Normalized $\Delta[Na^+]_{i(after)}$ 6 – 10 DIV	11 – 14 DIV
2 μM MK-801 + 20 μM CNQX	1.25 ± 0.13 (3)	1.06 ± 0.25 (2)
1 μM TTX	0.98 ± 0.20 (5)	0.92 ± 0.02 (2)
250 μM lidocaine	n.d.	0.89 ± 0.29 (3)
100 μM bumetanide[1]	0.91 ± 0.27 (3)	1.21 ± 0.25 (4)
50 μM bepridil	0.43 ± 0.12 (6)*	n.d.
1 μM KB-R7943	1.56 ± 0.25 (3)*	n.d.
10 μM KB-R7943	0.67 ± 0.09 (5)*	n.d.

To generate Normalized $\Delta[Na^+]_{i(after)}$ values, measurements of $\Delta[Na^+]_{i(after)}$ under a given experimental test condition were normalized to $[Na^+]_i$ measurements made in age-matched sister cultures under control conditions. Statistical comparisons were performed by comparing absolute $\Delta[Na^+]_{i(after)}$ values (i.e. not normalized) made under a given experimental test condition to measurements made in age-matched sister cultures under control conditions. * indicates statistical significance ($P < 0.05$) compared to measurements made in sister age-matched neurons in the absence of treatment. Numbers in brackets denote the number of neuronal populations (i.e. coverslips) from which data were obtained. [1]Experiments examining the effect of bumetanide on the increase in $[Na^+]_i$ observed following anoxia were performed using 500 μM ouabain rather than $[K^+]$-free medium to inhibit Na^+/K^+-ATPase activity following anoxia. DIV, days *in vitro*; n.d., not determined.

Fig. 7.1. Ionotropic glutamate receptor-operated channels do not contribute to the increase in $[Na^+]_i$ observed during anoxia under the present experimental conditions. *A*, the rise in $[Na^+]_i$ evoked by anoxia under control conditions (filled circles) was not significantly affected by the presence of 2 μM MK-801 and 20 μM CNQX (open circles). *Inset*, in a different neuronal culture, MK-801 (2 μM) and CNQX (20 μM) abolished the increase in $[Na^+]_i$ evoked by 30 s applications of 20 μM NMDA and 20 μM AMPA in the presence of 2 μM glycine (denoted by short bars above the record); the record is representative of results obtained in 2 neuronal cultures 6 or 9 DIV and the same result was obtained in 4 neuronal cultures 12 - 13 DIV (not shown).

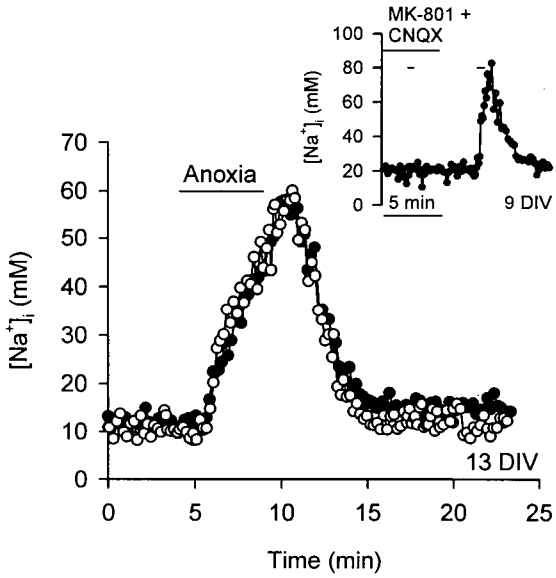
MK-801 +
CNQX
100
80
60
40
20
0
[Na+]i (mM)
5 min
9 DIV
Anoxia
70
60
50
40
30
20
10
0
[Na+]i (mM)
13 DIV
0
5
10
15
20
25
Time (min)

Fig. 7.2. Role of voltage-activated Na^+ channels, Na^+/Ca^{2+} exchange and $Na^+/K^+/2Cl^-$ cotransport in the increase in $[Na^+]_i$ observed during anoxia. Shown in *A, B* and *C* are superimposed records of the changes in $[Na^+]_i$ observed in response to 5 min anoxia in the presence (open symbols) and absence (filled circles) of an experimental treatment. *A*, 1 μM TTX had no effect on the increase in $[Na^+]_i$ observed during anoxia. *Inset*, TTX (1 μM) reduced the increase in $[Na^+]_i$ evoked by 60 s applications of 50 mM K^+_o (denoted by the short bars above the record). *B*, compared with observations made in age-matched cultures, 1 μM KB-R7943 (open circles) or 50 μM bepridil (open diamonds) did not influence the increase in $[Na^+]_i$ observed during anoxia. *C*, 100 μM bumetanide reduced the rise in $[Na^+]_i$ observed during anoxia in 14 DIV neuronal cultures. In all cases, pharmacological treatments were present throughout the duration of the records shown.

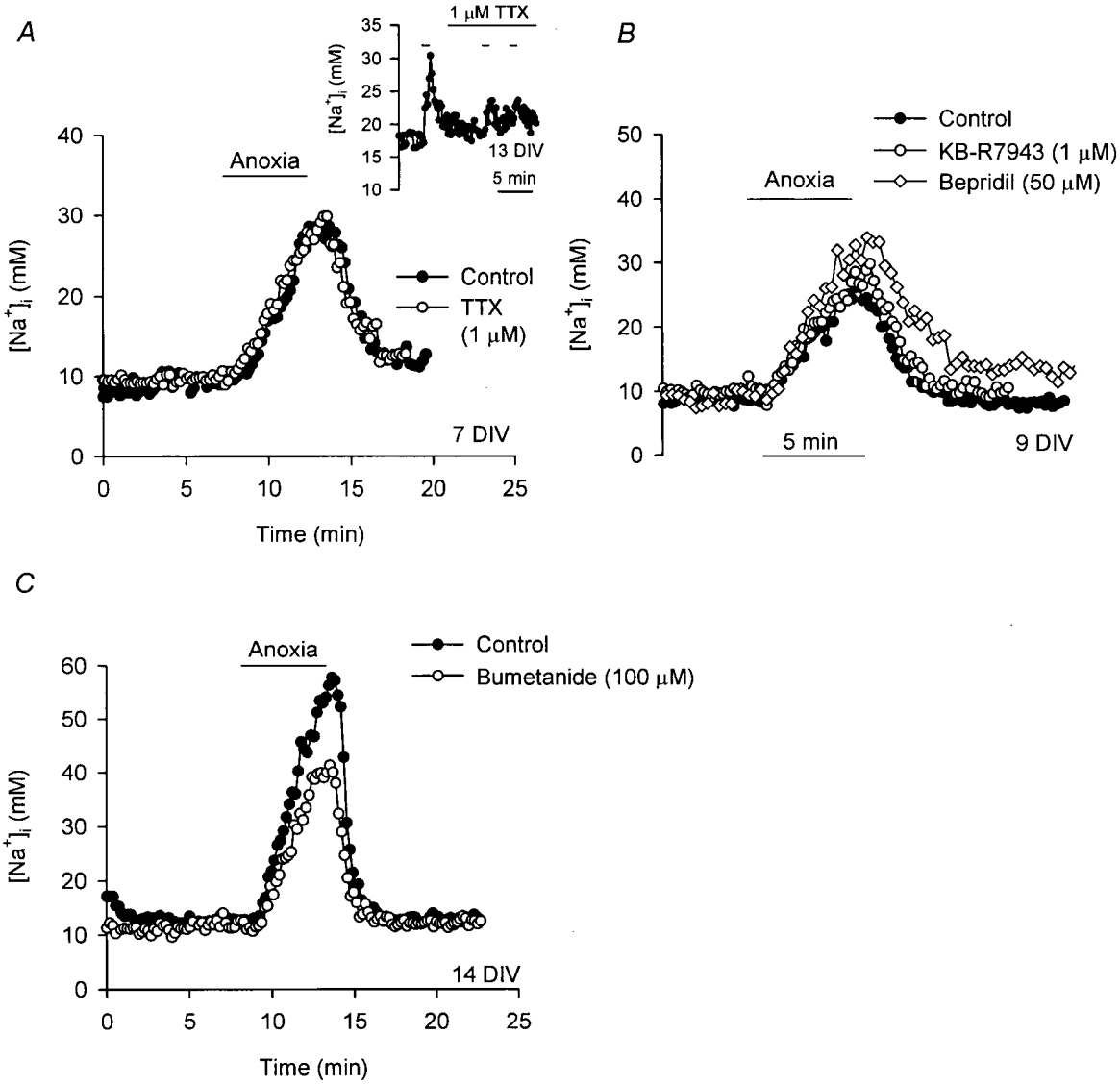
A
Anoxia
1 μM TTX
13 DIV
5 min
Control
TTX
(1 μM)
7 DIV
[Na+]i (mM)
Time (min)
B
Anoxia
Control
KB-R7943 (1 μM)
Bepridil (50 μM)
5 min
9 DIV
[Na+]i (mM)
C
Anoxia
Control
Bumetanide (100 μM)
14 DIV
[Na+]i (mM)
Time (min)

Fig. 7.3. Effect of Gd^{3+} on the increase in $[Na^+]_i$ observed during anoxia. *A*, compared with changes observed in an age-matched sister culture in the absence of Gd^{3+} (filled circles), the magnitude of the increase in $[Na^+]_i$ observed during anoxia was reduced in the presence of 30 μM Gd^{3+} (open circles). *B*, 100 mM mannitol failed to inhibit the increase in $[Na^+]_i$ observed during anoxia. *C*, applied in the presence of 100 mM mannitol, 30 μM Gd^{3+} continued to reduce the increase in $[Na^+]_i$ observed during anoxia (compare with *B*). *D*, summary of the effects of Gd^{3+}, hyperosmolar conditions and inhibitors of voltage-activated Ca^{2+} channels on the increase in $[Na^+]_i$ observed during anoxia. Data were obtained from neuronal cultures 6 - 10 DIV. In the presence or absence of mannitol, Gd^{3+} significantly reduced the increase in $[Na^+]_i$ observed during anoxia. * indicates statistical significance ($P < 0.05$).

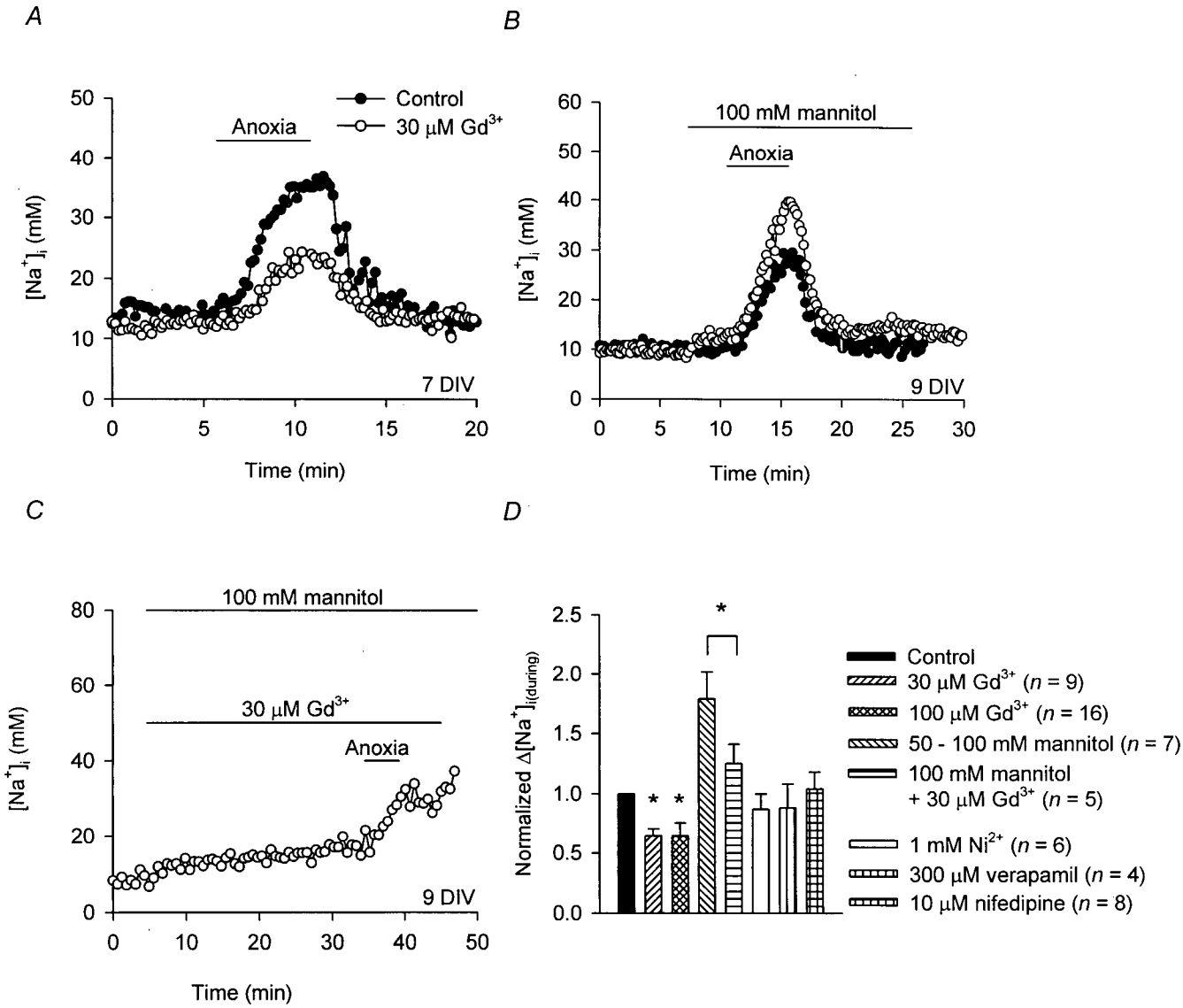
A
Control
30 μM Gd3+
Anoxia
[Na+]i (mM)
7 DIV
Time (min)
B
100 mM mannitol
Anoxia
[Na+]i (mM)
9 DIV
Time (min)
C
100 mM mannitol
30 μM Gd3+
Anoxia
[Na+]i (mM)
9 DIV
Time (min)
D
Normalized Δ[Na+]i(during)
Control
30 μM Gd3+ (n = 9)
100 μM Gd3+ (n = 16)
50 - 100 mM mannitol (n = 7)
100 mM mannitol
+ 30 μM Gd3+ (n = 5)
1 mM Ni2+ (n = 6)
300 μM verapamil (n = 4)
10 μM nifedipine (n = 8)

Fig. 7.4. Role of reactive oxygen species in the increase in $[Na^+]_i$ observed during anoxia. *A*, pretreatment with 1 mM trolox (open circles) reduced the increase in $[Na^+]_i$ observed during anoxia, compared to the increase in $[Na^+]_i$ observed in age-matched sister neurons not treated with trolox (filled circles). Observed in sister neurons also treated with 1 mM trolox, 30 μM Gd^{3+} failed to further attenuate the increase in $[Na^+]_i$ observed during anoxia (open diamonds). All records illustrated in *A* were obtained from sister neuronal cultures. *B*, summary of the effects of antioxidants and inhibitors of free radical production on the increase in $[Na^+]_i$ observed during anoxia in neurons 6 - 10 DIV. Following trolox pretreatment, 30 μM Gd^{3+} failed to exert an additional inhibitory effect on the increase in $[Na^+]_i$ observed during anoxia. $AACOCF_3$ (a PLA_2 inhibitor) failed to significantly influence the increase in $[Na^+]_i$ observed during anoxia. Similarly, although L-NAME (a NOS inhibitor) appeared to reduce the increase in $[Na^+]_i$ observed during anoxia, this effect failed to reach statistical significance ($P = 0.60$, compared to measurements made in age-matched sister neurons). * indicates statistical significance ($P < 0.05$) compared to measurements made in age-matched sister neurons under control conditions. N.S. indicates no statistically significant difference between the increase in $[Na^+]_i$ observed during anoxia in presence and absence of Gd^{3+} in neurons pretreated with trolox ($P = 0.54$).

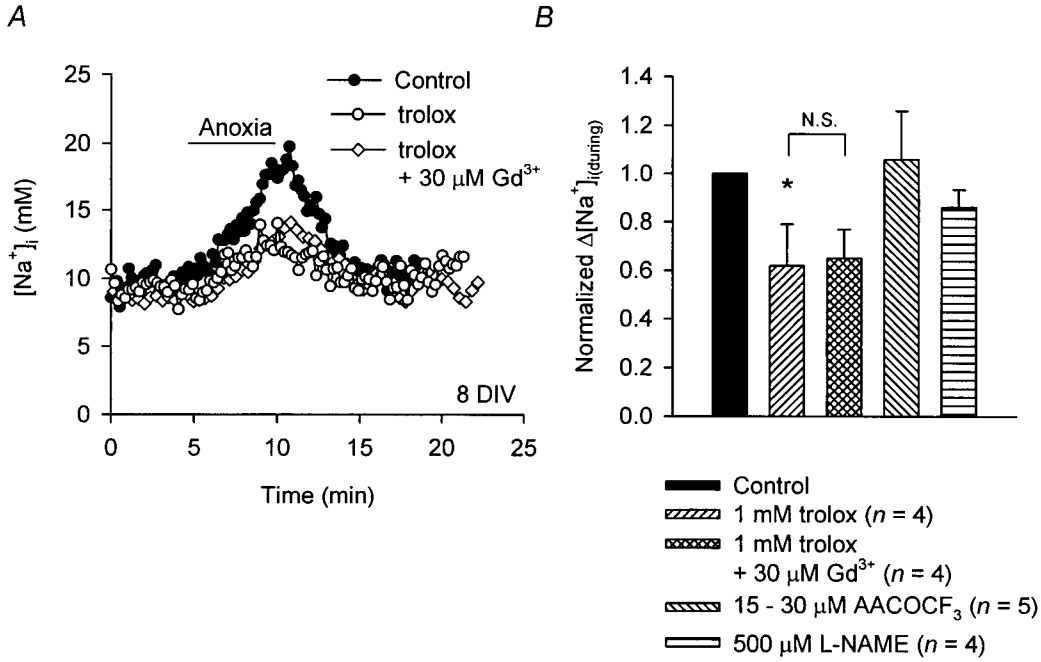
A
B
Control
trolox
trolox
+ 30 μM Gd3+
Anoxia
8 DIV
[Na+]i (mM)
Time (min)
N.S.
*
Normalized Δ[Na+]i(during)
Control
1 mM trolox (n = 4)
1 mM trolox
+ 30 μM Gd3+ (n = 4)
15 - 30 μM AACOCF3 (n = 5)
500 μM L-NAME (n = 4)

Fig. 7.5. Effects of maneuvers which modulate Na^+/Ca^{2+} exchange activity on the increase in $[Na^+]_i$ observed after anoxia (Na^+,K^+-ATPase inhibited). *A*, at the end of 5 min anoxia, neurons were exposed to K^+-free medium for 7 min. Compared with the increase in $[Na^+]_i$ observed under control conditions (filled circles), the increase in $[Na^+]_i$ after anoxia was reduced in the presence of 50 μM bepridil (open diamonds) or 10 μM KB-R7943 (open circles) and was enhanced in the presence of 1 μM KB-R7943 (open squares). Pharmacological treatments began at the end of 5 min anoxia and were continued for the duration of the trace.

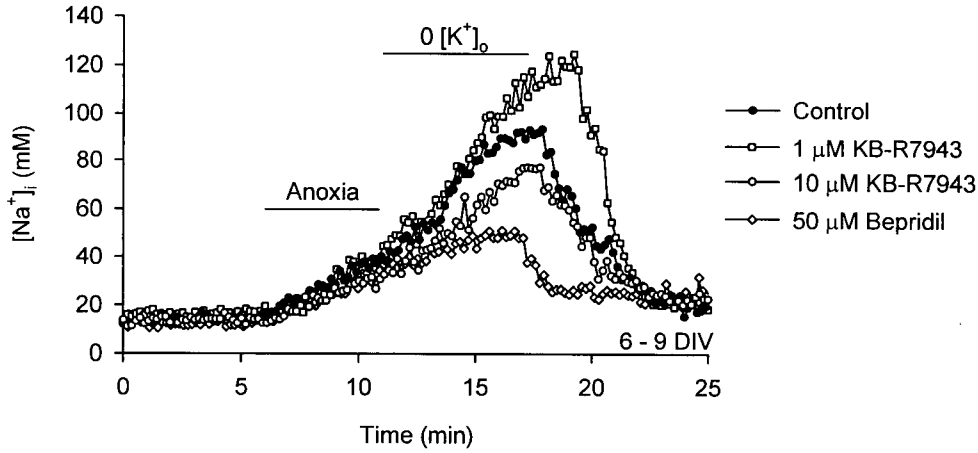
140
120
100
80
60
40
20
0
$[Na^+]_i$ (mM)
0 $[K^+]_o$
Anoxia
6 - 9 DIV
0
5
10
15
20
25
Time (min)
Control
1 μM KB-R7943
10 μM KB-R7943
50 μM Bepridil

Fig. 7.6. Effects of Gd^{3+} on the increase in $[Na^+]_i$ observed after anoxia (Na^+,K^+-ATPase inhibited). *A,* exposure to 30 μM Gd^{3+} immediately following anoxia under K^+_o-free conditions (open circles) reduced the increase in $[Na^+]_i$ observed after anoxia, compared to the change in $[Na^+]_i$ observed in age-matched sister neurons under control conditions (filled circles). *B,* summary of the effects hyperosmolar conditions, antioxidants, inhibitors of free radical production and Gd^{3+} on the magnitude of the increase in $[Na^+]_i$ observed after anoxia (Na^+,K^+-ATPase inhibited). 30 μM Gd^{3+} reduced significantly the increase in $[Na^+]_i$ observed following anoxia. Similar to its effects on the increase in $[Na^+]_i$ observed during anoxia (see Figs. 7.3 and 7.4), the inhibitory effects of Gd^{3+} on the increase in $[Na^+]_i$ observed following anoxia were not altered in the presence of 100 mM mannitol and were occluded by pretreatment with 1 mM trolox. $AACOCF_3$ (15 - 30 μM) caused a significant reduction while L-NAME (500 μM) had no influence on the increase in $[Na^+]_i$ observed following anoxia. * indicates statistical significance ($P < 0.05$) compared to measurements made in age-matched sister cultures under control conditions. N.S. indicates no statistically significant difference between the increase in $[Na^+]_i$ observed following anoxia in presence and absence of Gd^{3+} in neurons pretreated with trolox ($P = 0.67$). Data obtained from neuronal cultures 6 - 10 DIV.

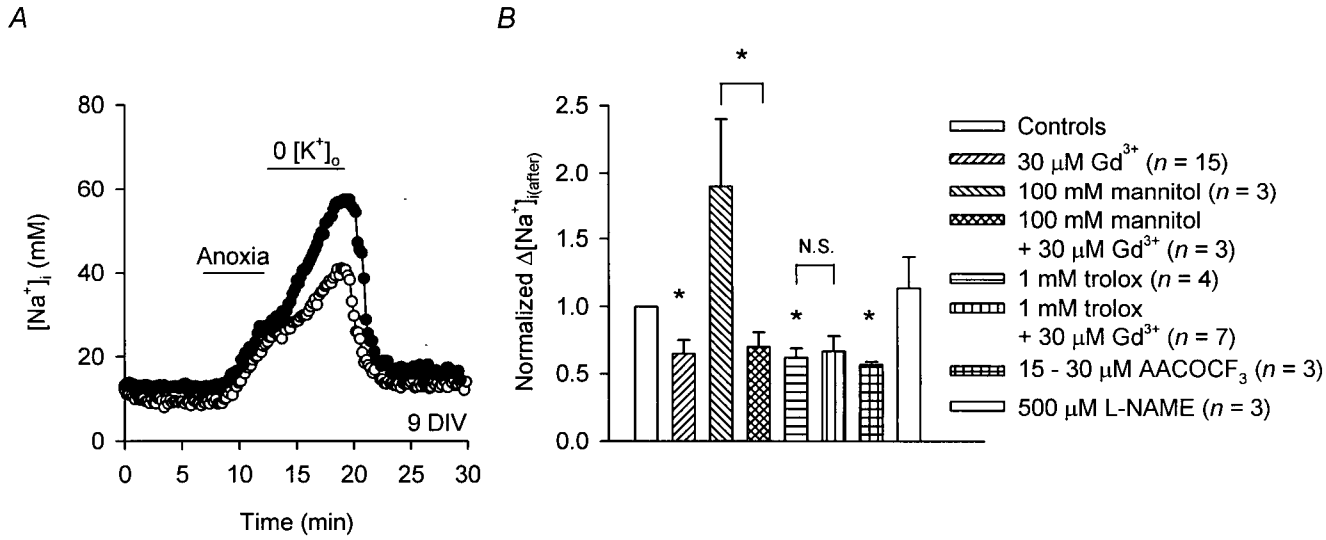
A
B
80
60
40
20
0
$[Na^+]_i$ (mM)
0 $[K^+]_o$
Anoxia
9 DIV
0 5 10 15 20 25 30
Time (min)
2.5
2.0
1.5
1.0
0.5
0.0
Normalized $\Delta[Na^+]_{i(after)}$
*
N.S.
Controls
30 μM Gd^{3+} (n = 15)
100 mM mannitol (n = 3)
100 mM mannitol
+ 30 μM Gd^{3+} (n = 3)
1 mM trolox (n = 4)
1 mM trolox
+ 30 μM Gd^{3+} (n = 7)
15 - 30 μM $AACOCF_3$ (n = 3)
500 μM L-NAME (n = 3)

CHAPTER EIGHT

SUMMARY AND CONCLUSIONS

It is well established that neurons respond to transient periods of anoxia or ischemia with internal shifts in $[Ca^{2+}]$, pH and $[Na^+]$. While the potential contribution of changes in $[Ca^{2+}]_i$ to neuronal injury has received particular attention, the early changes in pH_i and $[Na^+]_i$ that occur in response to anoxia or ischemia are also thought to participate in the pathophysiology of anoxic and ischemic neuronal death; however, the mechanisms contributing to these changes in pH_i and $[Na^+]_i$ have remained relatively ill-defined. Previous studies have documented the effects of anoxia and ischemia on pH_i and $[Na^+]_i$ in neurons *in vivo* and in slice preparations *in vitro* (e.g. Whittingham *et al.* 1984; Silver & Erecińska, 1990; Pisani *et al.* 1998a; Erecińska & Silver, 2001). The present study complements these earlier findings and represents one of the first detailed descriptions of the effects of anoxia on pH_i and $[Na^+]_i$ in mammalian central neurons under conditions in which the changes observed can be attributed to mechanisms intrinsic to the neurons under study.

8.1. Experimental protocols and preparations

As illustrated in Chapter 1 (Fig. 1.1), in response to periods of anoxia or ischemia, multiple pathways contribute to the development of subsequent neuronal dysfunction and death. In light of the facts that the immediate effects of ischemia (i.e. the cessation of energy production) are similar to those of anoxia (Somjen, 2004; also see Silver *et al.* 1997) and that marked oxygen deprivation is the fundamental common denominator amongst diverse conditions that can result in anoxic/ischemic damage (such as cardiac arrest, respiratory obstruction, cerebral trauma and stroke; Hansen, 1985), the present study has examined the neuronal response to transient periods

of anoxia. Moreover, in order to identify those components of the neuronal response to anoxia that are intrinsic to the cell itself, experiments were performed using isolated rat hippocampal neurons under conditions of constant superfusion. These experimental conditions offer a number of advantages. *First*, in studies performed *in vivo* or using brain slice preparations *in vitro*, it is difficult (if not impossible) to distinguish between the contributions of different cell types to volume-averaged measurements of anoxia-evoked changes in intracellular ion concentrations. *Second*, they allowed me to characterize the anoxia-evoked changes in pH_i and $[Na^+]_i$ (and $[Ca^{2+}]_i$) that occur independent of changes in the external microenvironment, such as the changes in pH_o, $[K^+]_o$ and $[glutamate]_o$, that take place *in vivo* and in brain slice preparations *in vitro*. These changes can affect pH_i, $[Na^+]_i$ and the activities of pH_i regulating mechanisms and complicate the characterization of underlying mechanisms contributing to anoxia-evoked changes in pH_i and $[Na^+]_i$. *Third,* they permitted the defined changes in the composition of external environment that are required to rigorously assess, for example, changes in Na^+/H^+ exchange activity in a cell type in which the antiport is insensitive to known selective pharmacological inhibitors. *Fourth,* not only are hippocampal neurons, in particular, vulnerable to the effects of anoxia or ischemia, they have also been the subject of extensive studies of pH_i regulation (Chesler, 2003).

On the other hand, it is evident that the neuronal response to global ischemia *in vivo* cannot be reproduced in its entirety in isolated neurons *in vitro*. For example, following the initiation of global ischemia *in vivo*, internal ATP levels are rapidly depleted to ~ 10% of pre-ischemic values after 2 - 3 min (Lipton, 1999), compared with reductions to 35 - 40% of preischemic values measured in the present study. In addition, measured in CA1 pyramidal neurons *in vivo* after 8 min low-flow global ischemia, Erecińska and Silver (2001) reported decreases in pH_i to 6.21,

increases in $[Na^+]_i$ and $[Ca^{2+}]_i$ to 72 mM and 30 μM, respectively, and membrane depolarizations to -17 mV. These changes are more pronounced than those observed in the cultured postnatal rat hippocampal neurons employed in the majority of the present studies. Possible exceptions include the sometimes ~40 mM increase in $[Na^+]_i$ observed at the end of 5 min anoxia in 11 - 14 DIV neurons, which approximated the 47 mM increase in $[Na^+]_i$ reported by Erecińska and Silver (2001), and the dramatic and persistant increase in $[Ca^{2+}]_i$ observed during anoxia in acutely isolated adult rat hippocampal CA1 pyramidal neurons (see Fig. 3.3), which likely reflects a marked depolarization in these cells (see Tanaka *et al.* 1997; Pisani *et al.* 1998b). Rather, the changes in the parameters measured during anoxia in the isolated neurons employed in the present studies appeared similar in many respects to those observed during focal ischemia *in vivo*, particularly those within the penumbral region. In contrast to neurons within the ischemic core, neurons within the penumbra exhibit smaller reductions in internal ATP and pH_i, less pronounced increases in $[Na^+]_i$ and $[Ca^{2+}]_i$ and are less likely to undergo 'anoxic depolarization' (Choi, 1990; Lipton, 1999). Nevertheless, it is important to note that the experimental protocols employed in the present study are associated with neuronal injury and death. Thus, in complementary series of experiments employing cultured postnatal rat hippocampal neurons, 5 min anoxia imposed under conditions identical to those used here reduced neuronal viability by ~40% at 4 h and ~70% at 24 h (Fernandes, 2001).

From studies performed early in the course of this thesis, it became clear that the changes in pH_i and $[Na^+]_i$ which occurred during anoxia differed from those taking place upon the return to normoxia (as did the mechanisms underlying the observed changes during *vs.* after transient periods of anoxia). That very few studies have examined the events that take place in neurons in the immediate post-anoxic period is surprising considering that reoxygenation does not always restore, and may actually worsen, intracellular ion homeostasis and that the ionic changes which

occur during early reoxygenation may be important determinants of subsequent neuronal dysfunction and death (Lipton, 1999; Taylor *et al.* 1999). For example, the extent of neuronal survival observed following transient periods of metabolic inhibition can be improved, not by lowering pH_o during the period of metabolic inhibition itself, but by maintaining an extracellular acidosis upon recovery (Vornov *et al.* 1996).

8.2. Changes in pH_i and $[Na^+]_i$ during *and* after anoxia

The first principal aim of the present studies was to characterize the changes in pH_i and $[Na^+]_i$ that occur in isolated rat hippocampal neurons during and following 5 min anoxia. The typical steady-state pH_i response to anoxia in acutely isolated adult rat hippocampal CA1 pyramidal neurons consisted of an initial fall in pH_i upon the induction of anoxia, a subsequent rise in pH_i in the continued absence of O_2, and a further internal alkalinization upon the return to normoxia. Although relatively few studies have examined the response of acutely isolated neurons to anoxia or ischemia, a similar sequence of pH_i changes has been observed in hippocampal slice preparations *in vitro* (e.g. Mabe *et al.* 1983; Pirttilä & Kauppinen, 1992; Melzian *et al.* 1996). In ~25% of neurons examined, and almost exclusively in neurons with resting pH_i values < 7.20 prior to the induction of anoxia (i.e. "low" pH_i neurons), a small internal acidification was observed that gave way to a marked internal alkalinization that began during anoxia and continued into the post-anoxic period. Similar to the anoxia-evoked changes in pH_i observed in these "low" pH_i rat hippocampal neurons, Yao *et al.* (2001) illustrated that, under HCO_3^--free, Hepes-buffered conditions, acutely isolated mouse hippocampal neurons respond to anoxia with an increase in pH_i that begins during anoxia and continues into the post-anoxic period.

In cultured rat hippocampal neurons, anoxia evoked a fall in pH_i that, upon the return to normoxia, increased to pre-anoxic values. Previous studies have similarly observed falls in pH_i

during and increases in pH_i after periods of anoxia or metabolic inhibition in cultured hippocampal and cortical neurons (Vornov *et al.* 1996; Diarra *et al.* 1999; Jørgensen *et al.* 1999; Messier *et al.* 2004; also see Maduh *et al.* 1990 for similar pH_i shifts observed in response to cyanide in PC12 cells). In some, but not all, of these studies, increases in pH_i during and pH_i 'overshoots' following anoxia were also observed (e.g. Diarra *et al.* 1999; Jørgensen *et al.* 1999). These variations may, in part, reflect differences in pre-anoxic resting pH_i values, as recently suggested by Messier *et al.* (2004) who observed variations in the pattern of anoxia-evoked changes in pH_i in cultured rat hippocampal neurons that appeared dependent on pre-anoxic pH_i values, and/or differences in the degree of membrane depolarization in response to anoxia with consequent differences in the extent of activation of a Zn^{2+}-sensitive H^+ efflux pathway found in the present study (also see Diarra *et al.* 1999) to contribute to acid extrusion during and following anoxia.

During transient periods of anoxia, an increase in $[Na^+]_i$ was consistently observed. Previous studies employing cultured neuronal preparations have observed similar increases in $[Na^+]_i$ during periods of anoxia (Friedman & Haddad, 1994a) or metabolic inhibition (Chen *et al.* 1999; also see Silver *et al.* 1997). Moreover, the increases in $[Na^+]_i$ observed during anoxia in the isolated neurons employed in the present study were also similar to those reported previously in response to hypoxia (Guatteo *et al.* 1998; Müller & Somjen, 2000a and b) or oxygen-glucose deprivation (Pisani *et al.* 1998a; Calabresi *et al.* 1999b; Fung *et al.* 1999) in brain slice preparations. Upon the return to normoxia, $[Na^+]_i$ recovered to pre-anoxic values despite ongoing Na^+ entry. Post-ischemic increases in $[Na^+]_i$ have been described by some (e.g. Taylor *et al.* 1999 and LoPachin *et al.* 2001 in rat hippocampal slices; Stys & LoPachin, 1998 in myelinated CNS axons), although not by others (e.g. Calabresi *et al.* 1999b and Guatteo *et al.* 1998 in rat striatal and midbrain slices, respectively). Nevertheless, the mechanism(s) that

underlie post-ischemic Na^+ entry have remained ill defined and the possibility that they may change during development has not been previously assessed. In addition, consistent with the present findings that the magnitude of the anoxia-evoked increases in $[Na^+]_i$ increased with culture 'age', Jiang *et al.* (1992) reported that the fall in $[Na^+]_o$ during anoxia was more pronounced in medullary slices taken from 'mature' *vs.* 'immature' rats.

Taken together, my results indicate that, during anoxia, hippocampal neurons typically exhibit falls in pH_i and increases in $[Na^+]_i$. In the post-anoxic period, rises in pH_i occur together with continued Na^+ entry. Recognizing the close inter-relationship and, in fact, linked regulation of pH_i and $[Na^+]_i$ via the activities of pH_i regulating mechanisms, subsequent experiments examined the hypothesis that changes in the activities of neuronal pH_i regulating mechanisms, and particularly changes in Na^+/H^+ exchange activity, contribute to anoxia-evoked changes in pH_i and $[Na^+]_i$. Further experiments also examined additional mechanisms contributing to the anoxia-evoked changes in $[Na^+]_i$. Based on findings made in the present study, schematic illustrations of the mechanisms found to contribute to the changes in pH_i and $[Na^+]_i$ observed during and immediately after anoxia in rat hippocampal neurons are illustrated in Figs. 8.1 and 8.2, respectively.

8.3. Contribution of pH_i regulating mechanisms to the changes in pH_i and $[Na^+]_i$ evoked by anoxia

8.3.1. HCO_3^--dependent pH_i regulating mechanisms

In rat hippocampal neurons, pH_i is regulated by the co-ordinated actions of HCO_3^--independent (e.g. Na^+/H^+ exchange) and HCO_3^--dependent (e.g. Na^+-dependent and Na^+-independent Cl^-/HCO_3^- exchange) mechanisms. In the present studies, I found that HCO_3^--dependent pH_i regulating mechanisms are not major determinants of anoxia-evoked changes in pH_i and $[Na^+]_i$ in

rat hippocampal neurons. Previous reports similarly illustrate that the pH_i response to anoxia in rat hippocampal neurons is not markedly influenced by the presence of HCO_3^- (Diarra *et al.* 1999; Roberts *et al.* 2000), although the present study contrasts with Yao *et al.* (2003) who reported that, under HCO_3^-/CO_2-buffered conditions, the pH_i response to 5 min anoxia in acutely isolated mouse hippocampal neurons reflected, in part, anoxia-induced changes in electrogenic Na^+/HCO_3^- cotransport activity. The reported differences in the contribution of HCO_3^--dependent mechanisms to anoxia-evoked changes in pH_i in rat *vs.* mouse hippocampal neurons may reflect the apparent lack of functional Na^+/HCO_3^- cotransport activity in rat hippocampal neurons (Schwiening & Boron, 1994; Baxter & Church, 1996). Nevertheless, from the experiments presented in this thesis, a possible contribution of HCO_3^--dependent pH_i regulating mechanisms to anoxia-evoked changes in pH_i and $[Na^+]_i$, especially in the post-anoxic period, cannot be fully discounted. As discussed in Chapter 5, rat hippocampal neurons possess multiple HCO_3^--dependent pH_i regulating mechanisms and, together with the complexities of the regulation of these mechanisms (Brett *et al.* 2002a), the possibility remains that the co-ordinate actions of multiple HCO_3^--dependent mechanisms may help to shape the anoxia-evoked changes in pH_i and/or $[Na^+]_i$ observed in the present study.

In support of a potential contribution of HCO_3^--dependent pH_i regulating mechanisms to the neuronal response to anoxia/ischemia, DIDS has previously been found to exert neuroprotective effects in rat cortical neurons (Tauskela *et al.* 2003) and other cell types (e.g. Zeevalk *et al.* 1989; Himi *et al.* 2002; Franco-Cea *et al.* 2004). Although these effects have previously been ascribed to the inhibition of HCO_3^--dependent pH_i regulating mechanisms, in the present study, DIDS (applied under HCO_3^-/CO_2-buffered conditions) was found to attenuate rises in $[Na^+]_i$ measured immediately after 5 min anoxia in the absence of any marked corresponding change in the pH_i response to anoxia (Sheldon & Church, 2002a) and, more importantly, reduced

Na^+ influx after anoxia, even in the absence of HCO_3^-. Thus, these results are consistent with the findings of Himi *et al.* (2002) who reported that the neuroprotective effects of DIDS were not dependent on the presence of HCO_3^-. Nevertheless, it remains unclear whether the neuroprotective effects of DIDS reflect an attenuation of Na^+ influx in response to anoxia or effects of the stilbene on other processes that contribute to the pathogenesis of anoxic neuronal injury and death.

8.3.2. <u>Na^+/H^+ exchange activity</u>

An examination of the contribution of changes in Na^+/H^+ exchange activity to the changes in pH_i and $[Na^+]_i$ observed in rat hippocampal neurons in response to anoxia is complicated by the lack of a specific pharmacological inhibitor (see Section 1.4.1; Raley-Susman *et al.* 1991; Schwiening & Boron, 1994; Baxter & Church, 1996). Therefore, I employed a number of complementary, albeit indirect, approaches to assess Na^+/H^+ exchange activity during and following anoxia. *First,* I determined the Na^+_o- (and Li^+_o-) dependencies of the anoxia-evoked changes in steady-state pH_i and the Na^+_o-dependency of rates of pH_i recovery from internal acid loads imposed either during or following anoxia under nominally HCO_3^--free, Hepes-buffered conditions (Chapters 3 and 4). *Second,* I examined the effects of a variety of maneuvres that have previously been found to influence Na^+/H^+ exchange activity in rat hippocampal neurons on the changes in pH_i and $[Na^+]_i$ evoked by anoxia (Chapters 3 - 5). *Finally,* I developed and characterized a novel microspectrofluorimetric technique that permitted concurrent measurements of pH_i and $[Na^+]_i$ in isolated rat hippocampal neurons and used this technique to directly examine the relationship between the changes in pH_i and $[Na^+]_i$ evoked by anoxia in the same cell (Chapter 6). Taken together, these approaches allowed me to assess the changes in Na^+/H^+ exchange activity that occur in rat hippocampal neurons during and following anoxia.

Although Na^+/H^+ exchange is a major acid-extruding mechanism under normoxic conditions in rat hippocampal neurons, my results indicate that transport activity in these cells becomes inhibited as internal ATP (and/or PIP_2) levels decline during anoxia. An anoxia-induced inhibition of Na^+/H^+ exchange activity may, along with other events (e.g. intracellular lactate accumulation; see Dennis *et al.* 1991) contribute to the fall in pH_i observed during anoxia; conversely, Na^+/H^+ exchange activity cannot be a major contributor to the rises in pH_i and $[Na^+]_i$ observed at this time. As detailed in Chapter 3, these findings support previous suggestions that Na^+/H^+ exchange activity in a variety of mammalian central neurons is reduced shortly (i.e. min) following the onset of ischemia *in vivo* (e.g. Taylor *et al.* 1996) and in slice preparations *in vitro* (e.g. Obrenovitch *et al.* 1990; Pirttilä & Kauppinen, 1992; Chambers-Kersh *et al.* 2000; LaManna *et al.* 2003). However, as alluded to above, they are in contrast to observations made in acutely isolated mouse hippocampal neurons, where Na^+/H^+ exchange activity is activated during periods of anoxia (Yao *et al.* 2001), a difference which may reflect species differences or variations in the expression and/or regulation of NHE isoforms.

In contrast to its reduced activity during anoxia, Na^+/H^+ exchange activity is enhanced upon the return to normoxia. Neither a decrease in pH_i during anoxia nor a return to normal pH_o values in the immediate post-anoxic period were absolute requirements for the rapid post-anoxic activation of Na^+/H^+ exchange activity; rather, it may be consequent upon anoxia-induced changes in the activities of intracellular second messenger systems that, in turn, act to regulate exchange activity. In the present study, I have provided evidence that an anoxia-induced activation of the cAMP/PKA pathway (e.g. Kobayashi *et al.* 1977; Whittingham *et al.* 1984; Blomqvist *et al.* 1985; Domanska-Janik, 1996; Small *et al.* 1996), at least in part, contributes to the activation of Na^+/H^+ exchange in the immediate post-anoxic period. Nevertheless, as discussed in Chapter 4, Na^+/H^+ exchange activity can be regulated concurrently by multiple signalling events and I

have not excluded the possible involvement of other signalling pathways (as reported by Yao *et al.* 2001 in mouse hippocampal neurons) or factors (e.g. reactive oxygen species; Mulkey *et al.* 2004) that can be affected by anoxia or ischemia. Whatever mechanism(s) contribute to its activation, Na^+/H^+ exchange activity contributes to acid extrusion and Na^+ influx in rat hippocampal neurons in the immediate post-anoxic period. These conclusions are analogous to findings made in cardiac myocytes, where the effects of anoxia and ischemia on Na^+/H^+ exchange activity have been investigated extensively (reviewed by Karmazyn, 1999; Avkiran, 2001) and are similar to findings recently presented by Kintner and colleagues (2004) in which either genetic ablation of NHE1 expression or the NHE1 inhibitor, HOE 642, reduced the rises in pH_i and $[Na^+]_i$ (measured in experiments performed in parallel) observed upon reperfusion following 2 h oxygen-glucose deprivation in cultured cortical astrocytes.

8.3.2.1. Potential implications of anoxia-evoked changes in Na^+/H^+ exchange activity

The potential consequences of anoxia- or ischemia-induced changes in Na^+/H^+ exchange activity remain unclear. During periods of anoxia, the apparent relationship between Na^+/H^+ exchange activity and internal ATP (and/or PIP_2) levels would act to link the activity of the exchanger with the metabolic state of the cell. In this way, reductions in antiport activity during a period of metabolic stress may, for example, limit its contribution to potentially detrimental elevations in $[Na^+]_i$ (and, possibly, $[Ca^{2+}]_i$), albeit at the expense of reduced acid extrusion (see Nottingham *et al.* 2001 who similarly suggested that the inhibition of Na^+/H^+ exchange activity by hypercapnic acidosis in mature hypoglossal neurons represents a neuroprotective mechanism to minimize the likelihood of internal Na^+ overload and cellular lysis during anoxia/ischemia). Although inhibition of Na^+/H^+ exchange activity may limit harmful elevations in $[Na^+]_i$ during anoxia, as noted in Chapter 1, falls in pH_i elicit a variety of effects with potentially different consequences

on neuronal viability. On the one hand, reductions in pH_i may be beneficial, for example, by reducing voltage-activated Ca^{2+} currents (e.g. Tombaugh & Somjen, 1997; Tombaugh, 1998), and neurotransmitter release (e.g. Chen *et al.* 1998b), and limiting synchronous neuronal activity (e.g. Xiong *et al.* 2000). Indeed, an enhanced internal acidification during anoxia has been correlated with improved recovery of synaptic transmission following anoxia (Roberts *et al.* 1998). On the other hand, falls in pH_i can initiate DNA damage, promote the production of free radicals (e.g. Siesjö *et al.* 1996; Vincent *et al.* 1999) and increase neuronal excitability by inhibiting a variety of K^+ channels (reviewed by Tombaugh & Somjen, 1998; also see Church *et al.* 1998; Liu *et al.* 1999; Kelly & Church, 2004). A fall in pH_i is also an early event that regulates caspase activation during apoptotic cell death (e.g. Matsuyama *et al.* 2000; Lagadic-Gossmann *et al.* 2004; Takahashi *et al.* 2004).

In contrast, enhanced Na^+/H^+ exchange activity immediately upon reperfusion will contribute to increases in pH_i and $[Na^+]_i$ at this time and, in this way, may have multiple harmful effects. For example, rises in pH_i, mediated by Na^+/H^+ exchange, will promote neuronal excitability (e.g. Church & Baimbridge, 1991; de Curtis *et al.* 1998; Bonnet *et al.* 2000a and b; Xiong *et al.* 2000), which, in the post-anoxic or post-ischemic period, represents an additional metabolic stress. Indeed, post-insult activity appears to be an important determinant of long-term neuronal viability (Gao *et al.* 1998; Graber & Prince, 1999; Lahtinen *et al.* 2001). In addition, a variety of intracellular enzymes, ranging from degradative enzymes (e.g. phospholipase A_2; Harrison *et al.* 1991; Stella *et al.* 1995; also see Lagadic-Gossmann *et al.* 2004) to those involved in free radical production (e.g. NOS; Conte, 2003) exhibit optimal levels of activity at neutral or slightly alkaline pH_i values. In cardiac myocytes (e.g. Bond *et al.* 1993; Harper *et al.* 1993) and cultured neocortical neurons (Vornov *et al.* 1996), cellular injury in response to metabolic inhibition appears to be initiated, not by the fall in pH_i that takes place during the insult, but by the rapidity with which pH_i increases in the period immediately

after the insult. By increasing $[Na^+]_i$, Na^+/H^+ exchange activity can also promote acute neuronal swelling (e.g. Jakubovicz *et al.* 1987; Melzian *et al.* 1996), and may enhance cAMP production (e.g. Reddy *et al.* 1995; Cooper *et al.* 1998), augment NMDA receptor-operated currents (Yu & Salter, 1998) and promote the reversal of plasmalemmal Na^+/Ca^{2+} exchange activity (leading to a subsequent rise in $[Ca^{2+}]_i$; Czyż *et al.* 2002), all of which may promote neuronal injury and death. Finally, in cardiac myocytes, Na^+/H^+ exchange-induced increases in $[Na^+]_i$ can alter mitochondrial $[Ca^{2+}]$, $[H^+]$ and membrane potential which may slow/prevent the recovery of internal ATP levels upon reperfusion (e.g. Hotta *et al.* 2001; Iwai *et al.* 2002; Teshima *et al.* 2003).

The contribution of Na^+/H^+ exchange to the pathophysiology of ischemic cell death may not be limited to acute ischemia-reperfusion injury. Within the myocardium, Na^+/H^+ exchange activity appears capable of activating various kinases involved in cell growth (e.g. Hayasaki-Kajiwara *et al.* 1999; Mukhin *et al.* 2004). As such, Na^+/H^+ exchange plays an important role in the pathogenesis of chronic maladaptive responses to injury, including myocardial remodeling, hypertrophy and, ultimately, cardiac failure (Karmazyn, 2001). That Na^+/H^+ exchange may be involved in the long-term response to periods of anoxia or ischemia in the central nervous system is supported by the observed alterations in Na^+/H^+ exchange protein expression following intense neuronal activity and periods of chronic hypoxia (Xia & Haddad, 1999; Kang *et al.* 2002; Douglas *et al.* 2003). A possible, although untested, hypothesis suggests that changes in Na^+/H^+ exchange activity and/or expression play a structural role in the central nervous system: Na^+/H^+ exchange proteins may be important for neurite outgrowth (e.g. Schwab, 2001; Putney *et al.* 2002) and, as such, may be involved, at least in part, in anoxia-induced alterations in spine structure and/or development of aberrant recurrant excitatory pathways (e.g. Jourdain *et al.* 2002; Carmichael, 2003).

8.3.2.2. Na^+/H^+ exchange inhibitors: neuroprotective actions and therapeutic potential

In myocardial tissue, increased Na^+/H^+ exchange activity contributes to increases in pH_i, $[Na^+]_i$ and $[Ca^{2+}]_i$ at reperfusion; by limiting these potentially detrimental ionic changes, Na^+/H^+ exchange inhibitors have been found, in animal studies, to limit reperfusion-induced ventricular fibrillations, contractile dysfunction and myocardial cell death (Karmazyn *et al.* 1999; Avkiran, 2001). In an analogous manner, the present study suggests that the neuroprotective effects of Na^+/H^+ exchange inhibitors are most likely to be mediated, not during anoxia, but in the immediate post-anoxic period by limiting the increases in pH_i, $[Na^+]_i$ and/or $[Ca^{2+}]_i$ that occur at this time. In support, cortical astrocytes cultured from NHE1 null mutant mice or astrocytes exposed to NHE1 inhibitors exhibit smaller increases in $[Na^+]_i$ and pH_i and, as a result, reduced cellular swelling during recovery from oxygen-glucose deprivation (Kintner *et al.* 2004). Moreover, Na^+/H^+ exchange inhibitors limit glutamate-induced cell swelling and internal Na^+ and Ca^{2+} accumulation in cultured cortical neurons and, thus, reduce neuronal death (Matsumoto *et al.* 2003; Yamamoto *et al.* 2003). Na^+/H^+ exchange inhibitors appear capable of influencing pH_i, $[Na^+]_i$ and cytotoxicity and, although the present study employed hippocampal neurons (and, where possible, CA1 pyramidal neurons), it would be of interest to examine any differences in the anoxia-induced changes in Na^+/H^+ exchange activity in a neuronal population less sensitive to anoxic/ischemic damage (i.e. CA3 pyramidal neurons).

In the present study, I did not address whether reducing Na^+/H^+ exchange activity immediately following anoxia was capable of limiting anoxia-induced neuronal death; however, as noted above, a growing body of evidence indicates that pharmacological inhibition of Na^+/H^+ exchange effectively protects against anoxia- and ischemia-induced neuronal injury *in vitro* and in animal models *in vivo* (e.g. Vornov *et al.* 1996; Kuribayashi *et al.* 1999; Phillis *et al.* 1999; Horikawa *et al.* 2001a and b). Moreover, in studies performed *in vivo*, Na^+/H^+ exchange

inhibitors reduce infarct size when administered prior to (Phillis *et al.* 1999; Kitayama *et al.* 2001) or during (Kuribayashi *et al.* 1999; Horikawa *et al.* 2001a and b; Suzuki *et al.* 2002) ischemia and Na^+/H^+ exchange inhibitors also reduce the extent of locomotor hyperactivity observed 6 days following a transient ischemic episode (Phillis *et al.* 1999). In contrast, in one study, it was found that administration of a Na^+/H^+ exchange inhibitor immediately upon reperfusion was not effective at reducing infarct size (Horikawa *et al.* 2001b). Together, these findings suggest that the utility of Na^+/H^+ exchange inhibitors as neuroprotective agents in stroke may be limited by the rapid activation of Na^+/H^+ exchange activity that occurs upon reperfusion, although they do not rule out the possibility that Na^+/H^+ exchange inhibitors may also prove useful under controlled conditions (e.g. cardiac bypass surgery) or as a prophylactic measure in patients at high risk for stroke. Even so, it is important to note that, despite the success of Na^+/H^+ exchange inhibitors as cardioprotective agents in preclinical animal studies, large-scale human clinical trials with Na^+/H^+ exchange inhibitors, cariporide or eniporide (e.g. the GAURDIAN and ESCAMI trials; Théroux *et al.* 2000, Zeymer *et al.* 2001; also see discussion by Avikran *et al.* 2002) have shown limited efficacy. Further studies to examine the neuroprotective effects of Na^+/H^+ exchange inhibitors appear justified; however, the possibility remains that, even if the compounds can be administered at the appropriate time point, they may prove similarly ineffective, an observation which may, at least in part, reflect the multiplicity of Na^+ entry pathways that contribute to the deleterious increases in $[Na^+]_i$ evoked by ischemia (see below).

8.3.3. Role of a putative voltage-activated proton conductance

Although Na^+/H^+ exchange is inhibited during anoxia, acid extrusion could sometimes occur. In these cases, the rise in pH_i during anoxia appeared to be associated temporally with a marked and persistent increase in $[Ca^{2+}]_i$, raising the possibility that anoxia-induced depolarizations may

activate H^+ efflux through a H^+-conductive pathway (a putative g_{H^+}). In support, the application of micromolar concentrations of Zn^{2+} (which blocks g_{H^+}s in all cell types studied to date; DeCoursey & Cherny, 1994a and 2000; Eder & DeCoursey, 2001) reduced significantly the increases in pH_i during and after anoxia. Moreover, pH_i recoveries from internal acid loads imposed during and following anoxia were slowed by brief applications of Zn^{2+}, an effect that was independent of both Na^+ and HCO_3^-. Additional experiments, conducted under normoxic conditions, also suggested that a H^+-conductive pathway contributes to acid extrusion from rat hippocampal neurons during high $[K^+]_o$-evoked depolarizations. Voltage-activated proton conductances have been found in snail neurons, macrophages and microglia, and while there is very little further evidence to indicate that they might contibute to pH_i regulation in vertebrate neurons (under normoxic or anoxic conditions), it seems teleologically reasonable for neurons to express proton channels whose main function is to alleviate the potentially detrimental internal acid loads associated with periods of high metabolic activity (reviewed by DeCoursey & Cherny, 1994a; Eder & DeCoursey, 2001; Chesler, 2003).

Evidence was also provided to suggest that, as in other cell types (see DeCoursey & Cherny, 1994b; Demaurex *et al.* 1995), the putative g_{H^+} might couple to Na^+/H^+ exchange activity in rat hippocampal neurons. This has a number of potential consequences: *i)* inhibition of Na^+/H^+ exchange would promote the activation of a g_{H^+} *during* anoxia, thereby preventing the fall in pH_i from reaching a critical (damaging) threshold; and *ii)* activation of a g_{H^+} *after* anoxia would limit the potentially detrimental activation of forward Na^+/H^+ exchange that may occur at this time. These considerations suggest that the neurotoxic effects associated with micromolar concentrations of Zn^{2+} (Choi & Koh, 1998; Weiss *et al.* 2000; Dineley *et al.* 2003) may, at least in part, reflect an inhibition of g_{H^+}s and a consequent augmentation of the fall in pH_i observed

during anoxia and/or a further promotion of Na^+/H^+ exchange activity upon reoxygenation. In fact, a marked accumulation of Zn^{2+} occurs in hippocampal slices following ischemia (Wei *et al.* 2004) and Zn^{2+}-induced increases in $[Na^+]_i$ have been suggested to underlie the post-ischemic upregulation of NMDA receptor activity (Yu & Salter, 1998; Manzerra *et al.* 2001). These considerations suggest that a formal assessment of the contribution of the putative proton conductance to acid extrusion in rat hippocampal neurons would be worthwhile. It is of interest that g_{H^+}s in non-neuronal cell types can be modulated by the activities of second messengers, including PKC and PLA_2 (e.g. Kapus *et al.* 1994; Suszták *et al.* 1997; Calonge & Ilundain, 1996; also see Morihata *et al.* 2000 for an illustration of the potentiation of voltage-activated proton currents by increases in cell volume), the activities of which are altered by anoxia (e.g. Wieloch *et al.* 1996; Sapirstein & Bonventre, 2000; Phillis & O'Regan, 2004). It will be also of interest to determine whether these pathways may promote the activation of g_{H^+}s during anoxia.

8.4. On the mechanisms contributing to anoxia-evoked changes in $[Na^+]_i$

Because changes in the activities of pH_i regulating mechanisms did not contribute to increases in $[Na^+]_i$ during anoxia and could account for only a portion of the Na^+ influx found to occur after anoxia, further experiments were undertaken to systematically explore the potential contributions of other mechanisms integral to the cell to the changes in $[Na^+]_i$ observed during and following anoxia in isolated rat hippocampal neurons. These studies provided additional insights into the mechanism(s) underlying the detrimental increases in $[Na^+]_i$ in rat hippocampal neurons (see Section 8.3.1 for a description of the potential consequences of elevations in $[Na^+]_i$).

It has been observed previously that isolated rat hippocampal neurons respond to anoxia with increases in $[Na^+]_i$ (Friedman & Haddad, 1994a; also see Chen *et al.* 1999 for a description

of the changes $[Na^+]_i$ observed in rat cerebellar granule cells in response to metabolic inhibition). In the present study, these findings were confirmed and, in addition, it was found that: *i)* the magnitudes of the increases in $[Na^+]_i$ observed during and after (Na^+,K^+-ATPase blocked) anoxia were dependent on the duration of time that neurons had been maintained in culture; *ii)* despite the recovery of $[Na^+]_i$ to pre-anoxic levels, Na^+ influx continued into the immediate post-anoxic period; and *iii)* perhaps most importantly, as previously suggested for Ca^{2+} (see Silver & Erecińska, 1990 and 1992; Lipton, 1999), Na^+ influx during and following anoxia was mediated by different complements of mechanisms, the respective contributions of which differed in 6 - 10 and 11 - 14 DIV neurons. These observations may contribute to our understanding of the enhanced vulnerability of more phenotypically mature neurons to anoxic damage *in vitro* (e.g. Rothman, 1983; Di Lorteo & Balestrino, 1997) and the aggravation of anoxic neuronal injury that occurs upon reperfusion (Lipton, 1999; Taylor *et al.* 1999). They may also, in part, help to explain the apparent inconsistencies in the literature regarding the contributions of different Na^+ entry pathways to anoxia-induced increases in $[Na^+]_i$.

In the present studies, the increase in $[Na^+]_i$ observed during anoxia reflected, in part, reduced Na^+,K^+-ATPase activity consequent upon declining ATP levels acting in concert with Na^+ influx via a putative Gd^{3+}-sensitive NSCC (6 - 10 DIV neurons) or $Na^+/K^+/2Cl^-$ cotransport activity (11 - 14 DIV neurons). In light of the fact that activation of NSCCs and $Na^+/K^+/2Cl^-$ cotransport, as well as inhibition of Na^+,K^+-ATPase, can initiate and promote cell swelling (e.g. Chen & Simard, 2001; Xiao *et al.* 2002; Beck *et al.* 2003), Na^+ influx via these mechanisms may contribute to the acute neurotoxic effects of anoxia.

Although a number of studies have suggested that the Na^+ entry that occurs after anoxia or ischemia may be particularly neurotoxic (e.g. Strijbos *et al.* 1996; Crumrine *et al.* 1997), the pathways mediating Na^+ influx at this time have not been previously investigated in mammalian

central neurons. In the present study, compared to the mechanisms contributing to the increase in $[Na^+]_i$ during anoxia, a different set of mechanisms contributed to Na^+ entry in the immediate post-anoxic period. Thus, Na^+/H^+ exchange, acting in concert with a Gd^{3+}-sensitive presumed NSCC and forward-mode Na^+/Ca^{2+} exchange activity were found to contribute to post-anoxic Na^+ influx, while concomitant reverse-mode Na^+/Ca^{2+} exchange appeared to contribute to Na^+ extrusion at this time. Reactive oxygen species, levels of which increase upon reoxygenation (see Lipton, 1999) were found to contribute to the activation of the Gd^{3+}-sensitive presumed NSCC and, though not directly investigated, reactive oxygen species may also contribute to the activation of Na^+/H^+ exchange (e.g. Sabri *et al.* 1998; but see Mulkey *et al.* 2004) and Na^+/Ca^{2+} exchange (e.g. Goldhaber, 2003; Takuma *et al.* 1996) as well as the reduction in $Na^+/K^+/2Cl^-$ cotransport activity (e.g. Ortiz *et al.* 2001), observed upon reoxygenation (also see review by Kourie, 1998). These interactions may, at least in part, account for the observation that the detrimental effects of increases in $[Na^+]_i$ and oxidative stress appear to be additive: exposure of isolated synaptosomes to veratridine (to induce an internal Na^+ load) and H_2O_2 in combination (i.e. conditions mimicking those observed in the immediate post-anoxic period) elicits more marked increases in $[Na^+]_i$ (and $[Ca^{2+}]_i$) and decreases in internal ATP compared to changes observed with either maneuver individually (Trettler & Adam-Vizi, 1996; Chinopoulos *et al.* 2000).

While the mechanisms outlined above appear to account for much of the Na^+ influx that takes place in rat hippocampal neurons during or immediately after anoxia, it is nevertheless clear that additional Na^+ entry routes must also contribute. This emphasizes the multifactorial nature of the Na^+ influx pathways that contribute to the detrimental increases in $[Na^+]_i$ that occur in rat hippocampal neurons in response to anoxia. In turn, these findings indicate that therapeutic strategies directed toward individual Na^+ entry pathways may not be successful in limiting neuronal death;

rather, as discussed by Lo *et al.* (2003), combination therapies directed towards inhibiting multiple Na^+ entry pathways may prove more useful in preventing the potentially disastrous consequences of stroke.

Fig. 8.1. A schematic representation of the mechanisms (*A*) found in the present studies to contribute to the changes in pH_i (*B*) observed during and after anoxia in rat hippocampal neurons. Solid green and dashed red lines indicate activation or inhibition of the indicated pH_i regulating mechanism. Also shown are the potential mechanisms underlying the observed change in transport activity. **During anoxia,** Na^+/H^+ exchange activity is reduced, possibly as a result of declining internal ATP levels. Na^+/H^+ exchange does not contribute to the increase in pH_i observed during anoxia. Rather, alongwith a variety of intracellular events, inhibition of Na^+/H^+ exchange activity may augment the fall in pH_i observed during anoxia. HCO_3^--dependent mechanism(s) do not appear to contribute to anoxia-evoked changes in pH_i observed during anoxia. A Zn^{2+}-sensitive H^+ efflux pathway, possibly a voltage-activated H^+ conductance activated by membrane depolarization, contributes to the increase in pH_i observed during anoxia. **After anoxia,** Na^+/H^+ exchange activity is stimulated and contributes to the increase in pH_i observed at this time. An anoxia-induced activation of the cAMP/PKA pathway contributes to the post-anoxic increase in Na^+/H^+ exchange activity. A Zn^{2+}-sensitive H^+ efflux pathway also contributes to acid extrusion after anoxia. HCO_3^--dependent mechanism(s) are not major contributors to the changes in pH_i observed after anoxia; however, indicated by the **?**, further experiments are required to examine the contribution of specific HCO_3^--dependent pH_i regulating mechanisms to the anoxia-evoked changes in pH_i. See text for further details.

NHE = Na^+/H^+ exchange.

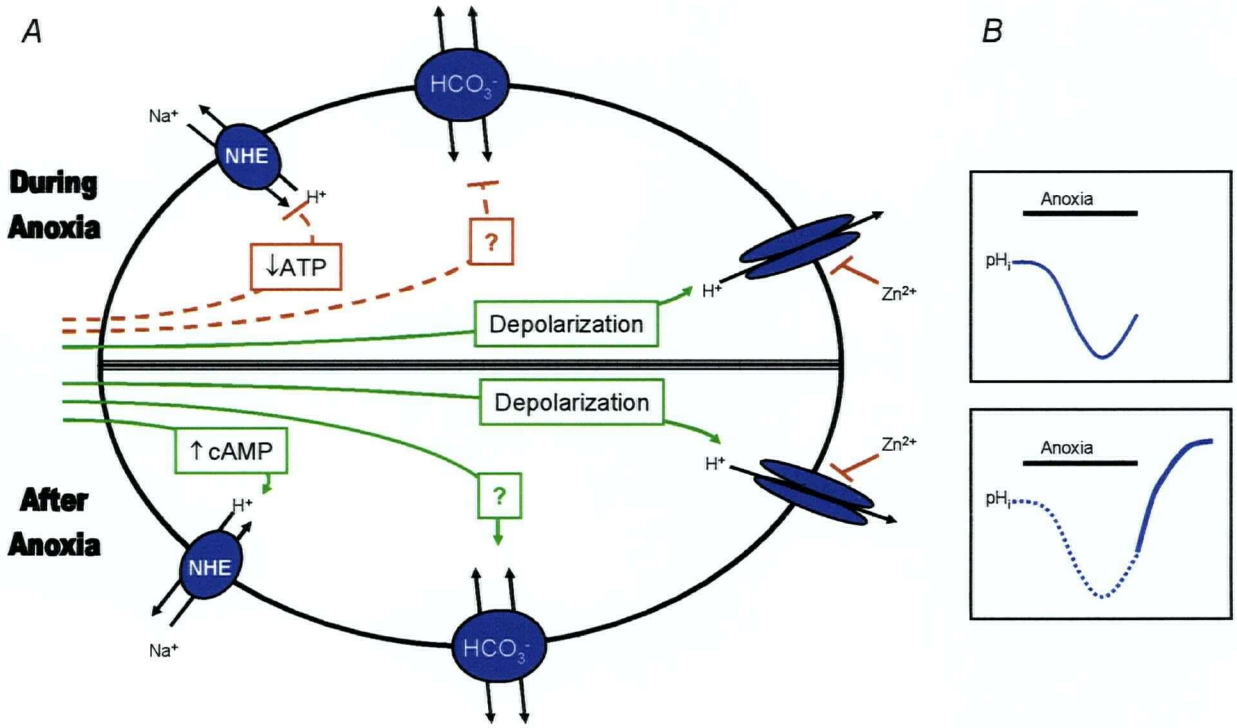
A
B
During Anoxia
After Anoxia
HCO3-
Na+
NHE
H+
↓ATP
?
Depolarization
Zn2+
↑ cAMP
Anoxia
pHi

Fig. 8.2. A schematic representation of the mechanisms (*A*) found in the present studies to contribute to the changes in $[Na^+]_i$ (*B*) observed during and after anoxia in rat hippocampal neurons. Solid Green and dashed red lines indicate activation or inhibition of the indicated Na^+-dependent mechanism, respectively. Also shown are the potential mechanisms contributing to the observed change in transport activity. **During anoxia,** Na^+/H^+ exchange and Na^+,K^+-ATPase activities are reduced, likely as a result of declining ATP levels during anoxia. Inhibition of Na^+,K^+-ATPase activity contributes to the accumulation of Na^+_i observed during anoxia. $Na^+/K^+/2Cl^-$ cotransport activity (in 11 - 14 DIV neurons) and putative Gd^{3+}-sensitive NSCCs (in 6 - 10 DIV neurons) contribute to Na^+ influx during anoxia. Neither HCO_3^--dependent mechanism(s) nor Na^+/Ca^{2+} exchange activity appear to contribute to the changes in $[Na^+]_i$ observed during anoxia. **After anoxia,** Na^+,K^+-ATPase activity is re-established and mediates the recovery of $[Na^+]_i$. The recovery of $[Na^+]_i$ occurs in the face of ongoing Na^+ influx in the post-anoxic period: Na^+/H^+ exchange activity is increased, HCO_3^--dependent mechanisms appear to be activated (the indentity of these mechanism(s) remains unclear; **?**) and Gd^{3+}-sensitive NSCCs also contribute to Na^+ influx. Na^+/Ca^{2+} exchange activity also influences the changes in $[Na^+]_i$ observed following anoxia (the double-headed arrows indicate that forward- and/or reverse-mode Na^+/Ca^{2+} exchange may be involved). See text for additional details.

NHE = Na^+/H^+ exchange; ATPase = Na^+,K^+-ATPase; NKCC = $Na^+/K^+/2Cl^-$ cotransport; NCX = Na^+/Ca^{2+} exchange; ROS = reactive oxygen species.

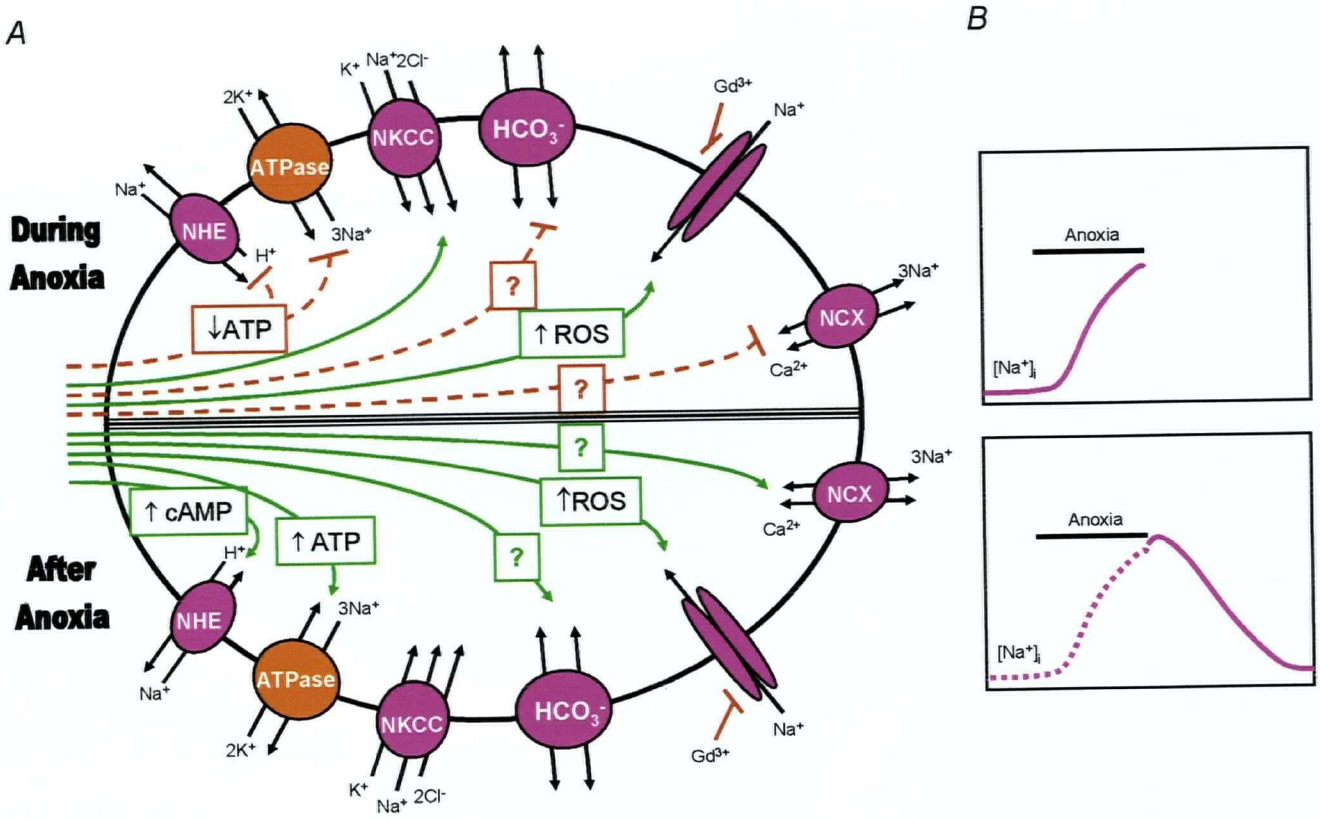
A
B
During Anoxia
After Anoxia
ATPase
NKCC
HCO3-
NHE
NCX
K+ Na+2Cl-
2K+
Na+
H+
3Na+
Gd3+
Ca2+
↓ATP
↑ ROS
↑ cAMP
↑ ATP
↑ROS
?
Anoxia
[Na+]i

BIBLIOGRAPHY

Aarts M., Iihara K., Wei W.-L., Xiong K.-G., Arundine M., Cerwinski W., MacDonald J.F. and Tymianski M. (2003) A key role for TRPM7 channels in anoxic neuronal death. Cell 115: 863 - 877.

Abdul-Ghani M.A., Valiante T.A., Carlen P.L. and Pennefather P.S. (1996) Metabotropic glutamate receptors coupled to IP_3 production mediate inhibition of I_{AHP} in rat dentate granule neurons. J. Neurophysiol. 76: 2691 - 2700.

Aharonovitz O., Zaun H.C., Balla T., York J.D., Orlowski J. and Grinstein S. (2000) Intracellular pH regulation by Na^+/H^+ exchange requires phosphatidylinositol-4,5-bisphosphate. J. Cell Biol. 150: 213 - 224.

Ahmed Z. and Connor J.A. (1980) Intracellular pH changes induced by electrical activity in molluscan neurons. J. Gen. Physiol. 75: 403 - 426.

Aickin C.C. and Thomas R.C. (1977) An investigation of the ionic mechanism of intracellular pH regulation in mouse soleus muscle fibers. J. Physiol. 273: 295 - 316.

Aickin, C.C. (1984) Direct measurement of intracellular pH and buffering power in smooth muscle cells of guinea-pig vas deferens. J. Physiol. 349: 571-585.

Aickin, C.C. and Brading, A.F. (1984) The role of chloride-bicarbonate exchange in the regulation of intracellular chloride in guinea-pig vas deferens. J. Physiol. 349: 587-606.

Alojado M.E., Morimoto Y., Morimoto Y. and Kemmotsu O. (1996) Mechanisms of cellular swelling induced by extracellular lactic acidosis in neuroblastoma-glioma hybrid (NG108-15) cells. Anesth. Analg. 83, 1002 - 1008.

Amaral D.G. and Witter M.P. (1995) Hippocampal formation. In: Paxinos G. (ed) The Rat Nervous System. 2nd ed. Academic Press, San Diego, pp. 443 - 493

An J., Varadarajan S.G., Camara A., Chen Q., Novalija E., Gross G.J. and Stowe D.F. (2001) Blocking Na^+/H^+ exchange reduces $[Na^+]_i$ and $[Ca^{2+}]_i$ load after ischemia and improves function in intact hearts. Am. J. Physiol. 281: H2398 - H2409.

Anderson R.E. and Meyer F.B. (2000) Is intracellular brain pH a dependent factor in NOS inhibition during focal cerebral ischemia? Brain Res. 856: 220 - 226.

Anderson S.E., Dickinson C.Z., Liu H. and Cala P.M. (1996) Effects of Na-K-2Cl cotransport inhibition on myocardial Na and Ca during ischemia and reperfusion. Am. J. Physiol. 270: C608 - C618.

Arai K., Ikegaya Y., Nakatani Y., Kudo I., Nishiyama N. and Matsuki N. (2001) Phospholipase A_2 mediates ischemic injury in the hippocampus: a regional difference of neuronal vulnerability. Eur. J. Neurosci. 13: 2319 - 2323.

Aram J.A. and Lodge D. (1987) Epileptiform activity induced by alkalosis in rat neocortical slices: block by antagonists of N-methyl-D-aspartate. Neurosci. Lett. 83: 345 - 350.

Archer S.L., Hampl V., Nelson D.P., Sidney E., Peterson D.A. and Weir E.K. (1995) Dithionite increases radical formation and decreases vasoconstriction in the lung. Circ. Res. 77: 174 - 181.

Aronson P.S. (1985) Kinetic properties of the plasma membrane Na^+-H^+ exchanger. Annu. Rev. Physiol. 47: 545 - 560.

Assaf H.M., Ricci A.J., Whittingham T.S., LaManna J.C., Ratcheson R.A. and Lust W.D. (1990) Lactate compartmentation in hippocampal slices: evidence for a transporter. Metab. Brain Dis. 5: 143 - 154.

Attaphitaya S., Nehrke K. and Melvin J.E. (2001) Acute inhibition of brain-specific Na^+/H^+ exchanger isoform 5 by protein kinases A and C and cell shrinkage. Am. J. Physiol. 281: C1146 - C1157.

Attaphitaya S., Park K. and Melvin J.E. (1999) Molecular cloning and functional expression of a rat Na^+/H^+ exchanger (NHE5) highly expressed in brain. J. Biol. Chem. 274: 4383 - 4388.

Austin C., Dilly K., Eisner D. and Wray S. (1996) Simultaneous measurement of intracellular pH, calcium and tension in rat mesenteric vessels: effects of extracellular pH. Biochem. Biophys. Res. Commun 222; 537 - 540.

Avkiran M. (2001) Protection of the ischemic myocardium by Na^+/H^+ exchange inhibitors: potential mechanisms of action. Basic Res. Cardiol. 96: 306 – 311.

Avkiran M. and Haworth R.S. (1999) Regulation of cardiac sarcolemmal Na^+/H^+ exchanger activity by endogenous ligands: relevance to ischemia. Ann. NY Acad. Sci. 874: 335 - 345.

Avkiran M. and Marber M.S. (2000) Na^+/H^+ exchange inhibitors for cardioprotective therapy: progress, problems and prospects. J. Am. Coll. Cardiol. 39: 747 - 753.

Back T. (1998) Pathophysiology of the ischemic penumbra - revision of a concept. Cell. Mol. Neurobiol. 18: 621 - 638.

Baird N.R., Orlowski J., Szabó E.Z., Zaun H.C., Schultheis P.J., Menon A.G. and Shull G.E. (1999) Molecular cloning, genomic organization, and functional expression of Na^+/H^+ exchanger isoform 5 (NHE5) from human brain. J. Biol. Chem. 274: 4377 - 4382.

Balestrino M. and Somjen G.G. (1988) Concentration of carbon dioxide, interstitial pH and synaptic transmission in hippocampal formation of the rat. J. Physiol. 396: 247 – 266.

Balestrino M., Lensman M., Parodi M., Perasso L., Rebaudo R., Melani R., Polenov S. and Cupello A. (2002) Role of creatine and phosphocreatine in neuronal protection from anoxic and ischemic damage. Amino Acids 23: 221 - 229.

Balestrino M., Rebaudo R. and Lunardi G. (1999) Exogenous creatine delays anoxic depolarization and protects from hypoxic damage: dose-effect relationship. Brain Res. 816: 124 - 130.

Ballanyi K. and Kaila K. (1998) Activity-evoked changes in intracellular pH. In: Kaila K., Ransom B.R. (ed) pH and Brain Function. Wiley-Liss, New York, pp 291 - 308.

Banasiak K.J., Burenkova O. and Haddad G.G. (2004) Activation of voltage-sensitive sodium channels during oxygen deprivation leads to apoptotic neuronal death. Neuroscience 126: 31 - 44.

Barber D.L., McGuire M.E. and Ganz M.B. (1989) β-Adrenergic and somatostatin receptors regulate Na^+-H^+ exchange independent of cAMP. J. Biol. Chem. 264: 21038 - 21042.

Barros L.F., Stutzin A., Calixto A., Catalán M., Castro J., Hetz C. and Hermosilla T. (2001) Nonselective cation channels as effectors of free radical-induced rat liver cell necrosis. Hepatology 33: 114 - 122.

Bassnett S., Reinisch L. and Beebe D.C. (1990) Intracellular pH measurement using single excitation-dual emission fluorescence ratios. Am. J. Physiol. 258: C171 - C178.

Baxter K.A. and Church J. (1996) Characterization of acid extrusion mechanisms in cultured fetal rat hippocampal neurons. J. Physiol. 493: 457 - 470.

Beck J., Lenart B., Kintner D.B. and Sun D. (2003) Na-K-Cl cotransporter contributes to glutamate-mediated excitotoxicity. J. Neurosci. 23: 5061 - 5068.

Benveniste H., Drejer J., Schousboe A. and Diemer N.H. (1984) Elevation of the extracellular concentrations of glutamate and aspartate in rat hippocampus during transient cerebral ischemia monitored by intracerebral microdialysis. J. Neurochem. 43: 1369 - 1374.

Bers D.M., Barry W.H. and Despa S. (2003) Intracellular Na^+ regulation in cardiac myocytes. Cardiovasc. Res. 57: 897 - 912.

Bevensee M.O. and Boron W.F. (2000) Hypoxia stimulates acid extrusion and acid loading in cultured hippocampal astrocytes. Soc. Neurosci. Abstr. 26, 767.4.

Bevensee M.O., Bashi E. and Boron W.F. (1999a) Effect of trace levels of nigericin on intracellular pH and acid-base transport in rat renal mesangial cells. J. Membrane Biol. 169: 131 - 139.

Bevensee M.O., Bashi E., Schlue W.-R., Boyarsky G. and Boron W.F. (1999b) Shrinkage-induced activation of Na^+/H^+ exchange in rat renal mesangial cells. Am. J. Physiol. 276: C674 - C683.

Bevensee M.O., Cummins T.R., Haddad G.G., Boron W.F. and Boyarsky G. (1996) pH regulation in single CA1 neurons acutely isolated from the hippocampi of immature and mature rats. J. Physiol. 494: 315 - 328.

Bevensee M.O., Schmitt B.M., Choi I., Romero M.F. and Boron W.F. (2000) An electrogenic Na^+-HCO_3^- cotransporter (NBC) with a novel COOH-terminus, cloned from rat brain. Am. J. Physiol. 278: C1200 - C1211.

Bevensee M.O., Schwiening C.J. and Boron W.F. (1995) Use of BCECF and propidium iodide to assess membrane integrity of acutely isolated CA1 neurons from rat hippocampus. J. Neurosci. Meth. 58: 61 - 75.

Bevensee M.O., Weed, R.A. and Boron W.F. (1997) Intracellular pH regulation in cultured astrocytes from rat hippocampus I. Role of HCO_3^-. J. Gen. Physiol.110: 453 - 465.

Bickler P.E., Gallego S.M. and Hansen B.M. (1993) Developmental changes in intracellular calcium regulation in rat cerebral cortex during hypoxia. J. Cereb. Blood Flow Metab. 13: 811-819.

Blanco G. and Mercer R.W. (1998) Isozymes of the Na-K-ATPase: heterogeneity in structure, diversity in function. Am. J. Physiol. 275: F633 - F650.

Blank P.S., Silverman H.S., Chung O.Y., Hogue B.A., Stern M.D., Hansford R.G., Lakatta E.G. and Capogrossi M.C. (1992) Cytosolic pH measurements in single cardiac myocytes using carboxy-seminaphthorhodafluor-1. Am. J. Physiol. 263: H276 - H284.

Blaustein M.P. and Lederer W.J. (1999) Sodium/calcium exchange: it physiological implications. Physiol. Rev. 79: 763 - 854.

Blomqvist P., Lindvall O., Stenevi U., and Wieloch T. (1985) Cyclic AMP concentrations in rat neocortex and hippocampus during and following incomplete ischemia: effects of central noradrenergic neurons, prostaglandins, and adenosine. J. Neurochem. 44: 1345 - 1353.

Boening J.A., Kass I.S., Cottrell J.E. and Chambers, G. (1989) The effect of blocking sodium influx on anoxic damage in the rat hippocampal slice. Neuroscience 33: 263 - 268.

Boland L.M., Brown T.A. and Dingledine R. (1991) Gadolinium block of calcium channels: influence of bicarbonate. Brain Res. 563: 142 - 150.

Bond J.M., Chacon E., Herman B. and Lemasters J.J. (1993) Intracellular pH and Ca^{2+} homeostasis in the pH paradox of reperfusion injury to neonatal rat cardiac myocytes. Am. J. Physiol. 265: C129 - C137.

Bonnet U., Bingmann D. and Wiemann M. (2000a) Intracellular pH modulates spontaneous and epileptiform bioelectric activity of hippocampal CA3 neurons. Eur. Neuropsychopharmacol. 10: 97 - 103.

Bonnet U., Leniger T. and Wiemann M. (2000b) Alteration of intracellular pH and activity of CA3-pyramidal cells in guinea pig hippocampal slices by inhibition of transmembrane acid extrusion. Brian Res. 872: 116 - 124.

Bookstein C., Musch M.W., DePaoli A., Xie Y., Rabenau K., Villereal M., Rao M.C. and Chang E.B. (1996) Characterization of the rat Na^+/H^+ exchanger isoform NHE4 and localization in rat hippocampus. Am. J. Physiol. 271: C1629 - C1638.

Borgese F., Malapert M., Fievet B., Pouyssegur J., Motais R. (1992) The cytoplasmic domain to the Na^+/H^+ exchangers (NHEs) dictates the nature of the hormonal response: behavior of a chimeric domain NHE1/trout beta NHE antiporter. PNAS 91: 5431 - 5435.

Boron W.R. and DeWeer P. (1976) Intracellular pH transients in squid giant axons caused by CO_2, NH_3, and metabolic inhibitors. J. Gen. Physiol. 67: 91 - 112.

Boron W.R., Hogan R. and Russell J.M. (1988) pH-sensitive activation of the intracellular pH regulation

system in squid axons by ATP-γ-S. Nature 332: 262 - 265.

Boron W.R., McCormick W.C. and Roos, A. (1979) pH regulation in barnacle muscle fibres: dependence on intracellular and extracellular pH. Am. J. Physiol. 237: C185 - C193.

Bouron A. and Reuter H. (1996) A role of intracellular Na^+ in the regulation of synaptic transmission and turnover of the vesicular pool in cultured hippocampal cells. Neuron 17: 969 - 978.

Boyarsky G., Hanssen C. and Clyne L.A. (1996a) Inadequacy of high K^+/nigericin for calibrating BCECF. I. Estimating steady-state intracellular pH. Am. J. Physiol. 271: C1131 - C1145.

Boyarsky G., Hanssen C. and Clyne L.A. (1996b) Inadequacy of high K^+/nigericin for calibrating BCECF. II. Intracellular pH dependence of the correction. Am. J. Physiol. 271: C1146 - C1156.

Bramlett H.M. and Dietrich W.D. (2004) Pathophysiology of cerebral ischemia and brain trauma: similarities and differences. J. Cereb. Blood Flow Metab. 24: 133 - 150.

Breder J., Sabelhau C.F., Opitz T., Reymann K.G. and Schröder U.H. (2000) Inhibition of different pathways influencing Na^+ homeostasis protects organotypic hippocampal slice cultures from hypoxic/hypoglycemic injury. Neuropharm. 39: 1779 - 1787.

Brett C.L., Kelly T., Sheldon C. and Church J. (2002a) Regulation of Cl^-/HCO_3^- exchange by cAMP-dependent protein kinase in acutely isolated adult rat hippocampal CA1 neurons. J. Physiol. 15: 837 - 853.

Brett C.L., Wei Y., Donowitz M. and Rao R. (2002b) Human Na^+/H^+ exchanger isoform 6 is found in recycling endosomes of cells, not in mitochondria. Am. J. Physiol. 282: C1031 - C1041.

Broderick J.P. and Hacke W. (2002a) Treatment of acute ischemic stroke. Part I: recanalization strategies. Circulation 106: 1563 - 1569.

Broderick J.P. and Hacke W. (2002b) Treatment of acute ischemic stroke. Part II: neuroprotection and medical management. Circulation 106: 1736 - 1740.

Brown A.M., Westenbroek R.E., Catterall W.A. and Ransom B.R. (2001) Axonal L-type Ca^{2+} channels and anoxic injury in rat CNS white matter. J. Neurophysiol. 85: 900 - 911.

Bruehl C. and Witte O.W. (2003) Relation between bicarbonate concentration and voltage dependence of sodium currents in freshly isolated CA1 neurons of the rat. J. Neurophysiol. 89: 2489 - 2498.

Bruehl G., Wadman W.J. and Witte O.W. (2000) Concentration dependence of bicarbonate-induced calcium current modulation. J. Neurophysiol. 84: 2277 - 2283.

Buckler K.J. and Vaughan-Jones R.D. (1990) Application of a new pH-sensitive fluoroprobe (carboxy-SNARF-1) for intracellular pH measurement in small, isolated cells. Pflügers Arch. 17: 234 - 239.

Busa W.B. and Nuccitelli R. (1984) Metabolic regulation via intracellular pH. Am. J. Physiol. 246:

R409 - R438.

Byerly L. and Suen Y. (1989) Characterization of proton currents in neurones of the snail, Lymnaea stagnalis. J. Physiol. 413: 75 - 89.

Cabantchik Z.I. and Greger R. (1992) Chemical probes for anion transporters of mammalian cell membranes. Am. J. Physiol. 262: C803 - C827.

Calabresi P., Marfia G.A., Amoroso S., Pisani A. and Bernardi G. (1999a) Pharmacological inhibition of the Na^+/Ca^{2+} exchanger enhances depolarizations induced by oxygen/glucose deprivation but not responses to excitatory amino acids in rat striatal neurons. Stroke 30: 1687 - 1693.

Calabresi P., Marfia G.A., Centonze D., Pisani A. and Bernardi G. (1999b) Sodium influx plays a major role in membrane depolarization induced by oxygen and glucose deprivation in rat striatal spiny neurons. Stroke 30: 171 - 178.

Caldwell R.A., Clemo H.F. and Baumgarten C.M. (1998) Using gadolinium to identify stretch-activated channels: technical considerations. Am. J. Physiol. 275: C619 - C621.

Calonge M.L. and Ilundain A.A. (1996) PKC activators stimulate H^+ conductance in chicken enterocytes. Pflügers Arch. 431: 594 - 598.

Camacho R., Páez M.P., Blázquez G., Jiménez C. and Fernández M. (1995) Influence of pH on the oxygen absorption kinetics in alkaline sodium dithionite solutions. Chem. Eng. Sci. 50: 1181 - 1186.

Carmeliet E. (1999) Cardiac ionic currents and acute ischemia: from channels to arrhythmias. Physiol. Rev. 79: 917 - 1017.

Carmichael S.T. (2003) Plasticity of cortical projections after stroke. Neuroscientist 9: 64 - 75.

Carpenter E., Hatton C.J., Peers C. (2000) Effects of hypoxia and dithionite on catecholamine release from isolated type I cells of the rat carotid body. J. Physiol. 523: 719 - 729.

Carter A.J., Muller R.E., Pschorn U. and Stransky W. (1995) Preincubation with creatine enhances levels of creatine phosphate and prevents anoxic damage in rat hippocampal slices. J. Neurochem. 64: 2691 - 2699.

Castilho R.F., Hansson O., Ward M.W., Budd S.L. and Nicholls D.G. (1998) Mitochondrial control of acute glutamate excitotoxicity in cultured cerebellar granule cells. J. Neurosci. 18: 10277-10286.

Castillo M.R. and Babson J.R. (1998) Ca^{2+}-dependent mechanisms of cell injury in cultured cortical neurons. Neuroscience 86: 1133 - 1144.

Centonze D., Marfia G.A., Pisai A., Picconi B., Ciacornini P., Bernardi G. and Calabresi P. (2001) Ionic mechanisms underlying differential vulnerability to ischemia in striatal neurons. Prog. Neurobiol. 63: 687 - 696.

Ch'en F.F.-T., Dilworth E., Swietach P., Goddard R.S. and Vaughan-Jones R.D. (2003) Temperature dependence of Na^+-H^+ exchange, Na^+-HCO_3^- co-transport, intracellular buffering and intracellular pH in guinea-pig ventricular myocytes. J. Physiol. 552: 713 - 726.

Chambers-Kersh L., Ritucci N.A., Dean J.B. and Putnam R.W. (2000) Response of intracellular pH to acute anoxia in individual neurons from chemosensitive and nonchemosensitive regions of the medulla. Adv. Exp. Med. Biol. 475: 453 - 464.

Chambrey R., Achard J.M. and Warnock D.G. (1997a) Heterologous expression of rat NHE4: a highly amiloride-resistant Na^+/H^+ exchanger isoform. Am. J. Physiol. 272: C90 - C98.

Chambrey R., Achard J.M., St.John P.L., Abrahamson D.R. and Warnock, D.G. (1997b) Evidence for an amiloride-insensitive Na^+/H^+ exchanger in rat renal cortical tubules. Am. J. Physiol. 273: C1064 - C1074.

Chen M. and Simard J.M. (2001) Cell swelling and a nonselective cation channel regulated by internal Ca^{2+} and ATP in native reactive astrocytes from adult rat brain. J. Neurosci. 21: 6512 - 6521.

Chen Q., Olney J.W., Lukasiewicz P.D., Almli T. and Romano C. (1998a) Fenamates protect neurons against ischemic and excitotoxic injury in chick embryo retina. Neurosci. Letters 242: 163 - 166.

Chen Q.X., Perkins K.L., Choi D.W. and Wong R.K.S. (1997) Secondary activation of a cation conductance is responsible for NMDA toxicity in acutely isolated hippocampal neurons. J. Neurosci. 17: 4032 - 4036.

Chen W.-H., Chu K.-C., Wu S.-J., Wu J.-C., Shui H.-A. and Wu M.-L. (1999) Early metabolic inhibition-induced intracellular sodium and calcium increase in rat cerebellar granule cells. J. Physiol. 515: 133 - 146.

Chen Y., Cann M.J., Litvin T.N., Iourgenko V., Sinclair M.L., Levin L.R. and Buck J. (2000) Soluble adenylyl cyclase as an evolutionarily conserved bicarbonate sensor. Science 289: 625 - 628.

Chen Y.-H., Wu M-L. and Fu W.-M. (1998b) Regulation of acetylcholine release by intracellular acidification of developing motoneurons in *Xenopus* cell cultures. J. Physiol. 507: 41 - 53.

Cheng C., Fass D.M. and Reynolds I.J. (1999) Emergence of excitotoxicity in cultured forebrain neurons coincides with larger glutamate-stimulated $[Ca^{2+}]_i$ increases and NMDA receptor mRNA levels. Brain Res. 849: 97 - 108.

Cherny V.V. and DeCoursey T.E. (1999) pH-dependent inhibition of voltage-gated H^+ currents in rat alveolar epithelial cells by Zn^{2+} and other divalent cations. J. Gen. Physiol. 114: 819 - 838.

Chesler M. (1986) Regulation of intracellular pH in reticulospinal neurones of the lamprey, *Petromyzon marinus*. J. Physiol. 381: 241 - 261.

Chesler M. (2003) Regulation and modulation of pH in the brain. Physiol. Rev. 83: 1183 - 1221.

Chesler M. and Kaila K. (1992) Modulation of pH by neuronal activity. TINS 15: 396 - 402.

Chidekel A.S., Friedman J.E. and Haddad, G.G. (1997) Anoxia-induced neuronal injury: role of Na^+ entry and Na^+-dependent transport. Exp. Neurol. 146: 403 - 413.

Chinopoulos C., Tretter L., Rozsa A., and Adam-Vizi V. (2000) Exacerbated responses to oxidative stress by an Na^+ load in isolated nerve terminals: the role of ATP depletion and rise of $[Ca^{2+}]_i$. J. Neurosci. 20: 2094 - 2103.

Choi D.W. (1990) Cerebral hypoxia: some new approaches and unanswered questions. J. Neurosci. 10: 2493 - 2501.

Choi D.W. and Koh J.Y. (1998) Zinc and brain injury. Annu. Rev. Neurosci. 21: 347 - 375.

Chow E. and Haddad G.G. (1998) Differential effects of anoxia and glutamate on cultured neocortical neurons. Exp. Neurol. 150: 52 - 59.

Church J. and Baimbridge K.G. (1991) Exposure to high-pH medium increases the incidence and extent of dye coupling between rat hippocampal CA1 pyramidal neurons in vitro. J. Neurosci. 11: 3289 - 3295.

Church J., Baxter K.A. and McLarnon J.G. (1998) pH modulation of Ca^{2+} responses and a Ca^{2+}-dependent K^+ channel in cultured rat hippocampal neurones. J. Physiol. 511: 119 - 132.

Church J., Fan C. and Brett C. (2001) Calmodulin antagonists modulate Na^+/H^+ exchange in rat CA1 hippocampal neurons. Soc. Neurosci. Abstr. 27: 45.5.

Church J., Zeman S. and Lodge D. (1988) The neuroprotective actions of ketamine and MK-801 after transient cerebral ischemia in rats. Anesthesiology 69: 702 - 709.

Cingolani H.E., Chiappe G.E., Ennis I.L., Morgan P.G., Alvarez B.V., Casey J.R., Dulce R.A., Perez, N.G. and Camilion de Hurtado M.C. (2003) Influence of Na^+-independent Cl^--HCO_3^- exchange on the slow force response to myocardial stretch. Circ. Res. 93: 1082 - 1088.

Connor J.A. and Hockberger P. (1984) Intracellular pH changes induced by injections of cyclic nucleotides into gastropod neurones. J. Physiol. 354: 163 - 172.

Conte A. (2003) Physiologic pH changes modulate calcium ion dependence of brain nitric oxide synthase in *Carassius auratu.i* Biochim. Biophys. Acta. 1619: 29 - 38.

Cooper D.M., Schell M.J., Thorn P. and Irvine R.F. (1998) Regulation of adenylyl cyclase by membrane potential. J. Biol. Chem. 273: 27703 - 27707.

Cowan A.I. and Martin R.L. (1992) Ionic basis of membrane potential changes induced by anoxia in rat

dorsal vagal motoneurons. J. Physiol. 455: 89 - 109.

Cowan A.I. and Martin R.L. (1995) Simultaneous measurement of pH and membrane potential in rat dorsal vagal motoneurons during normoxia and hypoxia: a comparison of bicarbonate and HEPES buffers. J. Neurophys. 74: 2713 - 2721.

Crumrine C.R., Bergstrand K., Cooper A.T., Faison W.L. and Cooper B.R. (1997) Lamotrigine protects hippocampal CA1 neurons from ischemic damage after cardiac arrest. Stroke. 28: 2230 - 2236.

Cummins T.R., Donnelly D.R. and Haddad G.G. (1991) Effect of metabolic inhibition on the excitability of isolated hippocampal CA1 neurons: developmental aspects. J. Neurophysiol. 66: 1471 - 1482.

Cummins T.R., Jiang C. and Haddad G.G. (1993) Human neocortical excitability is decreased during anoxia via sodium channel modulation. J. Clin. Invest. 91: 608 - 615.

Currin R.T., Gores G.J., Thurman R.G. and Lemasters J.J. (1991) Protection by acidotic pH against anoxia cell killing in perfused rat liver: evidence for a pH paradox. FASEB J. 5: 207 - 210.

Czyż A. and Kiedrowski L. (2003) Inhibition of plasmalemmal Na^+/Ca^{2+} exchange by mitochondrial Na^+/Ca^{2+} exchange inhibitor 7-chloro-5-(2-chlorophenyl)-1,5-dihydro-4,1-benzothiazepin-2(3H)-one (CGP-37157) in cerebellar granule cells. Biochem. Pharmacol. 66: 2409 - 2411.

Czyż A., Baranauskas G. and Kiedrowski L. (2002) Instrumental role of Na^+ in NMDA excitoxicity in glucose-deprived and depolarized cerebellar granule cells. J. Neurochem. 81: 379 - 389.

DeCoursey T.E. and Cherny V.V. (2000) Common themes and problems of bioenergetics and voltage-gated proton channels. Biochim. Biophys. Acta 1458: 104 - 119.

DeCoursey TE and Cherny VV. (1994a) Voltage-activated hydrogen ion currents. J. Membrane Biol. 141: 203 - 223.

DeCoursey TE and Cherny VV. (1994b) Na^+-H^+ antiport detected through hydrogen ion currents in rat alveolar epithelial cells and human neutrophils. J. Gen. Physiol. 103: 755 - 785.

Deitmer J.W. and Ellis D. (1980) Interactions between the regulation of the intracellular pH and sodium activity of sheep cardiac Purkinje fibres. J. Physiol. 304: 471 - 488.

Deitmer J.W. and Schlue W.R. (1983) Intracellular Na^+ and Ca^{2+} in leech Retzius neurones during inhibition of the Na^+-K^+ pump. Pflügers Arch. 397: 195 - 201.

Deitmer J.W. and Schlue W.R. (1989) An inwardly directed electrogenic sodium-bicarbonate co-transport in leech glial cells. J. Physiol. 411: 179 - 194.

Deitmer J.W. and Schneider H.P. (1998) Acid/base transport across the leech giant glial cell membrane at low external bicarbonate concentration. J. Physiol. 512, 459 - 469.

Demaurex N. and Grinstein S. (1994) Na^+/H^+ antiport: modulation by ATP and role in cell volume regulation. J Exp. Biol. 196: 389 - 404.

Demaurex N., Orlowski J., Brisseau G., Woodside M. and Grinstein S. (1995) The mammalian Na^+/H^+ antiporters NHE-1, NHE-2 and NHE-3 are electroneutral and voltage independent, but can couple to an H^+ conductance. J. Gen. Physiol: 106: 85 - 111.

Demaurex N., Romanek R.R., Orlowski J. and Grinstein S. (1997) ATP dependence of Na^+/H^+ exchange. Nucleotide specificity and assessment of the role of phospholipids. J. Gen. Physiol. 109: 117 - 128.

Dennis S.C., Gevers W. and Opie L.H. (1991) Protons in ischemia: where do they come from, where do they go? J. Mol. Cell. Cardiol. 23: 1077 - 1086.

Despa S., Islam M.A., Pogwizd S.M. and Bers D.M. (2002) Intracellular $[Na^+]$ and Na^+ pump rate in rat and rabbit ventricular myocytes. J. Physiol. 539: 133 - 143.

DeVries S.H. (2001) Exocytosed protons feedback to suppress the Ca^{2+} current in mammalian cone photoreceptors. Neuron 32: 1107 - 1117.

Di Loreto S. and Balestrino M. (1997) Development of vulnerability to hypoxic damage in in vitro hippocampal neurons. Int. J. Devl. Neurosci. 15: 225 - 230.

Diarra A., Sheldon C. and Church J. (2001) In situ calibration and $[H^+]$ sensitivity of the fluorescent Na^+ indicator, SBFI. Am. J. Physiol. 280: C1623 - C1633.

Diarra A., Sheldon C., Brett C.L., Baimbridge K.G. and Church J. (1999) Anoxia-evoked intracellular pH and Ca^{2+} concentration changes in cultured postnatal rat hippocampal neurons. Neuroscience 93: 1003 - 1016.

Diemer N.H. and Siemkowicz E. (1981) Regional neurone damage after cerebral ischemia in the normo- and hypoglycemic rat. Neuropath. Appl. Neurobiol. 7: 217 - 227.

Dietrich W.D. (1998) Neurobiology of Stroke. Int. Rev. Neurobiol. 42: 55 - 101.

Dineley K.E., Brocard J.B. and Reynolds I.J. (2002) Elevated intracellular zinc and altered proton homeostasis in forebrain neurons. Neuroscience 114: 439 - 449.

Dineley K.E., Votyakova T.V. and Reynolds I.J. (2003) Zinc inhibition of cellular energy production: implications for mitochondria and neurodegeneration. J. Neurochem. 85: 563 - 570.

Ding D., Moskowitz S.I., Li R., Lee S.B., Esteban M., Tomaselli K., Chan J. and Bergold P.J. (2000) Acidosis induces necrosis and apoptosis of cultured hippocampal neurons. Exp. Neurol. 162: 1 - 12.

Domanska-Janik K. (1996) Protein serine/threonine kinases (PKA, PKC and CaMKII) involved in ischemic brain pathology. Acta Neurobiol. Exp. 56: 579 - 585.

Domanska-Janik K. and Pylova S. (1989) Rapid enhancement of cAMP accumulation in rat brain particulate fraction after ischemia. Int. J. Tissue Reactions 11: 73 - 79.

Douglas R.M., Schmitt B.M., Xia Y., Bevensee M.O., Biemesderfer D., Boron W.F. and Haddad G.G. (2001) Sodium-hydrogen exchangers and sodium-bicarbonate co-transporters: ontogeny of protein expression in the rat brain. Neuroscience 102: 217 - 228.

Douglas R.M., Xue J., Chen J.Y., Haddad C.G., Alper S.L. and Haddad G.G. (2003) Chronic intermittent hypoxia decreases the expression of Na^+/H^+ exchangers and HCO_3^--dependent transporters in mouse CNS. J. Appl. Physiol. 95: 292 - 299.

Drapeau P. and Nachshen D.A. (1988) The regulation of cytosolic pH in isolated presynaptic terminals from rat brain. J. Gen. Physiol. 91: 289 - 303.

Dringen R., Peters H., Wiesinger H. and Hamprecht B. (1995) Lactate transport in cultured glial cells. Dev. Neurosci.17: 63 - 69.

Ebine Y., Fujiwara N. and Shimoji K. (1994) Mild acidosis inhibits the rise in intracellular Ca^{2+} concentration in response to oxygen-glucose deprivation in rat hippocampal slices. Neurosci. Lett. 168: 155 - 158.

Eder C. and DeCoursey T.E. (2001) Voltage-gated proton channels in microglia. Prog. Neurobiol. 64: 277 - 305.

Ekholm A., Katsura K., Kristián T., Liu M., Folbergrova J. and Siesjö B.K. (1993) Coupling of cellular energy state and ion homeostasis during recovery following brain ischemia. Brain Res. 604: 185 - 191.

Elinder F. and Århem P. (1994) Effects of gadolinium on ion channels in the myelinated axon on Xenopus laevis: four sites of action. Biophys. J. 67: 71 - 83.

El-Sherif Y., Wieraszko A., Banerjee P. and Penington N.J. (2001) ATP modulates Na^+ channel gating and induces a non-selective cation current in a neuronal hippocampal cell line. Brain Res. 904: 301 - 317.

Erecińska M. and Dagani F. (1990). Relationships between the neuronal sodium/potassium pump and energy metabolism: effects of K^+, Na^+ and adenosine triphosphate in isolated brain synaptosomes. J. Gen. Physiol. 95: 591 - 616.

Erecińska M. and Silver I.A. (1989) ATP and brain function. J. Cereb. Blood Flow Metab. 9: 2 - 19.

Erecińska M. and Silver I.A. (1994) Ions and energy in mammalian brain. Prog. Neurobiol: 43, 37 - 71.

Erecińska M. and Silver I.A. (2001) Tissue oxygen tension and brain sensitivity to hypoxia. Respiration Physiol. 128: 263 - 276.

Erecińska M., Dagani F., Nelson D., Deas J., and Silver I.A. (1991) Relations between intracellular ions and energy metabolism: A study with monensin in synaptosomes, neurons, and C6 glioma cells. J. Neurosci. 11: 2410 - 2421.

Estevez A.Y., Song D., Phillis J.W. and O'Regan M.H. (2000) Effects of the anion channel blocker

DIDS on ouabain- and high K^+-induced release of amino acids from the rat cerebral cortex. Brain Res. Bull. 52: 45 - 50.

Féraille E. and Doucet A. (2001) Sodium-potassium-adenosinetriphosphatase-dependent sodium transport in the kidney: hormonal control. Physiol. Rev. 81: 345 - 418.

Fernandes H.B. (2001) Characterization of anoxia-induced neuronal death in hippocampal neurons. University of British Columbia, Dept. Physiology. M.Sc. Thesis.

Fliegel L. (2001) Regulation of myocardial Na^+/H^+ exchanger activity. Basic Res. Cardiol. 96: 301-305.

Florez-McClure M.L., Linseman D.A., Chu C.T., Barker P.A., Bouchard R.J. Le S.S., Laessig T.A. and Heidenreich K.A. (2004) The p75 neurotrophin receptor can induce autophagy and death of cerebellar Purkinje neurons. J. Neurosci. 24: 4498 - 4509.

Fowler J.C. and Li Y. (1998) Contributions of Na^+ flux and the anoxic depolarization to adenosine 5'-triphosphate levels in hypoxic/hypoglycemic rat hippocampal slices. Neuroscience 83: 717 - 722.

Franco-Cea A., Valencia A., Sánchez-Armass S., Domínquez G. and Morán J. (2004) Role of ionic fluxes in the apoptotic cell death of cultured cerebellar granule neurons. Neurochem. Res. 29: 227 - 238

Frelin C., Vigne P. and Lazdunski M. (1984) The role of the Na^+/H^+ exchange system in cardiac cells in relation to the control of the internal Na^+ concentration. J. Biol. Chem. 259: 8880 - 8885.

Fried E., Amorim P., Chambers G., Cottrell J.E. and Kass I.S. (1995) The importance of sodium for anoxic transmission damage in rat hippocampal slice: mechanisms of protection by lidocaine. J. Physiol. 489: 557 - 565.

Friedman J.E. and Haddad G.G. (1993) Major differences in $Ca^{2+}{}_i$ response to anoxia between neonatal and adult rat CA1 neurons: role of $Ca^{2+}{}_o$ and $Na^+{}_o$. J. Neurosci. 13: 63 - 72.

Friedman J.E. and Haddad G.G. (1994a) Anoxia induces an increase in intracellular sodium in rat central neurons in vitro. Brain Res. 663: 329 - 334.

Friedman J.E. and Haddad G.G. (1994b) Removal of extracellular sodium prevents anoxia-induced injury in freshly dissociated rat CA1 hippocampal neurons. Brain Res. 641, 57 - 64.

Fujiwara N, Abe T, Endoh H, Warashina A, and Shimoji K. (1992) Changes in intracellular pH of mouse hippocampal slices responding to hypoxia and/or glucose depletion. Brain Res. 572: 335-339.

Fujiwara N., Higashi H., Shimoji K. and Yoshimura M. (1987) Effects of hypoxia on rat hippocampal neurones in vitro. J. Physiol. 384:131 - 151.

Fung M.-L., Croning M.D.R. and Haddad G.G. (1999) Sodium homeostasis in rat hippocampal slices during oxygen and glucose deprivation: role of voltage-sensitive sodium channels. Neurosci. Lett.

275:41 - 44.

Fung, M.-L. and Haddad, G.G. (1997) Anoxia-induced depolarization in CA1 hippocampal neurons: role of Na^+-dependent mechanisms. Brain Res. 762:97 - 102.

Gaillard S. and Dupont J.L. (1990) Ionic control of intracellular pH in rat cerebellar Purkinje cells maintained in culture. J. Physiol. 425:71 - 83.

Galeffi F., Sah R., Pond B.B., George A. and Schwartz-Bloom, R.D. (2004) Changes in intracellular chloride after oxygen-glucose deprivation of the adult hippocampal slice: effect of diazepam. J. Neurosci. 24: 4478 - 4488.

Gao T.-M., Pulsinelli W.A. and Xu Z.C. (1998) Prolonged enhancement and depression of synaptic transmission in CA1 pyramidal neurons induced by transient forebrain ischemia *in vivo*. Neuroscience 87: 371 - 383.

Gatto C. and Milanick MA. (1993) Inhibition of the red blood cell calcium pump by eosin and other fluorescein analogues. Am. J. Physiol. 264: C1577 - C1586.

Gebhardt C. and Heinemann U. (1999) Anoxic decrease in potassium outward currents of hippocampal cultured neurons in absence and presence of dithionite. Brain Res. 837: 270 - 276.

Gibney G.T., Zhang J.H., Douglas R.M., Haddad G.G. and Xia Y. (2002) Na^+/Ca^{2+} exchanger expression in the developing rat cortex. Neuroscience 112: 65 - 73.

Giffard R.G., Lee Y-S., Ouyang Y-B., Murphy S.L. and Monyer H. (2003) Two variants of the rat brain sodium-driven chloride bicarbonate exchanger (NCBE): developmental expression and addition of a PDZ motif. Eur. J. Neurosci. 18: 2935 - 2945.

Giffard R.G., Monyer H., Christine C.W. and Choi, D.W. (1990) Acidosis reduces NMDA receptor activation, glutamate neurotoxicity, and oxygen-glucose deprivation neuronal injury in cortical cultures. Brain Res. 506: 339 - 342.

Giffard R.G., Papadopoulos M.C., van Hooft J.A., Xu L., Giuffrida R. and Monyer H. (2000) The electrogenic sodium bicarbonate cotransporter: developmental expression in rat brain and possible role in acid vulnerability. J. Neurosci. 20, 1001 - 1008.

Ginsburg K.S., Weber C.R., Despa S. and Bers D.M. (2002) Simultaneous measurement of $[Na^+]_i$, $[Ca^{2+}]_i$ and I_{NCX} in intact cardiac myocytes. Ann. N. Y. Acad. Sci. 976: 157 - 158.

Gleitz J., Tosch C., Beile A. and Peters T. (1996) The protective action of tetrodotoxin and (±)-kavain on anaerobic glycolysis, ATP content and intracellular Na^+ and Ca^{2+} of anoxic brain vesicles. Neuropharmacology 35: 1743 - 1752.

Goldberg M.P. and Choi, D.W. (1993) Combined oxygen and glucose deprivation in cortical cell culture: calcium-dependent and calcium-independent mechanisms of neuronal injury. J. Neurosci. 13: 3510 - 3524.

Goldberg M.P., Weiss J.H., Pham P.C. and Choi D.W. (1987) *N*-methyl-D-aspartate receptors mediate hypoxic neuronal injury in cortical culture. J. Pharmacol. Exp. Ther. 243: 784 - 791.

Goldhaber J.I. (1996) Free radicals enhance Na^+/Ca^{2+} exchange in ventricular myocytes. Am. J. Physiol. 271: H823 - H333.

Gordienko, D.V., Tare, M., Parveen, S., Fenech, C.J., Robinson, C. and Bolton, T.B. (1996) Voltage-activated proton current in eosinophils from human blood. J. Physiol. 496: 299 - 316.

Gosmanov A.R., Schneider E.G. and Thomason D.B. (2003) NKCC activity restores muscle water during hyperosmotic challenge independent of insulin, ERK and p38 MAPK. Am. J. Physiol. 284: R655 - R665.

Graber K.D. and Prince D.A. (1999) Tetrodotoxin prevents posttraumatic epileptogenesis in rats. Ann. Neurol. 46: 234 - 242.

Grant E.R., Dubin A.E., Zhang S.-P., Zivin R.A. and Zhong Z. (2002) Simultaneous intracellular calcium and sodium flux imaging in human vanilloid receptor 1 (VR1)-transfected human embryonic kidney cells: a method to resolve ionic dependence of VR1-mediated cell death. J. Pharmacol. Exp. Ther. 300: 9 - 17.

Green J. and Kleeman C.R. (1992) Role of calcium and cAMP messenger systems in intracellular pH regulation of osteoblastic cells. Am. J. Physiol. 262: C111 - C121.

Green J., Yamaguchi D.T., Kleeman C.R. and Muallem S. (1988) Cytosolic pH regulation in osteoblasts. Interaction of Na^+ and H^+ with the extracellular and intracellular faces of the Na^+/H^+ exchanger. J. Gen. Physiol. 92: 239 - 261.

Grichtchenko I.I., Choi I., Zhong X., Bray-Ward P., Russell J.M. and Boron W.F. (2001) Cloning, characterization, and chromosomal mapping of human electroneutral Na^+-driven Cl^--HCO_3^- exchanger. J. Biol. Chem. 276: 8358 - 8363.

Grinstein S., Cohen S. and Rothstein A. (1984) Cytoplasmic pH regulation in thymic lymphocytes by an amiloride-sensitive Na^+/H^+ antiport. J. Gen. Physiol. 83: 341 - 369.

Gu X.Q., Yao H. and Haddad G.G. (2000) Effect of extracellular HCO_3^- on Na^+ channel characteristics in hippocampal CA1 neurons. J. Neurophysiol. 84: 2477 - 2483.

Guatteo E., Mercuri N.B., Bernardi G. and Knopfel T. (1998) Intracellular sodium and calcium homeostasis during hypoxia in dopamine neurons of rat substantia nigra pars compacta. J. Neurophysiol. 80: 2237 - 2243.

Haddad G.G. and Jiang C. (1993) Mechanisms of anoxia-induced depolarization in brainstem neurons: in vitro current and voltage clamp studies in the adult rat. Brain Res. 625: 261 - 268.

Hall R.A., Premont R.T., Chow C.-W., Blitzer J.T., Pitcher J.A., Claing A., Stoffel R.H., Barak L.S., Shenolikar S., Weinman E.J., Grinstein S. and Lefkowitz, R.J. (1998) The β_2-adrenergic receptor interacts with the Na^+/H^+-exchanger regulatory factor to control Na^+/H^+ exchange. Nature 392: 626 -

630.

Hammarström A.K. and Gage P.W. (1998) Inhibition of oxidative metabolism increases persistant sodium current in rat CA1 hippocampal neurons. J. Physiol. 510: 735 - 741.

Hammarström A.K. and Gage P.W. (2000) Oxygen-sensing persistant sodium currents in rat hippocampus. J. Physiol. 529: 107 - 118.

Han D., Antunes R., Canali R., Rettori D. and Cadenas E. (2003) Voltage-dependent anion channels control the release of the superoxide anion from mitochondria to cytosol. J. Biol. Chem. 278: 5557 - 5563.

Hansen A.J. (1985) Effect of anoxia on ion distribution in the brain. Physiol. Rev. 65: 101 - 148.

Harper L.S., Bond J.M., Chacon E., Reece J.M., Herman B. and Lemasters J.J. (1993) Inhibition of Na^+/H^+ exchange preserves viability, restores mechanical function, and prevents the pH paradox in reperfusion injury to rat neonatal myocytes. Basic Res. Cardiol. 88: 430 - 442.

Harrison D.C., Lemasters J.J. and Herman B. (1991) A pH-dependent phospholipase A_2 contributes to loss of plasma membrane integrity during chemical hypoxia in rat hepatocytes. Biochem. Biophys. Res. Comm. 174: 654 - 659.

Harrison N.L. and Gibbons S.J. (1994) Zn^{2+}: an endogenous modulator of ligand- and voltage-gated ion channels. Neuropharmacology 33: 935 - 952.

Hartley Z. and Dubinsky J.M. (1993) Changes in intracellular pH associated with glutamate excitotoxicity. J. Neurosci. 13: 4690 - 4699.

Hasbani M.J., Hyrc K.L., Faddis B.T., Romano C. and Goldberg M.P. (1998) Distinct roles for sodium, chloride, and calcium in excitotoxic dentritic injury and recovery. Exp. Neurol. 154: 241 - 258.

Hayasaki-Kajiwara Y., Kitano Y., Iwasaki T., Shimamura T., Naya N., Iwaki K. and Nakajima M. (1999) Na^+ influx via Na^+/H^+ exchange activates protein kinase C isozymes σ and ε in cultures neonatal rat cardiac myocytes. J. Mol. Cell. Cardiol. 31: 1559 - 1572.

Hayashi H., Szaszi K. and Grinstein S. (2002) Multiple modes of regulation of Na^+/H^+ exchangers. Ann. N.Y. Acad. Sci. 976: 248 - 258.

He S., Ruknudin A., Bambrick L.L., Lederer W.J. and Schulze D.H. (1998) Isoform-specific regulation of the Na^+/Ca^{2+} exchanger in rat astrocytes and neurons by PKA. J. Neurosci. 18: 4833 - 4841.

Herman B., Gores G.J., Nieminen A.-L., Kawanishi T., Harman A. and Lemasters J.J. (1990) Calcium and pH in anoxic and toxic injury. Crit. Rev. Toxicol. 21: 127 - 148.

Herson P.S. and Ashford M.L.J. (1999) Reduced glutathione inhibited β-NAD^+-activated non-selective cation currents in the CRI-G1 rat insulin-secreting cell line. J. Physiol. 514: 47 - 57.

Hess P., Lansman J.B. and Tsien R.W. (1986) Calcium channel selectivity for divalent and

monovalent cations. Voltage and concentration dependence of single channel current in ventricular heart cells. J. Gen. Physiol. 88: 293 - 319.

Hill C., Giesberts A.N. and White S.J. (2002) Expression of isoforms of the Na^+/H^+ exchanger in M-1 mouse cortical collecting duct cells. Am. J. Physiol. 282: F649 - 654.

Himi T., Ishizaki Y. and Murota S.-I. (2002) 4,4'-Diisothiocyano-2,2'-stilbenedisulfonate protects cultured cerebellar granule neurons from death. Life Sci. 70: 1235 - 1249.

Hodgkin A.L. and Keynes R.D. (1955) Active transport of cations in giant axons from *Sepia* and *Lolgio*. J. Physiol. 128: 28 - 60.

Hope P.L., Cady E.B., Delpy D.T., Ives N.K., Gardiner R.M. and Reynolds, E.O.R. (1988) Brain metabolism and intracellular pH during ischemia: effects of systemic glucose and bicarbonate administration studied by ^{31}P and ^{1}H nuclear magnetic resonance spectroscopy in vivo in the lamb. J. Neurochem. 50: 1394 - 1402.

Horikawa N., Kuribayashi Y., Matsui K. and Ohashi N. (2001b) Relationship between the neuroprotective effect of Na^+/H^+ exchanger inhibitor SM-20220 and the timing of its administration in a transient middle cerebral artery occlusion model in rats. Biol. Pharm. Bull. 24: 767 - 771.

Horikawa N., Nishioka M., Itoh N., Kuribayashi Y., Matsui K. and Ohashi N. (2001a) The Na^+/H^+ exchanger SM-20220 attenuates ischemic injury in in vitro and in vivo models. Pharmacology 63: 76 - 81.

Hotta Y., Ishikawa N., Ohashi N. and Matsui K. (2001) Effects of SM-20550, a selective Na^+-H^+ exchange inhibitor, on ion transport of myocardial mitochondria. Mol. Cell. Biochem. 219: 83 - 90.

Hou Y. and Delamere N.A. (2002) Influence of ANG II on cytoplasmic sodium in cultured rat nonpigmented ciliary epithelium. Am. J. Physiol. 283: C552 - C559.

Hoyt K.R., Arden S.R., Aizenman E. and Reynolds I.J. (1998) Reverse Na^+/Ca^{2+} exchange contributes to glutamate-induced intracellular Ca^{2+} concentration increases in cultured rat forebrain neurons. Mol. Pharmacol. 53: 742 - 749.

Huettner J.E., Stack E. and Wilding T.J. (1998) Antagonism of neuronal kainate receptors by lanthanum and gadolinium. Neuropharmacology 37: 1239 - 1247.

Hurn P.C., Koehler R.C., Norris S.E., Blizzard K.K. and Traystman R.J. (1991) Dependence of cerebral energy phosphate and evoked potential recovery on end-ischemic pH. Am. J. Physiol. 260: H532 - H541.

Hurn P.D., Koehler R.C. and Traystman R.J. (1997) Alkalemia reduces recovery from global cerebral ischemia by NMDA receptor-mediated mechanism. Am. J. Physiol. 272: H2557 - H2562.

Hurn P.D., Koehler R.C., Norris S.E., Schwentker A.E. and Traystman R.J. (1991) Bicarbonate conservation during incomplete cerebral ischemia with superimposed hypercapnia. Am. J. Physiol. 261: H853 - H859.

Hurtado C. and Pierce G.N. (2001) Sodium-hydrogen exchange inhibition: pre- versus post-ischemic treatment. Basic Res. Cardiol. 96: 312 - 317.

Ikeda U., Arisaka H., Takayasu T., Takeda K., Natsume T. and Hosoda S. (1988) Protein kinase C activation aggravates hypoxic myocardial injury by stimulating Na^+/H^+ exchange. J. Mol. Cell. Cardiol. 20: 493 - 500.

Inglefield J.R. and Schwartz-Bloom R.D. (1998a) Optical imaging of hippocampal neurons with a chloride-sensitive dye: early effects of in vitro ischemia. J. Neurochem. 70: 2500 - 2509.

Inglefield J.R. and Schwartz-Bloom R.D. (1998b) Activation of excitatory amino acid receptors in the rat hippocampal slice increases intracellular Cl^- and cell volume. J. Neurochem. 71: 1396 - 1404.

Inoue M., Fujishiro N. and Imanaga I. (1999) Na^+ pump inhibition and non-selective cation channel activation by cyanide and anoxia in guinea-pig chromaffin cells. J. Physiol. 519: 385 - 396.

Irie T., Hara M., Yasukura T., Minamino M., Omori K., Matsuda H., Inoue K. and Inagaki (1998) Chloride concentration in cultured hippocampal neurons increases during long-term exposure to ammonia through enhanced expression of an anion exchanger. Brain Res. 806: 246 - 256.

Irwin R.P., Lin S.-Z., Long R.T. and Paul S.M. (1994) *N*-methyl-D-aspartate induces a rapid, reversible, and calcium-dependent intracellular acidosis in cultured fetal rat hippocampal neurons. J. Neurosci. 14: 1352 - 1357.

Isagai T., Fujimura N., Tanaka E., Yamamoto S. and Higashi H. (1999) Membrane dysfunction induced by in vitro ischemia in immature rat hippocampal CA1 neurons. J. Neurophysiol. 81: 1866 - 1871.

Isom L.L., Cragoe Jr. E.J. and Limbird L.E. (1987) Multiple receptors linked to inhibition of adenylate cyclase accelerate Na^+/H^+ exchange in neuroblastoma x glioma cells via a mechanism other than decreased cAMP accumulation. J. Biol. Chem. 262: 17504 - 17509.

Iwai T., Tanonaka K., Inoue R., Kasahara S., Kamo N. and Takeo S. (2002) Mitochondrial damage during ischemia determine post-ischemic contractile dysfunction in perfused rat heart. J. Mol. Cell. Cardiol. 34: 725 - 738.

Iwamoto T., Watano T. and Shigekawa M. (1996) A novel isothiourea derivative selectively inhibits reverse mode of Na^+/Ca^{2+} exchange in cells expressing NCX1. J. Biol. Chem. 271: 22391 - 22397.

Jakubovicz D.E., Grinstein S. and Klip A. (1987) Cell swelling following recovery from acidification in C6 glioma cells: an in vitro model of postischemic brain edema. Brain Res. 435: 138 - 146.

Jakubovicz, D.E. and Klip, A. (1989) Lactic acid-induced swelling in C6 glial cells via Na^+/H^+ exchange. Brain Res. 485: 215 - 224.

Jarolimek W., Misgeld U. and Lux H.D. (1989) Activity dependent alkaline and acid transients in

guinea pig hippocampal slices. Brain Res. 505: 225 - 232.

Jean T., Frelin C., Vigne P., Barbry P. and Lazdunski M. (1985) Biochemical properties of the Na^+/H^+ exchange system in rat brain synaptosomes. J. Biol. Chem. 260: 9678 - 9684.

Jensen F.E. (2002) The role of glutamate receptor maturation in perinatal seizures and brain injury. Int. J. Devl. Neurosci. 20: 339 - 347.

Jiang C., Aqulian S. and Haddad G.G. (1992) Cl^- and Na^+ homeostasis during anoxia in rat hypoglossal neurons: intracellular and extracellular in vitro studies. J. Physiol. 448: 697 - 708.

Jørgensen N.K., Petersen S.F., Damgaard I., Schousboe A. and Hoffman E.K. (1999) Increases in $[Ca^{2+}]_i$ and changes in intracellular pH during chemical anoxia in mouse neocortical neurons in primary culture. J. Neurosci. Res. 56: 358-370.

Jourdain P., Nikonenko I., Alberi S. and Muller D. (2002) Remodeling of hippocampal synaptic networks by a brief anoxia-hypoglycemia. J. Neurosci. 22: 3108 - 3116.

Juel C. (1997) Lactate-proton cotransport in skeletal muscle. Physiol. Rev. 77: 321 - 358.

Juhaszuva M. and Blaustein M.P. (1997) Na^+ pump low and high ouabain affinity α subunits isoforms are differentially distributed in cells. Proc. Natl. Acad. Sci. 94: 1800 - 1805.

Jung D.W., Baysal K. and Brierley G.P. (1995) The sodium-calcium antiport of heart mitochondria is not electroneutral. J. Biol. Chem. 270: 672 - 678.

Kaila K. (1994) Ionic basis of $GABA_A$ receptor channel function in the nervous system. Prog. Neurobiol. 42: 489 - 537.

Kaila K. and Vaughan-Jones R.D. (1987) Influence of sodium-hydrogen exchange on intracellular pH, sodium and tension in sheep cardiac Purkinje fibres. J Physiol. 390: 93 - 118.

Kaila K. and Voipio J. (1987) Postsynaptic fall in intracellular pH induced by GABA-activated bicarbonate conductance. Nature 330: 163 - 165.

Kaila K., Vaughan-Jones R.D. and Bountra C. (1987) Regulation of intracellular pH in sheep cardiac Purkinje fibre: interactions among Na^+, H^+ and $Ca^{2+}{}_i$. Can. J. Physiol. Pharmacol. 65: 963 - 969.

Kaku D.A., Giffard R.G. and Choi D.W. (1993) Neuroprotective effects of glutamate antagonists and extracellular acidity. Science 260: 1516 - 1518.

Kalaria R.N., Premkumar D.R.D., Lin C.-W., Kroon S.N., Bae J.-Y., Sayre L.M. and LaManna J.C. (1998) Identification and expression of the Na^+/H^+ exchanger in mammalian cerebrovascular and choroidal tissues: characterization by amiloride-sensitive [^{3}H]MIA binding and RT-PCR analysis. Mol. Brain Res. 58: 178 - 187.

Kaneishi K., Sakuma Y., Kobayashi H. and Kato M. (2002) 3',5'-cyclic adenosine monophosphate augments intracellular Ca^{2+} concentration and gonadotropin hormone (GnRH) release in immortalized GnRH neurons in an Na^{+}-dependent manner. Endocrinology 143: 4210 - 4217.

Kang T.-C., An S.J., Park S.-K., Hwang I.-K., Suh J.-G., Oh Y.-S., Bae J.C. and Won M.H. (2002) Alterations in Na^{+}/H^{+} exchanger and Na^{+}/HCO_3^{-} cotransporter immunoreactivities within the gerbil hippocampus following seizure. Mol. Brain Res. 109: 226 - 232.

Kapus A., Romanek R. and Grinstein S. (1994) Arachidonic acid stimulates the plasma membrane H^{+} conductance of macrophages. J. Biol. Chem. 269: 4736 - 4745.

Kapus A., Romanek R., Qu A.Y., Rotstein O.D. and Grinstein, S. (1993) A pH-sensitive and voltage-dependent proton conductance in the plasma membrane of macrophages. J. Gen. Physiol. 102: 729 - 760.

Karmazyn M. (1988) Amiloride enhances postischemia ventricular recovery: possible role of Na^{+}-H^{+} exchange. Am J Physiol 255: H608 - H615.

Karmazyn M. (1999) Mechanisms of protection of the ischemic and reperfused myocardium by sodium-hydrogen exchange inhibition. J. Thrombosis Thrombolysis 8: 33 - 38.

Karmazyn M. (2001) Role of sodium-hydrogen exchange in cardiac hypertrophy and heart failure: a novel and promising therapeutic target. Basic Res. Cardiol. 96: 325 - 328.

Karmazyn M., Gan X.T., Humphreys R.A., Yoshida H. and Kusumoto K. (1999) The myocardial Na^{+}-H^{+} exchanger. Structure, regulation, and its role in heart disease. Circ. Res. 85: 777 - 786.

Karwatowska-Prokopczuk E., Nordberg J.A., Li H.L., Engler R.L. and Gottleib R.A. (1998) Effect of vacuolar proton ATPase on pH_i, Ca^{2+}, and apoptosis in neonatal cardiomyocytes during metabolic inhibition/recovery. Circ. Res. 82: 1139 - 1144.

Kass I.S. and Lipton P. (1982) Mechanisms involved in irreversible anoxic damage to the in vitro rat hippocampal slice. J. Physiol. 332: 459-472.

Kass I.S. and Lipton P. (1989) Protection of hippocampal slices from young rats against anoxic transmission damage is due to better maintenance of ATP. J. Physiol. 413: 1 - 11.

Katsura K., Kristián T., Smith M.-L. and Siesjö, B.K. (1994) Acidosis induced by hypercapnia exaggerates ischaemic brain damage. J. Cereb. Blood Flow Metab. 14: 243 - 250.

Kauppinen R.C, and Williams S.R. (1990) Cerebral energy metabolism and intracellular pH during severe hypoxia and recovery: a study using ^{1}H, ^{31}P, and $^{1}H[^{13}C]$ nuclear magnetic resonance spectroscopy in the guinea pig cerebral cortex in vitro. J. Neurosci. Res. 26: 356 - 369.

Kay A.R. and Wong R.K.S. (1986) Isolation of neurons suitable for patch-clamping from adult mammalian central nervous systems. J. Neurosci. Meth. 16: 227 – 238.

Keelan J., Vergun O. and Duchen M.R. (1999) Excitotoxic mitochondrial depolarization requires both calcium and nitric oxide in rat hippocampal neurons. J. Physiol. 520: 797 - 813.

Kelly T. and Church J. (2004) pH modulation of currents that contribute to the medium and slow afterhyperpolarizations in rat CA1 pyramidal neurones. J. Physiol. 554: 449 - 466.

Kent T.A., Soukup V.M. and Fabian R.H. (2001) Heterogeneity affecting outcome from acute stroke therapy. Stroke 32: 2318 - 2327.

Khandoudi N., Albadine J., Robert P., Krief S., Berrebi-Bertrand I., Martin X., Bevensee M.O., Boron W.F. and Bril A. (2001) Inhibition of the cardiac electrogenic sodium bicarbonate cotransporter reduces ischemic injury. Cardiovasc. Res. 52: 387 - 396.

Kiedrowski L. (1999) *N*-methyl-D-aspartate excitotoxicity: Relationships among plasma membrane potential, Na^+/Ca^{2+} exchange, mitochondrial Ca^{2+} overload, and cytoplasmic concentrations of Ca^{2+}, H^+, and K^+. Mol. Pharmacol. 56: 619 - 632.

Kiedrowski L., Brooker G., Costa E., and Wroblewski J.T. (1994) Glutamate impairs neuronal calcium extrusion while reducing sodium gradient. Neuron 12: 295 - 300.

Kilb W. and Schlue W.R. (1999) Mechanism of the kainate-induced intracellular acidification in leech Retzius neurons. Brain Res. 824:168 - 182.

Kimura M. and Aviv A. (1993) Regulation of the cytosolic pH set point for activation of the Na^+/H^+antiport in human platelets: the roles of the Na^+/Ca^{2+} exchange, the Na^+-K^+-$2Cl^-$ cotransport and cellular volume. Pflügers Arch. 422: 585 - 590.

Kimura M., Sawada K., Miyagawa T., Kuwada M., Katayama K. and Nishizawa Y. (1998) Role of glutamate receptors and voltage-dependent calcium and sodium channels in the extracellular glutamate/aspartate accumulation and subsequent neuronal injury induced by oxygen/glucose deprivation in cultured hippocampal neurons. J. Pharmacol. Exp. Ther. 285: 178 - 185.

Kinsella J.L. and Aronson P.S. (1981) Interaction of NH_4^+ and Li^+ with the renal microvillus membrane Na^+-H^+ exchanger. Am. J. Physiol. 241: C220 - C226.

Kintner D.B., Su G., Lenart B.A., Ballard A.J., Meyer J.W., Ng L.L., Shull G.E. and Sun D. (2004) Increased tolerance to oxygen and glucose deprivation in astrocytes from Na^+/H^+ exchanger isoform 1 null mice. Am. J. Physiol. 287: C12 - C21.

Kitayama J., Kitazono T., Yao H., Ooboshi H., Takaba H., Ago T., Fujishima M. and Ibayashi S. (2001) Inhibition of Na^+/H^+ exchanger reduces infarct volume of focal cerebral ischemia in rats. Brain Res. 922: 223 - 228.

Knöpfel T., Anchisi D., Alojado M.E., Tempia F. and Strata P. (2000) Elevation of intradendritic sodium concentration mediated by synaptic activation of metabotropic glutamate receptors in cerebellar Purkinje cells. Eur. J. Neurosci. 12: 2199 - 2204.

Kobayashi M., Lust W.D. and Passonneau, J.V. (1977) Concentrations of energy metabolites and cyclic nucleotides during and after bilateral ischemia in the gerbil cerebral cortex. J. Neurochem. 29: 53 -

59.

Kobayashi S., Morgans C.W., Casey J.R. and Kopito R.R. (1994) AE3 anion exchanger isoforms in the vertebrate retina: developmental regulation and differential expression in neurons and glia. J. Neurosci. 14: 6266 - 6279.

Koch R.A. and Barish M.E. (1994) Perturbation of intracellular calcium and hydrogen regulation in cultured mouse hippocampal neurons by reduction of the sodium ion concentration gradient. J. Neurosci. 14, 2585 - 2593.

Kohr G. and Mody I. (1991) Endogenous intracellular calcium buffering and the activation/inactivation of HVA calcium currents in rat dentate gyrus granule cells. J. Gen. Physiol. 98: 941 - 967.

Konorev E.A., Zhang H., Joseph J., Kennedy M.C. and Kalyanaraman B. (2000) Bicarbonate exacerbates oxidative injury induced by antitumor antibiotic doxorubicin in cardiomyocytes. Am. J. Physiol. 279: H2424 - H2430.

Kourie J.I. (1998) Interaction of reactive oxygen species with ion transport mechanisms. Am. J. Physiol. 275: C1 - C24.

Kraig R.P., Petito C.K., Plum F. and Pulsinelli, W.A. (1987) Hydrogen ions kill brain at concentrations reached in ischemia. J. Cereb. Blood Flow Metab. 7: 379 - 386.

Kramer R.H. and Tibbs G.R. (1996) Antagonists of cyclic nucleotide-gated channels and molecular mapping of their site of action. J. Neurosci. 16: 1285 - 1293.

Kreisman N.R. and LaManna J.C. (1999) Rapid and slow swelling during hypoxia in the CA1 region of rat hippocampal slices. J. Neurophysiol. 82: 320 - 329.

Krishek B.J., Amato A., Connolly C.N., Moss S.J. and Smart T.G. (1996) Proton sensitivity of the $GABA_{(A)}$ receptor is associated with the receptor subunit composition. J. Physiol. 492: 431 - 443.

Krishtal O.A., Osipchuk Y.V., Shelest T.N. and Smirnoff S.V. (1987) Rapid extracellular pH transients related to synaptic transmission in rat hippocampal slices. Brain Res. 436: 352 - 356.

Kristián T. and Siesjö B.K. (1997) Calcium in ischemic cell death. Stroke 29: 705 - 718.

Krnjević K. and Walz W. (1990) Acidosis and blockage of orthodromic responses caused by anoxia in rat hippocampal slices at different temperatures. J. Physiol. 422: 127 - 144.

Kubo T., Yokoi T., Hagiwara Y., Fukumori R., Goshima Y. and Misu Y. (2001) Characteristics of protective effects of NMDA antagonist and calcium channel antagonist on ischemic calcium accumulation in rat hippocampal CA1 region. Brain Res. Bull. 54: 413 - 419.

Kuribayashi Y., Itoh N., Kitano M. and Ohashi N. (1999) Cerebroprotective properties of SM-20220, a potent Na^+/H^+ exchange inhibitor, in transient cerebral ischemia in rats. Eur. J. Pharmacol. 383: 163 - 168.

Kurtz I. (1987) Apical Na^+/H^+ antiporter and glycolysis-dependent H^+-ATPase regulate intracellular pH in the rabbit S_3 proximal tubule. J. Clin. Invest. 80: 928 - 935.

Lagadic-Gossmann D., Huc L. and Lecureur V. Alterations of intracellular pH homeostasis in apoptosis: origins and roles. Cell Death and Diff. 11: 953 - 961.

Lahtinen H., Autere A.-M., Paalasmaa P., Lauri S.E. and Kaila K. (2001) Post-insult activity is a major cause of delayed neuronal death in organotypic hippocampal slices exposed to glutamate. Neuroscience 105: 131 - 137.

LaManna J.C., Neal M., Xu K. and Haxhiu M.A. (2003) Differential expression of intracellular acidosis in rat brainstem regions in response to hypercapnic ventilation. Adv. Exp. Med. Biol. 536: 407 - 413.

Lambeth D.O. and Palmer G. (1973) The kinetics and mechanism of reduction of electron transfer proteins and other compounds of biological interest by dithionite. J. Biol. Chem. 248: 6095 - 6103.

Lamers J.M.J. (2001) Unmasking of a novel target for blocking harmful Na^+ coupled acid extrusion: electrogenic Na^+-HCO_3^- symport. Cardiovasc. Res. 52: 339 - 344.

Lang F., Busch G.L. and Völkl H. (1998) The diversity of volume regulatory mechanisms. Cell. Physiol. Biochem. 8: 1 - 45.

Lansman J.B., Hess P. and Tsien R.W. (1986) Blockade of current through single calcium channels by Cd^{2+}, Mg^{2+} and Ca^{2+}. Voltage and concentration dependence of calcium entry into the pore. J. Gen. Physiol. 88: 321 - 347.

Lasser-Ross N. and Ross W.N. (1992) Imaging voltage and synaptically activated sodium transients in cerebellar Purkinje cells. Proc. R. Soc. Lond. B. 247: 35 - 39.

Lazdunski M., Frelin C. and Vigne P. (1985) The sodium/hydrogen exchange system in cardiac cells: its biochemical and pharmacological properties and its role in regulating internal concentrations of sodium and internal pH. J. Mol. Cell. Cardiol. 17: 1029 - 1042.

LeBlanc M.H., Huang M., Vig V., Patel D. and Smith E.E. (1993) Glucose affects the severity of hypoxic-ischemic brain injury in newborn pigs. Stroke 24: 1055 - 1062.

Leblond J. and Krnjević K. (1989) Hypoxic changes in hippocampal neurons. J. Neurophysiol. 62: 1 -14.

Lee J.M., Zinfel G.J. and Choi D.W. (1999) The changing landscape of ischaemic brain injury mechanisms. Nature 399: A7 - 14.

Lees K.R., Asplund K., Carolei A., Davis S.M., Diener H.-C., Kaste M., Orgogozo J.-M. and Whitehead J. for the GAIN International Investigators. (2000) Glycine antagonist (gavestinel) in neuroprotection (GAIN International) in patients with acute stroke: a randomised controlled trial. Lancet 355: 1949 - 1954.

Lei S. and MacDonald J.F. (2001) Gadolinium reduces AMPA receptor desensitization and deactivation in hippocampal neurons. J. Neurophysiol. 86: 173 - 182.

Lemars J.M.J. (2001) Unmasking of a novel target for blocking harmful Na^+ coupled acid extrusion: electrogenic Na^+-HCO_3^- symport. Cardiovasc. Res. 52: 339 - 344.

Lenart B., Kintner D.B., Shull G.E. and Sun D. (2003) Genetic ablation of Na^+-K^+-Cl^- cotransporter isoform 1 (NKCC1) protects astrocytes from OGD-mediated damage. Soc. Neurosci. Abstr. 31: 308.1

Leslie C.C. (1997) Properties and regulation of cytsolic phospholipase A_2. J. Biol. Chem. 272: 16709 - 16712.

Levine S.A., Montrose M.H., Tse C.M. and Donowitz, M. (1993) Kinetics and regulation of three cloned mammalian Na^+/H^+ exchangers stably expressed in a fibroblast cell line. J. Biol. Chem. 268: 25527 - 25535.

Li H. and Buchan A.M. (1993) Treatment with an AMPA antagonist 12 hours following severe normothermic forebrain ischemia prevents CA1 neuronal injury. J. Cereb. Blood Flow Metab. 13: 933 - 939.

Li P.-A., Kristián T., Shamloo M. and Siesjö B.K. (1996) Effects of preischemic hyperglycemia on brain damage incurred by rats subjected to 2.5 or 5 minutes of forebrain ischemia. Stroke 27: 1592 - 1602.

Li P.-A., Shamloo M. Katsura K., Smith M.-L. and Siesjö B.K. (1995) Critical values for plasma glucose in aggravating ischemic brain damage: correlation to extracellular pH. Neurobiol. Dis. 2: 97 - 104.

Li. S., Jiang Q. and Stys P.K. (2000) Important role of reverse Na^+-Ca^{2+} exchange in spinal cord white matter injury at physiological temperature. J. Neurophysiol. 84: 1116 - 1119.

Limbrick Jr. D.D., Sombati S., and DeLorenzo R.J. (2003) Calcium influx constitutes the ionic basis for the maintenance of glutamate-induced extended neuronal depolarization associated with hippocampal neuronal death. Cell Calcium 33: 69 - 81.

Lin M.R., Henteleff H.B., and Nemoto E.M. (1983) Noradrenaline-inducible cyclic-AMP accumulation in rat cerebral cortex: changes during complete global ischemia. J. Neurochem. 40: 595 - 598.

Lipton P. (1999) Ischemic cell death in brain neurons. Physiol. Rev. 79: 1431 - 1568.

Lipton P. and Whittingham T.S. (1982) Reduced ATP concentration as a basis for synaptic transmission failure during hypoxia in the in vitro guinea-pig hippocampus. J. Physiol. 325: 51 - 65.

Liu H., Moczydlowski E. and Haddad G.G. (1999) O_2 deprivation inhibits Ca^{2+}-activated K^+ channels via cytosolic factors in mice neocortical neurons. J. Clin. Invest. 104: 577 - 588.

Liu J., Diwu Z., Leung W.-Y. (2001) Synthesis and photophysical properties of new fluorinated benzo[c]xanthene dyes as intracellular pH indicators. Bioorgan. Med. Chem. Lett. 11: 2903 - 2905.

Ljunggren, D., Norberg, K. and Siesjö, B.K. (1974) Influence of tissue acidosis upon restitution of brain energy metabolism following total ischemia. Brain Res. 77: 173 - 186.

Lo E.H., Dalkara T. and Moskowitz M.A. (2003) Mechanisms, challenges and opportunities in stroke. Nat. Rev. Neurosci. 4: 399 - 415.

LoPachin R.M., Gaughan C.L., Lehning E.J., Weber M.L. and Taylor C.P. (2001) Effects of ion channel blockade on the distribution of Na^+,K^+, Ca^{2+} and other elements in oxygen-glucose deprived CA1 hippocampal neurons. Neuroscience 103: 971 - 983.

Ludt J., Tønnessen T.I., Sandvig K. and Olsnes S. (1991) Evidence for involvement of protein kinase C in regulation of intracellular pH by Cl^-/HCO_3^- antiport. J. Membrane Biol. 119: 179 - 186.

Lukacs G.L., Kapus A., Nanda A., Romanek R. and Grinstein, S. (1993) Proton conductance of the plasma membrane: properties, regulation, and functional role. Am. J. Physiol. 265, C3 - C14.

Ma E. and Haddad G.G. (1997) Expression and localization of Na^+/H^+ exchangers in rat central nervous sytem. Neuroscience 79: 591 - 603.

Mabe H., Blomqvist P., and Siesjö B.K. (1983) Intracellular pH in the brain following transient ischemia. J. Cereb. Blood Flow Metab. 3: 109 - 114.

MacLeod K.T. (1989) Effects of hypoxia and metabolic inhibition on the intracellular sodium activity of mammalian ventricular muscle. J. Physiol. 416: 455 - 468.

Maddaford T.G. and Pierce G.N. (1997) Myocardial dysfunction is associated with activation of Na^+/H^+ exchange immediately during reperfusion. Am. J. Physiol. 273: H2232 - H2239.

Maduh E.U., Borowitz J.L. and Isom G.E. (1990) Cyanide-induced alterations of cytosolic pH: involvement of cellular hydrogen ion handling processes. Tox. Appl. Pharm. 106: 201 - 208.

Malek S.A., Coderre E. and Stys P.K. (2003) Aberrant chloride transport contributes to anoxic/ischemic white matter injury. J. Neurosci. 23: 3826 - 3836.

Manzerra P., Behrens M.M., Canzoniero L.M.T., Wang X.Q., Heidinger V., Ichinose T., Yu S.P. and Choi D.W. (2001) Zinc induces a Src family kinase-mediated up-regulation of NMDA receptor activity and excitotoxicity. Proc. Natl. Acad. Sci. 98: 11055 - 11061.

Marks J.D., Bindokas V.P. and Zhang X-M. (2000) Maturation of vulnerability to excitotoxicity: intracellular mechanisms in cultured postnatal hippocampal neurons. Dev. Brain Res. 12: 101 - 116.

Martin R.L., Lloyd H.G.E. and Cowan A.I. (1994) The early events of oxygen and glucose deprivation: setting the scene for neuronal death? Trends Neurosci.17: 251 - 257.

Martínez-Zaguilán R., Martínez G.M., Lattanzio F. and Gillies R.J. (1991) Simultaneous measurement of intracellular pH and Ca^{2+} using the fluorescence of SNARF-1 and fura-2. Am. J. Physiol. 260: C297 - C307.

Martínez-Zaguilán R., Parnami G. and Lynch R.M. (1996) Selection of ion indicators for simultaneous measurements of pH and Ca^{2+}. Cell Calcium 19: 337 - 349.

Matsuda T., Arakawa N., Takuma K., Kishida Y., Kawasaki Y., Sakaue M., Takahashi K., Takahashi T., Suzuki T., Ota T., Hamano-Takahashi A., Onishi M., Tanaka Y., Kameo K., Baba A. (2001) SEA0400, a novel and selective inhibitor of the Na^{+}-Ca^{2+} exchanger, attenuates reperfusion injury in the in vitro and in vivo cerebral ischemic models. J. Pharmacol. Exp. 298: 249 - 256.

Matsumoto Y., Yamamoto S., Suzuki Y., Tsuboi T., Terakawa S., Ohashi N., Umemura K. (2003) Na^{+}/H^{+} exchanger inhibitor, SM-20220, is protective against excitotoxicity in cultured cortical neurons. Stroke 35: 185 - 190.

Matsuyama S., Llopis J., Deveraux Q.L., Tsien R.Y. and Reed J.C. (2000) Changes in intramitochondrial and cytosolic pH: early events that modulate caspase activation during apoptosis. Nature Cell Biol. 2: 318 - 325.

Mazza Jr. E., Edelman N.H. and Neubauer J.A. (2000) Hypoxic excitation in neurons cultured from the rostral ventrolateral medulla of the neonatal rat. J. Appl. Physiol. 88: 2319 - 2329.

Meech R. W. and Thomas R.C. (1987) Voltage-dependent intracellular pH in Helix aspersa neurones. J. Physiol. 390: 433 - 452.

Meldrum B.S. (1996) The role of nitric oxide in ischemic damage, in Advances in Neurology, Vol. 71: Cellular and Molecular Mechanisms of Ischemic Brain Damage, (Siesjö B.K. and Wieloch T., eds), pp. 355 - 363. Lippincott-Raven, Philadelphia.

Melzian D., Scheufler E., Grieshaber M. and Tegtmeier F. (1996) Tissue swelling and intracellular pH in the CA1 region of anoxic rat hippocampus. J. Neurosci. Methods 65: 183 - 187.

Menna G., Tong C.K. and Chesler M. (2000) Extracellular pH changes and accompanying cation shifts during ouabain-induced spreading depression. J. Neurophysiol. 83: 1338 - 1345.

Messier M.L., Bouyer P., Lavoie C. and Boron W.F. (2004) Effect of acute and chronic hypoxia on intracellular pH regulation in cultured rat hippocampal neurons. FASEB Exp. Biol. Abstr. 674.3.

Meyer T.M., Munsh T. and Pape H.C. (2000) Activity-related changes in intracellular pH in rat thalamic relay neurons. NeuroReport 11: 33 - 37.

Minta A. and Tsien R.Y. (1989) Fluorescent indicators for cytosolic sodium. J Biol. Chem. 264: 19449 - 19457.

Mironov S.L. and Richter D.W. (1999) Cytoskeleton mediates inhibition of the fast Na^{+} current in respiratory brainstem neurons during hypoxia. Eur. J. Neurosci. 11: 1831 - 1834.

Mitani A., Namba S., Ikemune K., Yanase H., Arai T. and Kataoka K. (1998) Postischemic enhancements of *N*-methyl-D-aspartic acid (NMDA) and non-NMDA receptor-mediated responses in hippocampal CA1 pyramidal neurons. J. Cereb. Blood Flow Metab. 18: 1088 - 1098.

Mitani A., Takeyasu S., Yanase H., Nakamura Y. and Kataoka K. (1994) Changes in intracellular Ca^{2+} and energy levels during in vitro ischemia in the gerbil hippocampal slice. J. Neurochem. 62, 626 - 634.

Mody I., Salter M.W. and MacDonald J.F. (1989) Whole-cell voltage-clamp recordings in granule cells acutely isolated from hippocampal slices of adult or aged rats. Neurosci. Lett. 96: 70 - 75.

Moody Jr, WJ (1981) The ionic mechanism of intracellular pH regulation in crayfish neurones. J Physiol 316: 293 - 308.

Moor A.N., Gan X.T., Karmazyn M. and Fliegel L. (2001) Activation of Na^+/H^+ exchanger-directed protein kinases in the ischemic and ischemic-reperfused rat myocardium. J. Biol. Chem. 276: 16113 - 16122.

Morris M.E., Baimbridge K.G., el-Beheiry H., Obrocea G.V. and Rosen A.S. (1995) Correlation of anoxic neuronal responses and calbindin-D28k localization in stratum pyramidale of rat hippocampus. Hippocampus 5: 25 - 39.

Motulsky H.J. and Ransnas L.A. (1987) Fitting curves to data using nonlinear regression: a practical and nonmathematical review. FASEB J. 1: 365 - 374.

Mukhin Y.V., Garnovskaya M.N., Ulliam M.E. and Raymond J.R. (2004) ERK is regulated by sodium-proton exchanger in rat aortic vascular smooth muscle cells. J. Biol. Chem. 279: 1845 - 1852.

Mulkey D.K., Henderson R.A. Ritucci N.A., Putnam R.W. and Dean J.B. (2004) Oxidative stress decreases intracellular pH and Na^+/H^+ exchange and increases excitability of solitary complex (SC) neurons from rat brain slices. Am. J. Physiol. 286: C940 - 951.

Müller M. (2000) Effects of chloride transport inhibition and chloride substitution on neuron function and on hypoxic spreading-depression-like depolarization in rat hippocampal slices. Neuroscience 97: 33 – 45.

Müller M. and Somjen G.G. (2000a) Na^+ dependence and the role of glutamate receptors and Na^+ channels in ion fluxes during hypoxia of rat hippocampal slices. J. Neurophysiol. 84: 1869 - 1880.

Müller M. and Somjen G.G. (2000b) Na^+ and K^+ concentrations, extra- and intracellular voltages, and the effect of TTX in hypoxic rat hippocampal slices. J. Neurophysiol. 83: 735 - 745.

Munsch T. and Deitmer J.W. (1997) Intracellular Ca^{2+}, Na^+ and H^+ transients evoked by kainate in the leech giant glial cells in situ. Neurosci. Res. 27: 45 - 56.

Mutch W.A.C. and Hansen A.J. (1984) Extracellular pH changes during spreading depression and cerebral ischemia: mechanisms of brain pH regulation. J. Cereb. Blood Flow Metab. 4: 17 - 27.

Myers R.E. and Yamaguchi S.-I. (1977) Nervous system effects of cardiac arrest in monkeys. Arch. Neurol. 34: 65 - 74.

Nabetani M, Okada Y, Takata T, Takada S, and Nakamura H. (1997) Neural activity and intracellular Ca^{2+} mobilization in the CA1 area of hippocampal slices from immature and mature rats during ischemia or glucose deprivation. Brain Res. 769: 158 - 162.

Nedergaard M. and Goldman S.A. (1993) Carrier-mediated transport of lactic acid in cultured neurons and astrocytes. Am. J. Physiol. 265: R282 - R289.

Nedergaard M., Goldman S.A., Desai S. and Pulsinelli W.A. (1991) Acid-induced death in neurons and glia. J. Neurosci. 11: 2489 - 2497.

Negulescu P.A. and Machen T.E. (1990) Intracellular ion activities and membrane transport in parietal cells measured with fluorescent dyes. Meth. Enzymol. 192: 38 - 81.

Nelson N. and Klionsky D.J. (1996) Vacuolar H^+-ATPase: from mammals to yeast and back. Experientia 52: 1101 - 1110.

Nett W. and Deitmer J.W. (1996) Simultaneous measurements of intracellular pH in the Leech giant glial cell using 2′,7′-bis-(2-carboxyethyl)-5(6)-carboxyfluorescein and ion-sensitive microelectrodes. Biophysical J. 71: 394 - 402.

Nett W. and Deitmer J.W. (1998) Intracellular Ca^{2+} regulation by the leech giant glial cell. J. Physiol. 507: 147 - 162.

Newell D.W., Barth A., Papermaster V. and Malouf A.T. (1995) Glutamate and non-glutamate receptor mediated toxicity caused by oxygen and glucose deprivation in organotypic hippocampal cultures. J. Neurosci. 15: 7702 - 7711.

NINDS study group (1995) Tissue plasminogen activator for acute ischemic stroke. The National Institute of Neurological Disorders and Stroke rt-PA Stroke Study Group. N. Engl. J. Med. 333: 1581 - 1587.

Nordmann J.J. and Stuenkel E.L. (1991) Ca^{2+}-independent regulation of neurosecretion by intracellular Na^+. FEBS Lett. 292: 37 - 41.

Nottingham S., Leiter J.C., Wages P., Buhay S. and Erlichman J.S. (2001) Developmental changes in intracellular pH regulation in medullary neurons of the rat. Am. J. Physiol. 281: R1940 - R1951.

Nowicky A.V. and Duchen M.R. (1998) Changes in $[Ca^{2+}]_i$ and membrane currents during impaired mitochondrial metabolism in dissociated rat hippocampal neurons. J. Physiol. 507: 131 - 145.

Numata M. and Orlowski J. (2001) Molecular cloning and characterization of a novel $(Na^+,K^+)/H^+$ exchanger located to the trans-Golgi network. J. Biol. Chem. 276: 17387 - 17394.

Numata M., Petrecca K., Lake N. and Orlowski J. (1998) Identification of a mitochondrial Na^+/H^+ exchanger. J. Biol. Chem. 273: 6951 - 6959.

Nurse S. and Corbett D. (1996) Neuroprotection after several days of mild, drug-induced hypothermia. J. Cereb. Blood Flow Metab. 16: 474 - 480.

O'Neill W.C. (1999) Physiological significance of volume-regulatory transporters. Am. J. Physiol. 276: C995 - C1011.

O'Reilly J.P., Cummins T.R. and Haddad G.G. (1997) Oxygen deprivation inhibits Na^+ currents in rat hippocampal neurons via protein kinase C. J. Physiol. 503: 479 - 488.

O'Reilly J.P., Jiang C. and Haddad, G.G. (1995) Major differences in response to graded hypoxia between hypoglossal and neocortical neurons. Brain Res. 683: 179 - 186.

Obeidat A.S., Jarvis C.R. and Andrew R.D. (2000) Glutamate does not mediate acute neuronal damage after spreading depression induced by O_2/glucose deprivation in the hippocampal slice. J. Cereb. Blood Flow Metab. 20: 412 - 422.

Obrenovitch T.P., Scheller D., Matsumoto T., Tegtmeier F., Höller M. and Symon L. (1990) A rapid redistribution of hydrogen ions is associated with depolarization and repolarization subsequent to cerebral ischemia reperfusion. J. Neurophysiol. 64: 1125 - 1133.

Ohno M., Obrenovitch T.P., Hartell N., Barratt S., Bachelard H.S. and Symon L. (1989) Simultaneous recording of tissue PCO_2, interstitial pH and potassium activity in the rat cerebral cortex during anoxia and the subsequent recovery period. Neurol. Res. 11: 153 - 159.

Olney J.W., Ho O.L. and Rhee V. (1971) Cytotoxic effects of acidic and sulphur containing amino acids on the infant mouse central nervous system. Exp. Brain Res. 14: 61 - 76.

Orlowski J. and Grinstein S. (2004) Diversity of the mammalian sodium/proton exchanger SLC9 gene family. Pflügers Arch. 447: 549 - 565.

Ortiz P.A., Hong N.J. and Garvin J.L. (2001) NO decreases thick ascending limb chloride absorption by reducing Na^+-K^+-$2Cl^-$ cotransporter activity. Am. J. Physiol. 281: F819 - F825.

Ou-Yang Y., Mellergard P. and Siesjö B.K. (1993) Regulation of intracellular pH in single rat cortical neurons in vitro: a microspectrofluorometric study. J. Cereb. Blood Flow Metab. 12: 827 - 840.

Ou-Yang Y.B., Kristián T., Mellergård P. and Siesjö B.K. (1994a) The influence of pH on glutamate- and depolarization-induced increases of intracellular calcium concentration in cortical neurons in primary culture. Brain Res. 646: 65 - 72.

Ou-Yang Y.B., Mellergård P., Kristián T., Kristiánova V. and Siesjö B.K. (1994b) Influence of acid-base changes on the intracellular calcium concentration of neurons in primary culture. Exp. Brain Res. 101: 265 - 271.

Papadopoulos M.C., Koumenis I.L., Yuan T.Y. and Giffard R.G. (1998) Increasing vulnerability of astrocytes to oxidative injury with age despite constant antioxidant defenses. Neuroscience 82: 915 – 925.

Paquet-Durand F. and Bicker G. (2004) Hypoxic/ischemic cell damage in cultured human NT-2 neurons. Brain Res. 1011: 33 - 47.

Park C.-O., Xiao X.-H. and Allen D.G. (1999) Changes in intracellular Na^+ and pH in rat heart during ischemia: role of Na^+/H^+ exchanger. Am. J. Physiol. 276: H1581 - H1590.

Parsons M.W., Barber P.A., Desmond P.M., Baird T.A., Darby D.G., Byrnes G., Tress B.M. and Davis S.M. (2002) Acute hyperglycemia adversely affects stroke outcome: a magnetic resonance imaging and spectroscopy study. Ann. Neurol. 52: 20 - 28.

Partridge L.D. and Valenzuela C.F. (2000) Block of hippocampal CAN channels by flufenamate. Brain Res. 867: 143 - 148.

Patel M., Day B.J., Crapo J.D., Fridovich I. and McNamara J.O. (1996) Requirement for superoxide in excitotoxic cell death. Neuron 16: 345 - 355.

Pedersen S.F., King S.A., Rigor R.R., Zhuang Z., Warren J.M. and Cala R.M. (2003) Molecular cloning of NHE1 from winter flounder RBCs: activation by osmotic shrinkage, cAMP, and calyculin A. Am. J. Physiol. 284: C1561 - C1576.

Pedersen, S.F., Jorgensen, N.K., Damgaard, I., Schousboe, A. and Hoffmann, E.K. (1998) Mechanisms of pH_i regulation studied in individual neurons cultured from mouse cerebral cortex. J. Neurosci. Res. 51: 431 - 441.

Pellegrini-Giampietro D.E., Gorter J.A., Bennett M.V.L. and Zukin R.S. (1997) The GluR2 (GluR-B) hypothesis: Ca^{2+}-permeable AMPA receptors in neurological disorders. Trends. Neurosci. 20: 464 - 470.

Pereira C., Ferreira C., Carvalho C., and Oliveira C. (1996) Contribution of plasma membrane and endoplasmic reticulum Ca^{2+}-ATPases to the synaptosomal $[Ca^{2+}]_i$ increase during oxidative stress. Brain Res. 713: 269 - 277.

Perez-Velazquez J.L., Valiante T.A. and Carlen P.L. (1994) Modulation of gap junctional mechanisms during calcium-free induced field burst activity: a possible role for electrotonic coupling in epileptogenesis. J. Neurosci. 14: 4308 - 4317.

Petrovic S., Spicer Z., Greeley T., Shull G.E. and Soleimani M. (2002) Novel Schering and ouabain-insensitive potassium-dependent proton secretion in the mouse cortical collecting duct. Am. J. Physiol. 282: F133 - F143.

Phillis J.W. and O'Regan M.H. (2004) A potentially critical role of phospholipases in central nervous system ischemic, traumatic and neurodegenerative disorders. Brain. Res. Rev. 44: 13 - 47.

Phillis J.W., Estevez A.Y., Guyot L.L. and O'Regan M.H. (1999) 5-(N-ethyl-N-isopropyl)-amiloride, an Na^+-H^+ exchange inhibitor, protects gerbil hippocampal neurons from ischemic injury. Brain Res. 839:199 - 202.

Phillis J.W., O'Regan M.H. and Song D. (1998) 5-(*N*-ethyl-*N*-isopropyl)-amiloride inhibits amino acid release from ischemic rat cerebral cortex: role of Na^+-H^+ exchange. Brain Res. 812: 297 - 300.

Pike M.M., Luo C.S., Clark M.D., Kirk K.A., Kitakaze M., Madden M.C., Cragoe Jr., E.J. and Pohost G.M. (1993) NMR measurements of Na^+ and cellular energy in ischemic rat heart: role of Na^+ - H^+ exchange. Am. J. Physiol. 265: H2017 - H2026.

Pilitsis J.G., Diaz F.G., O'Regan M.H. and Phillis J.W. (2001) Inhibition of Na^+/H^+ exchange by SM-20220 attenuates free fatty acid efflux in rat cerebral cortex during ischemia-reperfusion injury. Brain Res. 913: 156 - 158.

Pinelis V.G., Segal M., Greenberger V. and Khodorov B.I. (1994) Changes in cytosolic sodium caused by a toxic glutamate treatment of cultured hippocampal neurons. Biochem. Mol. Biol. Int. 32: 475 - 482.

Pirttilä T.-R.M. and Kauppinen R.A. (1992) Recovery of intracellular pH in cortical brain slices following anoxia studied by nuclear magnetic resonance spectroscopy: role of lactate removal, extracellular sodium and sodium/hydrogen exchange. Neuroscience 47: 155 - 164.

Pirttilä T.-R.M. and Kauppinen R.A. (1994) Regulation of intracellular pH in guinea pig cerebral cortex ex vivo studied by ^{31}P and ^{1}H nuclear magnetic resonance spectroscopy: Role of extracellular bicarbonate and chloride. J. Neurochem. 62: 656 - 664.

Pisani A., Calabresi P. and Bernardi G. (1997) Hypoxia in striatal and cortical neurons: membrane potential and Ca^{2+} measurements. Neuro Report 8: 1143 - 1147.

Pisani A., Calabresi P., Tozzi A., Bernardi G. and Knopfel T. (1998a) Early sodium elevations induced by combined oxygen and glucose deprivation in pyramidal cortical neurons. Eur. J. Neurosci. 10: 3572 - 3584.

Pisani A., Calabresi P., Tozzi A., D'Angelo V. and Bernardi G. (1998b) L-type Ca^{2+} channel blockers attenuate electrical changes and Ca^{2+} rise induced by oxygen/glucose deprivation in cortical neurons. Stroke 29: 196 - 202.

Plotkin M.D., Snyder E.Y., Hebert S.C. and Delpire E. (1997) Expression of the Na^+-K^+-$2Cl^-$ cotransporter is developmentally regulated in postnatal rat brains: a possible mechanism underlying GABA's excitatory role in immature brain. J. Neurobiol. 33: 781 - 795.

Pocock G. and Richards C.D. (1992) Hydrogen ion regulation in rat cerebellar granule cells studied by single-cell fluorescence microscopy. Eur. J. Neurosci. 4: 136 - 143.

Poole R.C. and Halestrap A.P. (1993) Transport of lactate and other monocarboxylates across mammalian plasma membranes. Am. J. Physiol. 264: C761 - 782.

Prast H. and Philippu A. (2001) Nitric oxide as modulator of neuronal function. Prog. Neurobiol. 64: 51 - 68

Probert A.W., Borosky S., Marcoux F.W. and Tayler C.P. (1997) Sodium channel modulators prevent oxygen and glucose deprivation injury and glutamate release in rat neocortical cultures. Neuropharmacology. 36: 1031 - 1038.

Pulsinelli W.A., Brierley J.B. and Plum F. (1982) Temporal profile of neuoronal damage in a model of transient forebrain ischemia. Ann. Neurol. 11: 491 - 498.

Putnam R.W. (2001) Intracellular pH regulation of neurons in chemosensitive and nonchemosensitive areas of brain slices. Respir. Physiol. 129: 37 - 56.

Putney L.K., Denker S.P. and Barber D.L. (2002) The changing face of the Na^+/H^+ exchange, NHE1: structure, regulation, and cellular actions. Ann. Rev. Pharmacol. Toxicol. 42: 527 - 52.

Rader R.K. and Lanthorn T.H. (1989) Experimental ischemia induces a persistent depolarization blocked by decreased calcium and NMDA antagonists. Neurosci. Lett. 99: 125 - 130.

Raley-Susman K.M., Cragoe Jr. E.J., Sapolsky R.M. and Kopito R.R. (1991) Regulation of intracellular pH in cultured hippocampal neurons by an amiloride-insensitive Na^+/H^+ exchanger. J. Biol. Chem. 266: 2739 - 2745.

Raley-Susman K.M., Kass I.S., Cottrell J.E., Newman R.B., Chambers G. and Wang J. (2001) Sodium influx blockade and hypoxic damage to CA1 pyramidal neurons in rat hippocampal slices. J. Neurophysiol. 86: 2715 - 2726.

Raley-Susman K.M., Sapolsky R.M. and Kopito R.R. (1993) Cl^-/HCO_3^- exchange function differs in adult and fetal rat hippocampal neurons. Brain Res. 614: 308 - 314.

Raley-Susman, K.M. and Barnes, J.R. (1998) The effects of extracellular pH and calcium manipulation on protein synthesis and response to anoxia/aglycemia in the rat hippocampal slice. Brain Res. 782: 281 - 289.

Reddy R., Smith D., Wayman G., Wu Z., Villacres E.C. and Storm D.R. (1995) Voltage-sensitive adenylyl cyclase activity in cultured neurons: a calcium-independent phenomenon. J. Biol. Chem. 270: 14340 - 14346.

Reese T., Bochelen D., Baumann D., Rausch M., Sauter A. and Rudin M. (2002) Impaired functionality of reperfused brain tissue following short transient focal ischemia in rat. Magn. Reson. Imaging 20: 447 - 454.

Richmond P.H. and Vaughan-Jones R.D. (1997) Assessment of evidence for K^+-H^+ exchange in isolated type-1 cells of neonatal rat carotid body. Pflügers Arch. 434: 429 - 437.

Ritucci N.A., Chambers-Kersh L., Dean J.B., and Putnam R.W. (1998) Intracellular pH regulation in neurons from chemosensitive and nonchemosensitive areas of the medulla. Am. J. Physiol. 275: R1152 - R1163.

Ritucci N.A., Dean J.B. and Putnam R.W. (1997) Intracellular pH response to hypercapnia in neurons from chemosensitive areas of the medulla. Am. J. Physiol. 273: R433 - R441.

Robello M., Baldelli P. and Cupello A. (1994) Modulation by extracellular pH of the activity of $GABA_A$ receptors on rat cerebellum granule cells. Neuroscience 61: 833 - 837.

Roberts Jr. E.L. and Chih, C.-P. (1997). The influence of age on pH regulation in hippocampal slices before, during, and after anoxia. J. Cereb. Blood Flow Metab. 17: 560 - 566.

Roberts Jr. E.L., He J. and Chih C.-P. (2000) Rat hippocampal slices need bicarbonate for the recovery of synaptic transmission after anoxia. Brain Res. 875: 171 - 174.

Roberts Jr. E.L., He J. and Chih, C.-P. (1998) The influence of glucose on intracellular and extracellular pH in rat hippocampal slices during and after anoxia. Brain Res. 783: 44 - 50.

Romero M.F., Fulton C.M. and Boron W.F. (2004) The SLC4 family of HCO_3^- transporters. Pflügers Arch. 447: 495 - 509.

Romero M.F., Henry D., Nelson S., Harte P.J., Dillon A.K. and Sciortino C.M. (2000) Cloning and characterization of a Na^+-driven anion exchanger (NDAE1). J. Biol. Chem. 275: 24552 - 24559.

Roos A. and Boron W.F. (1981) Intracellular pH. Physiol. Rev. 61: 296 - 434.

Rose C.R. (2002) Na^+ signals at central synapses. Neuroscientist 8: 532 - 539.

Rose C.R. and Deitmer J.W. (1995) Stimulus-evoked changes of extra- and intracellular pH in the leech central nervous system. II. Mechanisms and maintenance of pH homeostasis. J. Physiol. 73: 132 - 140.

Rose C.R. and Ransom B.R. (1997) Regulation of intracellular sodium in cultured rat hippocampal neurones. J. Physiol. 499: 573 - 587.

Rothman S.M. (1983) Synaptic activity mediates death of hypoxic neurons. Science 220: 536 - 537.

Rothman S.M. (1985) The neurotoxicity of excitatory amino acids is produced by passive chloride influx. J. Neurosci. 5: 1483 - 1489.

Russell J.M. (2000) Sodium-potassium-chloride cotransport. Physiol. Rev. 80: 211 - 276.

Ruβ U., Balser C., Scholz W., Albus U., Lang H.J., Weichert A., Scholkens B.A. and Gogelein H. (1996) Effects of the Na^+/H^+-exchange inhibitor Hoe 642 on intracellular pH, calcium and sodium in isolated rat ventricular myocytes. Pflügers Arch. 433: 26 - 34.

Sabri A., Byron K.L., Samarel A.M., Bell J. and Lucchesi P.A. (1998) Hydrogen peroxide activates mitogen-activated protein kinases and Na^+-H^+ exchange in neonatal rat cardiac myocytes. Circ. Res. 82: 1053 - 1062.

Sakaue M., Nakamura H., Kaneko I., Kawasaki Y., Arakawa N., Hashimoto H., Koyama Y., Baba A. and Matusda T. (2000) Na^+-Ca^{2+} exchanger isoforms in rat neuronal preparations: different changes in their expression during postnatal development. Brain Res. 881: 212 - 216.

Sánchez-Armass S, Martínez-Zaguilán R, Martínez GM, and Gillies RJ. (1994) Regulation of pH in

rat brain synaptosomes. I. Role of sodium, bicarbonate, and potassium. J. Neurophysiol. 71: 2236 - 2248.

Santos M.S., Moreno A.J. and Carvalho A.P. (1996) Relationships between ATP depletion, membrane potential, and the release of neurotransmitters in rat nerve terminals. Stroke 27: 941 - 950.

Sapirstein A. and Bonventre J.V. (2000) Phospholipases A_2 in ischemic and toxic brain injury. Neurochem. Res. 25: 745 - 753.

Sapolsky R.M., Trafton J. and Tombaugh G.C. (1996) Excitotoxic neuron death, acidotic endangerment, and the paradox of acidotic protection, in Advances in Neurology, Vol. 71: Cellular and Molecular Mechanisms of Ischemic Brain Damage, (Siesjö B.K. and Wieloch T., eds), pp. 237-245. Lippincott-Raven, Philadelphia.

Sardet C., Franchi A. and Pouyssegur J. (1989) Molecular cloning, primary structure, and expression of the human growth factor-activatable Na^+/H^+ antiporter. Cell 56: 271 - 280.

Satoh H., Hayashi H., Katoh H., Terada H., Kobayashi A. (1995) Na^+/H^+ and Na^+/Ca^{2+} exchange in regulation of $[Na^+]_i$ and $[Ca^{2+}]_i$ during metabolic inhibition. Am. J. Physiol. 268: H1239 - H1248.

Satoh H., Hayashi H., Noda N., Terada H., Kobayashi A., Hirano M., Yamashita Y., Yamazaki N. (1994) Regulation of $[Na^+]_i$ and $[Ca^{2+}]_i$ in guinea pig myocytes: dual loading of fluorescent indicators SBFI and fluo 3. Am J Physiol 266: H568 - H576.

Satoh H., Sugiyama S., Nomura N., Terada H. and Hayashi H. (2001) Importance of glycolytically derived ATP for Na^+ loading via Na^+/H^+ exchange during metabolic inhibition in guinea pig ventricular myocytes. Clin. Sci. 101, 243 - 251.

Sattler R., Charlton M.P., Hafner M. and Tymianski M. (1998) Distinct influx pathways, not calcium load, determine neuronal vulnerability to calcium neurotoxicity. J. Neurochem. 71: 2349 - 2364.

Scanlon J.M., Brocard J.B., Stout A.K. and Reynolds I.J. (2000) Pharmacological investigation of mitochondrial Ca^{2+} transport in central neurons: studies with CGP-37157, an inhibitor of the mitochondrial Na^+-Ca^{2+} exchanger. Cell Calcium 28: 317 - 327.

Schäfer C., Ladilov Y.V., Schafer M. and Piper H.M. (2000) Inhibition of NHE protects reoxygenated cardiomyocytes independently of anoxic Ca^{2+} overload and acidosis. Am. J. Physiol. 279: H2143 - H2150.

Schellinger P.D., Kaste M. and Hacke W. (2004) An update on thrombolytic therapy for acute stroke. Curr. Opin. Neurol. 17: 69 - 77.

Schlue W.R. and Thomas R.C. (1985) A dual mechanism for intracellular pH regulation by leech neurones. J. Physiol. 364: 327 - 338.

Schmitt B.M., Berger U.V., Douglas R.M., Bevensee M.O., Hediger M.A., Haddad G.G. and Boron W.F. (2000) Na/HCO_3 cotransporters in rat brain: Expression in glia, neurons, and choroid plexus. J. Neurosci. 20: 6839 - 6848.

Schröder U.H., Breder J., Sabelhaus C.F. and Reymann K.G. (1999) The novel Na^+/Ca^{2+} exchange inhibitor KB-R7943 protects CA1 neurons in rat hippocampal slices against hypoxic/hypoglycemic injury. Neuropharmacology. 38: 319 - 321.

Schurr A., Payne R.S., Tseng M.T., Miller J.J. and Rigor B.M. (1999) The glucose paradox in cerebral ischemia: new insights. Ann. N Y. Acad. Sci. 893: 386 - 390.

Schwab A. (2001) Function and spatial distribution of ion channels and transporters in cell migration. Am. J. Physiol. 280: F739 - F747.

Schwiening C.J. (2002) pH phantoms - a physiological phenomenon? Physiol. News 46: 15 - 19.

Schwiening C.J. and Boron W.F. (1994) Regulation of intracellular pH in pyramidal neurones from the rat hippocampus by Na^+-dependent Cl^--HCO_3^- exchange. J. Physiol. 475: 59 - 67.

Schwiening C.J. and Thomas R.C. (1992) Mechanism of pH_i regulation by locust neurones in isolated ganglia: a microelectrode study. J. Physiol. 447: 693 - 709.

Schwiening C.J., Kennedy H.J. and Thomas R.C. (1993) Calcium-hydrogen exchange by the plasma membrane Ca-ATPase of voltage-clamped snail neurons. Proc. R. Soc. Lond. B. 253: 285-289.

Seksek O. and Bolard J. (1996) Nuclear pH gradient in mammalian cells revealed by laser microspectrofluorimetry. J. Cell. Sci. 109: 257 - 262.

Seksek O., Henry-Toulmé N., Sureau F. and Bolard J. (1991) SNARF-1 as an intracellular pH indicator in laser microspectrofluorometry: a critical assessment. Anal. Biochem. 193: 49 - 54.

Serrano O.K., Jovanovic A. and Terzic A. (1999) Inhibition of both Na^+/H^+ and bicarbonate-dependent exchange is required to prevent recovery of intracellular pH in single cardiomyocytes exposed to metabolic stress. Biosci. Reports 19: 99 - 107.

Sheldon C. and Church J. (2002a) Intracellular pH response to anoxia in acutely dissociated adult rat hippocampal CA1 neurons. J. Neurophysiol. 87: 2209 - 2224.

Sheldon C. and Church J. (2002b) Na^+/H^+ exchange: molecular regulation to therapeutic development. Clin. Invest. Med. 25: 229 - 232.

Sheldon C. and Church J. (2004) Reduced contribution from Na^+/H^+ exchange to acid extrusion during anoxia in adult rat hippocampal CA1 neurons. J. Neurochem. 88: 594 - 603.

Sheldon C., Cheng Y.M. and Church J. (2004) Concurrent measurements of the free cytosolic concentrations of H^+ and Na^+ ions with fluorescent indicators. Pflügers Arch. In press.

Sheline C.T., Behrens M.M. and Choi D.W. (2000) Zinc-induced cortical neuronal death: contribution of energy failure attributable to loss of NAD(+) and inhibition of glycolysis. J. Neurosci. 20: 3139 - 3146.

Shibata S., Kodama K., Tominaga K., Ueki S. and Watanabe S. (1992) Assessment of the role of adrenoceptor function in ischemia-induced impairment of 2-deoxyglucose uptake and CA1 field potential in rat hippocampal slices. Eur. J. Pharmacol. 221: 255 - 260.

Shrode L.D., Klein J.D., Douglas P.B., O'Neill W.C. and Putnam R.W. (1997) Shrinkage-induced activation of Na^+/H^+ exchange: role of cell density and myosin light chain phosphorylation. Am. J. Physiol. 272: C1968 - C1979.

Sidky A.O. and Baimbridge K.G. (1997) Calcium homeostatic mechanisms operating in cultured postnatal rat hippocampal neurones following flash photolysis of nitrophenyl-EGTA. J. Physiol. 504: 579 - 90.

Siemkowicz C. and Hansen A.J. (1981) Brain extracellular ion composition and EEG activity following 10 minutes ischemia in normo- and hyperglycaemic rats. Stroke 12: 236 - 240.

Siesjö B.K., Katsura K. and Kristián T. (1996) Acidosis-related damage, in Advances in Neurology, Vol. 71: Cellular and Molecular Mechanisms of Ischemic Brain Damage, (Siesjö B.K. and Wieloch T., eds), pp. 209-236. Lippincott-Raven, Philadelphia.

Silver I.A. and Erecińska M. (1990) Intracellular and extracellular changes in $[Ca^{2+}]_i$ in hypoxia and ischemia in rat brain in vivo. J. Gen. Physiol. 95: 837 - 866.

Silver I.A. and Erecińska M. (1992) Ion homeostasis in rat brain in vivo: intra- and extracellular $[Ca^{2+}]$ and $[H^+]$ in the hippocampus during recovery from short-term, transient ischemia. J. Cereb. Blood Flow. Metab. 12: 759 - 772.

Silver I.A. and Erecińska, M. (1994) Extracellular glucose concentration in mammalian brain: continuous monitoring of changes during increased neuronal activity and upon limitation in oxygen supply in normo-, hypo-, and hyperglycemic animals. J. Neurosci. 14: 5068 - 5076.

Silver I.A., Deas J. and Erecińska M. (1997) Ion homeostasis in brain cells: differences in intracellular ion responses to energy limitation between cultured neurons and glial cells. Neuroscience 78: 589 - 601.

Simon R.P., Swan J.H., Griffiths T. and Meldrum B.S. (1984) Blockade of *N*-methyl-D-aspartate receptors may protect against ischemic damage in the brain. Science 226: 850 - 852.

Small D.L., Monette R., Chakravarthy B., Durkin J., Barbe G., Mealing G., Morley P., and Buchan A.M. (1996) Mechanisms of 1S,3R-ACPD-induced neuroprotection in rat hippocampal slices subjected to oxygen and glucose deprivation. Neuropharmacology 35: 1037 - 1048.

Small D.L., Morley P. and Buchan A.M. (1999) Biology of ischemic cerebral cell death. Prog. Cardiovasc. Dis. 42: 185 - 207.

Smart T.G., Xie X. and Krishek B.J. (1994) Modulation of inhibitory and excitatory amino acid receptor ion channels by zinc. Prog. Neurobiol. 42: 393 - 441.

Smith G.A.M., Brett C.L. and Church J. (1998) Effects of noradrenaline on intracellular pH in acutely dissociated adult rat hippocampal CA1 neurones. J. Physiol. 512: 487 - 505.

Smith M.A., Herson P.S., Lee K., Pinnock R.D. and Ashford M.L. (2003) Hydrogen-peroxide-induced toxicity of rat striatal neurons involves activation of a non-selective cation channel. J. Physiol. 547: 417 - 425.

Smith M.L., von Hanwehr R. and Siesjö B.K. (1986) Changes in extra- and intracellular pH in the brain during and following ischemia in hyperglycemic and in moderately hypoglycemic rats. J. Cereb. Blood Flow Metab. 6: 574 - 583.

Snider B.J., Gottron F.J. and Choi D.W. (1999) Apoptosis and necrosis in cerebrovascular disease. Ann. N.Y. Sci. 893: 243 - 253.

Somjen G.G. (2002) Ion regulation in the brain: implications for pathophysiology. Neuroscientist 8: 254 - 267.

Somjen G.G. *Ions in the Brain. Normal Functions, Seizures, and Stroke.* New York: Oxford University Press, 2004

Spray, D.C. and Bennett, M.V.L. (1985) Physiology and pharmacology of gap junctions. Annu. Rev. Physiol. 47: 281 - 303.

Staley K.J., Soldo B.L. and Procter W.R. (1995) Ionic mechanisms of neuronal excitation by inhibitory $GABA_A$ receptors. Science 269: 977 - 981.

Stella N., Pellerin L. and Magistretti P.J. (1995) Modulation of the glutamate-evoked release of arachidonic acid from mouse cortical neurons: involvement of a pH-sensitive membrane phospholipase A_2 J. Neurosci. 15: 3307 - 3317.

Strijbos P.J.L.M., Leach M.J. and Garthwaite J. (1996) Vicious cycle involving Na^+ channels, glutamate release, and NMDA receptors mediates delayed neurodegeneration through nitric oxide formation. J. Neurosci. 15: 5004 - 5013.

Stys P.K. (1998) Anoxic and ischemic injury in myelinated axons in CNS white matter: from mechanistic concepts to therapeutics. J. Cereb. Blood Flow Metab. 18: 2 - 25.

Stys P.K. and LoPachin R.M. (1998) Mechanisms of calcium and sodium fluxes in anoxic myelinated central nervous system axons. Neuroscience 82: 21 - 32.

Su G., Kintner D.B. and Sun D. (2002) Contribution of Na^+-K^+-Cl^- cotransport to high-$[K^+]_o$-induced swelling and EAA release in astrocytes. Am. J. Physiol. 282: C1136 - C1146.

Sun D. and Murali S.G. (1999) Na^+-K^+-$2Cl^-$ cotransporter in immature cortical neurons: a role in intracellular Cl^- regulation. J. Neurophysiol. 81: 1939 - 1948.

Sun G.Y. and Hsu C.Y. (1996) Poly-phosphoinositide-mediated messengers in focal cerebral ischemia and reperfusion. J. Lipid Med. Cell. Signal. 14: 137 - 145.

Suszták K., Mocsai A., Ligeti E. and Kapus A. (1997) Electrogenic H^+ pathway contributes to stimulus-induced changes of intracellular pH and membrane potential in intact neutrophils: role of cytoplasmic phospholipase A_2. Biochem. J. 325: 501 - 510.

Suzuki Y., Matsumoto Y., Ikeda Y., Kondo K., Ohashi N. and Umemura K. (2002) SM-20220, a Na^+/H^+ exchanger inhibitor: effects on ischemic brain damage through edema and neutrophil accumulation in a rat middle cerebral artery occlusion model. Brain Res. 945: 242 - 248.

Szabó E.Z., Numata M., Shull G.E. and Orlowski J. (2000) Kinetic and pharmacological properties of human brain Na^+/H^+ exchanger isoform 5 stably expressed in Chinese hamster ovary cells. J. Biol. Chem. 275: 6302 - 6307.

Szászi K., Kurashima K., Kaibushi K., Grinstein S., Orlowski J. (2001) Role of the cytoskeleton in mediating cAMP-dependent protein kinase inhibition of the epithelial Na^+/H^+ exchanger NHE3. J. Biol. Chem. 276: 40761 - 40768.

Szászi K., Paulsen A., Szabó E.Z., Numata M., Grinstein S. and Orlowski J. (2002) Clathrin-mediated endocytosis and recycling of the neural Na^+/H^+ exchanger NHE5 isoform: regulation by phosphatidylinositol 3'-kinase and the actin cytoskeleton. J. Biol. Chem. 277: 42623 - 42632.

Takahashi A., Masuda A., Sun M., Centonze V.E. and Herman B. (2004) Oxidative stress-induced apoptosis is associated with alterations in mitochondrial caspase activity and Bcl-2-dependent alterations in mitochondrial pH (pH_m). Brain Res. Bull. 62: 497 - 504.

Takahashi K. and Copenhagen D.R.(1996) Modulation of neuronal function by intracellular pH. Neurosci. Res. 24: 109 - 116.

Takahashi M., Billups B., Rossi D., Sarantis M., Hamann M. and Attwell D. (1997) The role of glutamate transporters in glutamate homeostasis in the brain. J. Exp. Biol. 200: 401 - 409.

Takuma K., Matsuda T., Hashimoto H., Kitanaka J., Asano S., Kishida Y. and Baba A. (1996) Role of Na^+-Ca^{2+} exchanger in agonist-induced Ca^{2+} signalling in cultured rat astrocytes. J. Neurochem. 67: 1840 - 1845.

Tanaka E., Niiywan S., Sato S., Yamada A. and Higashi H. (2003) Arachidonic acid metabolites contribute to the irreversible depolarization induced by in vitro ischemia. J. Neurophysiol. 90: 3213 - 3223.

Tanaka E., Yamamoto S., Inokuchi H., Isagai T. and Higashi H. (1999) Membrane dysfunction induced by in vitro ischemia in rat hippocampal CA1 pyramidal neurons. J. Neurophysiol. 81: 1872 - 1880.

Tanaka E., Yamamoto S., Kudo Y., Mihara S. and Higashi H. (1997) Mechanisms underlying the rapid depolarization produced by deprivation of oxygen and glucose in rat hippocampal CA1 neurons in vitro. J. Neurophysiol. 78: 891 - 902.

Tanaka K. (2001) Alteration of second messengers during acute cerebral ischemia - adenylate cyclase, cyclic AMP-dependent protein kinase, and cyclic AMP response element binding protein. Prog. Neurobiol. 65: 173 - 207.

Tani M. and Neely J.R. (1989) Role of intracellular Na^+ in Ca^{2+} overload and depressed recovery of ventricular function of reperfused ischemic rat hearts. Circ. Res. 65: 1045 - 1056.

Tauskela J.S., Mealing G., Comas R., Brunette E., Monette R., Small D.L. and Morley P. (2003) Protection of cortical neurons against oxygen-glucose deprivation and *N*-methyl-D-aspartate by DIDS and SITS. Eur. J. Pharmacol. 464: 17 - 25.

Taylor C.P., Burke S.P. and Weber M.L. (1995) Hippocampal slices: glutamate overflow and cellular damage from ischemia are reduced by sodium channel blockade. J. Neurosci. Methods 59: 121 - 128.

Taylor C.P., Weber M.L., Gaughan C.L., Lehning E.J. and LoPachin R.M. (1999) Oxygen/glucose deprivation in hippocampal slices: altered intraneuronal elemental composition predicts structural and functional damage. J. Neurosci. 19: 619 - 629.

Taylor D.L., Obrenovitch T.P. and Symon L. (1996) Changes in extracellular acid-base homeostasis in cerebral ischemia. Neurochem. Res. 21: 1013 - 1021.

Teshima Y., Akao M., Jones S.P. and Marban E. (2003) Cariporide (HOE 642), a selective Na^+-H^+ exchange inhibitor, inhibits the mitochondrial death pathway. Circulation 108: 2275 - 2281.

Théroux P., Chaitman B.R., Danchin N., Erhardt L., Meinertz T., Schoreder J.S., Tosnoni G., White H.D., Willerson J.T., Jessel A. for the GUARDAIN investigators. (2000) Inhibition of sodium-hydrogen exchanger with cariporide to prevent myocardial infarction in high-risk ischemic situations. Circulation 102: 3032 - 3038.

Thomas R.C. (1972) Intracellular sodium activity and the sodium pump in snail neurones. J. Physiol. 220: 55 - 71.

Thomas R.C. (1977) The role of bicarbonate, chloride and sodium ions in the regulation of intracellular pH in snail neurones. J. Physiol. 273: 317 - 338.

Tombaugh G.C. (1998) Intracellular pH buffering shapes activity-dependent Ca^{2+} dynamics in dendrites of CA1 interneurons. J. Neurophysiol. 80: 1702 - 1712.

Tombaugh G.C. and Sapolsky R.M. (1990) Mild acidosis protects hippocampal neurons from injury induced by oxygen and glucose deprivation. Brain Res. 506: 343 - 345.

Tombaugh G.C. and Sapolsky R.M. (1993) Evolving concepts about the role of acidosis in ischemic neuropathology. J. Neurochem. 61: 793 - 803.

Tombaugh G.C. and Somjen G.G. (1996) Effects of extracellular pH on voltage-gated Na^+, K^+ and Ca^{2+} currents in isolated rat CA1 neurons. J. Physiol. 493: 719 - 732.

Tombaugh G.C. and Somjen G.G. (1997) Differential sensitivity to intracellular pH among high- and

low-threshold Ca^{2+} currents in isolated rat CA1 neurons. J. Neurophysiol. 77: 639 - 653.

Tombaugh G.C. and Somjen G.G. (1998) pH modulation of voltage-gated ion channels. In: Kaila K., Ransom B.R. (ed) pH and Brain Function. Wiley-Liss, New York, pp 395 - 416.

Tombaugh, G.C. (1994) Mild acidosis delays hypoxic spreading depression and improves neuronal recovery in hippocampal slices. J. Neurosci. 14: 5635 - 5643.

Tong C.K. and Chesler M. (2000) Modulation of spreading depression by changes in extracellular pH. J. Neurophysiol. 84: 2449 - 2457.

Trafton J., Tombaugh G., Yang S. and Sapolsky R. (1996) Salutary and deleterious effects of acidity on an indirect measure of metabolic rate and ATP concentrations in CNS cultures. Brain Res. 731: 122 - 131.

Trapp S., Lückermann M., Brooks P.A. and Ballanyi K. (1996a) Acidosis of rat dorsal vagal neurons in situ during spontaneous and evoked activity. J. Physiol. 496: 695 - 710.

Trapp S., Lückermann M., Kaila K. and Ballanyi K. (1996b) Acidosis of hippocampal neurones mediated by a plasmalemmal Ca^{2+}/H^{+} pump. NeuroReport 7: 2000 - 2004.

Traynelis S.F. and Cull-Candy S.G. (1991) Pharmacological properties and H^{+} sensitivity of excitatory amino acid receptor channels in rat cerebellar granule neurons. J. Physiol. 433: 727 - 763.

Tretter L. and Adam-Vizi V. (1996) Early events in free radical-mediated damage of isolated nerve terminals: effects of peroxides on membrane potential and intracellular Na^{+} and Ca^{2+} concentrations. J. Neurochem. 66: 2057 - 2066.

Trudeau L.-E., Parpura V. and Haydon P.G. (1999) Activation of neurotransmitter release in hippocampal nerve terminals during recovery from intracellular acidification. Am. J. Physiol. 81: 2627 - 2635.

Tse M., Levine S., Yun C., Brant S.R., Counillon L.T., Pouysségur J. and Donowitz M. (1993) Structure/function studies of the epithelial isoforms of the mammalian Na^{+}/H^{+} exchanger gene family. J. Membrane Biol. 135: 93 - 108.

Tymianski M., Charlton M.P., Carlen P.L. and Tator C.H. (1993) Source specificity of early calcium neurotoxicity in cultured embryonic spinal neurons. J. Neurosci. 13: 2085 - 2104.

Tyson R., Peeling J. and Sutherland G. (1993) Metabolic changes associated with altering blood glucose levels in short duration forebrain ischemia. Brain Res. 608: 288 - 298.

Urenjak J. and Obrenovitch T.P. (1996) Pharmacological modulation of voltage-gated Na^{+} channels: a rational and effective strategy against ischemic brain damage. Pharmacol. Rev. 48: 21 - 67.

Van Driel I.R. and Callaghan J.M. (1995) Proton and potassium transport by H^{+}/K^{+}-ATPases. Clin. Exp. Physiol. Pharmacol. 22: 952 - 960.

Van Emous J.G., Schreur J.H., Ruigrok T.J. and Van Echteld C.J. (1998) Both Na^+,K^+-ATPase and Na^+/H^+ exchanger are immediately active upon post-ischemic reperfusion in isolated rat hearts. J. Mol. Cell. Cardiol. 30: 337 - 342.

Vandenberg J.I., Metcalfe J.C. and Grace A.A. (1993) Mechanisms of pH_i recovery after global ischemia in the perfused heart. Circulation Res 72: 993 - 1003.

Vaughan-Jones R.D. (1979) Regulation of chloride in quiescent sheep-heart Purkinje fibres studies using intracellular chloride and pH-sensitive micro-electrodes. J. Physiol. 295: 111 - 137.

Vaughan-Jones R.D. (1988) Regulation of intracellular pH in cardiac muscle. CIBA Foundation Symposium 139: 23 - 46.

Vaughan-Jones R.D. and Wu M.-L. (1990) Extracellular H^+ inactivation of Na^+-H^+ exchange in the sheep cardiac Purkinje fibre. J. Physiol. 428: 441 - 466.

Vaz R., Sarmento A., Borges N., Cruz C. and Azevedo I. (1998) Effect of mechanogated membrane ion channel blockers on experimental traumatic brain oedema. Acta Neurochir. 140: 371 - 375.

Verdru P., DeGreef C., Mertens L., Carmeliet E. and Callewaert G. (1997) Na^+-Ca^{2+} exchange in rat dorsal root ganglion neurons. J. Neurophysiol. 77: 484 - 490.

Vergun O., Sobolevsky A.I., Yelshansky M.V., Keelan J., Khodorov B.I. and Duchen M.R. (2001) Exploration of the role of reactive oxygen species in glutamate neurotoxicity in rat hippocampal neurons in culture. J. Physiol. 531: 147 - 163.

Vigne P., Breittmayer J.-P., Frelin C. and Lazdunski M. (1988) Dual control of the intracellular pH in aortic smooth muscle cells by a cAMP-sensitive HCO_3^-/Cl^- antiporter and a protein kinase C-sensitive Na^+/H^+ antiporter. J. Biol. Chem. 263: 18023 - 18029.

Vincent A.M., TenBroeke M. and Maiese K. (1999) Neuronal intracellular pH directly mediates nitric oxide-induced programmed cell death. J. Neurobiol. 40: 171 - 184.

Voipio J. (1998) Ion-sensitive microelectrodes. In: Kaila K., Ransom B.R. (ed) pH and Brain Function. Wiley-Liss, New York, pp 95 - 108.

Vornov J.J., Thomas A.G. and Jo D. (1996) Protective effects of extracellular acidosis and blockade of sodium/hydrogen ion exchange during recovery from metabolic inhibition in neuronal tissue culture. J. Neurochem. 67: 2379 - 2389.

Vyklicky L, Vlachova A. and Krusek J. (1990) The effect of external pH changes on responses to excitatory amino acids in mouse hippocampal neurons. J. Physiol. 430: 497 - 517.

Wakabayashi S., Shigekawa M. and Pouysségur J. (1997) Molecular physiology of vertebrate Na^+/H^+ exchangers. Physiol. Rev. 77: 51 - 74.

Wang C.-Z., Yano H., Nagashima K. and Seino S. (2000) The Na^+-driven Cl^-/HCO_3^- exchanger. J. Biol. Chem. 275: 35486 - 35490.

Wang D., King S.M., Quill T.A., Doolittle L.K. and Garbers D.L. (2003a) A new sperm-specific Na^+/H^+ exchanger required for sperm motility and fertility. Nature Cell Biol. 5: 1117 - 1122.

Wang G.J., Randall R.D. and Thayer S.A. (1994) Glutamate-induced intracellular acidification of cultured hippocampal neurons demonstrates altered energy metabolism resulting from Ca^{2+} loads. J. Neurophysiol. 72: 2563 - 2569.

Wang Y., Meyer J.W., Ashraf M. and Shull G.E. (2003b) Mice with a null mutation in NHE1 Na^+/H^+ exchange are resistant to cardiac ischemia-reperfusion injury. Circ. Res. 93: 776 - 782.

Watano T., Kimura J., Morita T. and Nakanishi H. (1996) A novel antagonist, No. 7043, of the Na^+/Ca^{2+} exchange current in guinea-pig cardiac ventricular cells. Br. J. Pharmacol. 119: 555 - 563.

Wei G., Hough C.J., Li Y. and Sarvey J.M. (2004) Characterization of extracellular accumulation of Zn^{2+} during ischemia and reperfusion of hippocampal slices in rat. Neuroscience 125: 867 - 877.

Wei S., Rothstein E.C., Fliegel L., Dell'Italia L.J. and Lucchesi P.A. (2001) Differential MAP kinase activation and Na^+/H^+ exchanger phophorylation by H_2O_2 in rat cardiac myocytes. Am. J. Physiol. 281: C1542 - C1550.

Weiss J.H., Sensi S.L., and Koh J.Y. (2000) Zn^{2+}: a novel ionic mediator of neural injury in brain disease. Trends Pharmacol. Sci. 21: 395 - 401.

Whitaker J.E., Haugland R.P. and Prendergast F.G. (1991) Spectral and photophysical studies of benzo[c]xanthene dyes: Dual emission pH sensors. Biochemistry 194: 330 - 344.

White R.J. and Reynolds I.J. (1995) Mitochondria and Na^+/Ca^{2+} exchange buffer glutamate-induced calcium loads in cultured cortical neurons. J. Neurosci. 15: 1318 - 1326.

Whittingham T.S., Lust W.D. and Passonneau J.V. (1984) An in vitro model of ischemia: Metabolic and electrical alterations in the hippocampal slice. J. Neurosci. 4: 793 - 802.

Wiegmann T.B., Welling L.W., Beatty D.M., Howard D.E., Vamos S. and Morris S.J. (1993) Simultaneous imaging of intracellular $[Ca^{2+}]$ and pH in single MDCK and glomerular epithelial cells. Am. J. Physiol. 265: C1184 - C1190.

Wieloch T., Hu B., Boris-Moller A., Cardell M., Kamme F., Kurihara J. and Sakata K. (1996) Intracellular signal transduction in the postischemic brain. Advances in Neurology, Vol. 71: Cellular and Molecular Mechanisms of Ischemic Brain Damage, (Siesjö B.K. and Wieloch T., eds), pp. 371 - 388.

Wiemann M., Schwark J.-R., Bonnet U., Jansen H.W., Grinstein S., Baker R.E., Lang H.-J., Wirth K. and Bingmann D. (1999) Selective inhibition of the Na^+/H^+ exchanger type 3 activates CO_2/H^+-sensitive medullary neurons. Pflügers Arch. 438: 255 - 262.

Wilding T.J., Cheng B. and Roos A. (1992) pH regulation in adult rat carotid body glomus cells. J. Gen. Physiol. 100: 593 - 608.

Willoughby D. and Schwiening C.J. (2002) Electrically evoked dendritic pH transients in rat cerebellar Purkinje cells. J. Physiol. 544: 487 - 499.

Willoughby D., Thomas R.C. and Schwiening C.J. (1998) Comparison of simultaneous pH measurements made with 8-hydroxypyrene-1,3,6-trisulphonic acid (HPTS) and pH-sensitive microelectrodes in snail neurones. Pflügers Arch. 436: 615 - 622.

Wu M.-L. and Vaughan-Jones R.D. (1994) Effect of metabolic inhibitors and second messengers upon Na^+-H^+ exchange in the sheep cardiac Purkinje fibre. J. Physiol. 478: 301 - 313.

Wu M.-L. and Vaughan-Jones R.D. (1997) Interaction between Na^+ and H^+ ions on Na-H exchange in sheep cardiac Purkinje fibers. J. Mol. Cell. Cardiol. 29: 1131 - 1140.

Wu M.-L., Chen J.-H., Chen W.-H., Chen Y.-J. and Chu K.-C. (1999) Novel role of the Ca^{2+}-ATPase in NMDA-induced intracellular acidification. Am. J. Physiol. 277: C717 - C727.

Wu M.-L., Tsai M.-L. and Tseng Y.-Z. (1994) DIDS-sensitive pH_i regulation in single rat cardiac myocytes in nominally HCO_3^--free conditions. Circ. Res. 75: 123 - 132.

Wu Q. and Delamere N.A. (1997) Influence of bafilomycin A_1 on pH_i responses in cultured rat nonpigmented ciliary epithelium. Am. J. Physiol. 273: C1700 - C1706.

Xia Y. and Haddad G.G. (1999) Effect of prolonged O_2 deprivation on Na^+ channels: differential regulation in adult versus fetal rat brain. Neuroscience 94: 1231 - 1243.

Xiao A.Y., Wei L., Xia S., Rothman S. and Yu S.P. (2002) Ionic mechanism of ouabain-induced concurrent apoptosis and necrosis in individual cultured cortical neurons. J. Neurosci. 22: 1350 - 1362.

Xiong Z.-Q., Saggau P. and Stringer J.L. (2000) Activity-dependent intracellular acidification correlates with the duration of seizure activity. J. Neurosci. 20: 1290 - 1296.

Xu Z.C. and Pulsinelli W.A. (1996) Electrophysiological changes of CA1 pyramidal neurons following transient forebrain ischemia: an in vivo intracellular recording and staining study. J. Neurophysiol. 76: 1689 - 1697.

Xu Z.C., Gao T.-M. and Ren Y. (1999) Neurophysiological changes associated with selective neuronal damage in hippocampus following transient forebrain ischemia Biol. Signals Recept. 8: 294 - 308.

Yamada Y., Fukuda A., Tanaka M., Shimano Y., Nishino H., Muramatsu K., Togari H. and Wada Y. (2001) Optical imaging reveals cation-Cl^- cotransporter-mediated transient rapid decrease in intracellular Cl^- concentration induced by oxygen-glucose deprivation in rat neocortical slices. Neurosci. Res. 39: 269 - 280.

Yamamoto S., Matsumoto Y., Suzuki Y., Tsuboi T., Terakawa S, Ohashi N. and Umemura K. (2003) An Na^+/H^+ exchanger inhibitor suppresses cellular swelling and neuronal death induced by glutamate in cultured cortical neurons. Acta. Neurochir. [Suppl] 86: 223 - 226.

Yamamoto S., Tanaka E., Shoji Y., Kudo Y., Inokuchi H. and Higashi H. (1997) Factors that reverse the persistent depolarization produced by deprivation of oxygen and glucose in rat hippocampal CA1 neurons in vitro. J. Physiol. 78: 903 - 911.

Yan Y., Dempsey R.J. and Sun D. (2001) Na^+-K^+-Cl^- cotransporter in rat focal cerebral ischemia. J. Cereb. Blood Flow Metab. 21: 711 - 721.

Yan Y., Dempsey R.J., Flemmer A., Forbush B. and Sun D. (2003) Inhibition of Na^+-K^+-Cl^- cotransporter during focal cerebral ischemia decreases edema and neuronal damage. Brain Res. 961: 22 - 31.

Yao H., Gu X.G. and Haddad GG. (2003) The role of HCO_3^--dependent mechanisms in pH_i regulation during O_2 deprivation. Neuroscience 117: 29 - 35.

Yao H., Gu X.-Q., Douglas R.M. and Haddad G.G. (2001) Role of Na^+/H^+ exchanger during O_2 deprivation in mouse CA1 neurons. Am. J. Physiol. 281: C1205 - C1210.

Yao H., Ma E., Gu X.-Q. and Haddad G.G. (1999) Intracellular pH regulation of CA1 neurons in Na^+/H^+ isoform 1 mutant mice. J. Clinical Invest. 104: 637 - 645.

Yasutake M. and Avkiran M. (1995) Exacerbation of reperfusion arrhythmias by α_1 adrenergic stimulation: A potential role for receptor mediated activation of sarcolemmal sodium-hydrogen exchange. Cardiovasc. Res. 29: 222 - 230.

Yoshinaka K., Kumanogoh H., Nakamura S. and Maekawa S. (2004) Identification of V-ATPase as a major component in the raft fraction prepared from the synaptic plasma membrane and the synaptic vesicle of rat brain. Neurosci. Lett. 363: 168 - 172.

Yu S.P. and Choi D.W. (1997) Na^+-Ca^{2+} exchange currents in cortical neurons: concomitant forward and reverse operation and effect of glutamate. Eur. J. Neurosci. 9: 1273 - 1281.

Yu X.-M. and Salter M.W. (1998) Gain control of NMDA-receptor currents by intracellular sodium. Nature 396: 469 - 474.

Yuan J., Lipinski M. and Degterev A. (2003) Diversity of the mechanisms of neuronal cell death. Neuron 40: 401 - 413.

Yun C.H.C., Tse C.-M., Nath S.K., Levine S.A., Brant S.R. and Donowitz M. (1995) Mammalian Na^+/H^+ exchanger gene family: structure and function studies. Am. J. Physiol. 269: G1 - G11.

Zaidi A. and Michaelis M.L. (1999) Effects of reactive oxygen species on brain synaptic plasma membrane Ca^{2+}-ATPase. Free Radical Biol. Med. 27: 810 - 821.

Zeevalk G.D., Hyndman A.G. and Nicklas, W.J. (1989) Excitatory amino acid-induced toxicity in chick retina: amino acid release, histology, and effects of chloride channel blockers. J. Neurochem. 53: 1610 - 1619.

Zeymer U., Suryapranata H., Monassier J.P., Opolski G., Davies J., Rasmanis G., Linssen G., Tebbe U., Schroder R., Tiemann R., Machnig T., Neuhaus K.-L. for the ESCAMI investigators. J. Am. Coll. Cardiol. 38: 1644 - 1650.

Zhan R.-Z., Fujiwara N., Tanaka E. and Shimoji K. (1998) Intracellular acidification induced by membrane depolarization in rat hippocampal slices: roles of intracellular Ca^{2+} and glycolysis. Brain Res. 780: 86 - 94.

Zhang Y. and Lipton P. (1999) Cytosolic Ca^{2+} changes during in vitro ischemia in rat hippocampal slices: major roles for glutamate and Na^{+}-dependent Ca^{2+} release from mitochondria. J. Neurosci. 19: 3307 - 3315.